AD-A072 095 ROCKWELL INTERNATIONAL THOUSAND OAKS CA SCIENCE CENTER F/G 20/6
FIR OPTICAL MODULATION PHENOMENA.(U)
MAY 79 J G PASKO DAAK70-78-C-0003
UNCLASSIFIED SC5149.31FR NL

1 OF 3
AD A072095

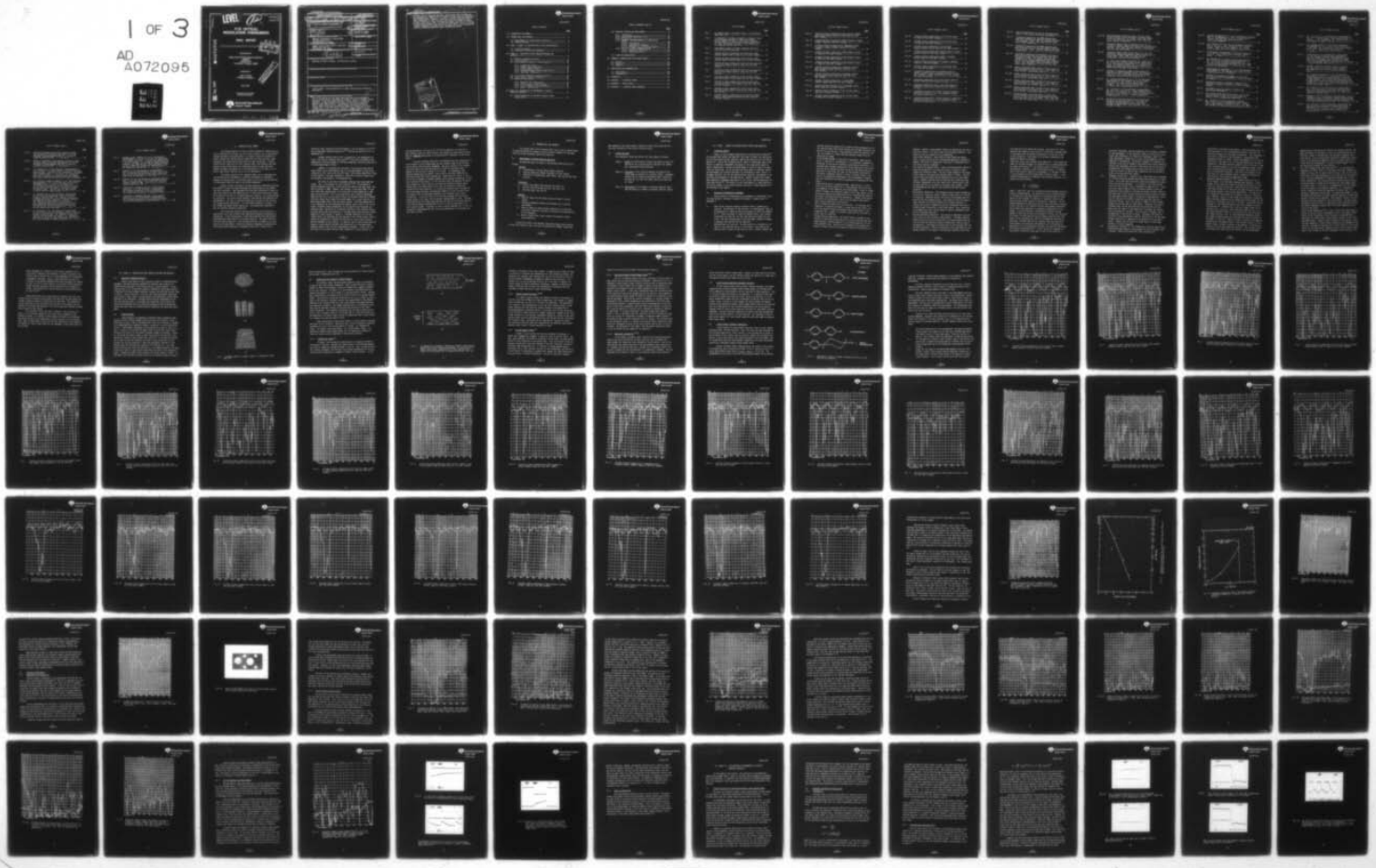

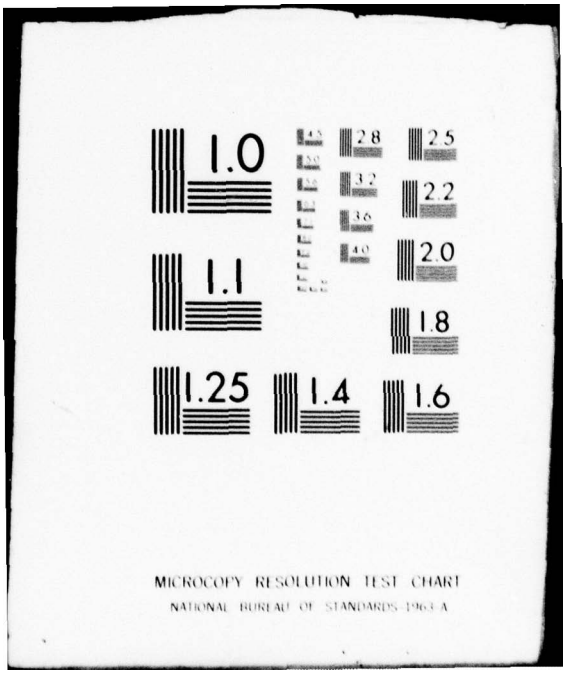
1.0
1.1
1.25
1.4
1.6
2.8
3.2
3.6
4.0
2.5
2.2
2.0
1.8
MICROCOPY RESOLUTION TEST CHART
NATIONAL BUREAU OF STANDARDS 1963 A

LEVEL II

SC5149.31FR

SC5149.31FR
Copy No. 46

FIR OPTICAL MODULATION PHENOMENA

FINAL REPORT

Sponsored by:

Night Vision & Electro-Optics Laboratory
W26P8H
Building 307
Fort Belvoir, Virginia 22060

Prepared by:

John G. Pasko
Principal Investigator

May 1979

Approved for public release.
Distribution unlimited.

Rockwell International
Science Center

Unclassified

SECURITY CLASSIFICATION OF THIS PAGE (When Data Entered)

REPORT DOCUMENTATION PAGE	READ INSTRUCTIONS BEFORE COMPLETING FORM
1. REPORT NUMBER (9) Final rept. 3 Jan 78—30 Apr 79. 2. GOVT ACCESSION NO.	3. RECIPIENT'S CATALOG NUMBER
4. TITLE (and Subtitle) (6) FIR OPTICAL MODULATION PHENOMENA.	5. TYPE OF REPORT & PERIOD COVERED (11) Final Report 01/03/78 through 04/30/79
	6. PERFORMING ORG. REPORT NUMBER (14) SC5149.31FR
7. AUTHOR(s) (10) John G. Pasko	8. CONTRACT OR GRANT NUMBER(s) (15) DAAK70-78-C-0003
9. PERFORMING ORGANIZATION NAME AND ADDRESS Rockwell International Science Center 1049 Camino Dos Rios Thousand Oaks, CA 91360	10. PROGRAM ELEMENT, PROJECT, TASK AREA & WORK UNIT NUMBERS
11. CONTROLLING OFFICE NAME AND ADDRESS Night Vision & Electro-Optics Laboratory W26P8H, Building 307 Fort Belvoir, VA 22060	12. REPORT DATE (11) May 1979 13. NUMBER OF PAGES 209
14. MONITORING AGENCY NAME & ADDRESS (if different from Controlling Office) (12) 211p.	15. SECURITY CLASS. (of this report) Unclassified 15a. DECLASSIFICATION/DOWNGRADING SCHEDULE

16. DISTRIBUTION STATEMENT (of this Report)

Approved for public release. Distribution unlimited.

17. DISTRIBUTION STATEMENT (of the abstract entered in Block 20, if different from Report)

18. SUPPLEMENTARY NOTES

19. KEY WORDS (Continue on reverse side if necessary and identify by block number)

Liquid crystal, infrared modulation, 8-12μm, Electro-Optical Modulator, Cholesteric

MICRON

20. ABSTRACT (Continue on reverse side if necessary and identify by block number)

The initial portion of this report describes the survey conducted of various electro-optical phenomena for potential use as an 8-12μm infrared modulator. Using the chosen candidate, liquid crystals, a prototype modulator has been fabricated and tested utilizing the cholesteric-nematic phase change effect. Cyano-biphenyl and phenylcyclohexane liquid crystals have been identified as materials having high infrared transmission. A one mil film of 4-cyano-4'-n-pentyl biphenyl has an average transmission of ≥87% over the whole 8-12μm region. A contrast

DD FORM 1 JAN 73 1473 EDITION OF 1 NOV 65 IS OBSOLETE

Unclassified

SECURITY CLASSIFICATION OF THIS PAGE (When Data Entered)

(APPROXIMATELY) 389947 (MICRON)

of ≈93%, turn-on time less than 1ms, and turn-off time of ≈125ms has been measured at λ = 8μm for an ≈f/3 optical system using the conventional phase change effect. However, a partially turned-on operating mode has been investigated in which turn-off times have been reduced to about 20-30ms, with turn-on times increased to ≈5-20ms, and having a contrast of about 60-70% measured over the whole 8-12μm region in an f/1.2 system. Trade-off between cell transmission, contrast, and turn-off time must be carefully optimized depending on the intended application.

TABLE OF CONTENTS

TABLE OF CONTENTS (Cont'd)

LIST OF FIGURES

LIST OF FIGURES (Cont'd)

LIST OF FIGURES (Cont'd)

LIST OF FIGURES (Cont'd)

LIST OF FIGURES (Cont'd)

LIST OF FIGURES (Cont'd)

LIST OF FIGURES (Cont'd)

LIST OF FIGURES (Cont'd)

LIST OF FIGURES (Cont'd)

1.0 INTRODUCTION AND SUMMARY

The advanced design of current infrared pyroelectric imaging devices, such as pyroelectric vidicons, has led to their potential use in man-portable systems and other field applications. At present, mechanical choppers are used to produce the required optical modulation, but they are bulky, power consuming, and contain moving parts which can wear and fatigue. A purely electro-optical modulator with fast response times, high contrast and transmission in the 8-12μm region, and compactness would be highly desirable. Another stringent requirement for a vidicon modulator is the need for it to have a large optical aperture and to be line addressable.

The primary purpose of this research effort was to investigate various electro-optical phenomena as a possible replacement for mechanical choppers for applications in the 8-12μm region, and to build and characterize an experimental modulator based on the chosen phenomenon.

Several surveys of potential infrared modulation techniques have been published[1-4] in which the many advantages and disadvantages of the methods have been elucidated. Some phenomena which have been considered in these surveys, but ruled out as less promising are: (1) free carrier absorption caused by injection of carriers in a forward-biased p-n junction, (2) reverse-biased p-n junctions, (3) strain-induced changes in the free carrier absorption of a semiconductor, (4) shift of absorption edge due to stress or free carriers, (5) Faraday rotation modulators, (6) Stark effect modulator in gases, (7) Kerr effect and Pockels effect modulators, (8) acousto-optic modulators, and (9) multiple reflection modulators.

One of the more favorable devices mentioned in the literature is a Fabry-Perot cavity with variable plate separation produced by piezoelectric transducers. In the 14-16μm band, a Fabry-Perot modulator has been tested[5] which modulates about 75% of the available radiation. The major difficulty with this type of modulator is the extreme difficulty in producing one that could be line addressable. Additional modulation phenomena studied were the Christiansen effect modulator,[6] suspended crystal cell,[7] electrically-

controlled light scattering and birefringence in the ferroelectric PLZT,[8-10] and the deformable membrane modulator,[11-14] offering the possibility of x-y addressability.

Another promising device that is potentially line addressable utilizes a thin film of vanadium oxide (VO_2)[15-17] which has an extremely sharp temperature transition between an infrared-transparent insulating state and an infrared-opaque metallic state.

However, in reviewing the literature, it was obvious that none of these effects could simultaneously meet all the requirements of high 8-12μm transmission, fast turn-on and turn-off times, high contrast modulation, large optical aperture, low power consumption, simplicity of design, construction and operation, and potential line addressability.

But there is one class of phenomena which has not as yet been mentioned. This is the subject of liquid crystals.[18-22] The existence of organic compounds exhibiting liquid crystalline behavior has been known since their discovery in 1888. However, only recently, since about 1965, has any real effort been concentrated in utilizing their unique properties in some type of actual device. The initial application was in display technology where the ability of liquid crystal films to be switched electrically between clear and cloudy states enabled the establishment of a visual contrast to be maintained between these clear and cloudy regions. Switching speeds were at first inadequate, but the technology has matured, and at least in the visible region, switching speeds approaching 1 ms are possible with contrasts approaching 100%. The wealth of information compiled in the literature discussing the applications and technology of the many known electro-optical effects present in liquid crystals is abundant. Although essentially all the published results are concerned with applications in the visible region, there is nothing in the physics to prevent the extension of liquid crystal electro-optical phenomena to the infrared. In addition, due to similar techniques employed in liquid crystal displays, the fabrication of a line-addressable modulator poses no new difficult technological problems. In fact, with the publication of the paper entitled "Some Properties of Liquid Crystals as

Infrared Modulators", by Fray et al.,[23] and the commercial availability of many different types of liquid crystals, this became the most promising candidate for immediate application as an electro-optical modulator in the 8-12μm region.

The major problems which had to be addressed were the transmission of liquid crystals in the 8-12μm region and the response times of the relevant liquid crystal electro-optical phenomena. The major portion of this contractual effort dealt with the investigation of these two important areas. A summary of the principal findings is as follows: 1) cyanobiphenyl and phenylcylohexane positive nematic liquid crystals have been identified as materials having high 8-12μm transmission. Neglecting cell losses, a 1 mil thick film of 4-cyano-4'-n-pentyl biphenyl has an average transmission of ≈87% over the whole 8-12μm region, 2) fast turn-off times are obtained for short-pitch cholesteric liquid crystals utilizing the cholesteric-nematic phase change effect, but these materials are less than optimum for efficient scattering of 8-12μm radiation, 3) a partially turned-on operating mode has been investigated yielding a considerable reduction in cell turn-off times, but however, with an associated decrease in cell contrast and on state transmission. A turn-off time of ≈5 ms has been achieved in the 8-11.5μm region using a 5 mil thick, 14% cholesteryl nonanoate/BDH E-1 cell. The best contrast/turn-off time combination measured was ≈55%, 20 ms and occurred for a 5 mil, 5% cholesteryl nonanoate/BDH E-1 cell in the 8-11.5μm region in an f/1.2 optical system. A contrast as high as 70% was measured for a 5 mil, 5% cholesteryl nonanoate/EM 684 cell, but was accompanied by an increased turn-off time of ≈40 ms.

2.0 PROGRAM GOALS AND APPROACH

The primary goal of this research effort was to find a suitable means of replacing mechanical choppers by electro-optical choppers for the modulation of 8-12μm incoherent unpolarized radiation.

2.1 Requirements for Electro-Optical Modulator

The modulator goals as stated in the purchase description are as follows:

Optical:

a. Transmittance in 8-12μm region greater than 95%.
b. Contrast modulation greater than 95% in 8-12μm region.
c. Variation of transmittance, when "OPEN", less than 5% over clear aperture.

Electrical:

a. Turn-on time (100% to 5% contrast) less than 1 ms.
b. Turn-off time (0% to 90% contrast) less than 1 ms.
c. Switching power less than 1W.

Chemical:

a. Material should not have major absorption bands in 8-12μm region.
b. Operating temperature should be consistent with a military environment.
c. Material should be stable against photolysis by visible and ultraviolet radiation, hydrolysis by humidity and contamination by the atmosphere.
d. Material should have a vapor pressure low enough to permit vacuum operation.

During the course of the program, encouraging results were observed in the 3-5μm regions as well, and with the permission of NV&EOL, experiments

were extended to the 3-5μm region in addition to the 8-12μm region during a four month extension to the original contract period.

2.2 Program Approach

The contractual effort was broken into three phases as follows:

Phase I: Survey of electro-optical effects and materials useful for application as an electro-optical modulator for incoherent, unpolarized 8-12μm radiation.

Phase II: Evaluation of most promising methods and materials selected based on analysis of literature survey. Parameters measured are to include transmittance and/or scattering for both the "on" and "off" modes, and turn-on and turn-off times.

Phase III: Optimization of performance of selected modulator candidate and delivery to NV&EOL of modulator material samples.

3.0 PHASE I: SURVEY OF ELECTRO-OPTICAL EFFECTS AND MATERIALS

3.1 Literature Search

Phase I of this program concentrated on surveying the literature[1-2] for any pertinent effects and materials that might be useful for application as an 8-12μm electro-optical modulator meeting the specifications outlined in Section 2.1. Due to the increasing use of lasers in technology, many of the efforts in modulator development are geared to this application where coherent, monochromatic, narrow collimated beams of radiation need to be modulated and controlled. Few of the many published papers on modulator design and development are directly applicable to the problem at hand, since it is extremely difficult for all the electro-optical modulator requirements to be satisfied simultaneously in the same device. Several surveys have already been completed of phenomena applicable as solid state infrared modulators for space application.[3-4] The majority of the requirements for these modulators are similar enough to the current problem to warrant a closer examination of the findings of the reports.

3.2 Discussion of Modulation Phenomena

Several possible infrared modulation phenomena are mentioned in the following synopsis, and many of these are discussed in greater detail in Reference 4.

1. Free carrier injection caused by forward biasing a germanium p-n junction: The presence of free carriers in a semiconductor leads to the absorption of radiation where the absorption coefficient depends on λ^2. Close tolerances on junction formation and p- and n-region thicknesses are required, but very high modulation depths are possible. The major disadvantage is the high power consumption needed to generate the required carrier densities.
2. Reverse-biased p-n junction: The application of a reverse-bias voltage to a p-n junction results in an increase in the junction depletion width in which no free carriers exist. However, whereas the

previous device can operate with incident radiation perpendicular to the junction plane, this device requires the incident radiation to be parallel to the junction. Since depletion widths are typically narrow, this results in a small aperture modulator useful only for narrow optical beams.

3. Strain-induced changes in free carrier absorption: When uniaxial strain is applied to a semiconductor, it is possible to generate an anisotropy in free carrier absorption under certain conditions. If radiation were incident perpendicular to the direction of the stress, the free carrier absorption would be high for the polarization perpendicular to the stress and lower for the parallel polarization, thus making a modulator possible in which a periodic stress is applied to an appropriate semiconductor such as germanium. However, very low transmission and effective modulation is predicted for this device.

4. Stress-induced shift in absorption edge: Application of a stress alters the interband absorption of a semiconductor due to the relative movements of the conduction and valence bands. Alloys of either PbSnTe or HgCdTe, with absorption edges in the 8-12μm region, can be used and by applying the appropriate strain, the absorption edge can be shifted, thus modulating the transmission. However, while moderate shifts can be obtained, a shift over the whole 8-12μm region would require excessively large strains.

5. Shift of absorption edge due to free carriers: In narrow-gap semiconductors like PbSnTe and HgCdTe, a large free carrier density can shift the absorption edge by occupying lower energy states in the conduction band. However, the material would have to be cooled to obtain good p-n junctions.

6. Faraday rotation modulators: The Faraday effect is defined as the rotation of the plane of polarization of a plane polarized beam when passed through a suitable material in a direction parallel to an applied magnetic field. Variation of the magnetic field changes the amount of rotation and thus the amount of radiation transmitted by an

analyzer. However, large magnetic fields are required and the use of polarizers results in a loss in 50% of the available radiation. This device is also not suitable for line addressing.

7. Stark effect modulator: High electric fields modify the energy levels in gases displacing the corresponding absorption frequencies. However, this shift is rather small resulting in a modulator with a very narrow spectral bandwidth.

8. Kerr effect and Pockels effect: These are electro-optical effects in which the application of an electric field to a solid or liquid changes the refractive index. The Kerr effect depends on the square of the electric field while the Pockels effect is linear. These effects are the most widely applied phenomena for use as laser modulators. However, materials such as GaAs and CdTe, which have high infrared transparency, also have rather small electro-optical coefficients resulting in the need for extremely high voltages. Other disadvantages are the need for two polarizers and small angular apertures.

9. Acousto-optic modulators: High-frequency acoustic waves propagating in solids or liquids can result in behavior reminiscent of a diffraction grating. Modulator devices can be built using Bragg angle diffraction from the induced grating. The problem is that the acoustic power required for efficient depletion of incident radiation increases with acoustic frequency and optical wavelength resulting in excessive power dissipation in the 8-12μm region. Also, scattering is strongest only over a narrow range of spectral wavelengths which satisfy the Bragg conditions.

10. Multiple-reflection modulators: This device is comprised of two parallel plates of high refractive index material. Incident radiation enters the device hitting the back wall at an angle greater than the critical angle and passes by multiple reflections to the far end of the modulator. Electrodes are placed close to and insulated from the reflecting surfaces. These are maintained at the same potential, and another contact in the center of the modulator enables a high field

to be applied at the reflecting surfaces. Application of a field modulates the number of free carriers at the surface, although there is some doubt that the modulation mechanism is truly due to free carrier absorption. Using KRS-5 or Ge surfaces, moderately high modulation depths are obtained.

11. Fabry-Perot cavity with variable plate separation: This concept was chosen as the most favorable for application as an infrared modulator for space applications.[3-4] Two parallel plates of reflectivity R separated by a distance d, form a Fabry-Perot cavity. If monochromatic plane parallel radiation of wavelength λ is incident at angle θ, the transmission of the system shows a series of peaks. I, the intensity transmitted as a fraction of the incident intensity, I_o, is given by the Airy function,

$$\frac{I}{I_o} = \frac{1}{1+F \sin^2 \delta/2}$$

where $F = 4R/(1-R)^2$, and δ is the phase difference between successive multiply reflected beams. For application as an infrared modulator, at one setting of the plate separation, the maximum possible transmission of the incident f/1 radiation is required, while at some other setting, minimum possible transmission is required. The differences between this application and the usual Fabry-Perot configuration is the use of f/1 radiation and the large spectral bandwidth. The variable plate separation is produced by piezoelectric transducers. In the 14-16μm band, a Fabry-Perot modulator has been tested[5] in which two cavities are connected in series, with the outer CdTe plates in fixed positions and one common vibrating inner CdTe plate. In this configuration, 75% of the transmitted radiation was modulated. Although enabling fast response times and large modulation depths to be attained, the extension of this technique to fabrication of a line addressable modulator cell would be formidable.

12. Christiansen effect modulator:[6] If small particles suspended in a liquid have a refractive index equal to that of the liquid at a

particular wavelength, then the suspension will be highly transparent at that wavelength. If the refractive indices of the particles and liquid vary differently as a function of wavelength, then at all other wavelengths, scattering will occur in the suspension causing a reduction in transmission. The optical bandwidth is inversely proportional to the rate of change of the particle and liquid refractive indices with wavelength, and also on the square root of the particle concentration, the average particle radius, and the cell thickness. It may be difficult to obtain high transmission over a bandwidth as large as the required 8-12μm region.

13. Suspended crystal cell:[7] Crystals with a high aspect ratio suspended in a fluid by Brownian movement have been used successfully as light valves. Cells have been successfully made using Herapathite crystals which are excellent absorbers. In an electric field the crystals rotate and the incident light is transmited through the cell. Otherwise, the random orientation due to Brownian movement causes the broadside of the crystals to intercept and absorb incident radiation. This same type of cell has been used with aluminum crystals and metal shavings where incident energy is reflected or backscattered. Occlusion of three and four orders of magnitude have been achieved in laboratory devices. Also, this device is useable in high f-number systems and the open axes at right angles. Therefore, for normally incident light, the two polarizations are individually shifted. While this will result in some smearing of the image, the contrast ratio variations will be small. For fast optical systems, light is incident over a wide variety of angles. Therefore, the effect of variation in the extraordinary index of refraction will be more complicated, resulting in a smearing of the image even for one polarization. However, the utilization of these types of birefringent devices is virtually unproven.

14. Ferroelectric devices:[8-10] Two fundamentally different electro-optic effects have been observed in hot-pressed PZT (lead zirconate, lead titanate): electrically-controlled light scattering and

electrically- controlled birefringence. These two effects have also been discovered in PLZT (lanthanum modified PZT), which has the additional property of being highly transparent. The transparency in the visible is 95% and at 8μm wavelength is approximately 90% neglecting reflective losses. Further improvements at 8 to 12μm are realizable. High quality PLZT and related compounds are available commercially, and these materials generally have a Curie point above 100°C, and would operate in the military temperature range. Wafers with interdigitated electrodes in the plane of the surface can be used as controllable scatterers. They have the advantage of very high speed (in the microsecond region), commercial availability, stability and a wide operating temperature range.

15. Deformable membrane modulator:[11-14] Another alternative for an 8-12μm chopper is the deformable membrane (DM) modulator. Several systems of this type have received considerable attention as light valves for projection television. Modulators which can disperse light beams through 18° of angle with low power dissipation and sub-microsecond response time have been demonstrated. Efficiencies of this system are from 50-80%, and f-numbers as low as 1.7 have been used. Moreover, several of the systems are constructed of materials whose important properties do not change significantly under the temperature or illuminated conditions of interest. One possible device composed of a few thousand Angstrom thick metal membrane (possibly electroplated Ni) stretched over a series of ridges formed from an insulator (e.g., SiO_2) on a rigid conducting substrate (e.g., Si). The distance between ridges will be typically 40μm and the height of the ridges typically 4-7μm. On other deformable membrane systems, the ridges and empty spaces may be replaced by other structures, an elastomer, or even PLZT. When no voltage is applied to the membrane, the tension of the membrane holds it taut and the surface is mirror smooth. When a voltage is applied to the membrane, it deforms parabolically, being pulled toward the substrate. The voltages applied in the device are large, typically a few KV, but may be decreased

substantially by decreasing film tension and insulator spacing. The power dissipation in the device is very low, consisting only of the frictional losses in deforming the film and small spreading resistance losses. Also, by constructing appropriate addressing circuitry on the Si and etching the membrane, a device is made in which individual cells may be modulated. The major drawback appears to be in the fabrication problems of such a device.

16. Thin film vanadium oxide (VO_2) modulator:[15-17] At the transition temperature of ~65°C, there is a very abrupt electrical conductivity change as high as 10^5 in single crystals of VO_2. Thus, in the insulating state, infrared transparency is very high while in the metallic state, infrared transparency is reduced considerably due to free carrier absorption. The insulator-to-metal transition can be driven by passing electric current pulses through thin film elements made from these films. In this way, a line-addressable thin film pattern can be delineated on a transparent substrate. At a frequency of 100 Hz, radiation at 337μm was modulated by ~70% with the film-substrate transmission close to 80%. At frequencies between 1-2 kHz, the modulation decreased to 50-60%, primarily because of insufficient external cooling of the substrate. Very recently, results using this technique have been reported in the 8-12μm region. The major disadvantages are the difficulty in producing pure VO_2 films and the need for careful temperature control due to the sharp temperature transition of the effect.

17. Liquid crystal modulators:[18-22] Liquid crystals have been primarily applied in optical display development, and for this reason, essentially all the information in the literature is concerned with a description of liquid crystal electro-optical effects in the visible wavelength region. However, there is nothing in the physics to prevent the extension of liquid crystal electro-optical phenomena to the infrared. Although the transmission of liquid crystals in the 8-12μm region and the electro-optic response times of liquid crystal phenomena in the infrared are not well documented in the literature, the

major advantages of a potential liquid crystal modulator are its large optical aperture, wide bandwidth, low power dissipation, and relative ease of fabrication of a line-addressable cell using photolithographic techniques. Many of these properties are just not available in the several phenomena previously discussed. As a matter of fact, the use of liquid crystals as an 8-12μm infrared modulator looked even more promising with the publication of the paper entitled, "Some Properties of Liquid Crystals as Infrared Modulators," by Fray et al.[23]

Other possiblities for an electro-optical modulator were also considered as well as those discussed above, but there just was not enough time to make a detailed analysis of feasibility for each case. The reference to the VO_2 modulator was not discovered until the end of the program, but this appears to be another good approach to the 8-12μm modulation problem currently being pursued by other people.

The literature survey, delivered to NV&EOL as the culmination of Phase I of this program, emphasizes the liquid crystal approach to the modulator problem. It contains a rather extensive collection of references describing the physics and technology of liquid crystals up to the present time. Many of these papers should find definite application in the extension of research of liquid crystal materials and phenomena to the 8-12μm region of the infrared.

4.0 PHASE II: EVALUATION OF MOST PROMISING METHODS AND MATERIALS

4.1 Modulator Candidate Selection

Based on the results of the literature survey of infrared modulator phenomena, the most promising candidate for immediate application as an electro-optical modulator in the 8-12μm region is liquid crystals. In the paper by Fray et al.,[23] modulation depths of 80%-90% at 10.6μm were reported in addition to 8-14μm average transmission greater than 70% and turn-off times of 100 ms. Equally important is the fact that photolithographic techniques could enable a rather simple, straightforward line-addressable liquid crystal modulator to be fabricated. Although state-of-the-art performance did not meet the specified goals, it was hoped that additional liquid crystal materials and techniques could be found and developed during the contractual period that would lead to an electro-optical modulator that would meet these goals.

4.2 Liquid Crystals

Liquid crystals are composed of elongated organic molecules representing a state of matter between crystalline solid and isotropic liquid in which there is only a one or two-dimensional ordering of molecules as opposed to a three-dimensional ordering of atoms or molecules in a solid crystalline lattice. Three general mesophases are distinguished as shown in Figs. 1a, b, and c. Figure 1a illustrates the nematic phase in which the liquid crystal molecules are parallel to one another although randomly distributed. Figure 1b illustrates the smectic phase in which the molecules are parallel to one another but stacked in well defined rows, and Fig. 1c illustrates the cholesteric phase in which the molecules are found in rows and parallel to one another, but with the molecules in each row subsequently twisted at a well defined angle from the molecular direction in a previous row. The longitudinal distance over which the molecules in a row become oriented in the same direction as those in some previous row defines the pitch of the cholesteric phase. Although the smectic phase posseses the highest degree of order, it is the nematic and cholesteric phases which have the greatest number of electro-

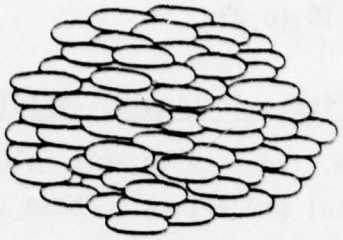

(a)

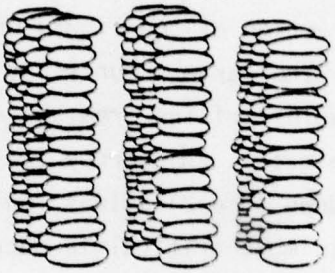

(b)

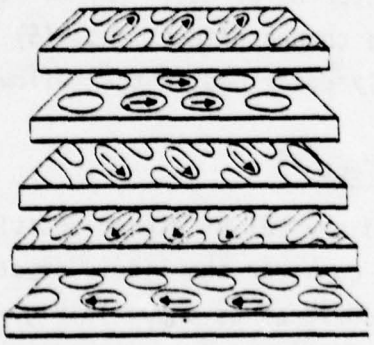

(c)

Fig. 1 (a) Nematic phase; (b) Smectic phase; (c) Cholesteric phase. (Ref. 42)

optical applications. Good introductions to the properties of liquid crystals can be found in References 18 to 22.

4.3 Electro-Optical Effects in Liquid Crystals

The ordered, large, rod-like organic molecules lead to anisotropies in many of the liquid crystal properties. These include dielectric constant, refractive index (birefringence), electrical conductivity, magnetic susceptibility, and viscosity. Of these, it is the dielectric anisotropy which determines the behavior of liquid crystals in applied electric fields. The magnetic susceptibility anisotropy serves a similar function for applied magnetic fields. The dielectric anisotropy is defined as $\Delta\varepsilon = \varepsilon_{11}-\varepsilon_{\perp}$, where ε_{11} and $\varepsilon_{\perp}$ refer to the dielectric constants parallel and perpendicular to the director (defined as the average direction of the liquid crystal rod-shaped molecular axes comprising a sample). The largest contributions to the dielectric constants are the permanent dipoles arising from the structure of the liquid crystal molecules. The dielectric anisotropy ($\Delta\varepsilon$) can take on both positive (up to ≈+15) or negative (down to ≈-2) values, and it is the sign as well as the magnitude of $\Delta\varepsilon$ which is most critical in determining how a liquid crystal will respond to an applied electric field.

Many electro-optical and optical effects in liquid crystals have been described in the literature. Those which were initially selected as possible candidates for use in the infrared modulator include: (1) Freedericksz effect, (2) dynamic scattering effect, (3) twisted nematic effect, (4) cholesteric-nematic phase change effect, and (5) guest-host interaction. These will each be briefly described in the following sections.

4.3.1 Freedericksz Effect [24]

A nematic liquid crystal of either positive or negative dielectric anisotropy is required. Consider the liquid crystal to be contained between two parallel conducting surfaces as shown in Fig. 2a. Here, by application of cell surface treatments, the molecules are oriented perpendicular to the conducting surface (homeotropic alignment of nematic liquid crystals). If the

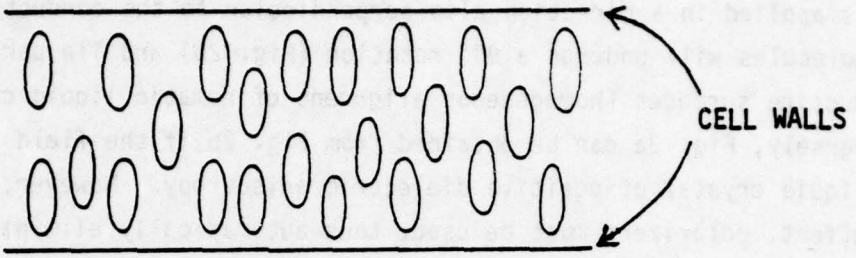

(a)

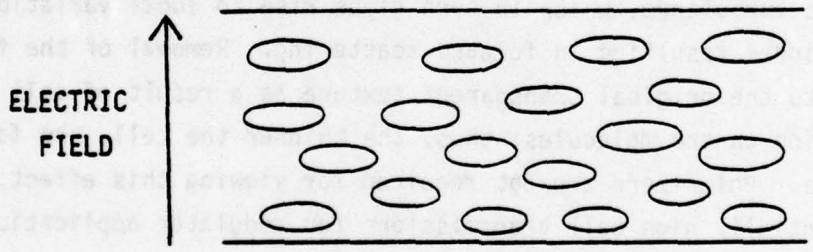

(b)

Fig. 2 (a) Homeotropic alignment of negative $\Delta\varepsilon$ nematic liquid crystal between two parallel conducting surfaces; (b) Reorientation of above liquid crystal molecules by 90° after application of electric field perpendicular to conducting surfaces. (Ref. 42)

dielectric anisotropy of the liquid crystal is negative and an electric field is applied in a direction also perpendicular to the conducting surfaces, the molecules will undergo a 90° rotation (Fig. 2b) and lie parallel to the conducting surfaces (homogeneous alignment of nematic liquid crystals). Conversely, Fig. 2a can be obtained from Fig. 2b if the field is applied to a liquid crystal of positive dielectric anisotropy. However, to observe the effect, polarizers must be used, thus automatically eliminating half the available incident radiation, a major disadvantage.

4.3.2 Dynamic Scattering Effect [25-26]

In a nematic liquid crystal with negative dielectric anisotropy, resistivity less than 10^{10}ohm-cm (slightly conducting), and aligned in a homeotropic orientation, the cell will initially be transparent. The application of an electric field perpendicular to the cell walls causes current to flow which interacts with the molecular dipoles leading to the generation of electrohydrodynamic turbulence, which in turn gives rise to local variations in the refractive index resulting in forward scattering. Removal of the field allows relaxation to the original transparent texture as a result of cell wall surface forces acting on the molecules; thus, the thinner the cell, the faster the relaxation time. Polarizers are not required for viewing this effect, thus allowing potentially high cell transmissions for modulator applications, assuming liquid crystal infrared absorption is small.

4.3.3 Twisted Nematic Effect [27]

A nematic liquid crystal with positive dielectric anisotropy is chosen and a homogeneous alignment is applied to each of the cell walls. However, when assembled, the molecular orientation on one plate is placed perpendicular to the orientation on the second plate. Thus, the director turns continuously through 90° across the thickness of the cell providing a guiding of polarized light through the cell. If the cell is placed between crossed polarizers with no field applied, the cell will be transparent; application of a field results in homeotropic alignment which negates the light guiding property and results in minimum transmission. The use of polarizers, however,

results in an initial loss of 50% of the available radiation.

4.3.4 Cholesteric-Nematic Phase Change Effect [28-31]

This is a scattering effect utilizing a cholesteric liquid crystal of high resistivity and positive dielectric anisotropy. Referring to Fig. 1c, a cholesteric liquid crystal forms a helical structure with an associated pitch. A cholesteric liquid crystal can be formed by adding varying amounts of an optically active material (such as another cholesteric liquid crystal) to a nematic liquid crystal. In this way, a mechanism exists for varying the pitch of the mixture by varying the concentration of the optically active material, thus optimizing the pitch length for efficient scattering of radiation of any desired wavelengh. There are two possible alignments, or textures present in cholesteric liquid crystals depending on the orientation of the helix axes. The Grandjean texture, in which the helix axes are perpendicular to the cell walls, is partially transparent, while the focal-conic texture, in which the helix axes are parallel to the cell walls, although not necessarily parallel to each other, is strongly scattering. The phase change occurs when an electric field is applied to the cell leading to an initial stretching of the helix and finally to a homeotropic alignment (transparent nematic phase) of the molecules when a specific threshold field is reached. The relaxation back to the cholesteric phase is a function of the helix elastic restoration force which acts throughout the bulk of the liquid crystal and not just on the wall surfaces. The advantage of this effect, like the dynamic scattering effect, is that polarizers are not needed for its operation.

4.3.5 Guest-Host Interaction [32-33]

In this effect, pleochroic dyes, consisting of long molecules which absorb light polarized parallel to their long axis, are introduced into a phase change cell containing a host cholesteric liquid crystal. With no voltage applied, the random directions of the dye molecules cause absorption of all incident polarization directions. Maximum cell transmission occurs with the cell turned-on and the dye molecules in a homeotropic alignment. The main advantage of this effect is that it is an absorbing rather than scattering

device providing a larger viewing angle. However, the dyes used are optimized for the visible region, not the infrared, making the search for a proper dye a pre-requisite before this effect can be utilized.

4.4 Liquid Crystal Modulator Candidate Selection

Of the liquid crystal electro-optical effects discussed, the dynamic scattering and cholesteric-nematic phase change effects are the most promising, especially since polarizers are not required for their operation. This is critical because the purpose of the modulator is to modulate 8-12μm radiation from an unpolarized radiation field; the use of polarizers in a cell would automatically reduce the cell transparency by 50% and could not be tolerated. Early in Phase II of the program, the choice between the dynamic scattering and cholesteric-nematic phase change effects could not be finalized until an investigation of the infrared transparencies and electro-optical response times of liquid crystal materials available for the effects could be completed. Infrared (8-12μm) transmission of greater than 95% and modulator turn-on and turn-off times of 1 ms were required. The remainder of Phase II dealt with a search for liquid crystal materials which could meet the requirements stated above.

4.5 Liquid Crystal Infrared Transmission

Liquid crystals are large organic molecules, and as a rule, organic molecules absorb infrared radiation. Very little work has been published on the infrared properties of liquid crystals, so the approach was to obtain as many different liquid crystal types as possible, measure the infrared transmission in the 8-12μm regions, and choose the material with the highest overall transmission which was simultaneously compatible with either the dynamic scattering or cholesteric-nematic phase change effect.

Several different organic compound groups can exhibit liquid crystalline properties; their structures are shown in Fig. 3, where the R and R''s can be some terminal group such as C_nH_{2n+1}, $C_nH_{2n+1}O$, or CN, etc. The cyanobiphenyls are unique in that the linking groups between the two benzene

SC79-4438

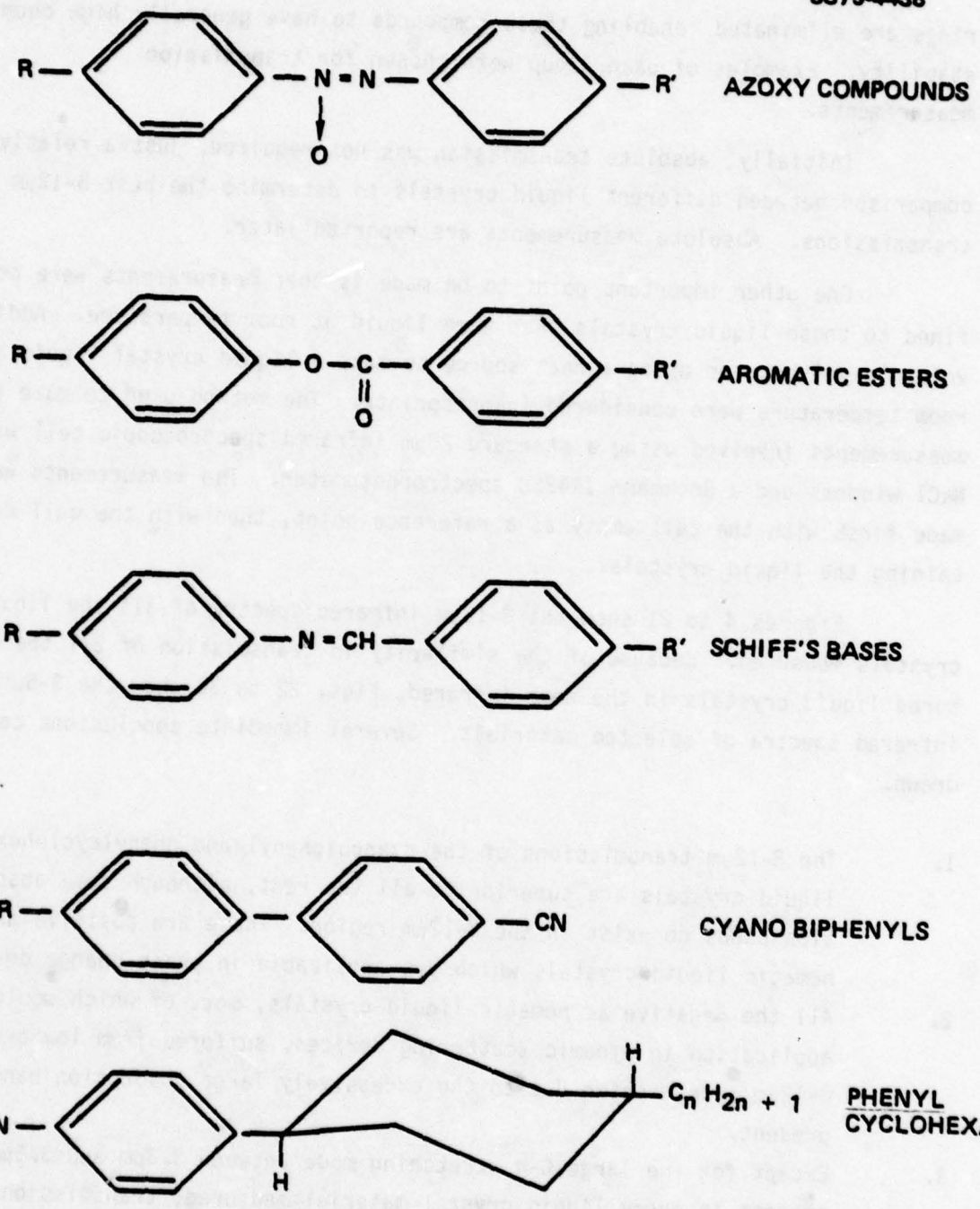

Fig. 3 Some general classes of organic compounds exhibiting liquid crystalline properties.

rings are eliminated enabling these compounds to have generally high chemical stability. Examples of each group were chosen for transmission measurements.

Initially, absolute transmission was not required, just a relative comparison between different liquid crystals to determine the best 8-12μm transmissions. Absolute measurements are reported later.

One other important point to be made is that measurements were confined to those liquid crystals that were liquid at room temperature. Adding volatile solvents or using a heat source to make a liquid crystal liquid at room temperature were considered inappropriate. The method used to make the measurements involved using a standard 25μm infrared spectroscopic cell with NaCl windows and a Beckmann IR4250 spectrophotometer. The measurements were made first with the cell empty as a reference point, then with the cell containing the liquid crystals.

Figures 4 to 21 show the 8-12μm infrared spectra of all the liquid crystals measured. Because of the similarity in transmission of all the measured liquid crystals in the near infrared, Figs. 22 to 30 show the 3-5μm infrared spectra of selected materials. Several immediate conclusions can be drawn.

1. The 8-12μm transmissions of the cyanobiphenyl and phenylcyclohexane liquid crystals are superior to all the rest, although some absorption bands do exist in the 8-12μm region. These are positive $\Delta\varepsilon$ nematic liquid crystals which are applicable in phase change devices.
2. All the negative $\Delta\varepsilon$ nematic liquid crystals, most of which would find application in dynamic scattering devices, suffered from low overall 8-12μm transmission due to the excessively large absorption bands present.
3. Except for the large C-H stretching mode between 3.3μm and 3.5μm present in every liquid crystal material measured, transmission in the 3-5μm region is high for both positive and negative $\Delta\varepsilon$ nematic liquid crystals. This is partly the basis by which the contract

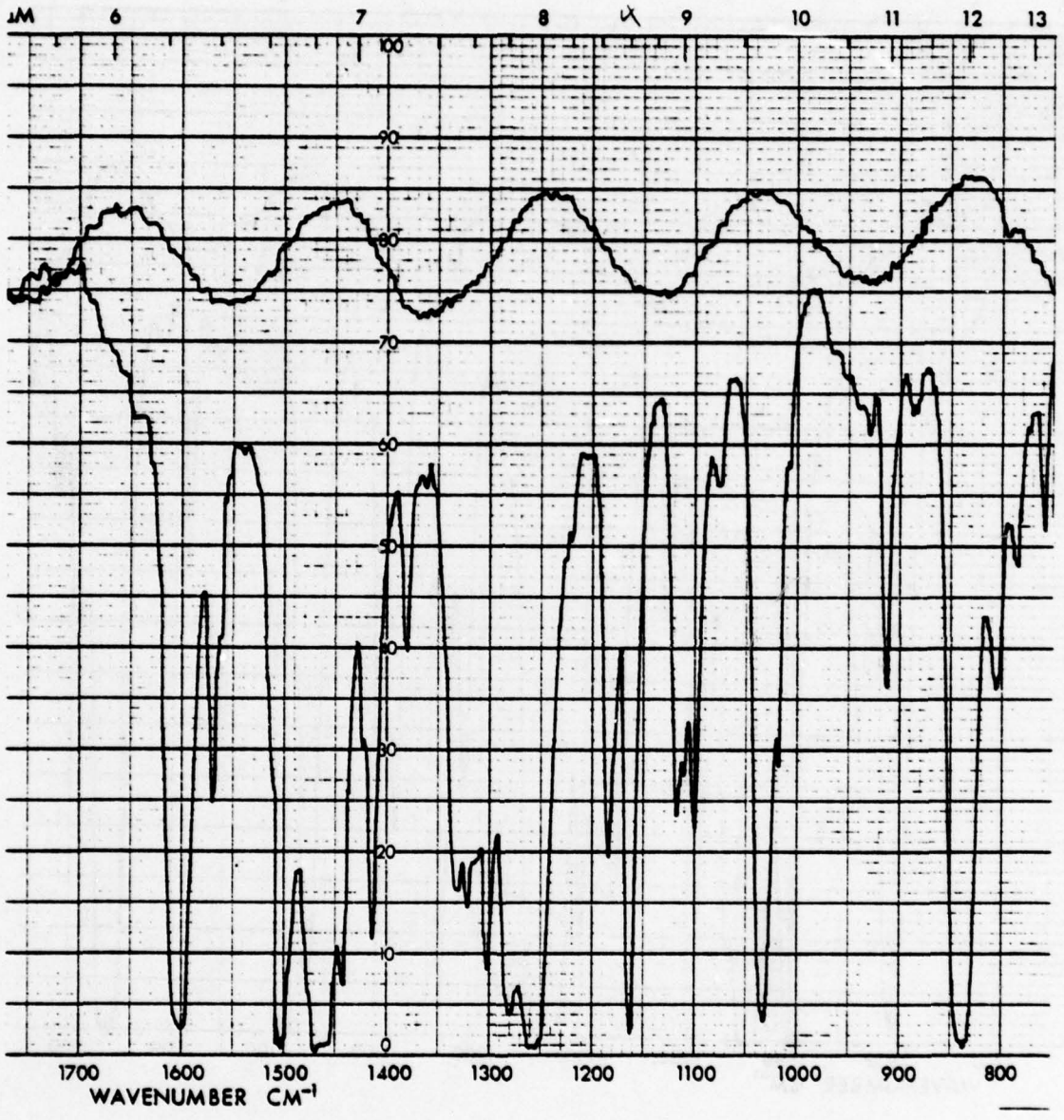

Fig. 4 Infrared (6-12μm) transmission of EM Licristal azoxy compound nematic phase 4 (25μm cell with NaCl windows).

SC5149.31FR

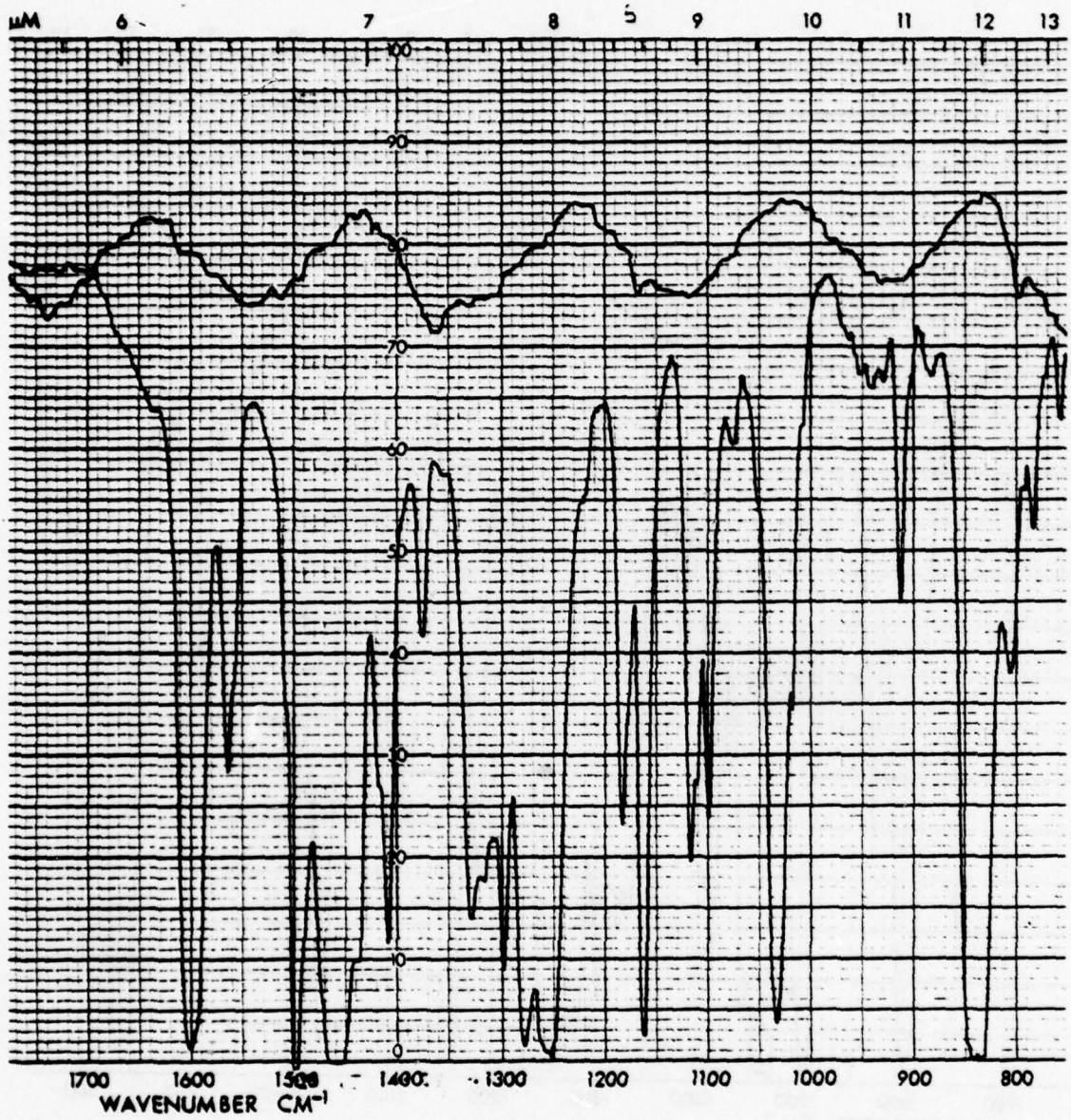

Fig. 5 Infrared (6-12μm) transmission of EM Licristal azoxy compound nematic phase 5A (25μm cell with NaCl windows).

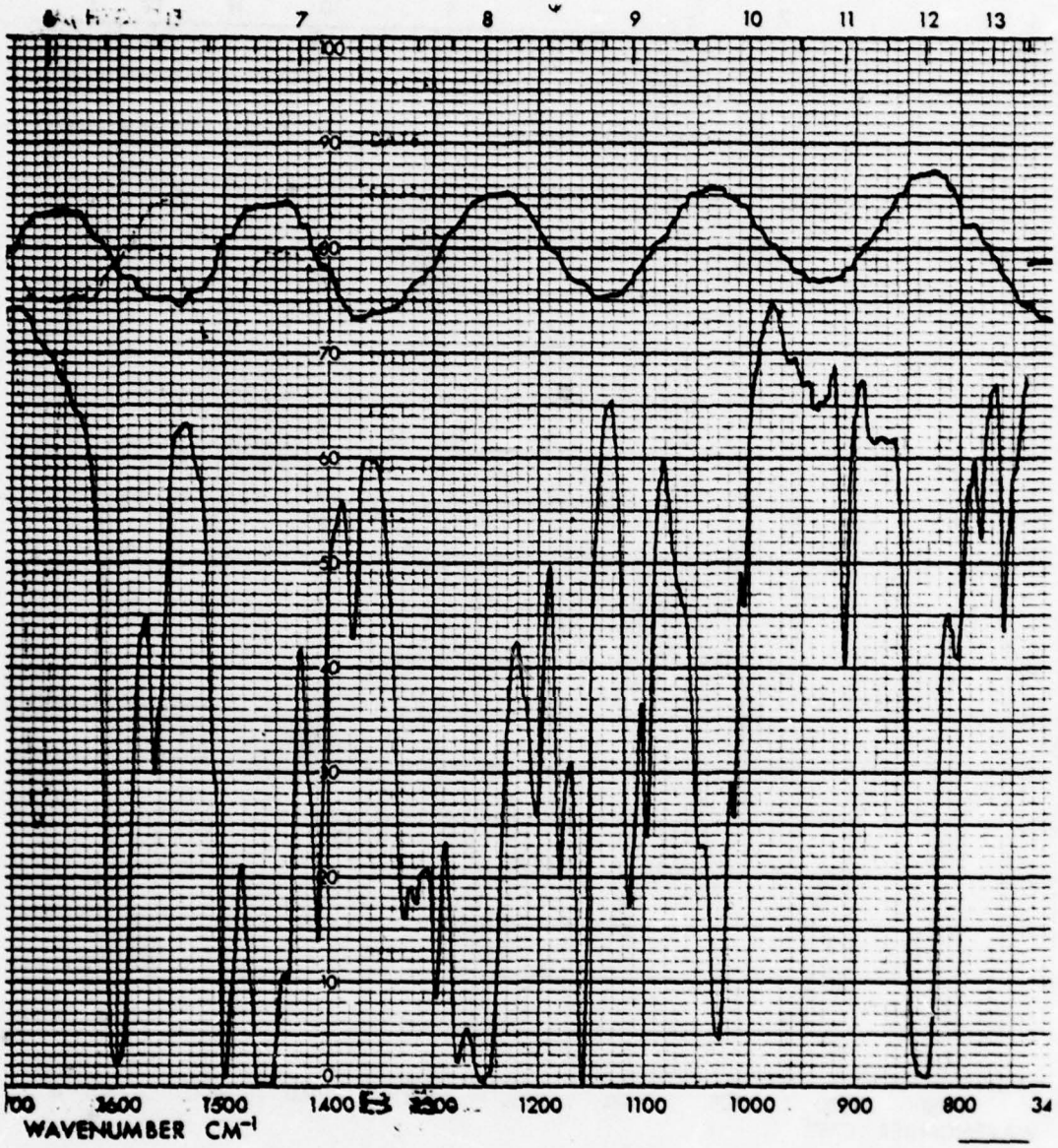

Fig. 6 Infrared (6-12μm) transmission of EM Licristal azoxy and ester mixture nematic phase 7A (25μm cell with NaCl windows).

SC5149.31FR

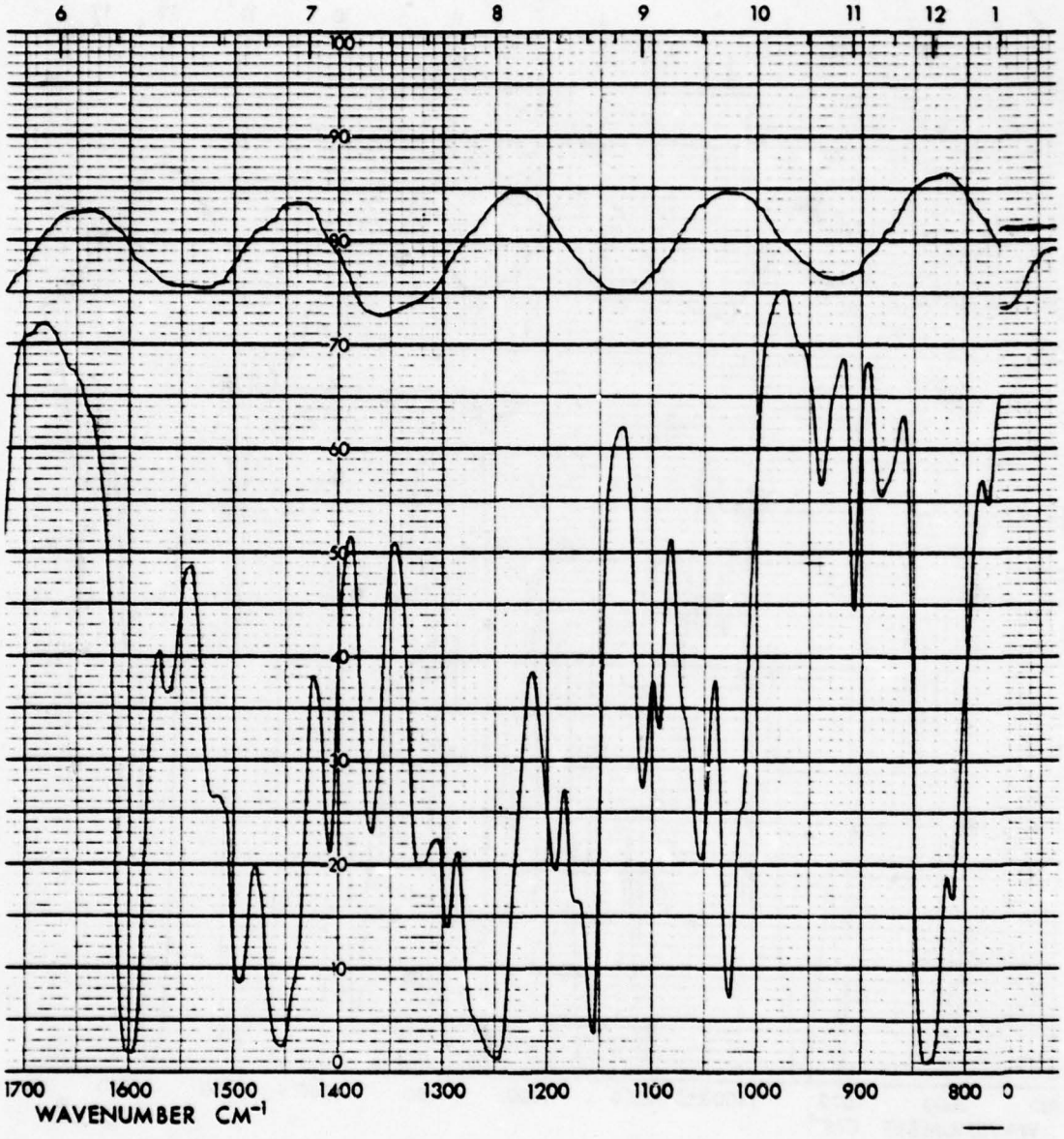

Fig. 7 Infrared (6-12μm) transmission of EM Licristal azoxy and ester mixture nematic phase 10 (25μm cell with NaCl windows).

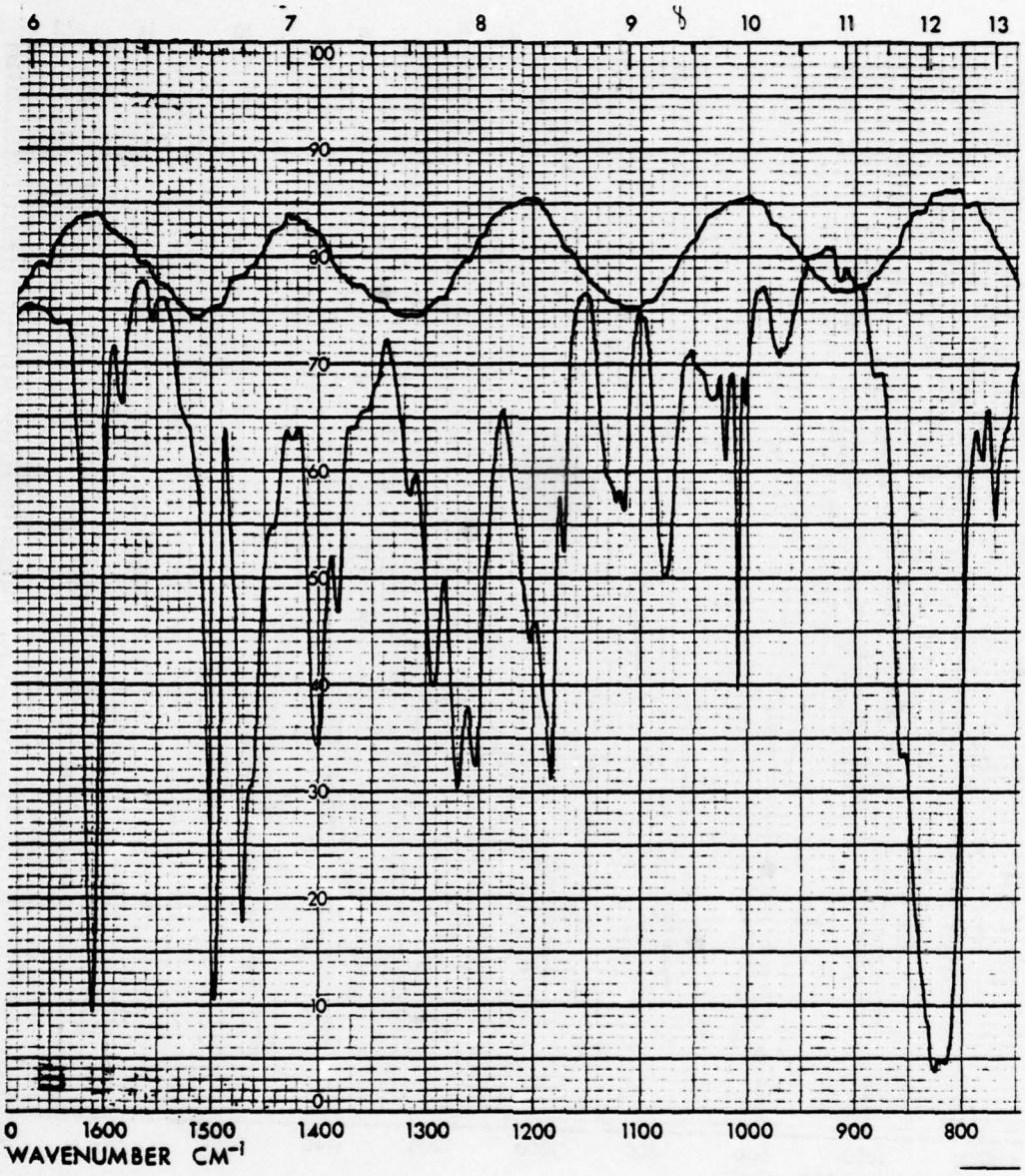

Fig. 8 Infrared (6-12μm) transmission of EM Licristal nematic phase 684 biphenyl mixture (25μm cell with NaCl windows).

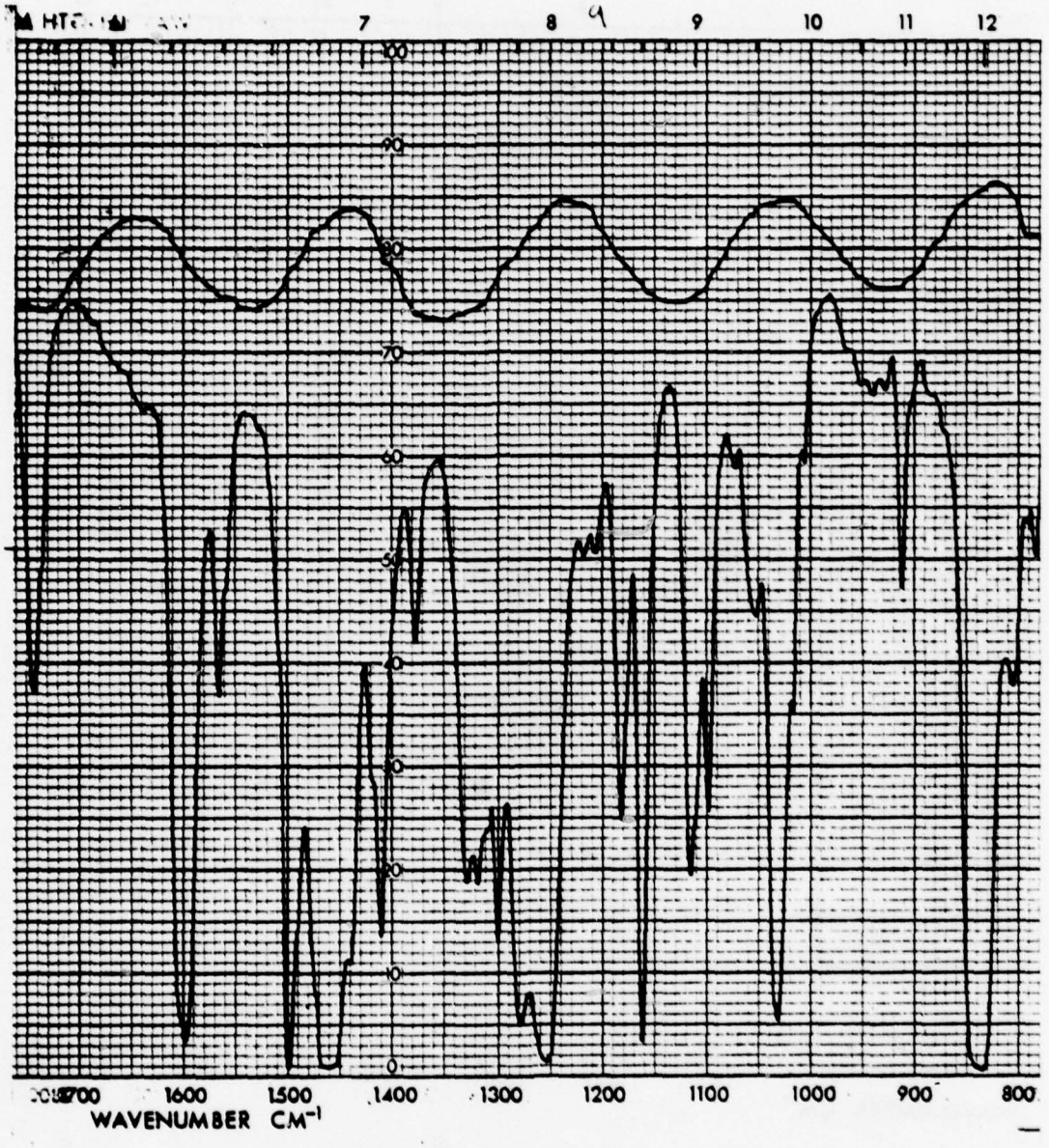

Fig. 9 Infrared (6-12μm) transmission of EM Licristal azoxy and biphenyl ester mixture nematic phase 997 (25μm cell with NaCl windows).

SC5149.31FR

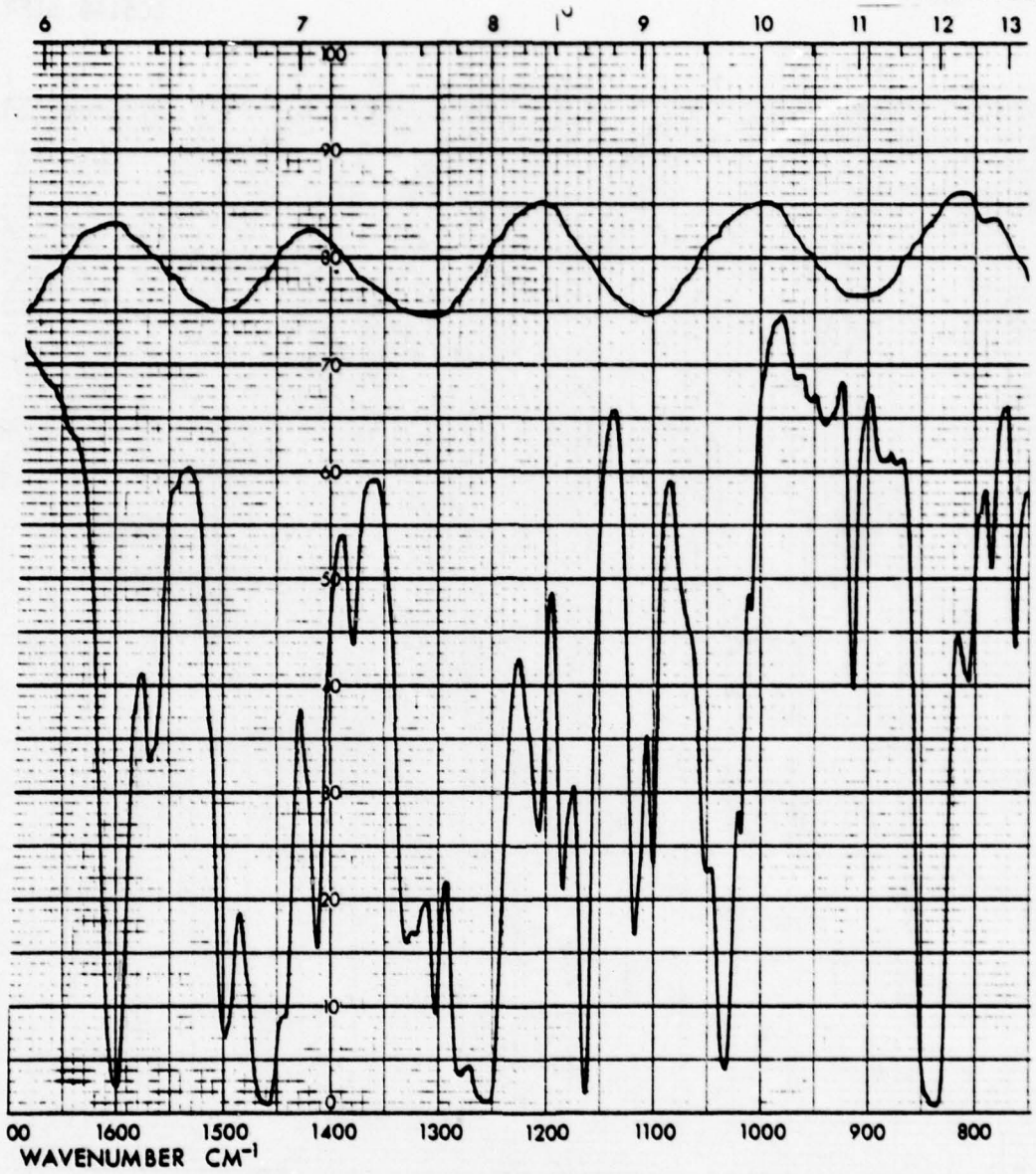

Fig. 10 Infrared (6-12μm) transmission of EM Licristal azoxy and ester mixture nematic phase ZLI-207 (25μm cell with NaCl windows).

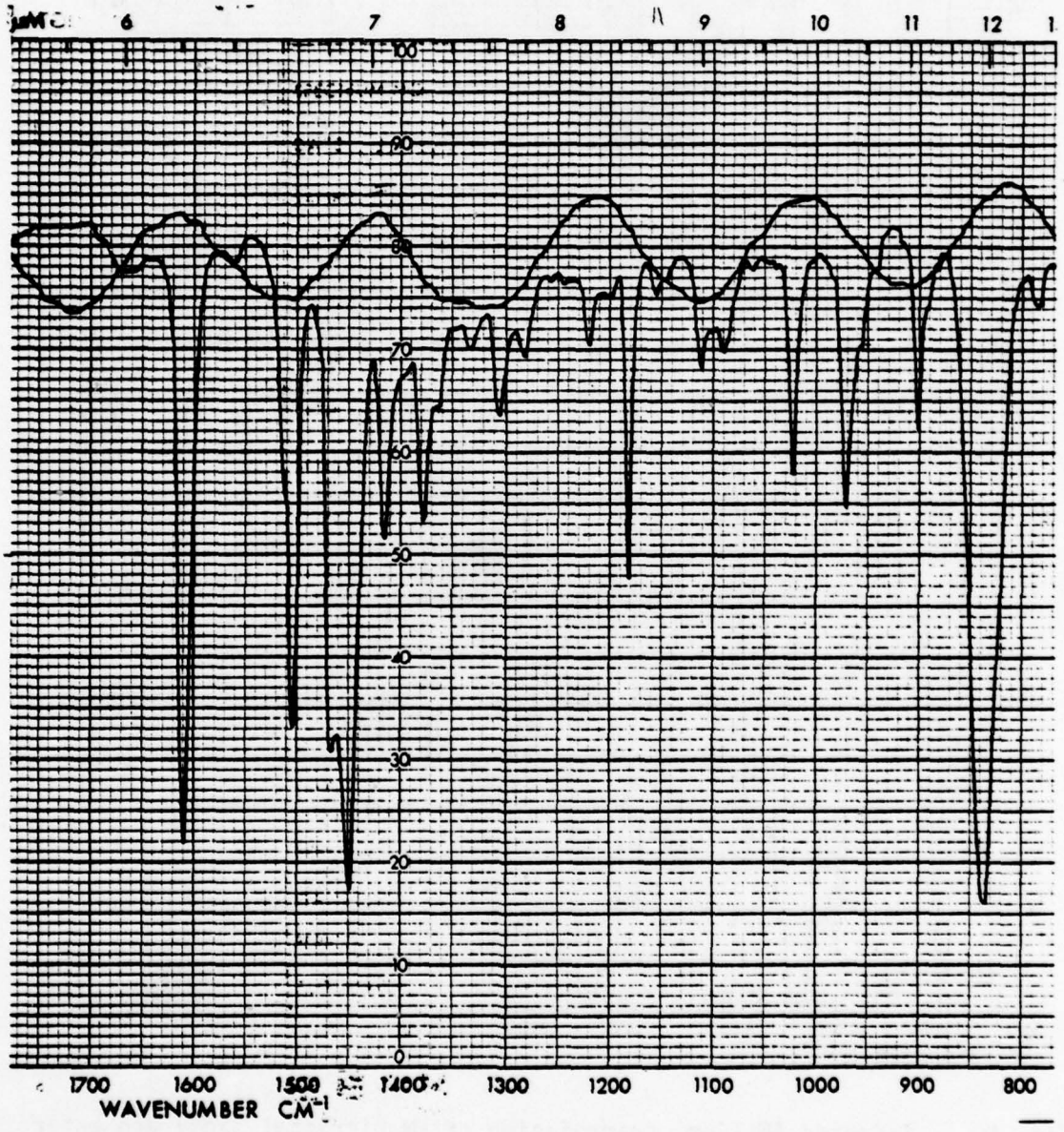

Fig. 11 Infrared (6-12μm) transmission of EM Licristal nematic phase ZLI-1083 (phenylcyclohexane mixture) (25μm cell with NaCl windows).

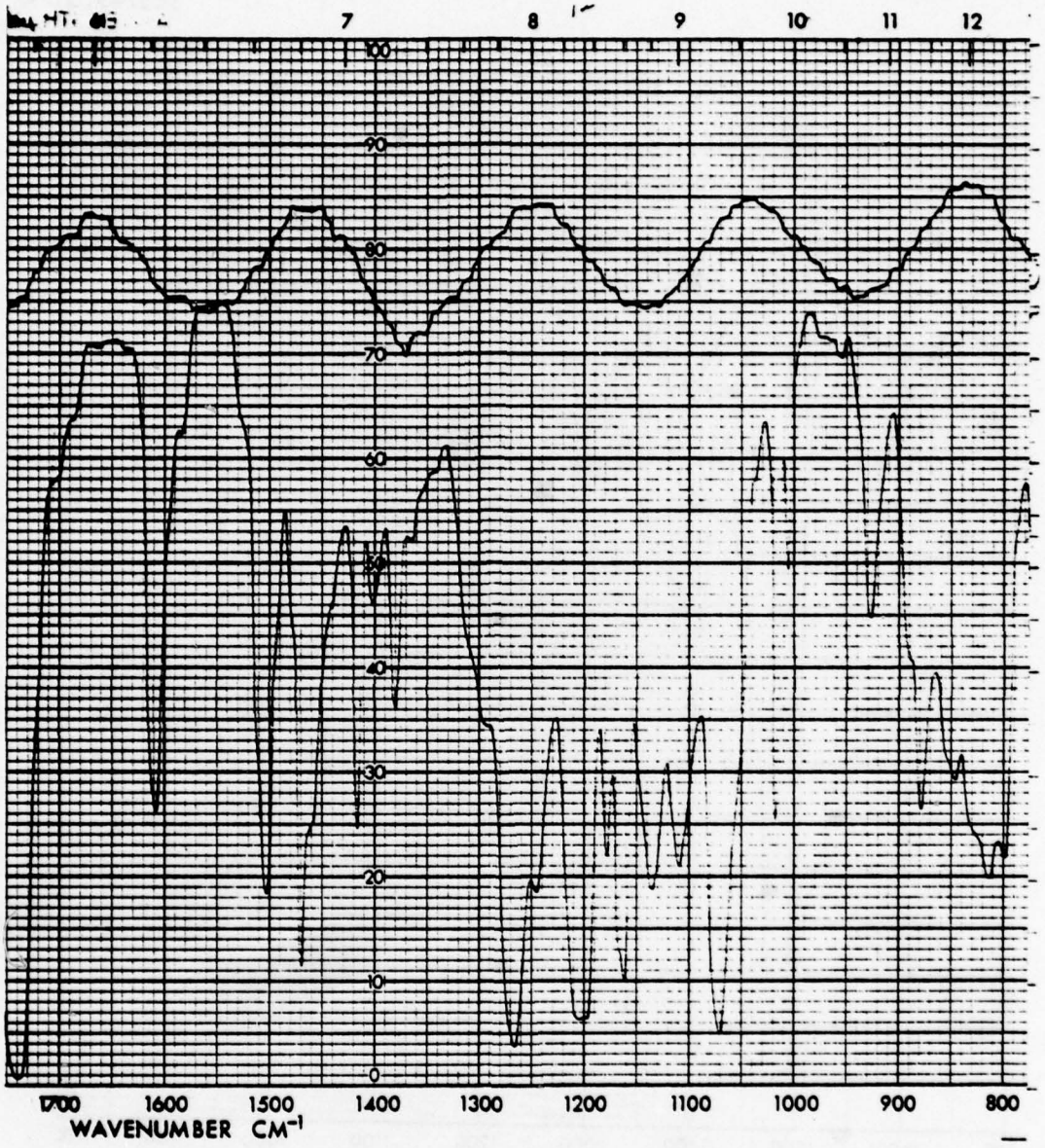

Fig. 12 Infrared (6-12μm) transmission of EM Licristal aromatic ester mixture nematic phase ZLI-1085 (25μm cell with NaCl windows).

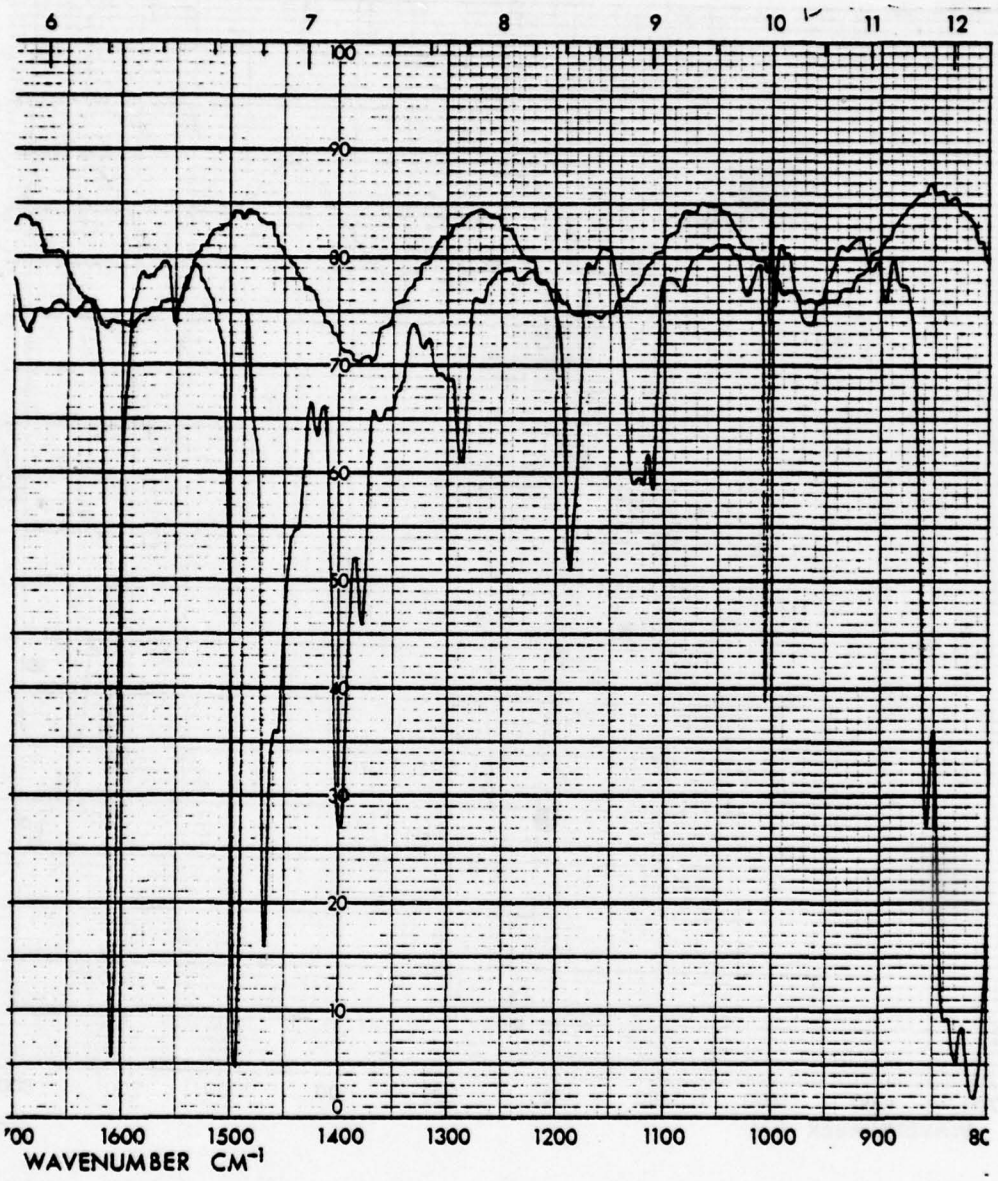

Fig. 13 Infrared (6-12μm) transmission of BDH 4-cyano-4'-n-pentyl biphenyl (25μm cell with NaCl windows).

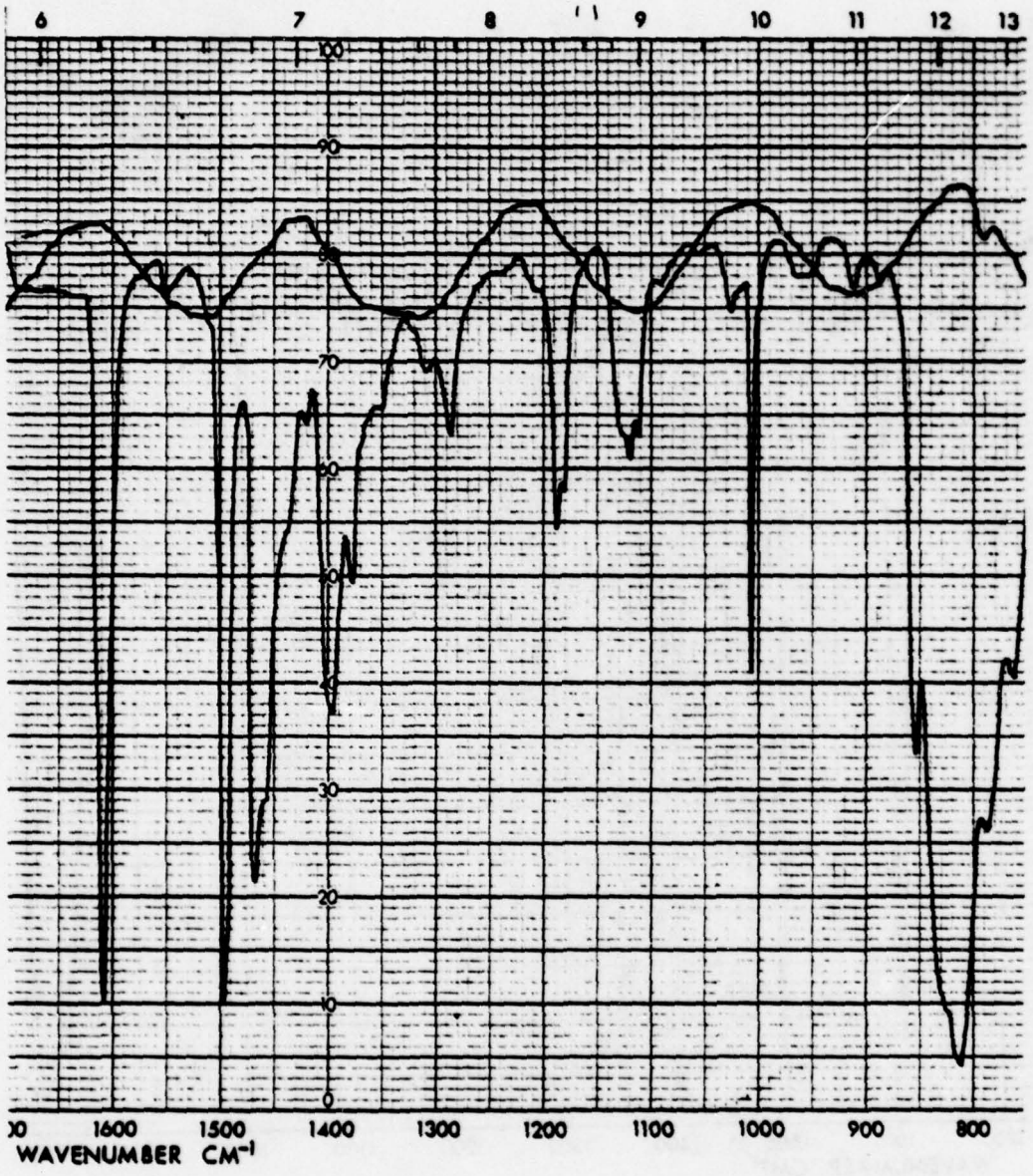

Fig. 14 Infrared (6-12μm) transmission of independent source 4-cyano-4'-heptyl biphenyl (25μm cell with NaCl windows).

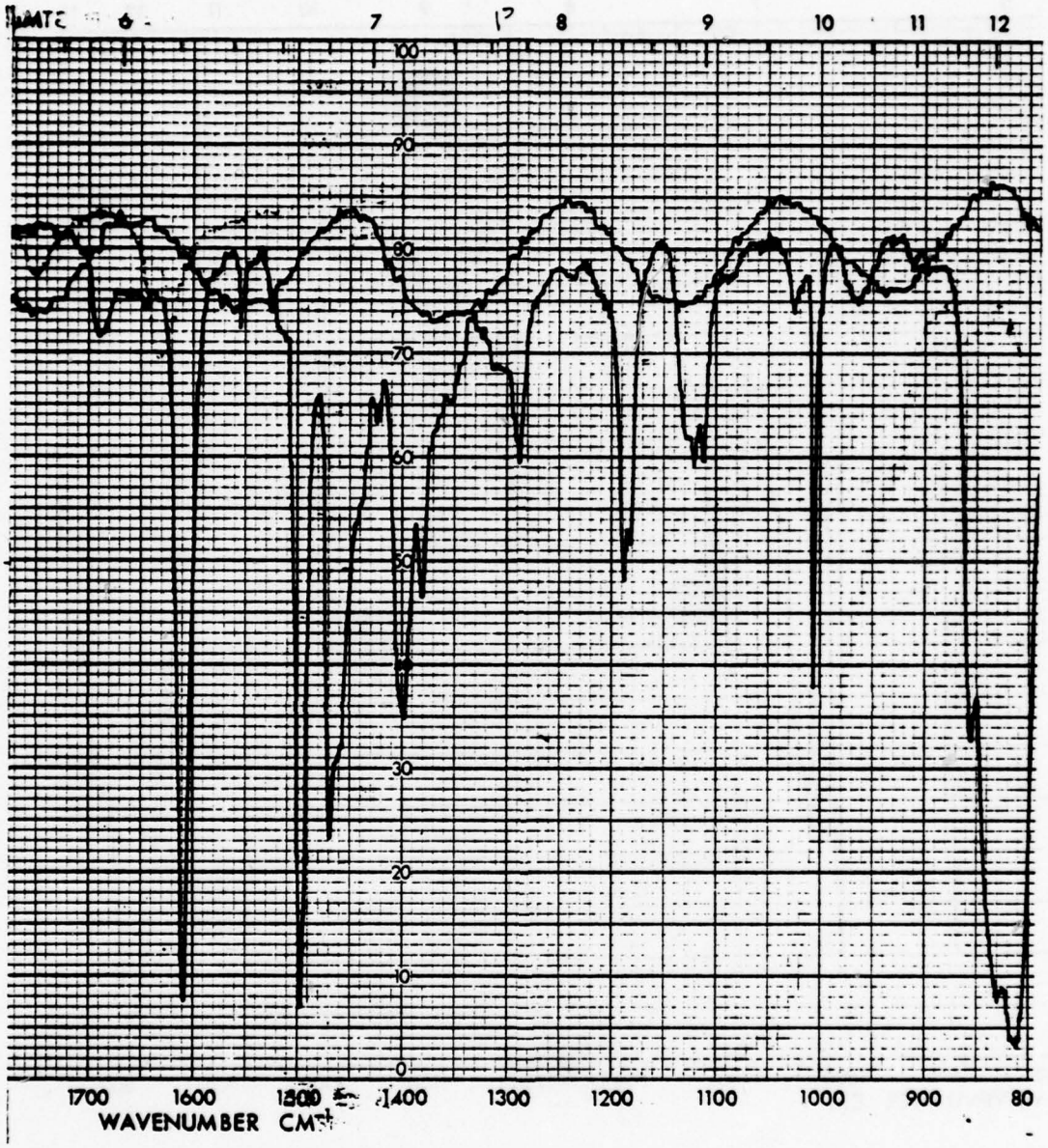

Fig. 15 Infrared (6-12μm) transmission of BDH biphenyl mixture E1 (25μm cell with NaCl windows).

SC5149.31FR

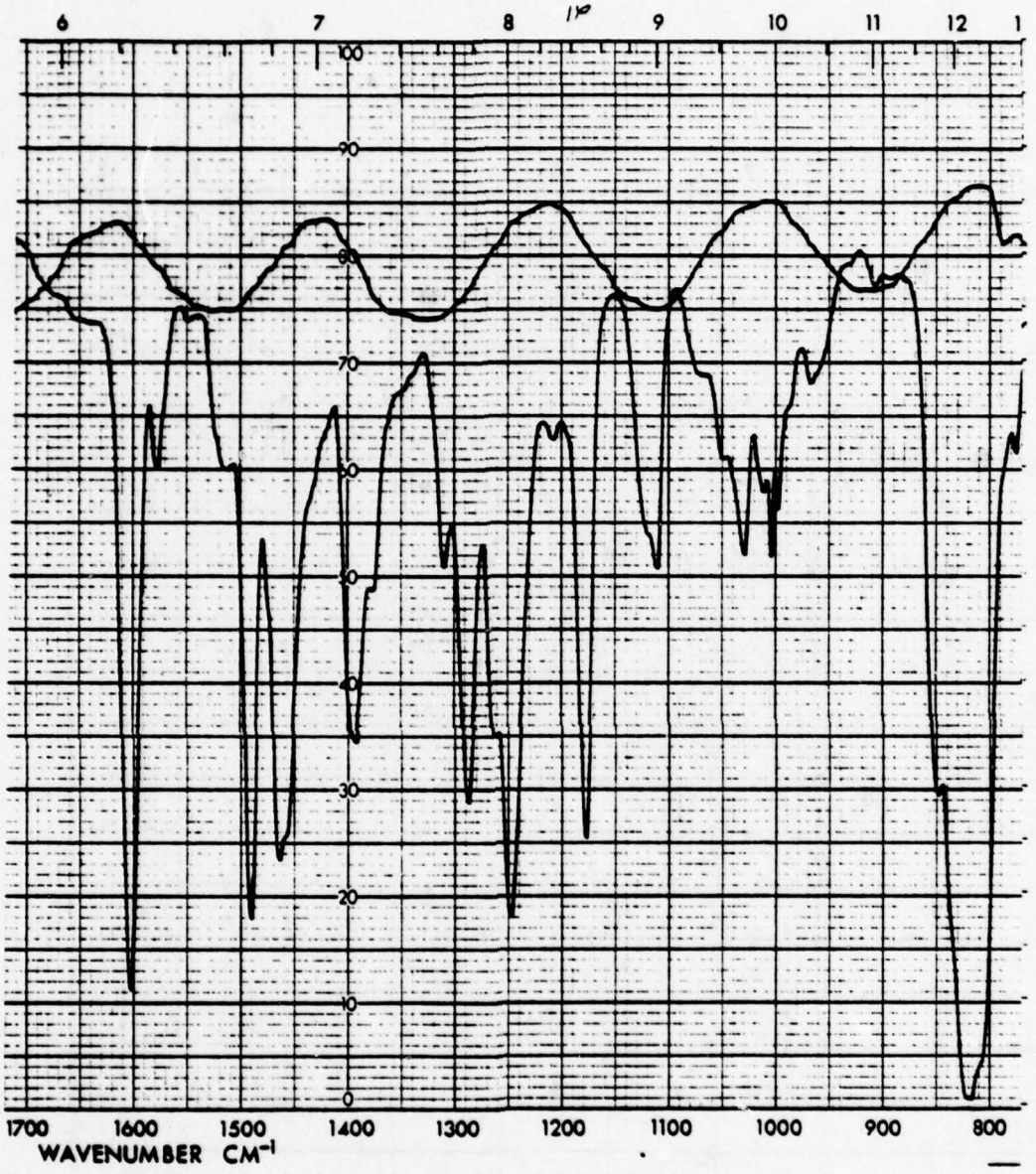

Fig. 16 Infrared (6-12μm) transmission of BDH biphenyl mixture E3 (25μm cell with NaCl windows).

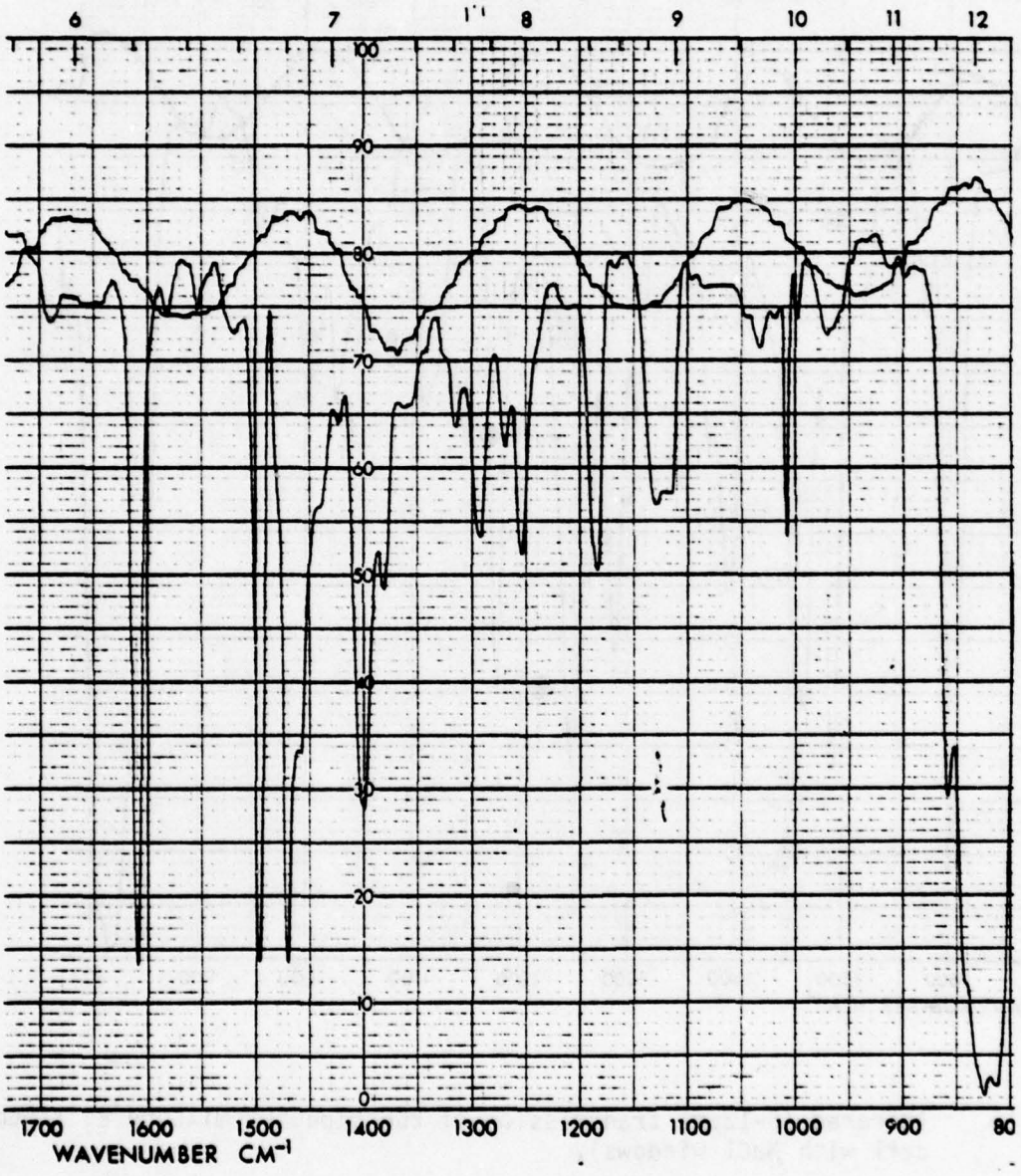

Fig. 17 Infrared (6-12μm) transmission of BDH biphenyl mixture E7 (25μm cell with NaCl windows).

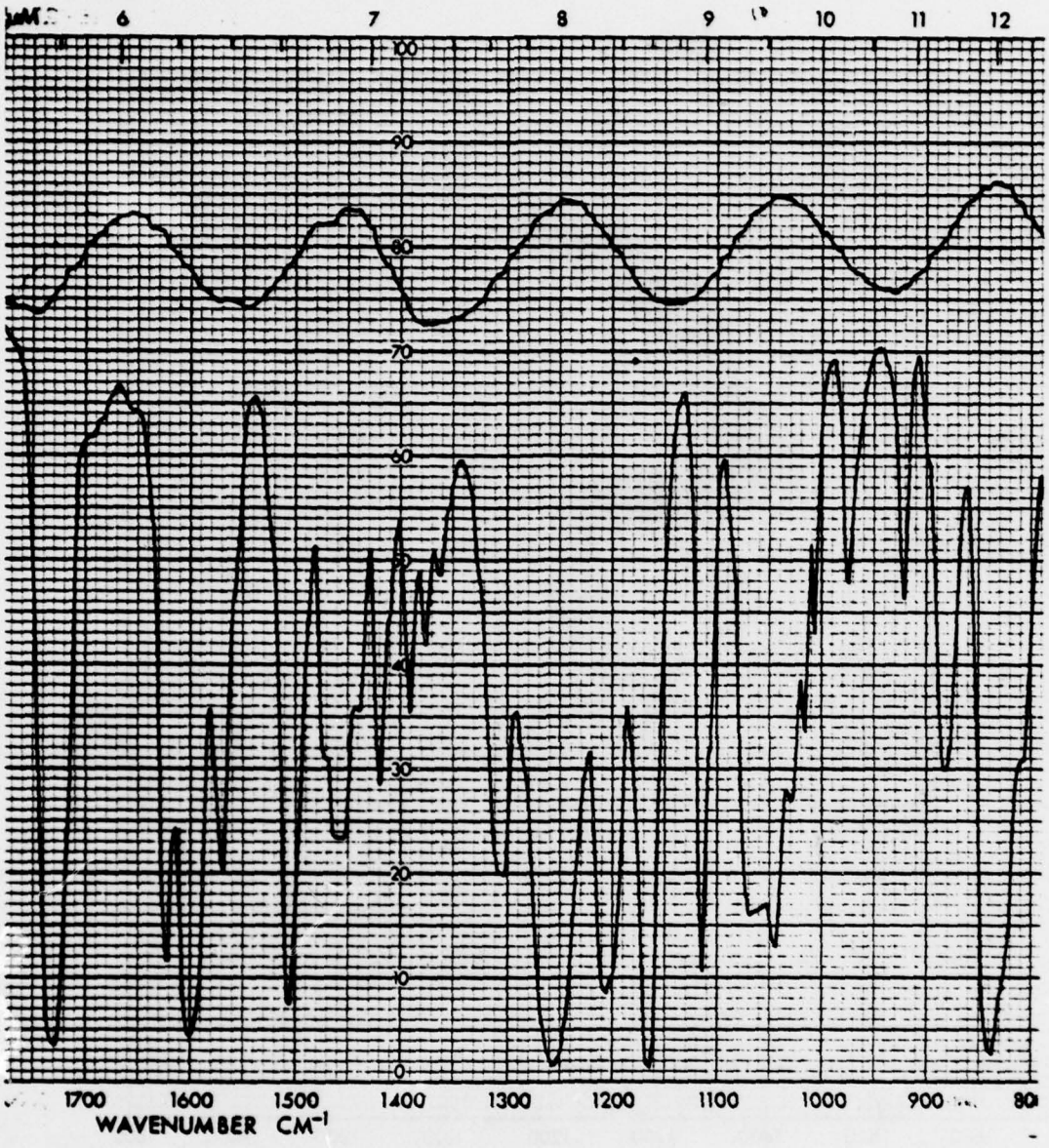

Fig. 18 Infrared (6-12μm) transmission of Atomergic Schiff's base and ester mixture LCNM 8212 (25μm cell with NaCl windows).

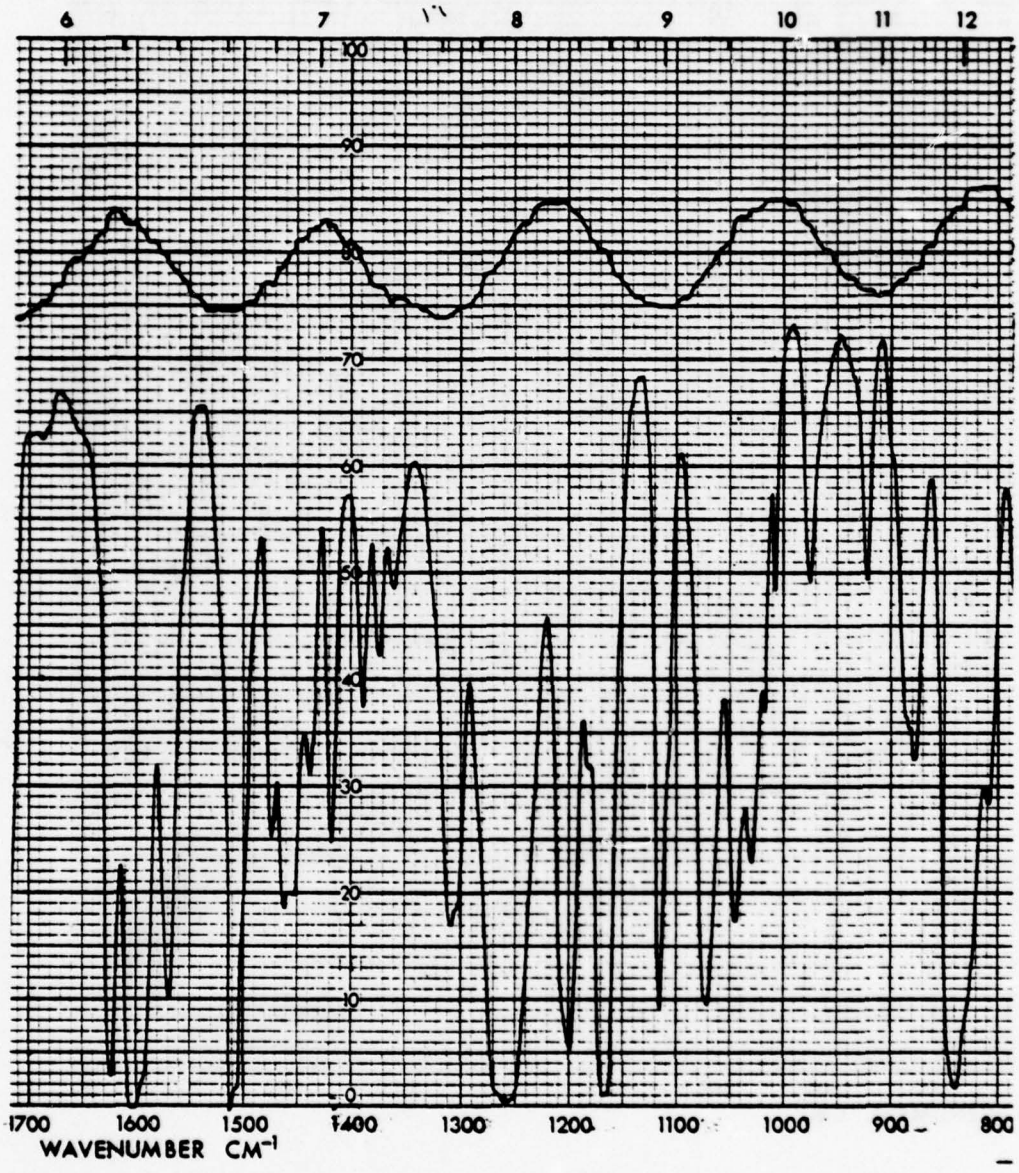

Fig. 19 Infrared (6-12μm) transmission of Atomergic Schiff's base and ester mixture LCNM 8243 (25μm cell with NaCl windows).

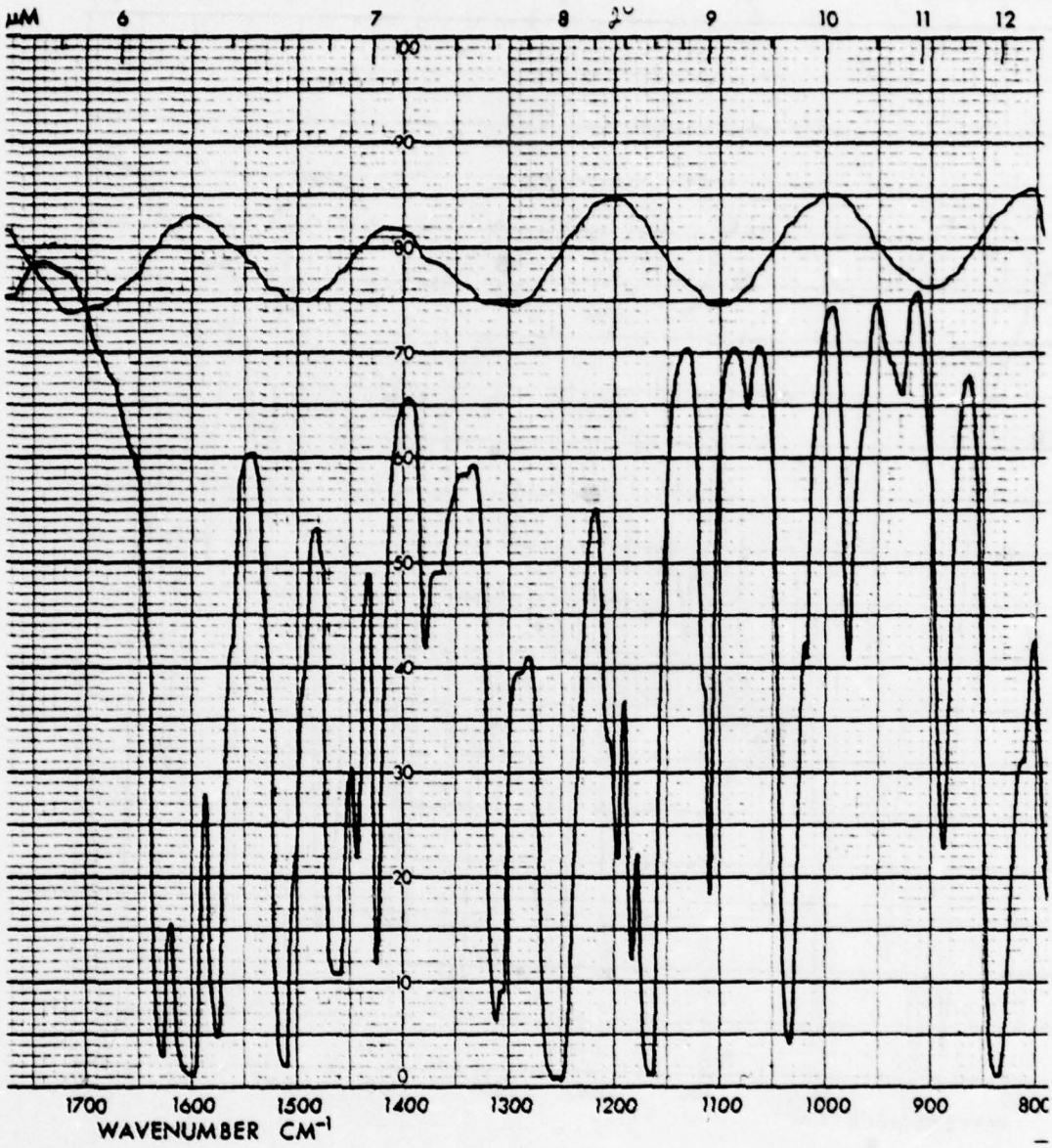

Fig. 20 Infrared (6-12μm) transmission of Eastman MBBA (Schiff's base) (25μm cell with NaCl windows).

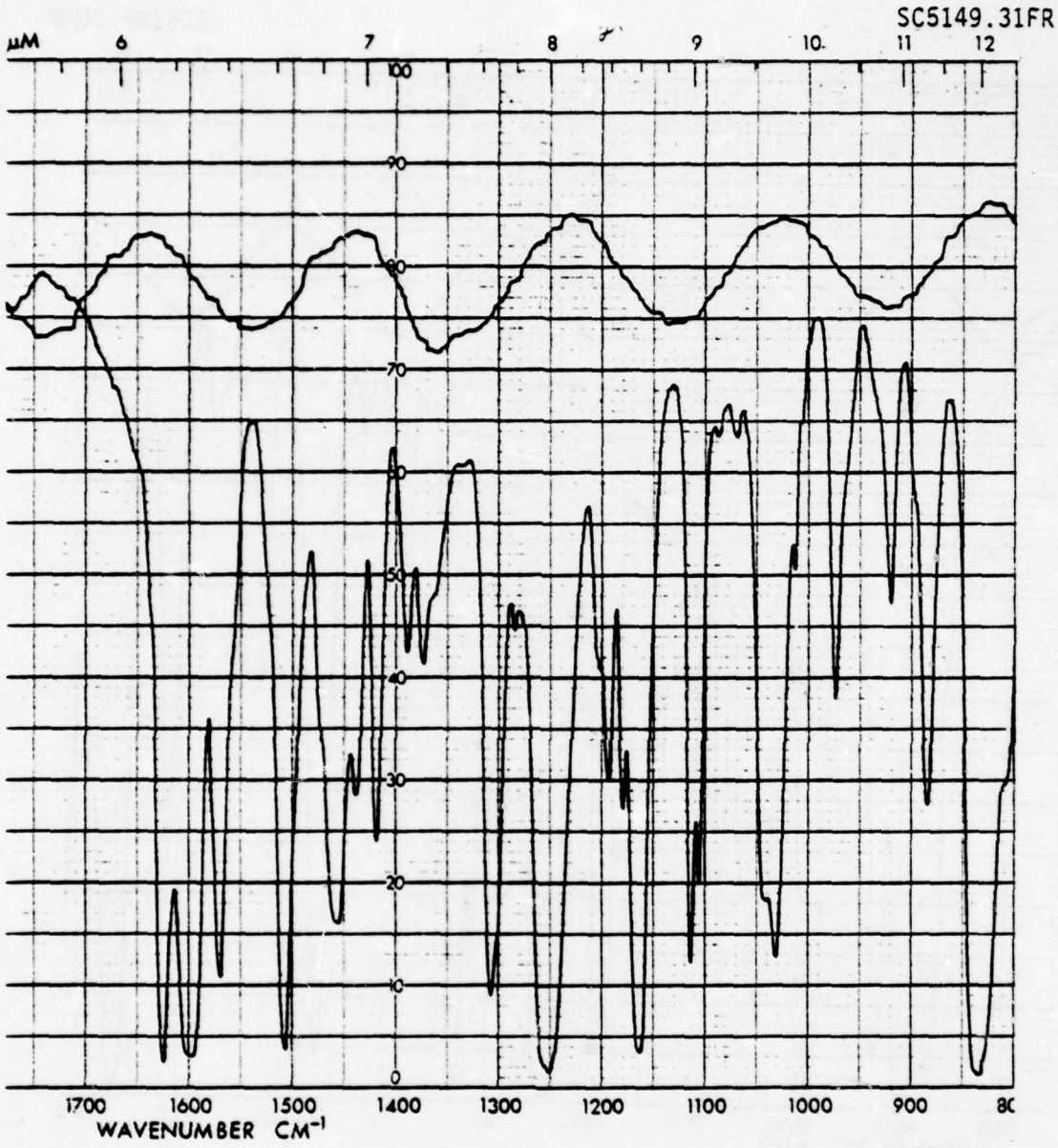

Fig. 21 Infrared (6-12μm) transmission of independent source TDS-21 (25μm cell with NaCl windows).

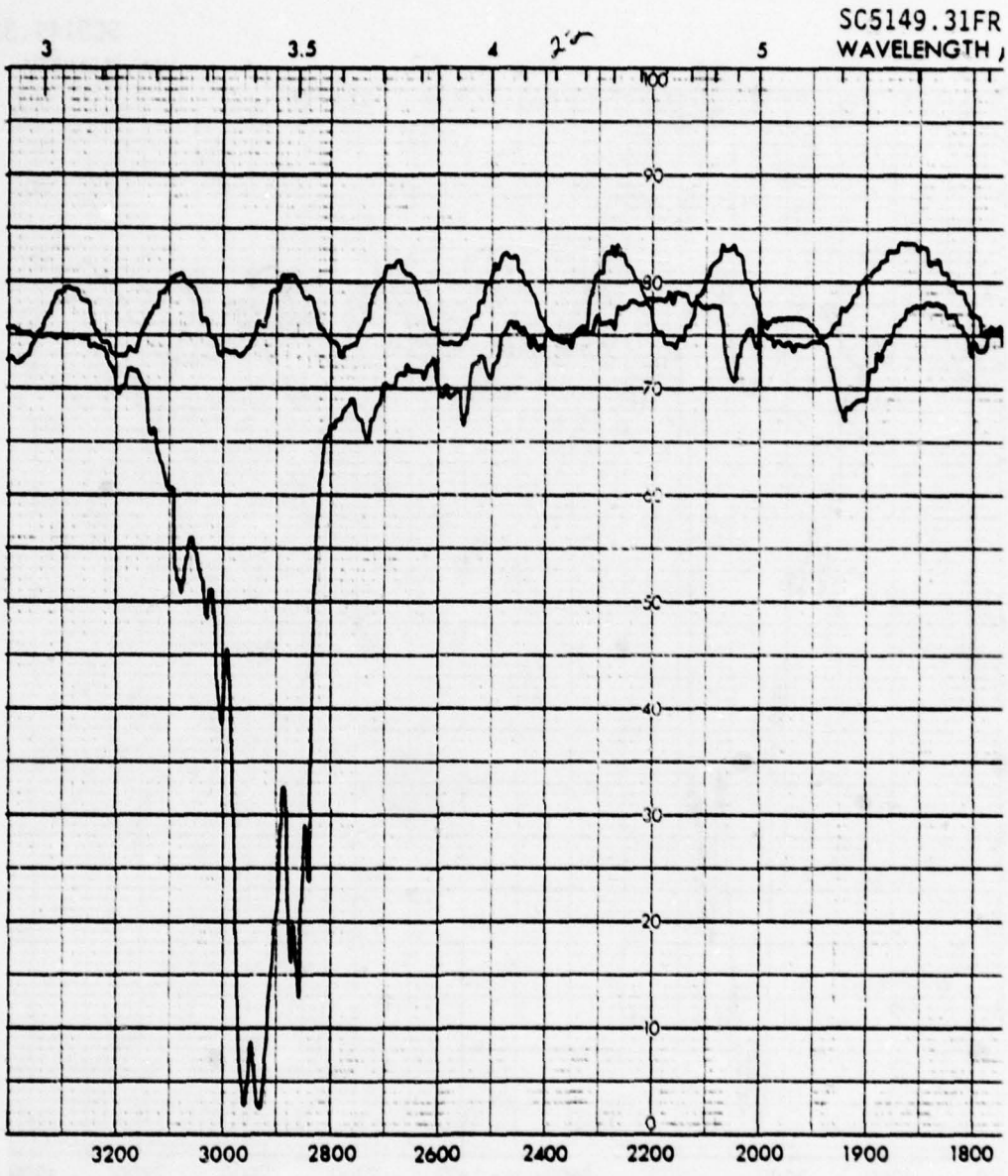

Fig. 22 Infrared (3-5μm) transmission of EM Licristal phase 4 (25μm cell with NaCl windows).

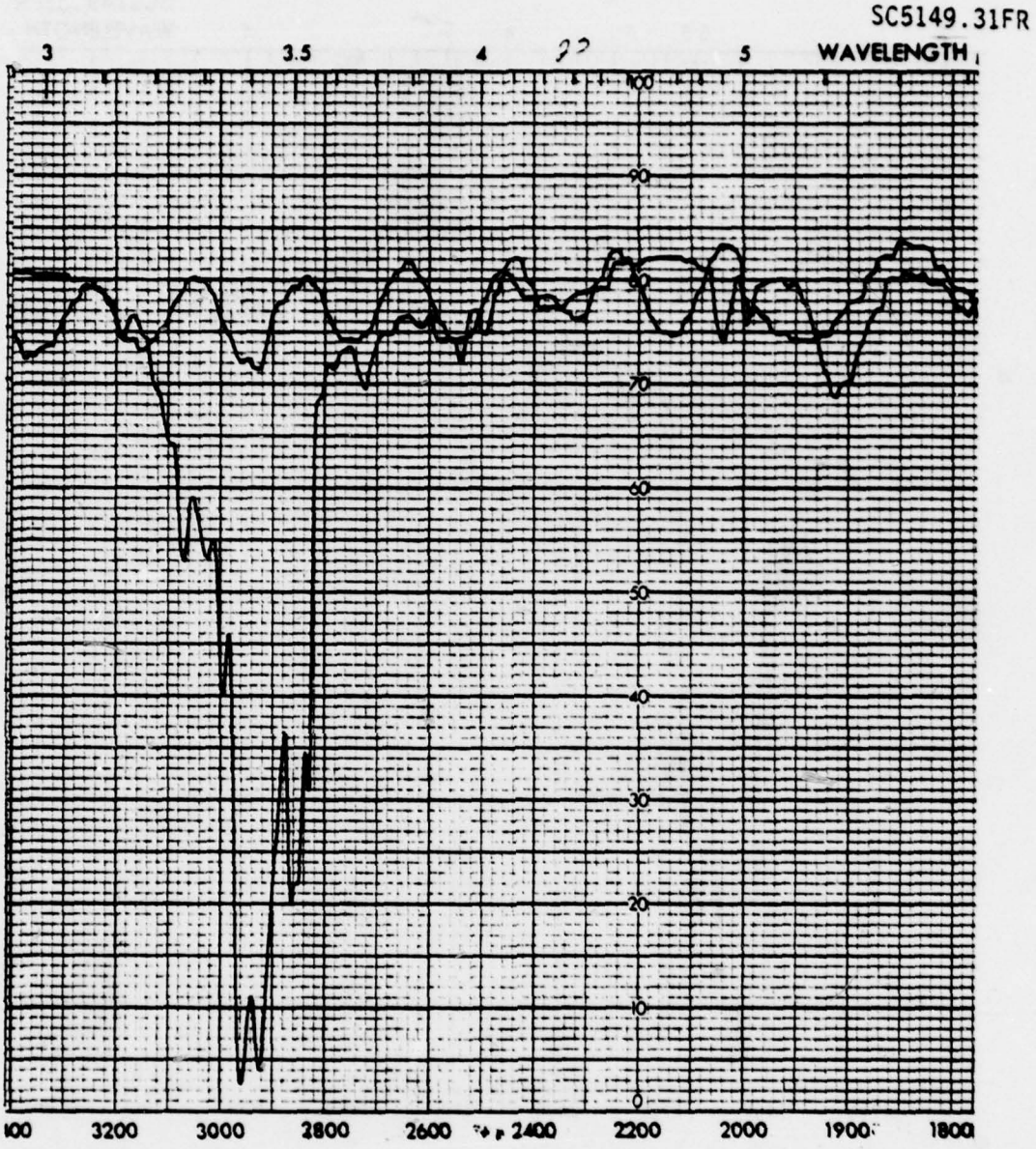

Fig. 23 Infrared (3-5μm) transmission of EM Licristal phase 5A (25μm cell with NaCl windows).

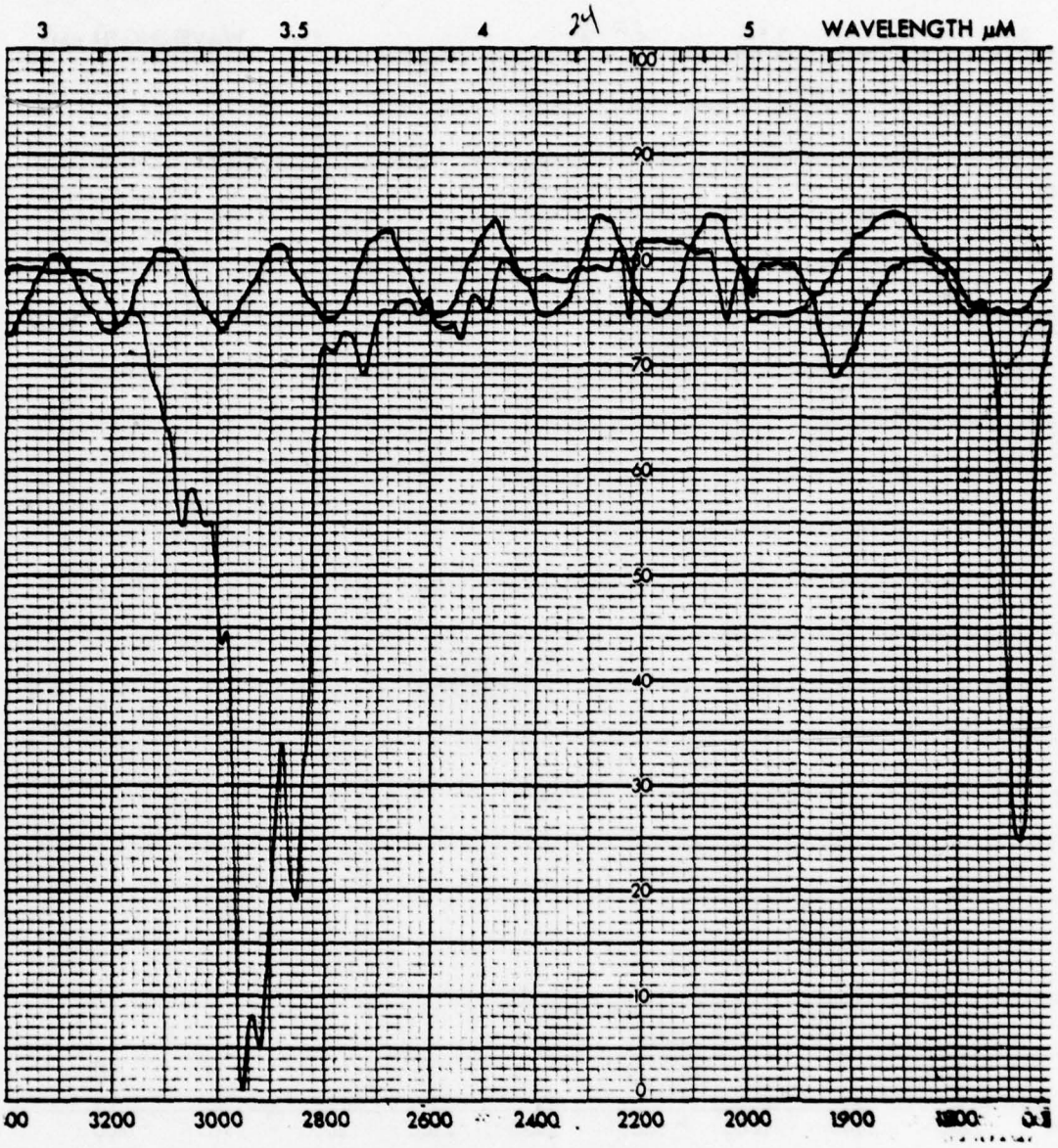

Fig. 24 Infrared (3-5μm) transmission of EM Licristal phase 7A (25μm cell with NaCl windows).

SC5149.31FR

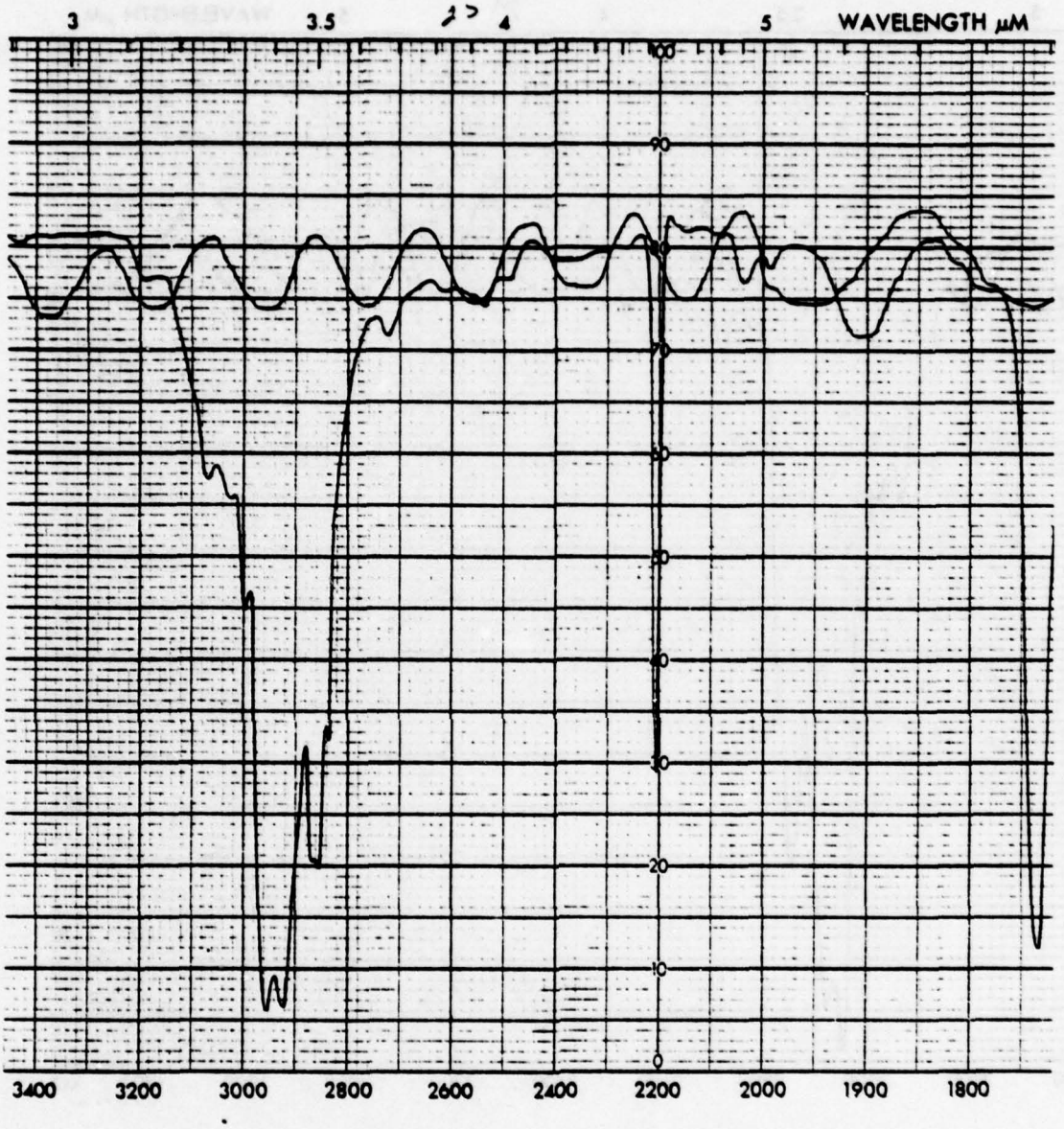

Fig. 25 Infrared (3-5μm) transmission of EM Licristal phase 10 (25μm cell with NaCl windows).

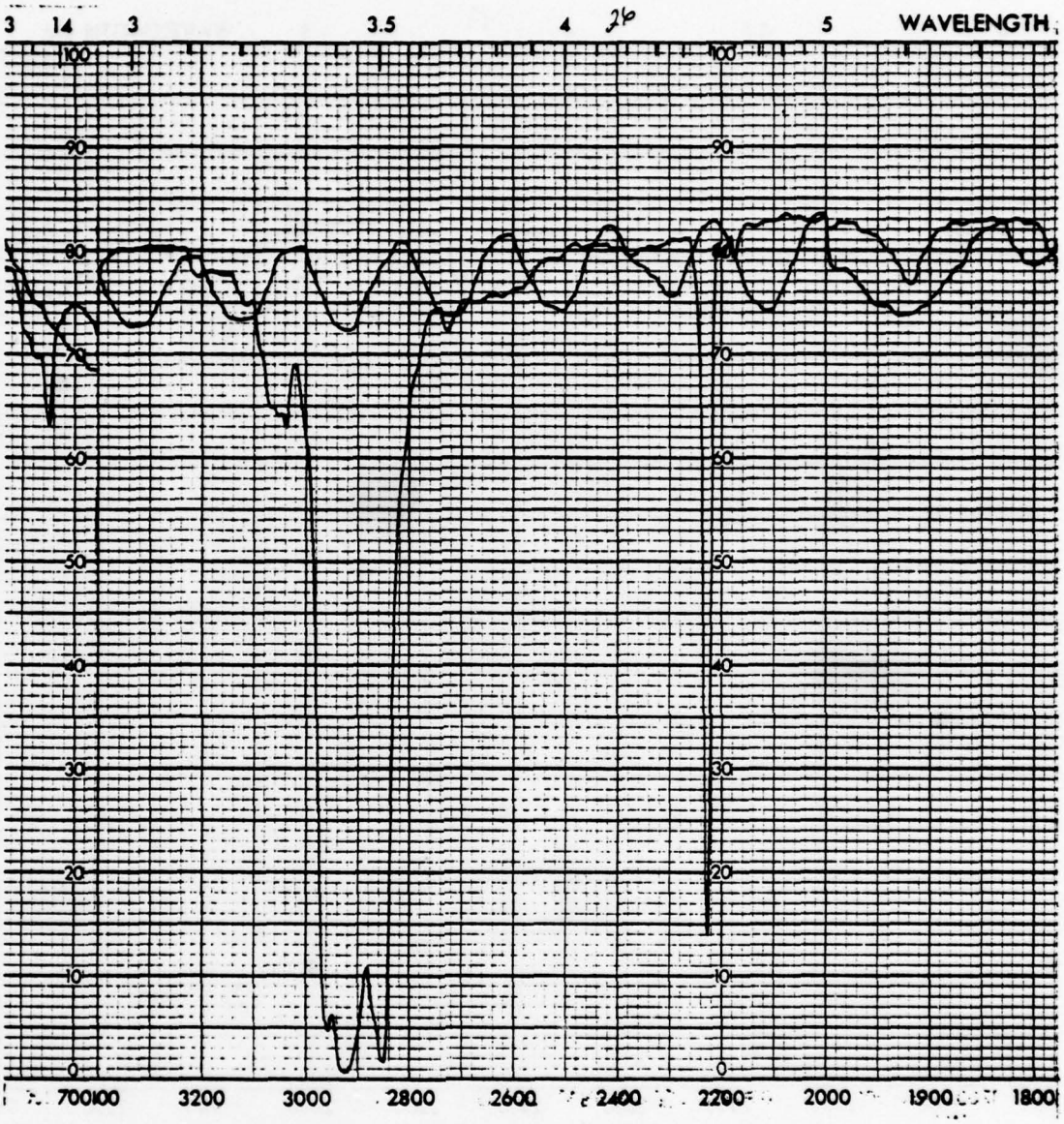

Fig. 26 Infrared (3-5μm) transmission of EM ZLI-1083 phenycyclohexane mixture (25μm cell with NaCl windows).

SC5149.31FR

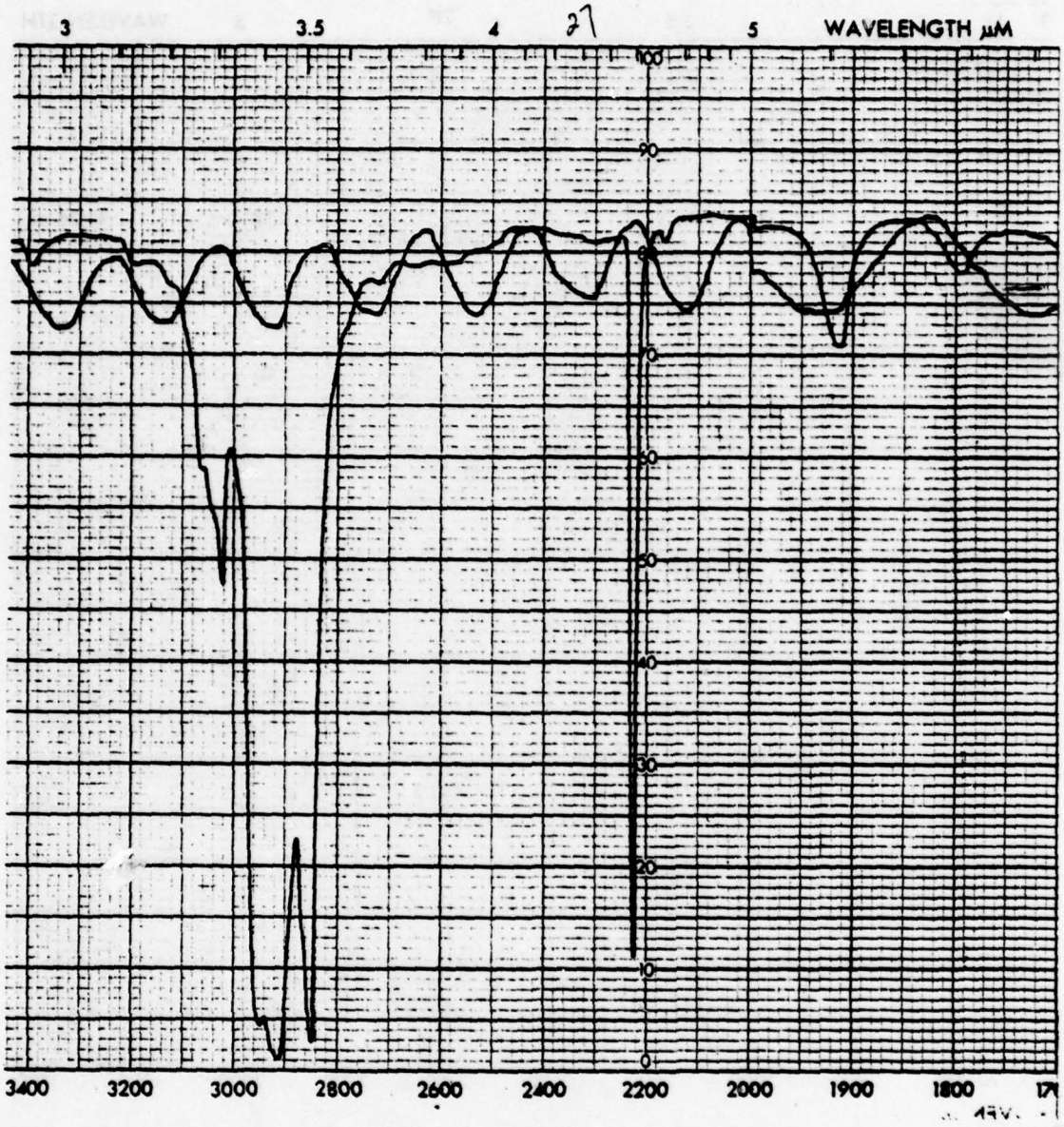

Fig. 27 Infrared (3-5μm) transmission of BDH 4-cyano-4'-n-pentyl biphenyl (25μm cell with NaCl windows).

SC5149.31FR

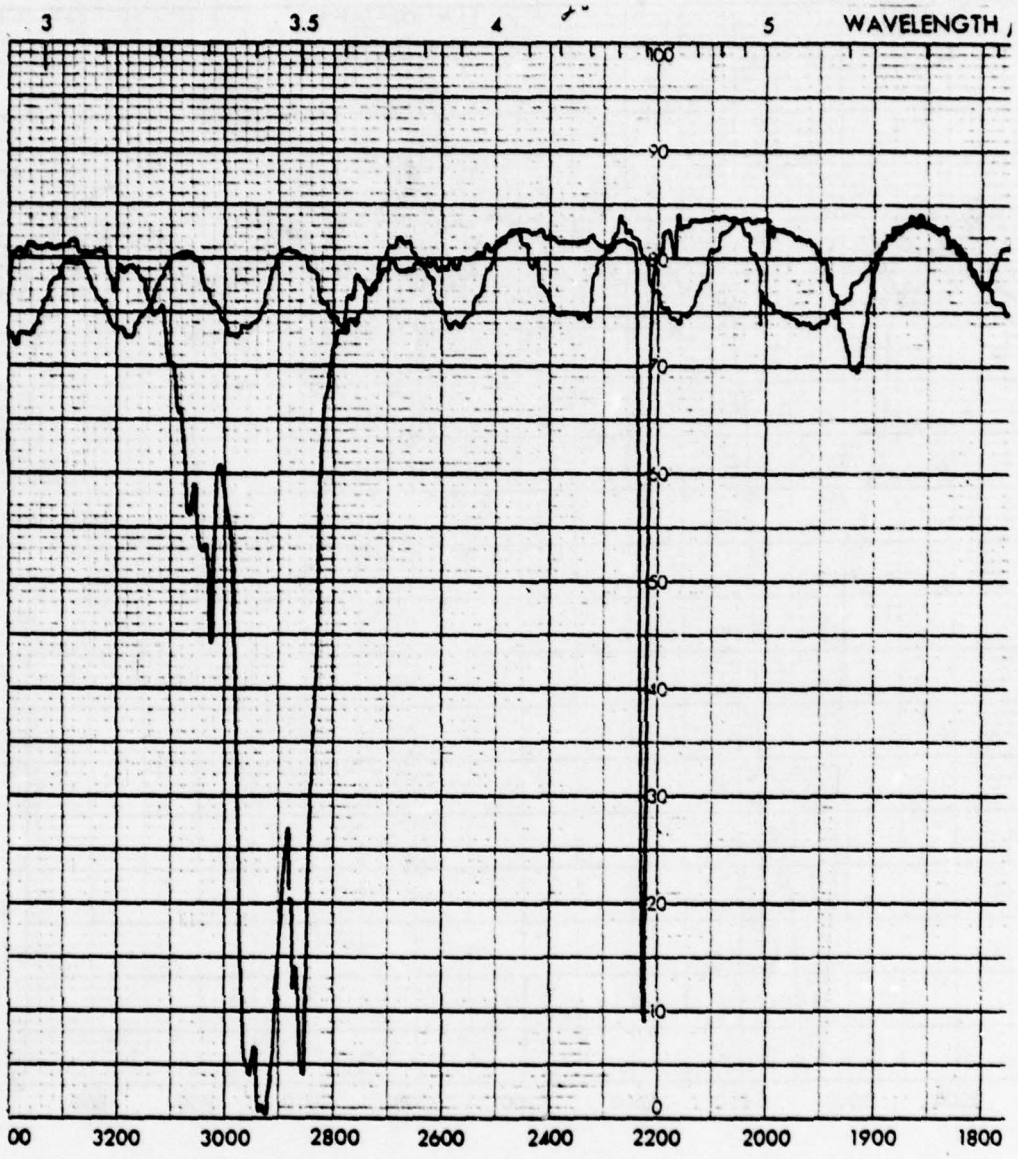

Fig. 28 Infrared (3-5μm) transmission of BDH E-1 biphenyl mixture (25μm cell with NaCl windows).

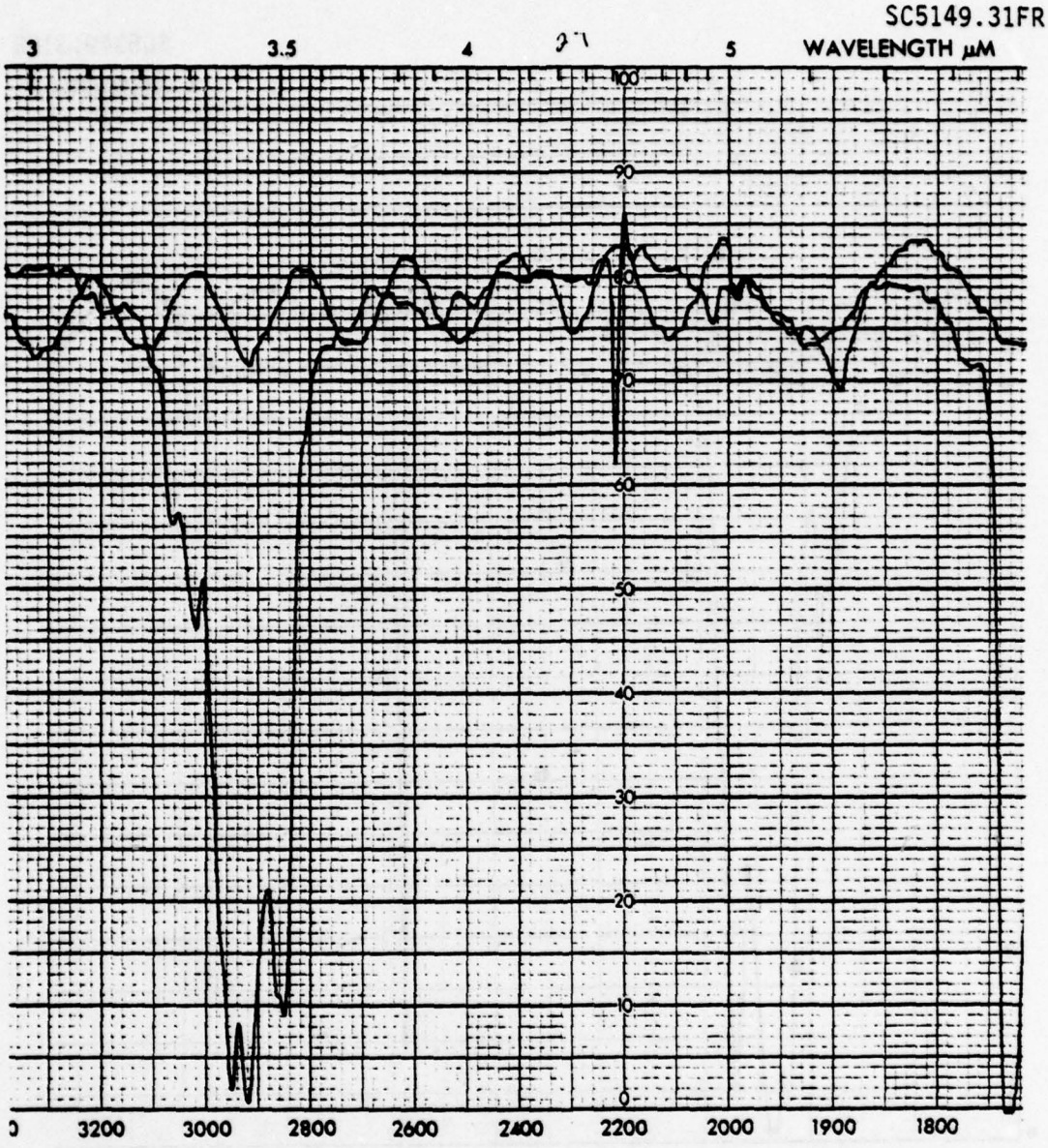

Fig. 29 Infrared (3-5μm) transmission of Atomergic LCNM 8243 (25μm cell with NaCl windows).

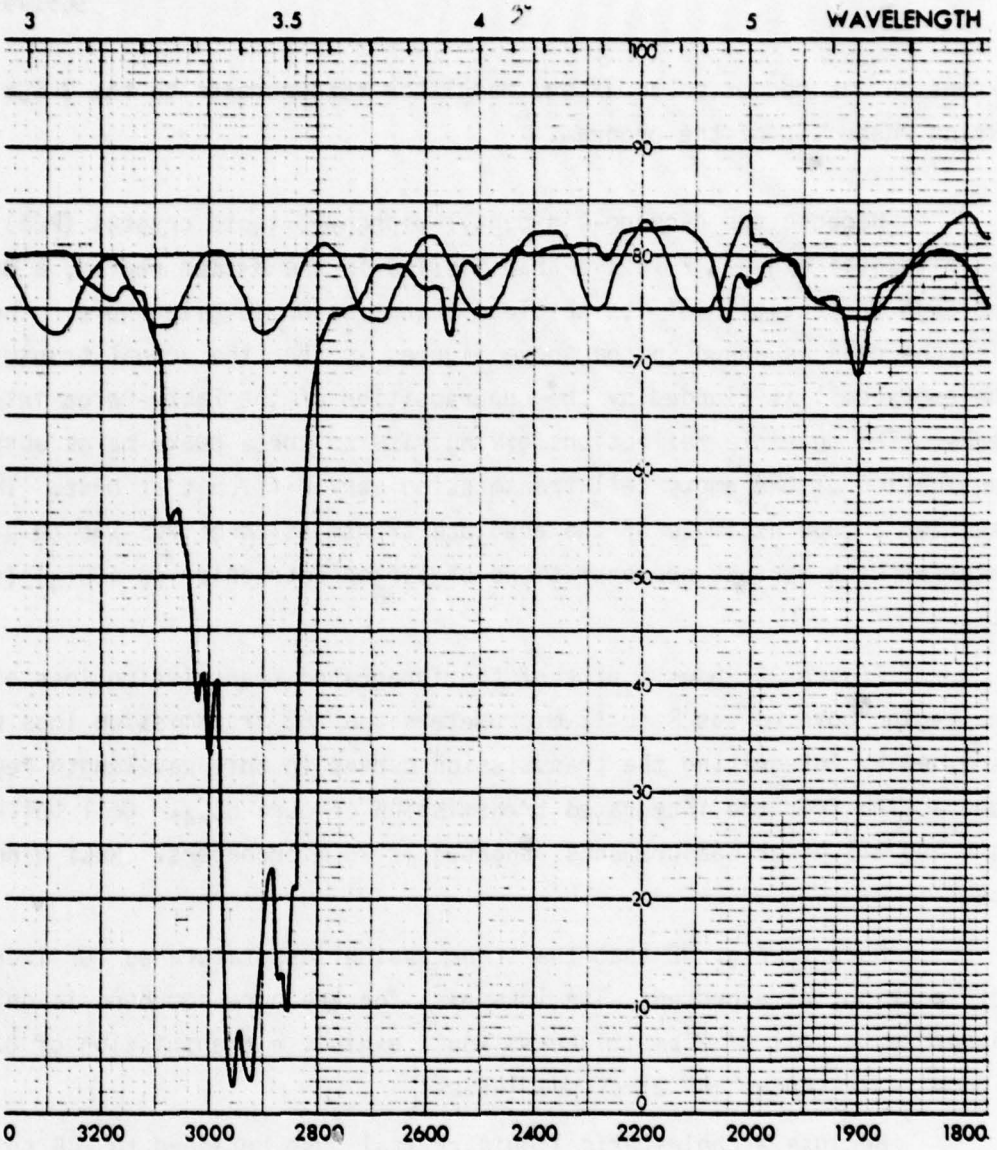

Fig. 30 Infrared (3-5μm) transmission of Eastman MBBA (25μm cell with NaCl windows).

extension was requested to extend modulator measurements to the 3-5μm region during Phase III of the program.

Because the 4-cyano-4'n-pentyl biphenyl liquid crystal (PCB) exhibited the highest relative transmission in the 8-12μm region, a more thorough presentation of its absolute transmission is given here. The problem with the data as shown in the above figures is that the actual transmission of the empty cell is clouded by the superposition of the Fabry-Perot interference peaks. The multiple reflections giving rise to these peaks makes absolute determination of the empty cell transmission very difficult at best. The method used for a good estimate of the absolute transmission of PCB was to dilute the material with various concentrations of carbon tetrachloride (CCl_4) (see Fig. 31).

Figure 32 shows a plot of the integrated transmission loss of PCB. The region covered was 8 to 12 micrometers and the transmission loss was determined by integrating the transmission curves in this wavelength region and subtracting from the integrated transmission of pure CCL_4. Cell thickness for this and all other measurements reported is 25 micrometers. NaCl windows were used.

Note in Fig. 32 that the transmission loss saturates for increasing mol fraction, as expected. The loss even for the pure compound is only 13%. Therefore, a cell of 25μm thickness would exhibit a transmission of 87%, less window reflectances and electrode losses.

Because a cholesteric liquid crystal must be added to PCB to make a cholesteric mixture suitable for the phase change effect, Fig. 33 shows a plot of transmission loss for one particular additive, cholesteryl chloride, using the same method as described above for PCB. For this material, the solubility limit in CCl_4 is about .24 mol fraction at 22°C. Here, the loss is only 9.5%. Since most of the mixtures utilized in the literature for cholesteric-nematic phase change studies utilize less than 10% of the cholesteric phase material, cholesteryl chloride will add negligibly to transmission loss.

Figure 34 shows the transmission spectrum of cholesteryl chloride

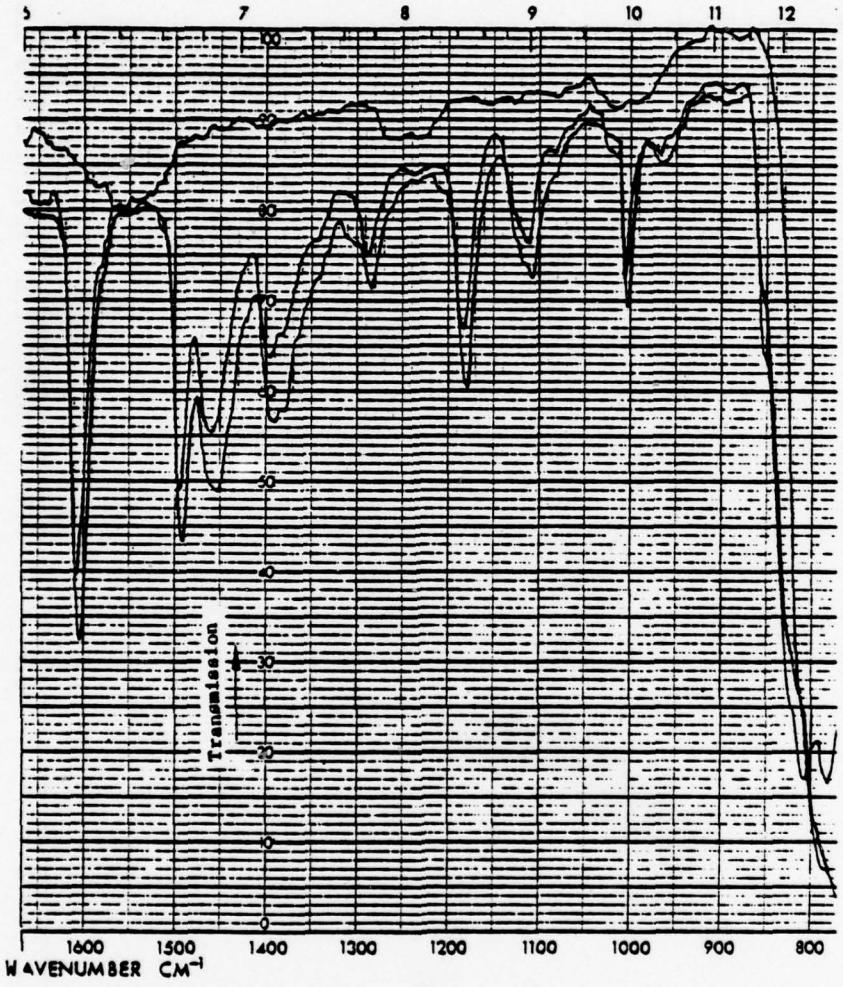

Fig. 31 Transmission spectrum of full strength and 52 mol percent 4-cyano-4'-n-pentyl biphenyl dissolved in CCl_4. Cell thickness is 25μm. Bottom trace is full strength. Top trace is pure CCl_4.

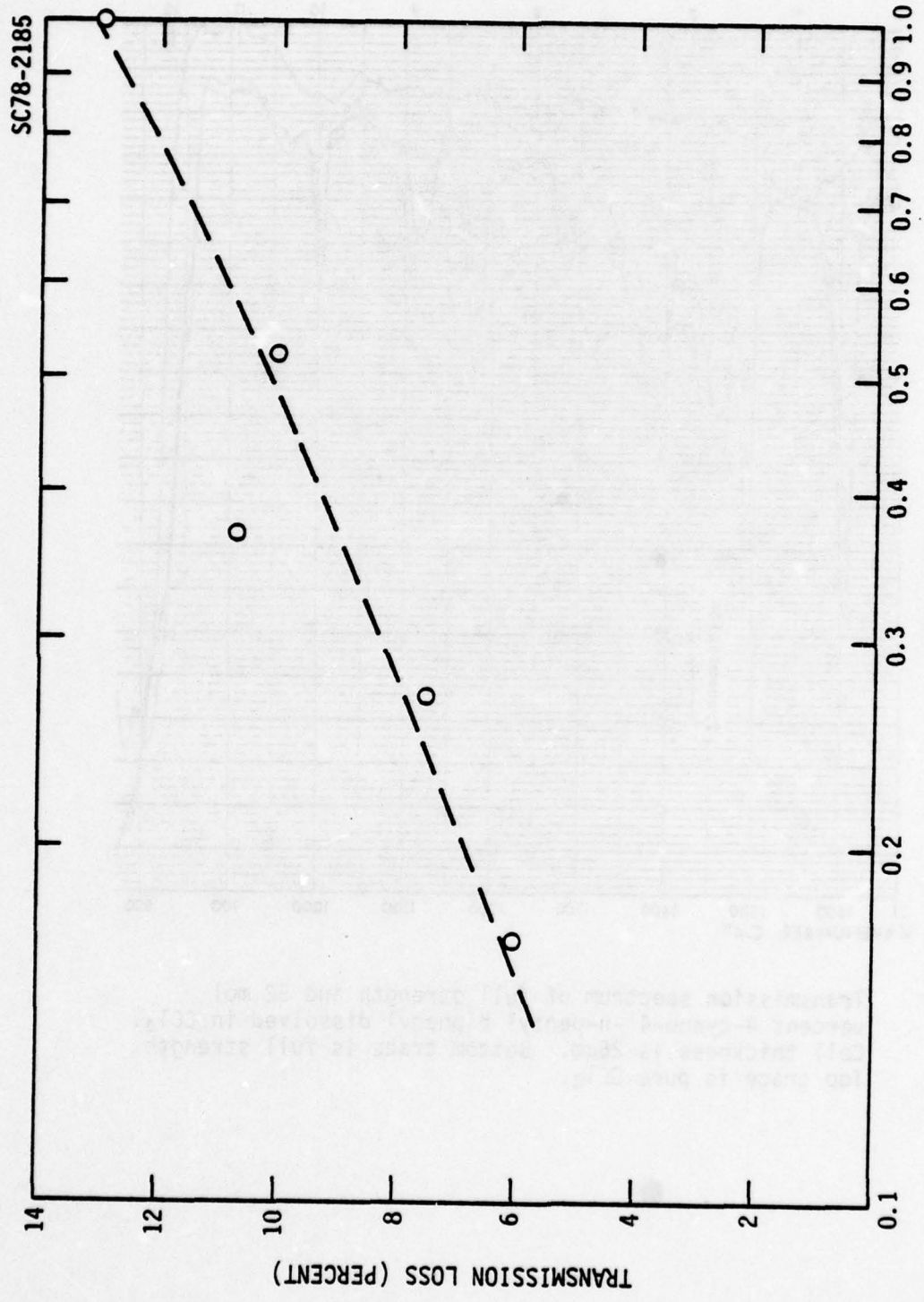

Fig. 32 Integrated transmission loss in the 8-12μm region for PCB as a function of mol fraction in CCl_4.

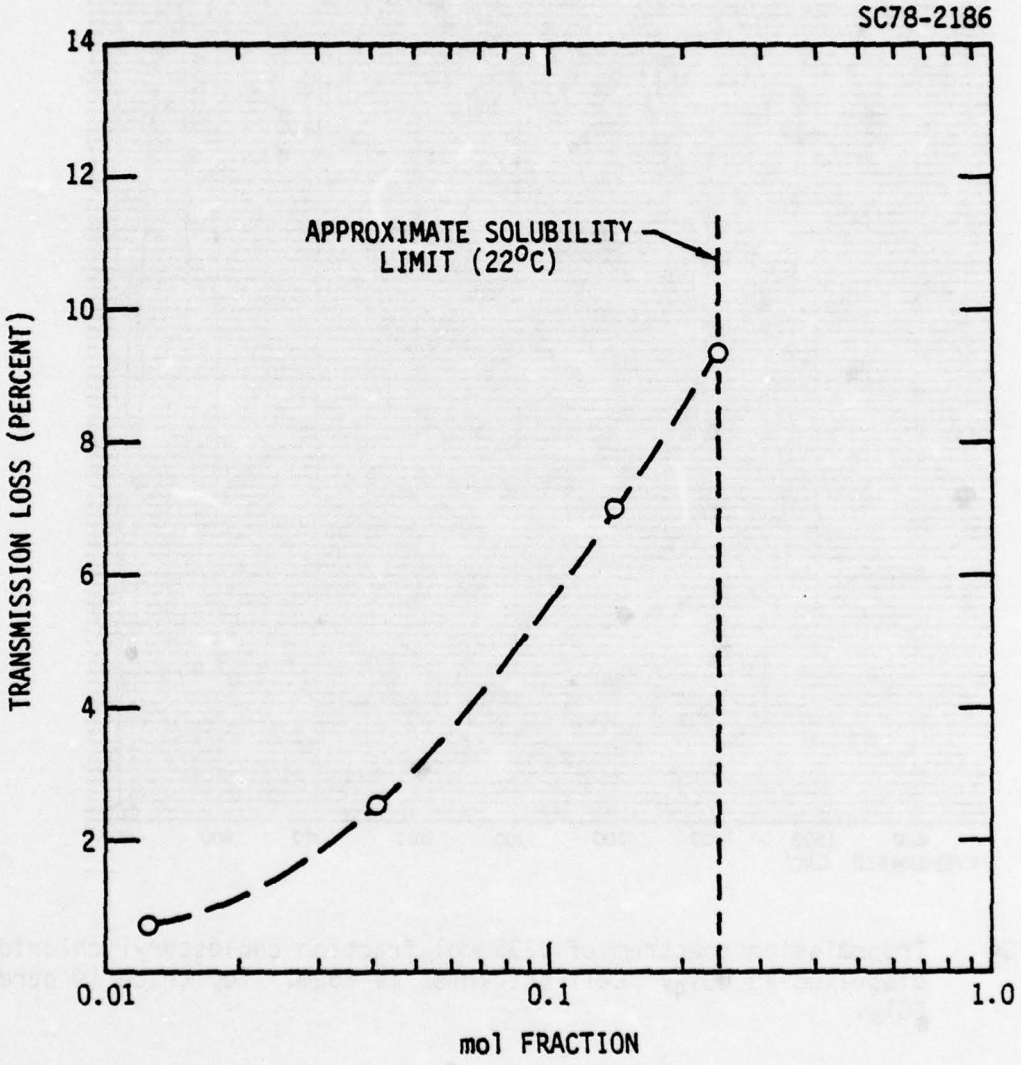

Fig. 33 Integrated transmission loss in the 8-12μm region for cholesteryl chloride as a function of mol fraction in CCl_4.

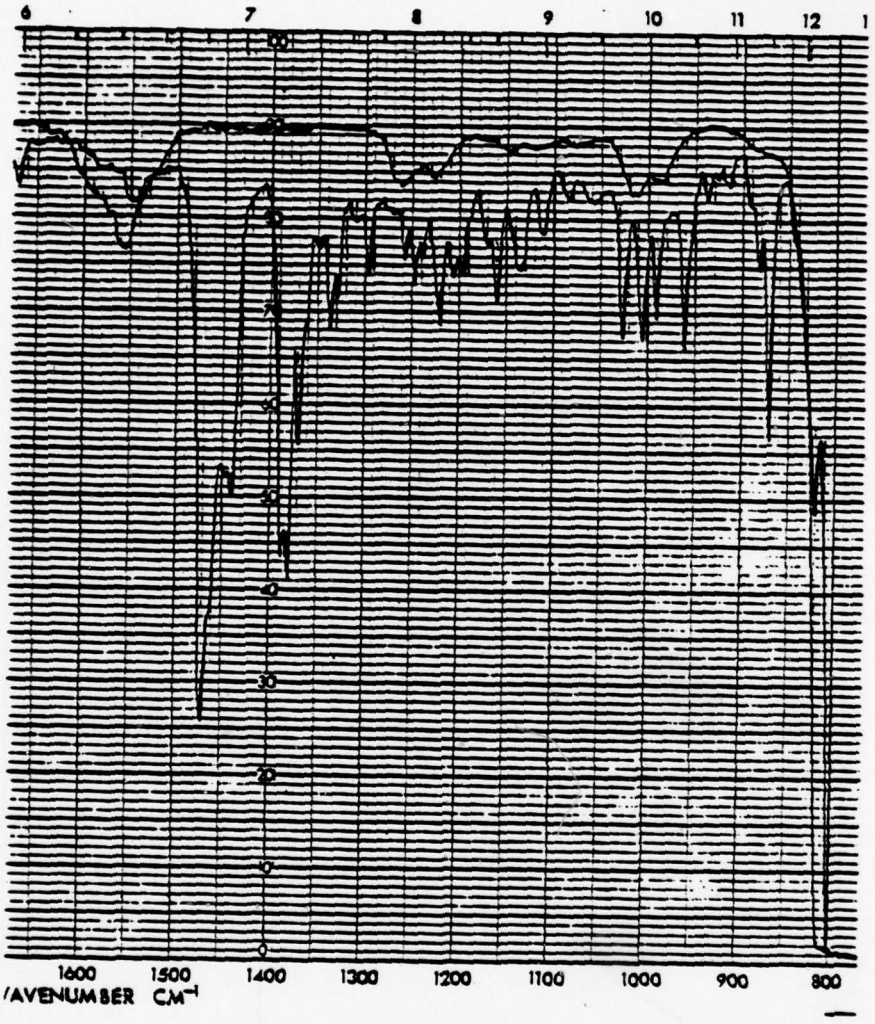

Fig. 34 Transmission spectrum of .235 mol fraction cholesteryl chloride dissolved in CCl_4. Cell thickness is 25μm. Top trace is pure CCl_4.

($C_{27}H_{45}Cl$) for .235 mol fraction (maximum solubility) in CCl_4. For comparison, Fig. 35 shows the spectrum for cholesteryl erucate ($C_{27}H_{45}OCO(CH_2)_{11}CH{=}CH(CH_2)_7CH_3$) for .106 mol fraction dissolved in CCl_4. Clearly, the cholesteryl portion of these molecules is not responsible for the large absorption in the latter material.

Toward the end of Phase II, after most of the infrared transmission spectra data had been compiled, the cholesteric-nematic phase change effect began to look like the more favorable effect to pursue based on the high infrared transmission of the positive $\Delta\varepsilon$ materials. However, before a final decision could be made, experimental measurements had to be first completed on response times and contrast determination for both the dynamic scattering and cholesteric-nematic phase change effects.

4.6 Modulation Experiments

4.6.1 Modulator Cell Construction

Figure 36 shows a photograph of the experimental cell used for the liquid crystal electro-optical measurements. The cell is composed of two conducting Ge infrared transmitting windows .120" thick and 1.00" in diameter, separated from one another by mylar spacers. A one by 4 mil gold wire lead is attached to the edge of each inner conducting surface so that an external voltage can be applied. The cell is held together by four screws enabling liquid crystal materials and cell spacing to be varied. Permanently sealed cells were impractical in this case because of the prohibitive expense which would be experienced in having to purchase dozens of optically flat infrared windows.

Initial measurements were performed in cells containing ZnSe windows coated with approximately 300A of a conductive, evaporated SnTe semiconducting material which was partially transparent out to and beyond 12μm. However, two windows of ZnSe coated with SnTe and placed together in a cell gave an average transmission of only 18% between 8-12μm. Also, the SnTe film was soft and easily scratched, making it unreliable to keep re-using the windows.

Germanium windows were then ordered and proved conductive enough so

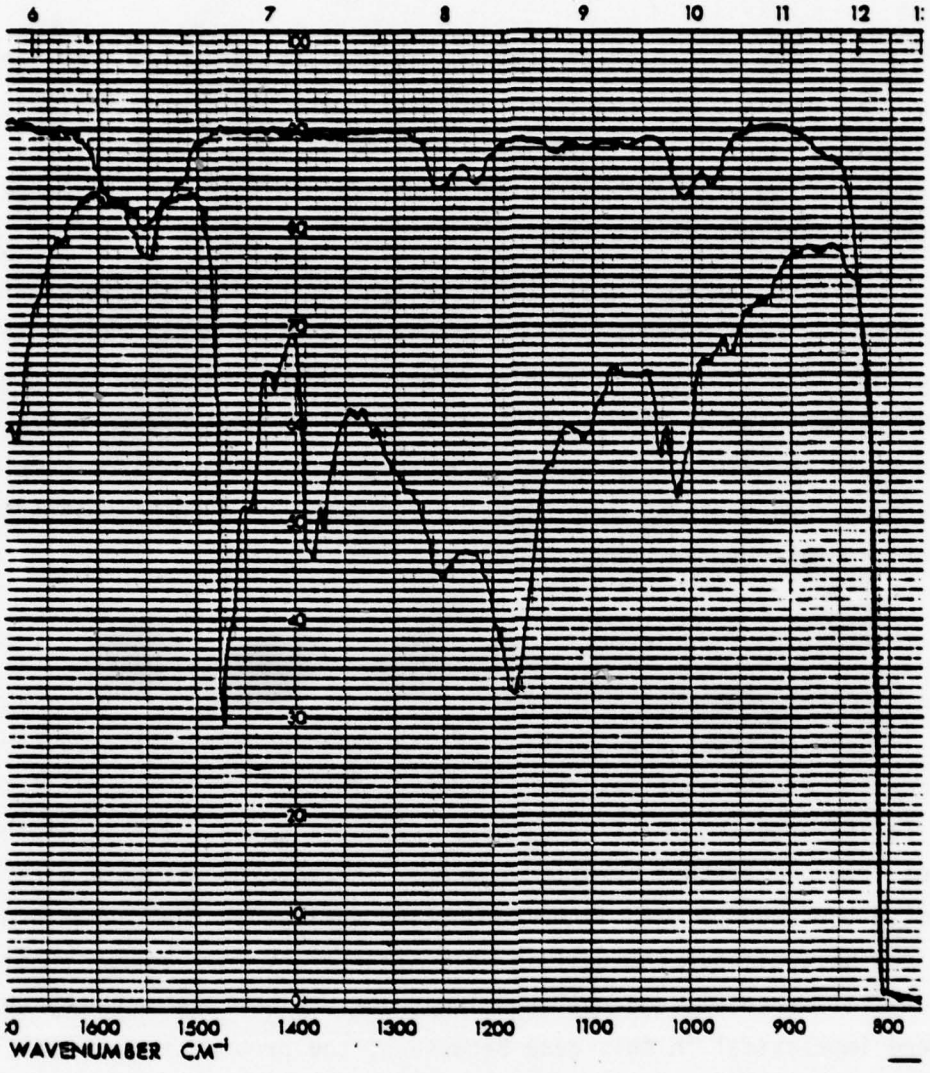

Fig. 35 Transmission spectrum of .106 mol fraction of cholesteryl erucate dissolved in CCl_4. Cell thickness is 25μm. Top trace is pure CCl_4.

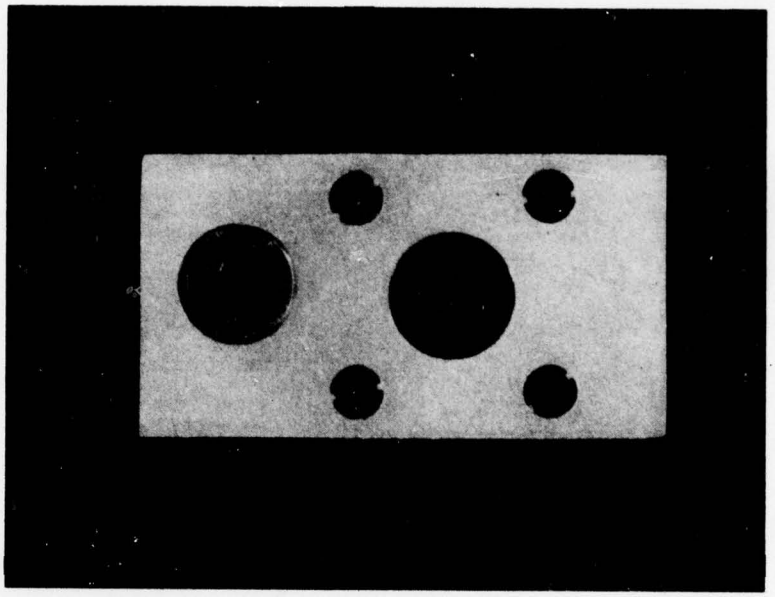

Fig. 36 Photo of experimental cell with Ge infrared windows used for liquid crystal modulation experiments.

that an additional conductive film did not have to be applied. The problem here was that the windows were not anti-reflection coated, thus giving an average transmission of about 30% between 8-12μm; but at least the inner surface of the Ge was more durable and relatively scratch resistant during the cell refilling operations.

Finally, the measurements made during Phase III used Ge windows (a total of four were purchased) which had both sides anti-reflection coated and optimized for 10.6μm. These proved to be best of all, but problems still did exist. First of all, an AR coating which was flat from 8-12μm would have been more optimum. Secondly, all the 3-5μm measurements made used these windows, although they were optimized for 10.6μm, thus limiting transmission in this region.

The cell filling operation was performed as follows: Windows were cleaned by rinsing in methanol to remove traces of the previous liquid crystal material used in the cell. New liquid crystal material was placed with an eyedropper into the shallow cavity defined by the mylar spacer and then the second Ge window was placed over the first window holding the liquid crystal and spacer, and the four screws tightened.

4.6.2 Initial Electric Field Effects

The very first liquid crystal studied was the negative nematic MBBA. Much has been written about this material because it was the first known room temperature liquid crystal. Also, since it is so well documented, the use of MBBA seemed a good test for the liquid crystal modulator cell and would provide experience in the interpretations of field effect data. The following measurements are all made with the Beckman 4250 spectrophotometer.

Figure 37 shows the 3-5μm infrared transmission spectrum of a 25μm cell of pure MBBA with and without an applied DC voltage of 40 volts. Figure 38 shows the 6-12μm infrared transmission spectrum of the same MBBA cell. The low transmission of MBBA in the 8-12μm region (Fig. 20) coupled with the low ZnSe cell transmission leads to a very low overall transmission in the 8-12μm region as Fig. 38 demonstrates. Nevertheless, there is modulation observable

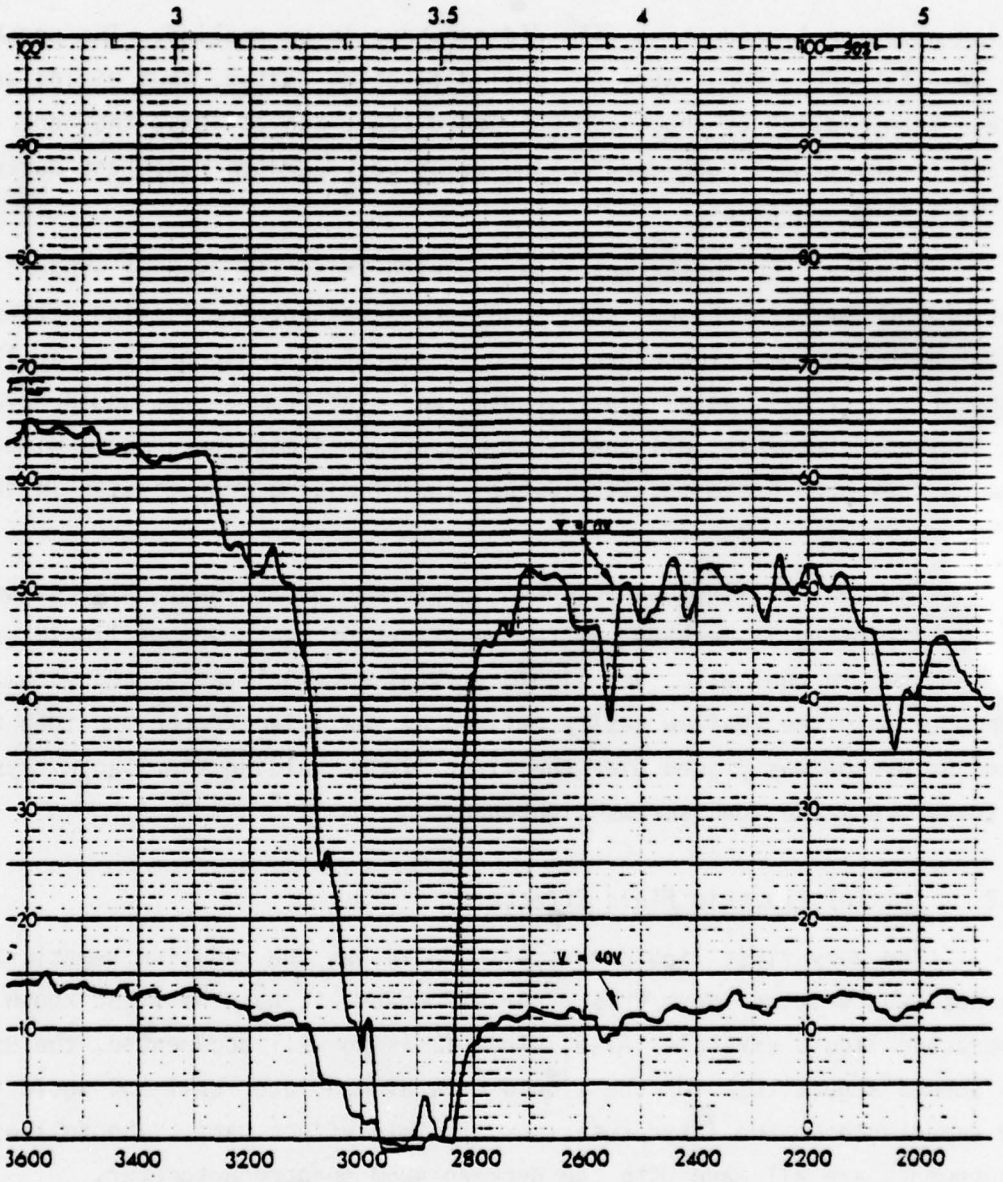

Fig. 37 Transmission spectrum of pure MBBA showing 3-5μm modulation obtained with applied voltage of 40 volts. Cell thickness is 25μm. Note that vertical scale covers 0-50% transmission.

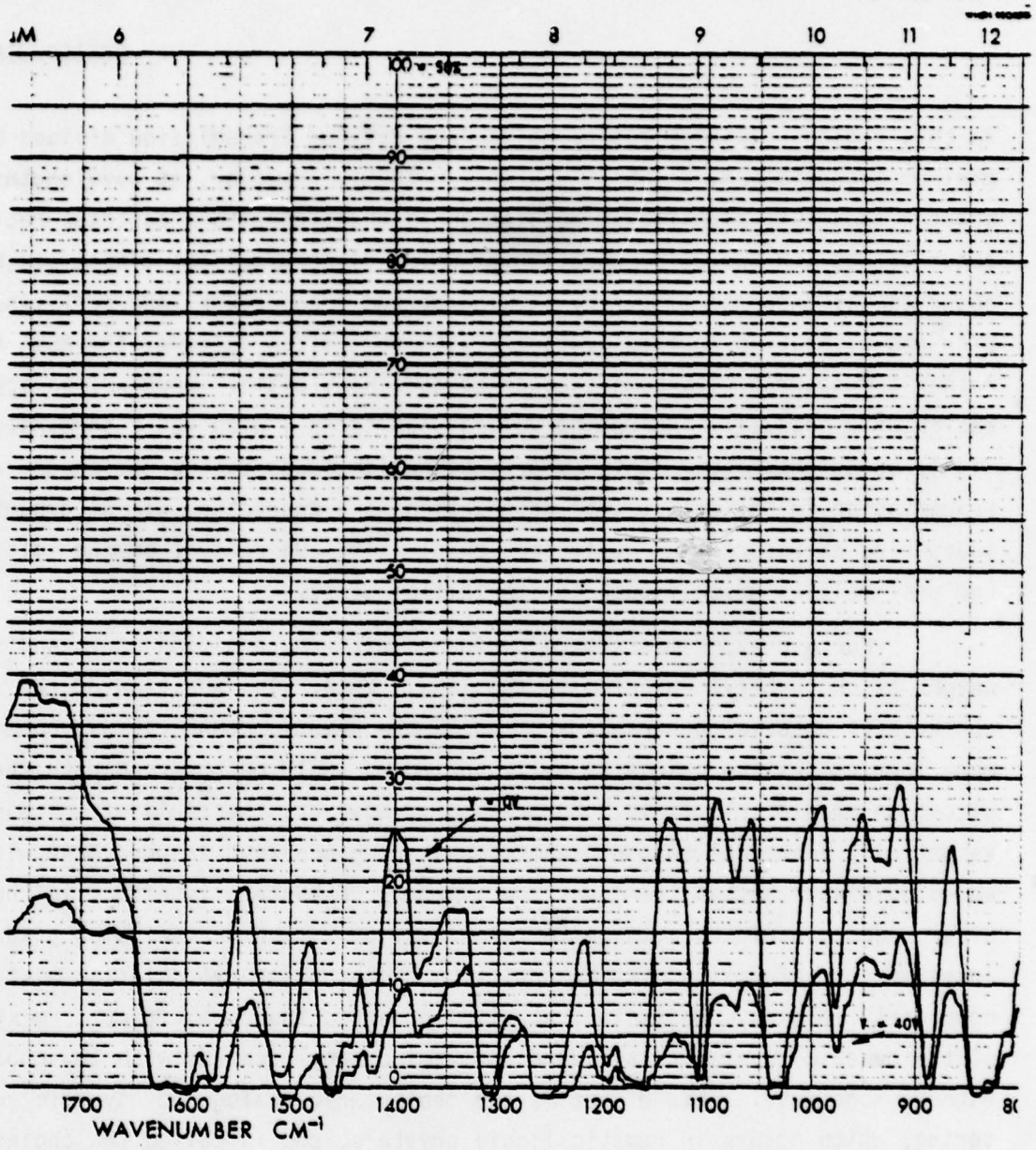

Fig. 38 Transmission spectrum of pure MBBA showing 6-12μm modulation obtained with applied voltage of 40 volts. Cell thickness is 25μm. Vertical scale covers 0-50% transmission.

in this region (contrast ratio, defined as maximum transmission divided by minimum transmission, is about 2:1 at λ = 10μm). However, at wavelengths shorter than 6μm, significant modulation is observed with a contrast ratio of about 4:1 at λ = 3μm. The question of which electro-optical effect was being observed was answered simply by looking at the transparent ZnSe cell visually with and without an applied voltage. With no applied voltage, the MBBA is rather transparent with some scattering domains visible. However, on application of a gradually increasing voltage (up to 40 V with ≈10 V threshold), a highly turbulent cloudy state is produced which leads to the decreased transmission in the cell. This observation is a characteristic of dynamic scattering as reported by Heilmeier, et al.[25-26] On removal of the voltage, the cell relaxes quickly back to its initial state.

Further experiments were performed with the addition of 1% and 5% by weight of cholesteryl chloride to the liquid MBBA. The addition of the cholesteryl material generates a pitch in the nematic MBBA. It was hoped that some form of texture change or helix unwinding would be observed with the application of electric field. Surprisingly, however, the field effect was essentially identical to the dynamic scattering observed in pure MBBA with the added observation that there was now a memory or hysteresis effect in the cell after reduction of the voltage to zero (Fig. 39). The transmission gradually increases as a function of time until the MBBA-cholesteryl chloride mixture completely relaxes. Heilmeier, et al.[34] observed the same effect in mixtures of the nematic crystal anisylidene para-aminophenyl acetate with 10% cholesteryl nonanoate. This effect is the cholesteric analogue of dynamic scattering, which occurs in nematic liquid crystals, and is called the cholesteric memory effect, also requiring electrically conducting material with negative dielectric anisotropy. When the voltage is switched off, the liquid crystal is initially in the focal-conic scattering state, indicative of the cholesteric phase, and gradually relaxes back to the starting transparent Grandjean state. This relaxation time is exponentially dependent on the ratio of the cell thickness to the pitch and can possibly last years. As noted by Heilmeier, the application of a 15 kHz, AC field quickly returns the liquid crystal to the transparent Grandjean state. This effect was, indeed, verified experimentally.

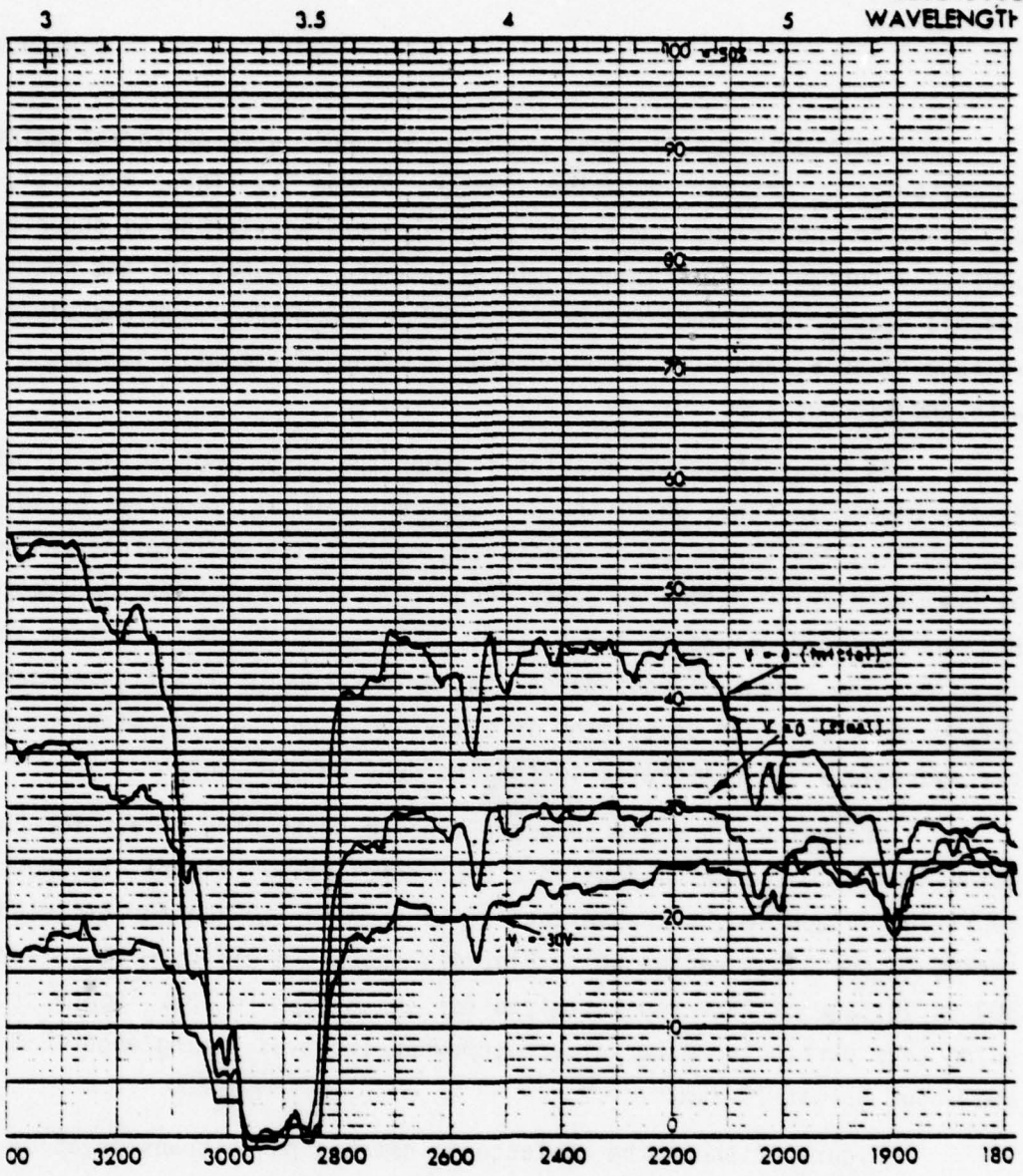

Fig. 39 Transmission spectrum of 5% cholesteryl chloride in MBBA showing 3-5μm modulation obtained with applied voltage of 30 volts. The center trace shows the transmission of the cell immediately after removal of the 30 volts and demonstrates the cholesteric memory effect. Cell thickness is 25μm and vertical scale covers 0-50% transmission.

Additional dynamic scattering experiments were performed using the EM Laboratories "Licristal" negative nematics 7A and 5A. These materials are pre-doped to the proper conductivity for dynamic scattering to occur and also contain a surfactant for homeotropic alignment. Figures 40a and 40c show the dynamic scattering effect for EM 7A at 3-5μm and 8-12μm with and without a DC voltage of 40 V, and Figs. 40b and 40d show the effect at 3-5μm and 8-12μm with and without a DC voltage of 10 V.

An interesting observation is that the 3-5μm modulation is optimized at the higher voltage, while the 8-12μm modulation is optimized at 10 V. This demonstrates the variation of scattering region size with voltage as mentioned by Fray et al. for Merck 5A. They found that at about 10 V, the scattering regions have dimensions of about 20μm, while at 30 V, they are less than 10μm in size. The effect of voltage on scattering shown in the figures demonstrates the fact that scattering is a maximum when the dimensions of the scattering regions are comparable to the incident wavelength.

Figures 41a and 41b show the dynamic scattering effect for EM 5A using non-AR coated Ge windows in a 25μm thick cell. Figure 41a shows the effect with an applied 500 Hz voltage of 54 V rms optimized for efficient scattering in the 3-5μm region while Fig. 41b shows the effect with an applied 500 Hz voltage of 29 V rms optimized for the 8-12μm region. Contrast ratios using this particular material are somewhat improved, being about 8:1 at 3μm and about 5:1 at 10.2μm.

Figure 42 shows the cholesteric-nematic phase transformation in the 8-12μm region for 4-cyano-4'n-pentyl biphenyl (PCB) and 3% by weight of cholesteryl chloride. The plot shows the maximum transmission at 40 V, and the minimum transmission at ≈3 V; at 0 V, the scattering was slightly less (a similar effect was noted by Fray et al.[23]). No pre-alignment was given to the 25μm thick cell. After switching the voltage on and off several times, the voltage at which maximum scattering occurs shifts slightly, probably because the focal-conic scattering state is metastable. The constrast ratio at $\lambda \approx 10.8\mu m$ is less than 2:1.

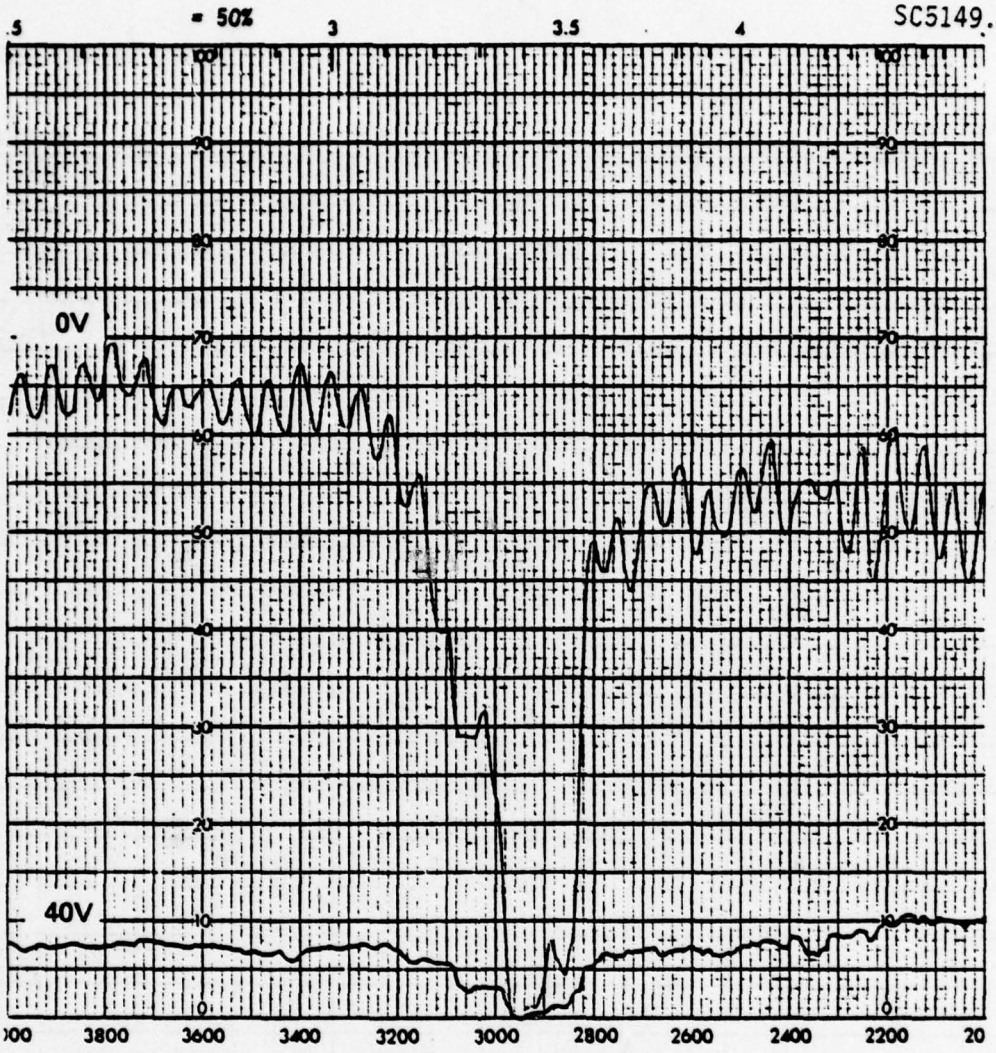

Fig. 40a Dynamic scattering effect (3-5μm) for EM Licristal 7A with and without DC voltage of 40 V. Note: 100% line equals 50% max. transmission; 25μm cell.

SC5149.31FR

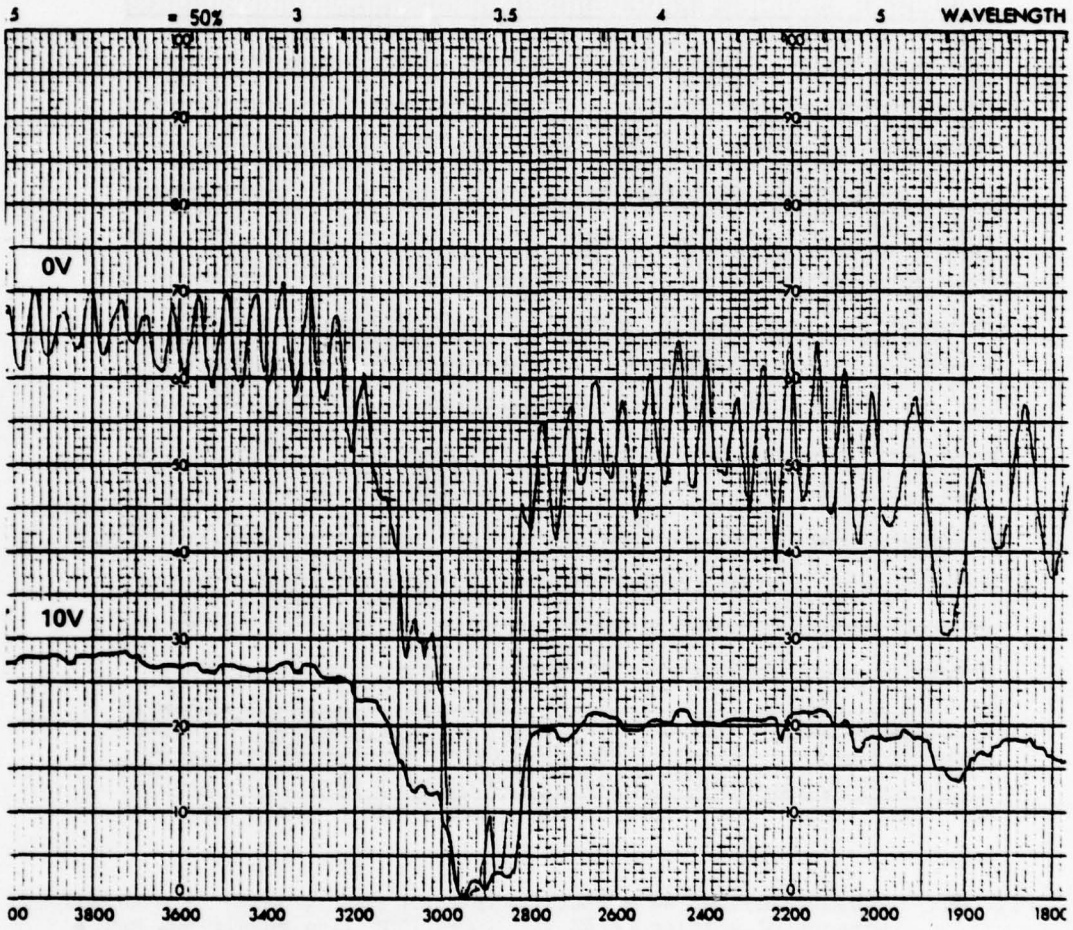

Fig. 40b Dynamic scattering effect (3-5μm) for EM Licristal 7A with and without DC voltage of 10 V. Note: 100% line equals 50% max. transmission; 25μm cell.

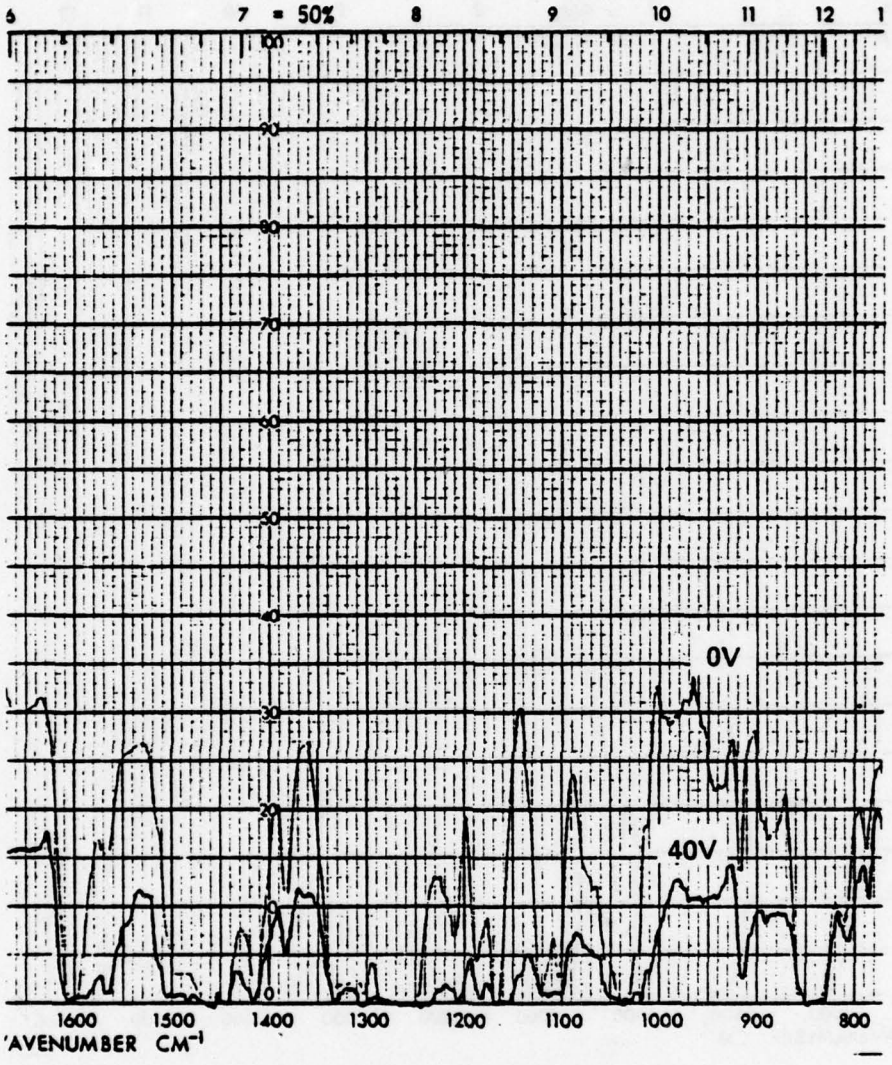

Fig. 40c Dynamic scattering effect (6-12μm) for EM Licristal 7A with and without DC voltage of 40 V. Note: 100% line equals 50% max. transmission; 25μm cell.

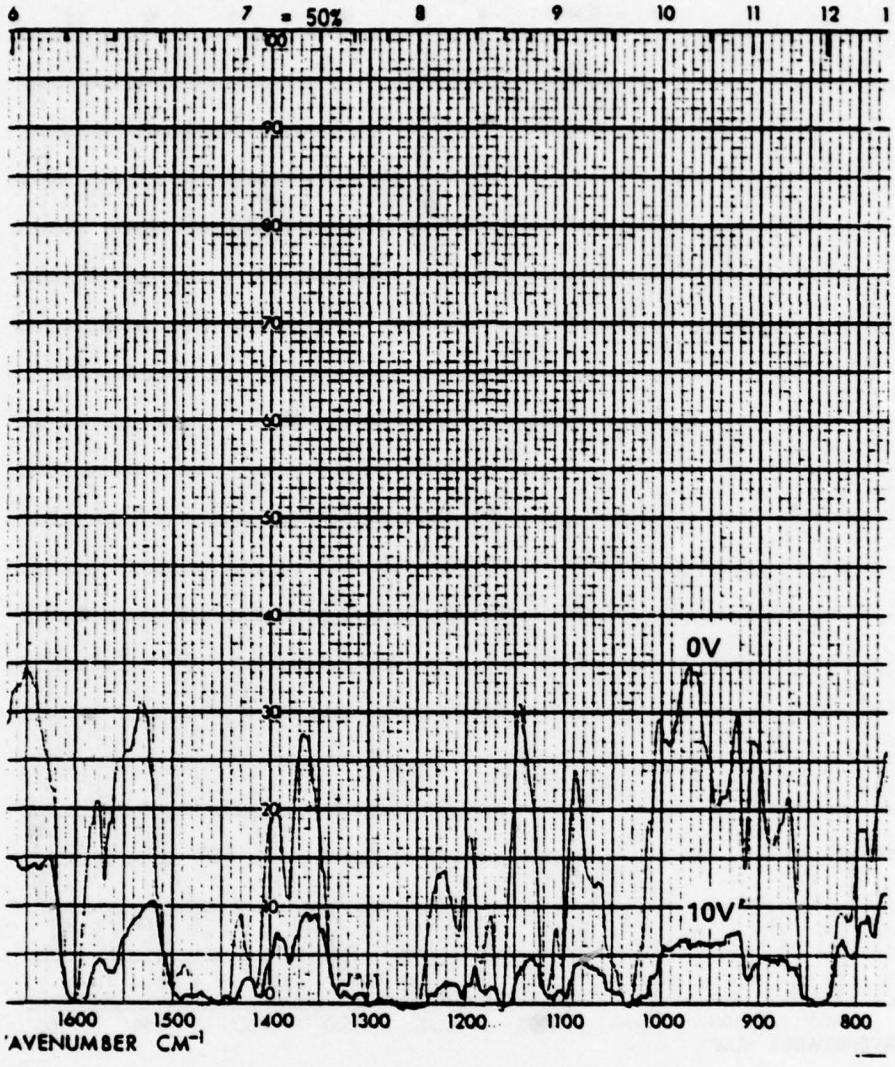

Fig. 40d Dynamic scattering effect (6-12μm) for EM Licristal 7A with and without DC voltage of 10 V. Note: 100% line equals 50% max. transmission; 25μm cell.

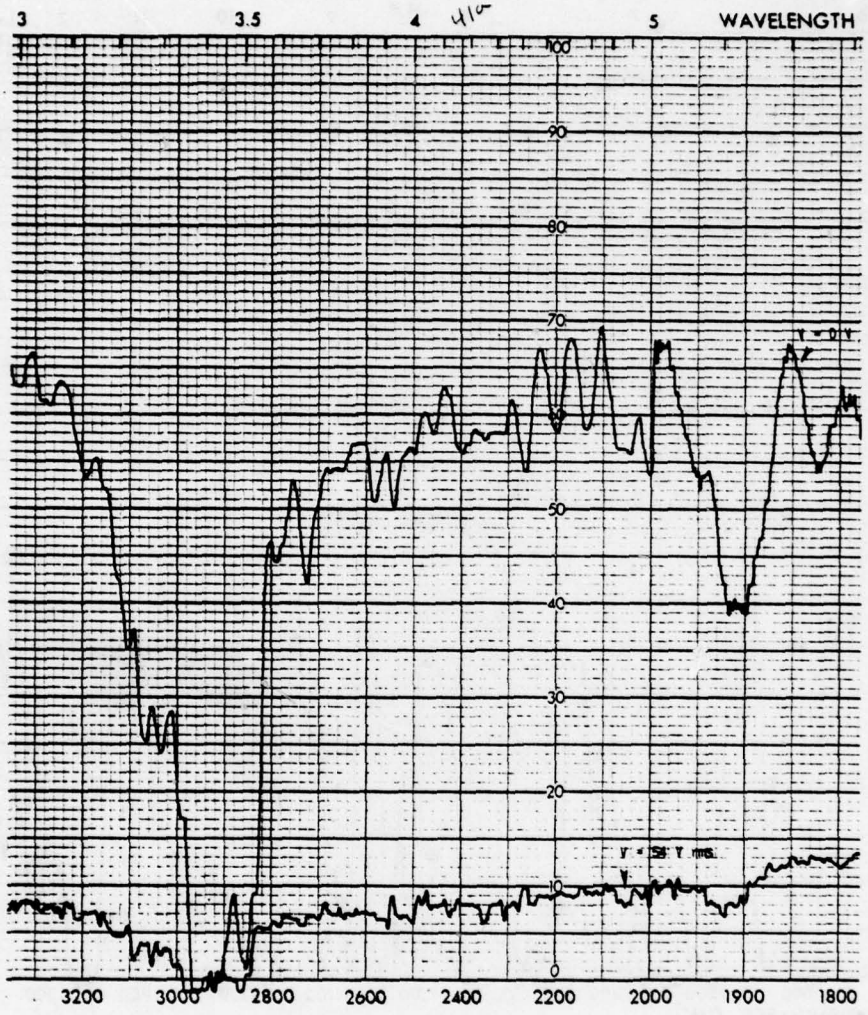

Fig. 41a Optimized dynamic scattering effect in 3-5μm region for EM Licristal 5A with and without 500 Hz AC voltage of 54 V rms (25μm cell, Ge windows). Note: 100% line equals 50% max. transmission.

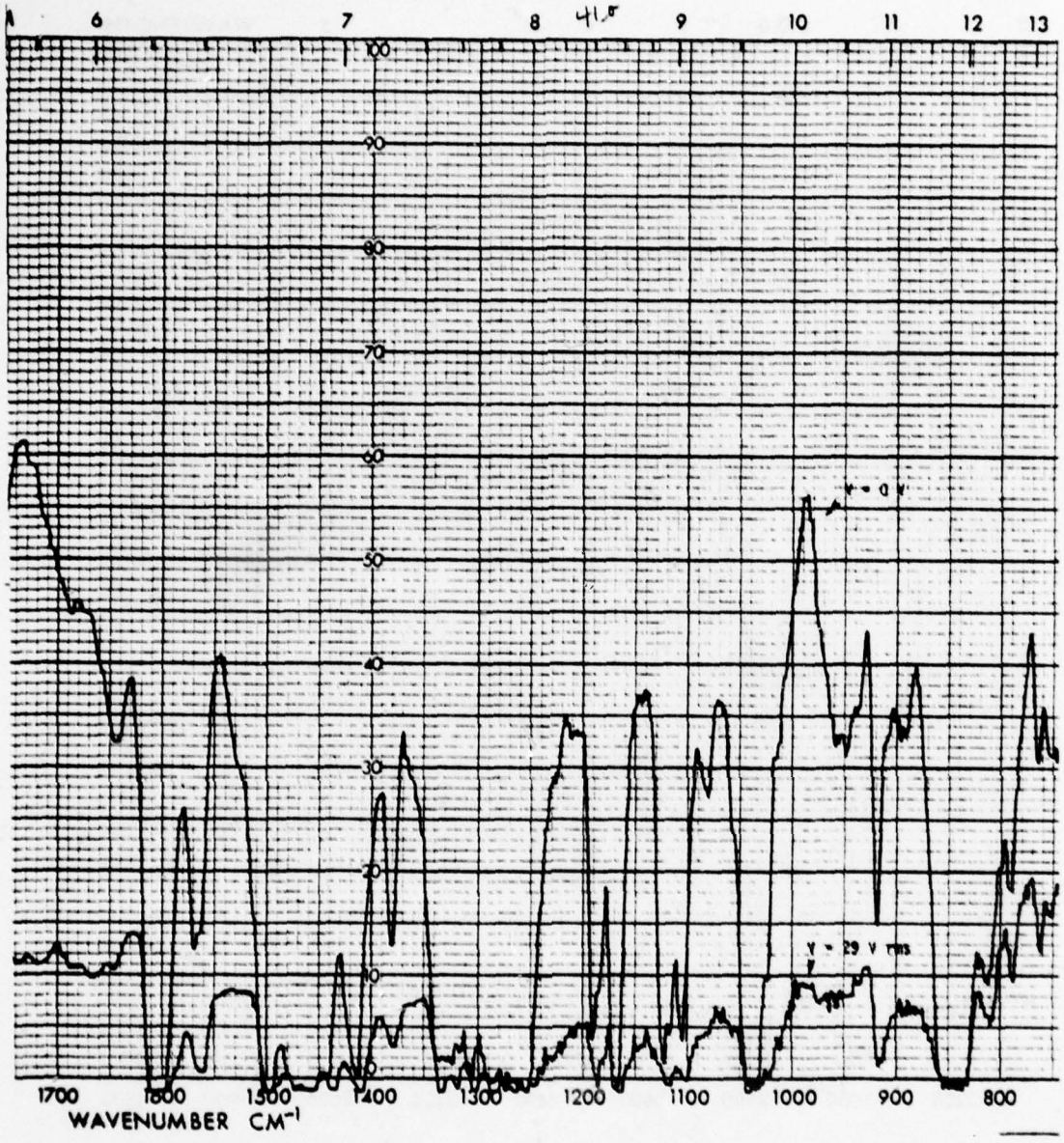

Fig. 41b Optimized dynamic scattering effect in 8-12μm region for EM Licristal 5A with and without 500 Hz AC voltage of 29 V rms (25μm cell, Ge windows. Note: 100% line equals 50% max. transmission.

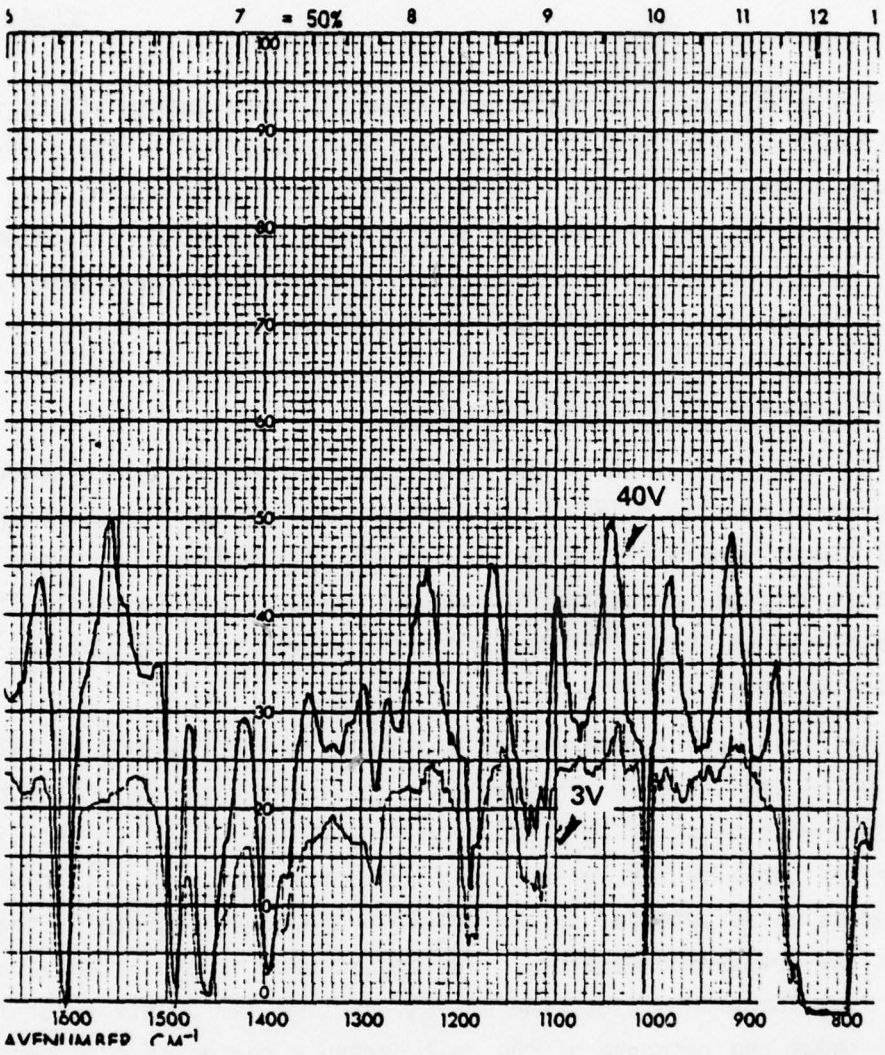

Fig. 42 Cholesteric-nematic phase transformation (6-12μm for 4-cyano-4'-n-pentyl biphenyl and 3% by weight of cholesteryl chloride. Note: 100% line equals 50% max. transmission; 25μm cell with ZnSe windows.

Figure 43 shows the cholesteric-nematic phase change effect for a 25μm thick cell containing 4.7% cholesteryl nonanoate/PCB in the 8-12μm region using non-AR coated Ge windows. The maximum transmission occurs at a 2 kHz voltage of 40 V rms, and the maximum scattering occurs at a voltage of 9 V rms. The overall turned-on transmission in this cell is now higher, and the contrast at $\lambda \approx 10.8\mu m$ is slightly better than 2:1.

4.6.3 Initial Response Time Measurements

The experimental setup was comprised of a Nernst glower/monochromator for the infrared source, a 77°K PbSnTe photodiode for the detector, an Exact model 7271 signal generator and Burleigh PZ-70 high voltage DC op-amp to provide variable voltage pulses to the modulator cell, and a Tektronix 7834 storage oscilloscope to monitor and store the waveforms. The optical setup corresponded to an ≈f/3 system.

The first measurement was on a dynamic scattering cell containing a 25μm film of EM Licristal 7A. Figure 44a shows the risetime of the cell when a 40 V square-wave pulse of long duration is applied. The straight line at the top of the photo is the voltage pulse, and the bottom plot is the relative cell transmission as detected by the PbSnTe photodiode (increasing transmission is in the downward direction). The measurement is conducted at a wavelength of 7μm. From this plot, the 10-90% risetime is roughly 60 or 70 ms. Figure 44b shows the response of the cell during a series of 40 V rectangular pulses. With the voltage applied, scattering is a maximum and cell transmission a minimum. When the pulse is switched off, the cell transmission increases very slowly; full relaxation takes about 4 seconds to complete.

Figure 45 shows the response of a cholesteric-nematic phase change cell, containing a 25μm film of BDH E3 biphenyl mixture-3% cholesteryl chloride, to a 40 V pulse. In this case, when the voltage is on, the transmission is a maximum, just opposite to the case of dynamic scattering. The turn-off time for this effect is expected to be faster than the turn-off for dynamic scattering because it is dependent upon the bulk properties of the cholesteric liquid crystal and not the wall surface forces as in the case of

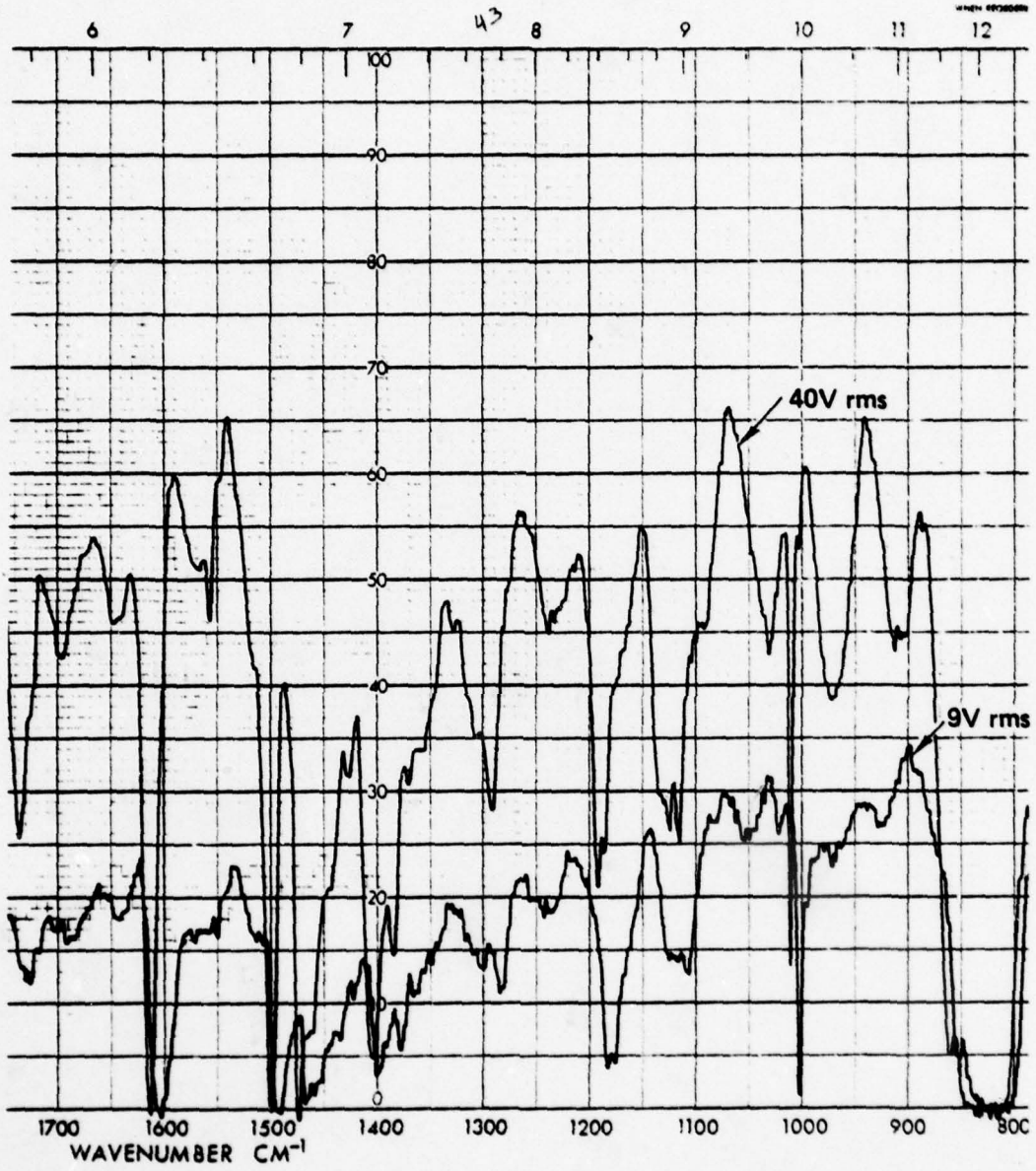

Fig. 43 Cholesteric-nematic phase change effect for 1 mil 4.7% cholesteryl nonanoate/4-cyano-4'-n-pentyl biphenyl cell in 8-12μm region. Note: 100% line equals 50 max. transmission; 25μm cell with Ge windows.

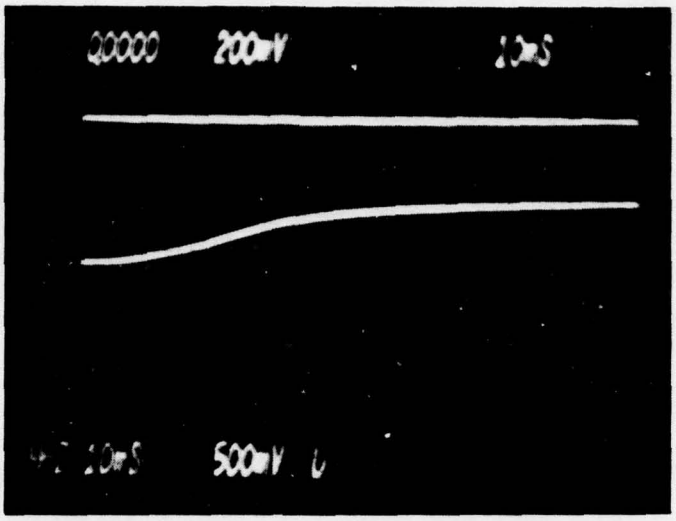

Fig. 44 (a) Rise time of dynamic scattering cell (25μm film of EM Licristal 7A) with application of 40 V square-wave pulse.

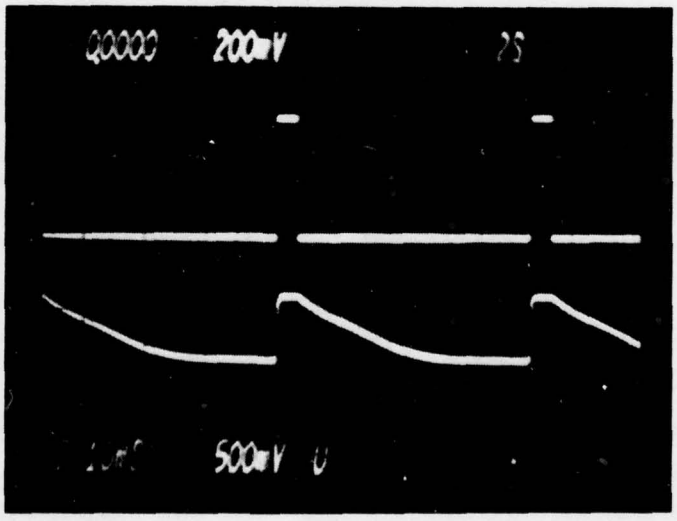

(b) Response of above cell to a series of 40 V square-wave pulses showing relaxation of scattering in dynamic scattering mode (lower curve).

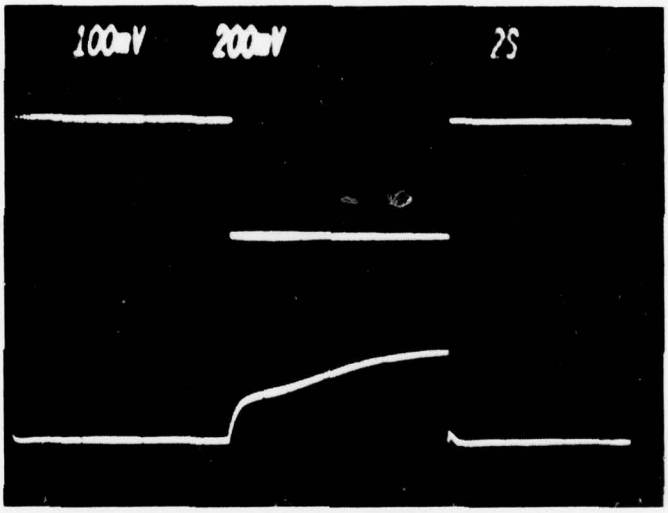

Fig. 45 Response of a cholesteric-nematic phase change cell (25μm film of BDH E3 biphenyl mixture: 3% cholesteryl chloride) to a 40 V pulse showing relaxation to the scattering focal-conic texture (lower curve).

dynamic scattering. However, the measured turn-off time is actually slower (≈6 sec for complete relaxation). As can be seen, the relaxation consists of two distinct regions, one fast and the other considerably slower. The fast region is most likely the elastic restoration of the cholesteric helixes from the homeotropic nematic phase, while the slow region is probably the rotation of the helices to a focal-conic texture. The modulation frequency can be increased considerably by utilizing this fast relaxation region but with a corresponding reduction in contrast ratio. This sort of trade-off may ultimately have to be made.

4.6.4 Phase II Conclusions

These measurements completed Phase II of the contract. The choice between the dynamic scattering and cholesteric-nematic phase change effects for application as an 8-12μm infrared modulator was based primarily on the measured infrared transmission spectra, since no hard conclusions could be made based on the response time measurements. Due to the superior transmission of the cyanobiphenyl and phenylcyclohexane liquid crystals used in the phase change effect, compared to any liquid crystal available for the dynamic scattering effect, it was decided to place almost complete emphasis on the optimization of the phase change effect during Phase III.

5.0 PHASE III: OPTIMIZATION OF PERFORMANCE OF SELECTED MODULATOR CANDIDATE

In this phase of the contract, the operation of the cholesteric-nematic phase change effect, chosen as the most promising modulator candidate, was to be optimized. In addition, with the permission of NV&EOL measurements were to be extended to the 3-5μm region during a four month extension of the contract.

5.1 Further Discussion of Cholesteric-Nematic Phase Change Effect

Now that the cholesteric-nematic phase change effect has been chosen for application in the 8-12μm electro-optical infrared modulator, a few additional words about this effect should be mentioned at this time.

As experiments progressed, one observation was very clear. It soon became obvious that the cholesteric-nematic phase change effect is much more complex than originally envisioned. Since three basic textures can be observed during the course of the phase change effect, the conditions for obtaining each one must be known and understood. What complicated matters in these experiments is the fact that visual observations could not be made of these texture changes through the opaque Ge windows in the cell. Knowledge gained about the cholesteric-nematic phase change processes was based primarily on the optical transmission data as monitored by the PbSnTe photodiode. A detailed analysis based on visual observations and polarizer experiments could not be carried out.

However, an excellent description of the theory and visual observations of the fundamental texture transitions occurring in the phase change effect is presented in a doctoral thesis by J.C. Varney.[35] He also discusses the interrelationships of cell thickness, pitch and surface alignment, and how they affect the electro-optical properties of the cell. The presentation is interesting in that it presents derivations for the critical fields required to go from one texture to another and also predicts the structures present both during and after the transitions. The processes of nucleation and

relaxation from the nematic state, however, are not describable by the theory and there is an uncertainty as to what recovery processes will actually exist from cell to cell. This is substantiated in the present work as well, especially with the high-voltage square-wave drive technique (next section) in which the cell is completely turned-on and allowed to relax. When the helicies are fully unwound during the modulation process, relaxation can terminate in the focal-conic texture, the Granojean texture, or possibly, in no well-defined state. The partially turned-on operating mode is considerably more predictable and reproducible and is discussed later in Section 5.2.5.

5.2 Response Time/Contrast Measurements

5.2.1 Introduction

The major areas of concern during Phase III were the turn-on and turn-off times associated with the cholesteric-nematic phase change effect. The few measurements made previously resulted in turn-off times of several seconds, and since the goal was 1 ms, major improvements would have to be made.

The approach was to investigate materials with various values of pitch, viscosity, and dielectric anisotropy, and to study the effects of these parameters on the response times. According to Jakeman and Raynes,[35] who report decay times of 60μs in a short pitch cholesteric mixture of MBBA, cholesteryl nonanoate and a cyano Schiff's base, the decay time and the rise time for the cholesteric-nematic phase change effect are given by the expressions

$$\tau_{decay} = \frac{\eta}{K_2 q^2}$$

$$\tau_{rise} = \frac{\eta}{\Delta\varepsilon\, E^2/4\pi - K_2 q^2}$$

where $\Delta\varepsilon = \varepsilon_{11} - \varepsilon_{\perp} > 0$ is the dielectric anisotropy, η is the twist viscosity, K_2 is the twist elastic constant, E is the electric field, and q is a function of E, but takes the value of the cholesteric helix wave vector $q_0 = \pi/\text{pitch}$

(P_o) when the electric field is equal to zero. From these expressions, the response times are of minimum value in materials having a large dielectric anisotropy, low viscosity and small pitch. The dielectric anisotropy and the viscosity (although it can be varied by heating the material) are fixed by the type of nematic liquid crystal used, but the pitch is one parameter that can be varied regardless of what the material is simply by adding various amounts of a short-pitch cholesteric to the particular nematic material being used. The results of such an experiment will be presented in Section 5.2.4. Unfortunately, fast response times are obtained with short pitch lengths, but short-pitch lengths also result in inefficient scattering of long wavelength (8-12μm) radiation. It is this critical trade-off between response times and modulator contrast, both dependent upon the pitch of the liquid crystal used, which must be clarified before the cholesteric-nematic phase change liquid crystal infrared modulator can ever become a reality.

In addition to optimizing the dielectric anisotropy, viscosity and pitch, another alternative for fast response times was to explore various modulator cell drive techniques. This is done in the following sections where high-voltage square-wave drive, AC drive, and partially turned-on operating mode drive techniques are discussed. Since one potential use of the liquid crystal modulator is to replace a mechanical chopper, a square-wave output from the modulator is desired. Thus, the driving waveforms were limited primarily to those that could provide a square-wave output with sharp rise and fall times.

5.2.2 High-Voltage Square-Wave Drive

From the last section, the risetime of the cholesteric-nematic phase transition is inversely proportional to the square of the applied electric field. The higher the applied electric field, or voltage for a cell of fixed electrode spacing, the faster the turn-on time will be, up to the point of the occurrence of dielectric breakdown in the liquid crystal. In addition, the critical electric field, E_c, for the cholesteric-nematic phase change to occur is given by

$$E_c = \frac{\pi^2}{P_o} (K_2/\Delta\varepsilon)^{1/2} \text{ or } V_c = \pi^2 \frac{d}{P_o} (K_2/\Delta\varepsilon)^{1/2}$$

where once again, $\Delta\varepsilon>0$ is the dielectric anisotropy, K_2 is the twist elastic constant, d is the cell thickness, and P_o is the pitch of the cholesteric helix. This expression implies that the critical electric field is reduced as the pitch becomes larger. Also, the voltage required to produce the critical electric field becomes larger as the cell spacing increases. Keeping these relationships in mind, the initial approach to the response time problem was to use a drive voltage much larger than that required for producing the critical field for the phase change, in order to at least be able to reduce the turn-on time to a value close to 1 ms.

For these initial measurements, the experimental setup used is the same as that described in Section 4.6.3. Also, Ge windows are now being used with both sides containing an AR coating optimized for 10.6μm. Figures 46a and 46b show the turn-on characteristics of a 5 mil thick, 5% cholesteryl nonanoate/BDH E-1 cell with a drive voltage of about 480 V and measured at λ = 8μm. The turn-on time (to maximum transparency) is about 30 ms (shown in Fig. 46b). Notice that the cell has a very fast initial turn-on (<1 ms) followed by a considerably slower region during which the liquid crystal molecules near the cell walls continue to align parallel to the electric field. Perhaps if a cell were really overdriven, this slow region would disapper. Figures 47a and 47b show the results of such an experiment. Figure 47a shows the turn-on of a 5 mil thick 5% cholesteryl nonanoate/BDH E-1 cell with a drive voltage of ≈320 V and Fig. 47b shows the turn-on of the same cell overdriven with a voltage of ≈610 V. Notice that in the overdriven condition, the turn-on is sharp as compared to the soft turn-on with the lower voltage. Thus, very fast turn-on times can indeed be achieved in a cholesteric-nematic phase change cell using large drive voltages.

However, the most significant finding is that the cell turn-off time is critically dependent on the minimum voltage level of the square wave pulses used to drive the cell. Figure 48 illustrates the effect on the turn-off of a 5 mil thick, 5% cholesteryl nonanoate/BDH E-1 cell when the bias level

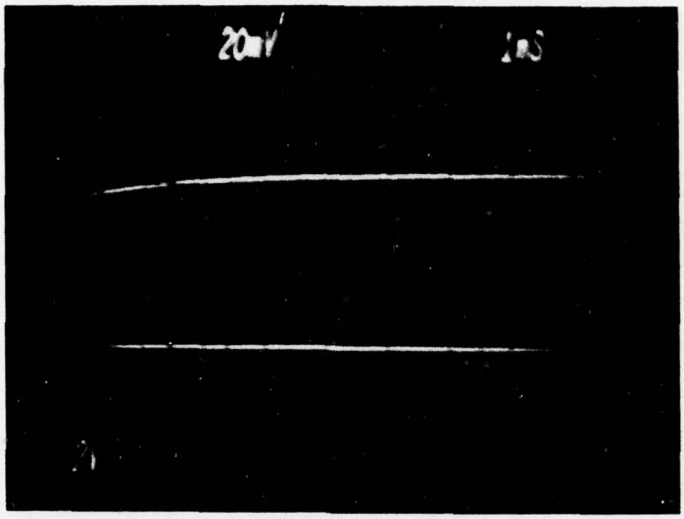

Fig. 46 (a) Turn-on characteristic of a 5 mil 5% cholesteryl nonanoate/BDH E-1 cell showing fast turn-on region. Lower line is DC level of drive voltage equal to ~480 V.

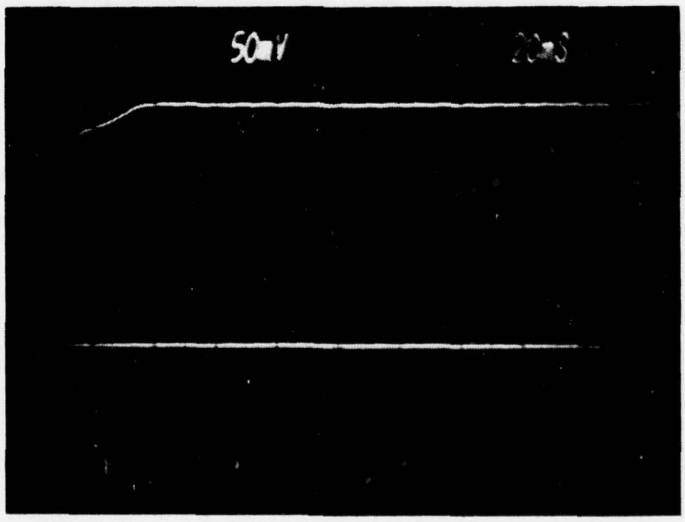

(b) Total turn-on time for above cell to nematic state is approximately 30 ms.

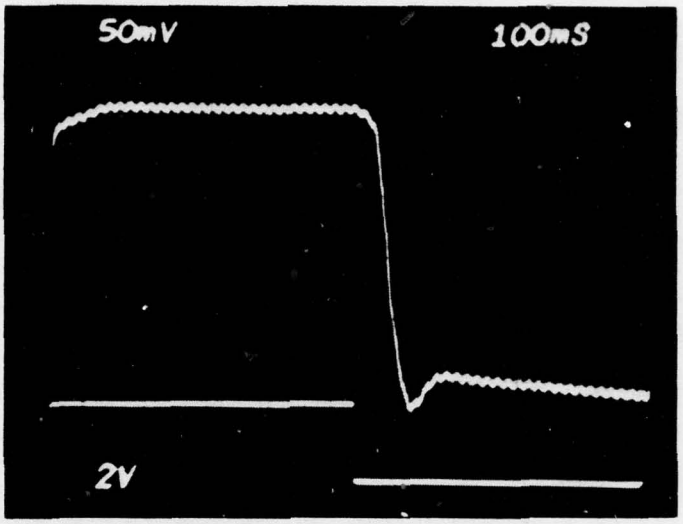

Fig. 47 (a) Turn-on of 5 mil 5% CN/E-1 cell with ~320 V square wave. (Lower voltage scale is 200 V/div, λ = 8-11.5μm.)

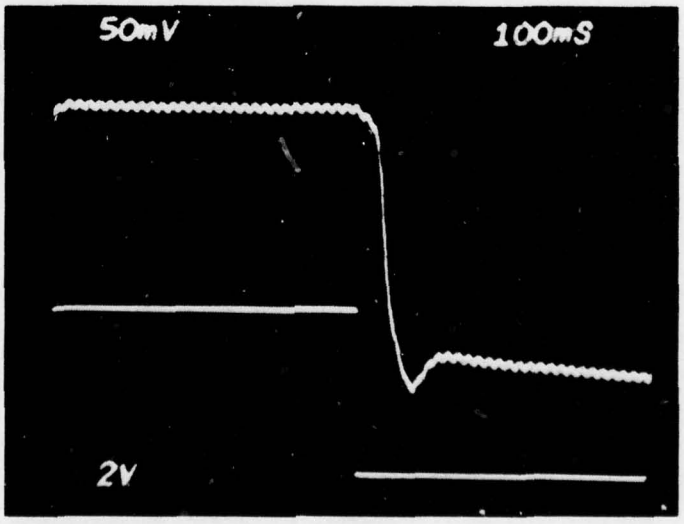

(b) Turn-on of above cell with overdrive voltage of ~610 V. (Lower voltage scale is 200 V/div.)

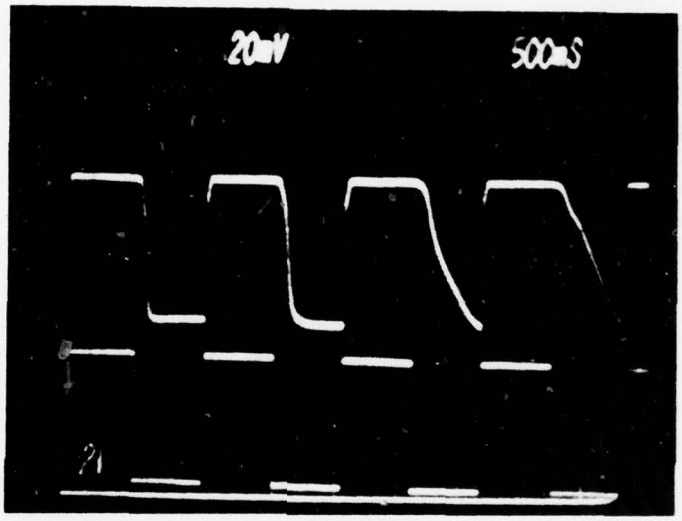

Fig. 48 The effect of varying the minimum of the square wave voltage on the turn-off time of a 5 mil thick, 5% cholesteryl nonanoate/BDH E-1 cell. Bias level (minimum voltage on lower trace) decreases from left to right (λ = 8μm).

AD-A072 095 ROCKWELL INTERNATIONAL THOUSAND OAKS CA SCIENCE CENTER F/G 20/6
FIR OPTICAL MODULATION PHENOMENA.(U)
MAY 79 J G PASKO DAAK70-78-C-0003
UNCLASSIFIED SC5149.31FR NL

2 OF 3
AD A072095

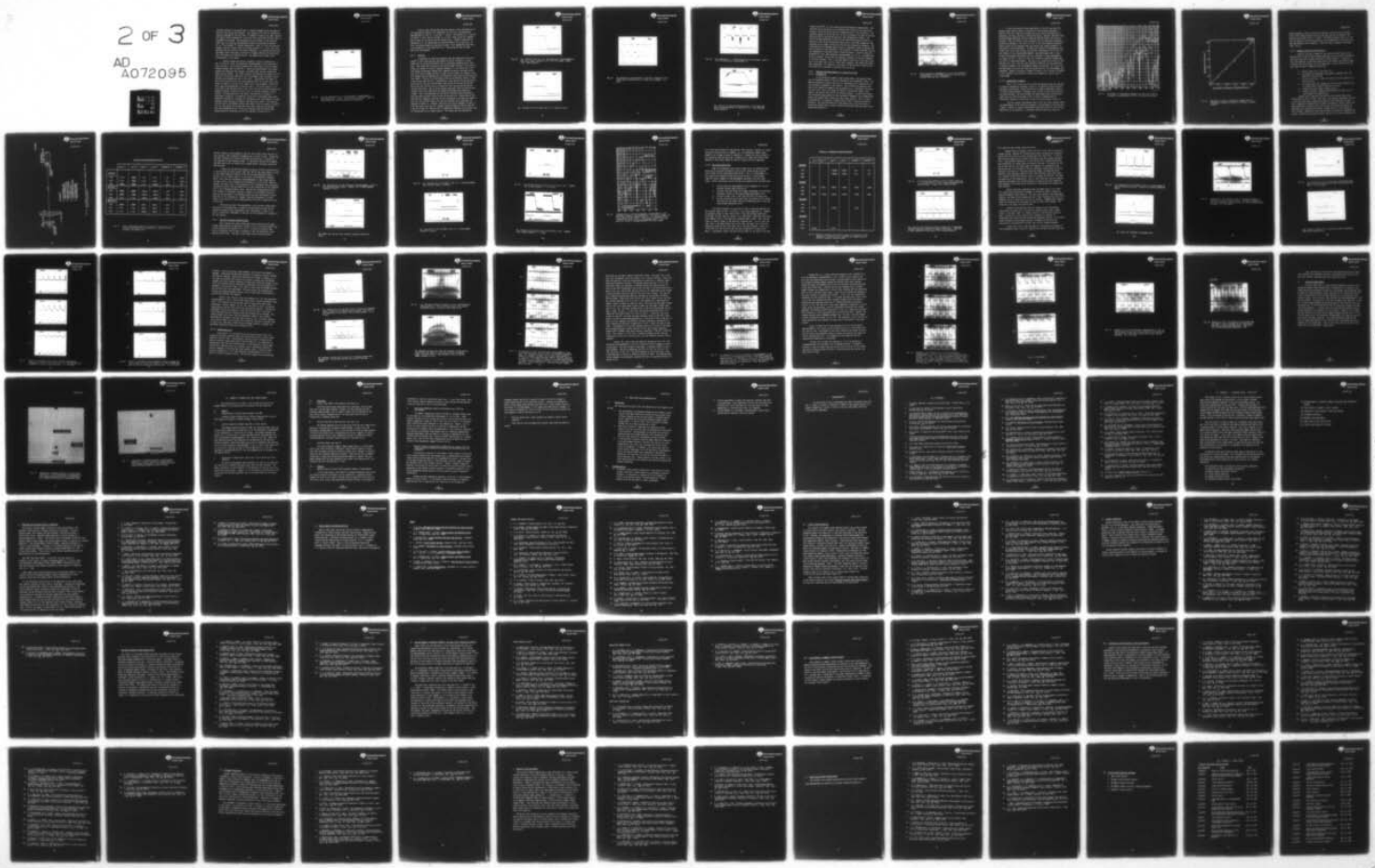

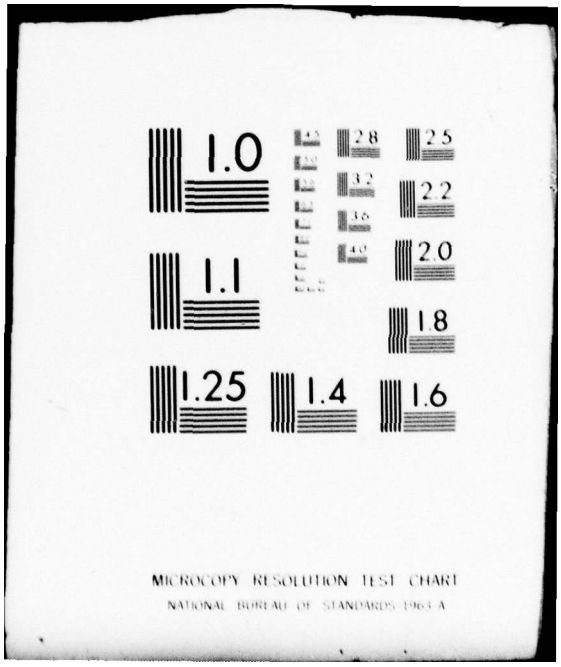
1.0
1.1
1.25
1.4
1.6
2.8
3.2
3.6
4.0
2.5
2.2
2.0
1.8
MICROCOPY RESOLUTION TEST CHART
NATIONAL BUREAU OF STANDARDS-1963-A

(minimum voltage) of the square wave is slightly changed during one sweep of pulses on the storage oscilloscope. The response on the left is optimum and gradually degrades as the bias level is reduced as shown on the lower trace of the figure; similar degradation in turn-off also occurs when the bias level is increased from optimum. The explanation for this effect is not precisely known, but is related to the hysteresis effects as described by Kashnow et al.,[37] and Greubel.[38] Another observation is that in a cell with bare Ge windows, the bias voltage level for optimum response is, in fact, zero volts agreeing with the results in the above references. So, perhaps the bias voltage effect might be related to surface or alignment effects with the dielectric films used for AR coating the Ge. The composition of these films, unfortunately, is not known.

Figure 49 shows the turn-off response of ≈125 ms, measured at λ = 8μm, of the 5 mil thick, 5% cholesteryl nonanoate/BDH E-1 cell described in Figs. 46a and b. The turn-off characteristic shown occurs with an optimum minimum voltage level of about 60 V. Notice the approximately 20 ms delay between the times when the voltage is switched lower and the transmission decay actually begins. This delay time was also observed by Kashnow et al.[37] and has to do with the particular cell pre-alignment used, although no preferential pre-alignment was used in this cell. They observe this delay in their cells with the helix axis pre-aligned parallel to the cell walls; the effect is reduced in thicker cells and/or with a pre-alignment in which the helix axes are perpendicular to the cell walls. From their results, it is surprising to see the delay time in the 5 mil thick cell used here because the purpose of going to thick cells was to try to eliminate potential surface effects. The bump observed in the decay, characteristic of nematic to cholesteric relaxation, is caused by a rotation of birefringent zones which temporarily maintain or increase cell transparency and then decrease in transparency as they continue to rotate to the focal-conic state. This measured turn-off time is considerably faster than those initially reported in Section 4.6.3 of this report giving hope that even faster times can be obtained. A much more comprehensive set of data was obtained using the high-voltage square-wave-drive technique, but will be reported in Section 5.2.4.

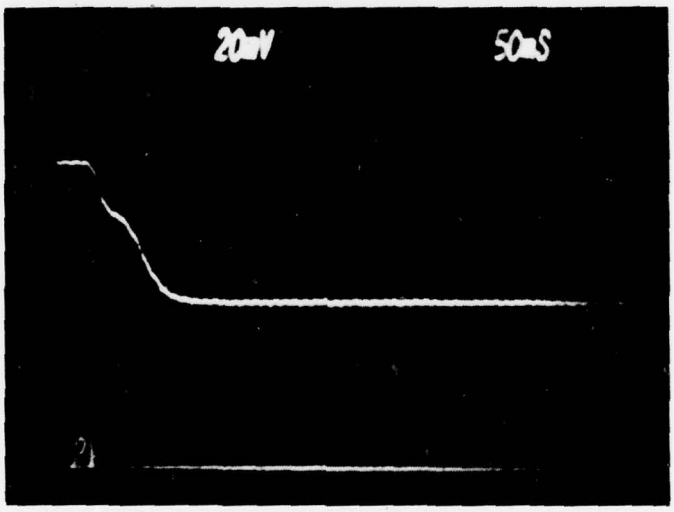

Fig. 49 Turn-off characteristic of 5% cholesteryl nonanoate/BDH E-1 cell measured at λ = 8μm. Turn-off time is ≈125 ms. Note the short delay time (≈20 ms) before decay commences.

Finally, Figs. 50a and 50b show the contrast ratios (defined here as "on" magnitude divided by "off" magnitude) for the 5 mil, 5% cholesteryl nonanoate-BDH E-1 cell at λ = 8μm and λ = 10.6μm. The contrast at λ = 8μm for f/3 optics is 14/1, while at 10.6μm, it is 5.5/1. These ratios will undoubtedly be less for f/1 optics and for thinner cells. Figure 51 shows the response due to a 1 Hz square wave rep rate followed by a 4 Hz rep rate. At 5 Hz, the contrast begins to decrease slightly. This demonstrates the modulation capability of the above cell at λ = 8μm during the time of these particular measurements.

5.2.3 AC Drive

A technique for improving response times was described by Oron and Labes[39] in which they applied simultaneous AC and DC voltages to a phase change cell by using two different sets of electrodes separated by an insulator. They found that using just a DC drive voltage resulted in fast turn-on times, but yielded a turn-off response composed of a fast region and a very slow region lasting many seconds until complete relaxation occurred; using just an AC drive voltage resulted in slower turn-on times, but yielded a turn-off response which eliminated the slow relaxation region while maintaining the fast region. The use of a simultaneous AC-DC drive technique results in both a fast turn-on and turn-off. Unfortunately, since the cell being used had no provisions for two sets of electrodes, just the AC drive alone was applied during the cell turn-on, while a non-zero DC level was applied during the turn-off half-cycle. Due to the DC op-amp being used, only the positive amplitude of the AC was amplified, the negative amplitude being completely clipped. Thus, the experiment did not exactly duplicate that described by Oron and Labes and their results could not be verified. Figures 52a and 52b show the cell response, using the AC drive technique of the same cell shown in Fig. 49. The turn-off times using the two different drive techniques are essentially identical. However, looking at the turn-on response in detail in Fig. 52b, notice that the cell response partially keeps up with the applied 1 kHz AC voltage, but when the cell is completely turned-on (flat region), the AC fluctuations are no longer present. This effect was also observed by

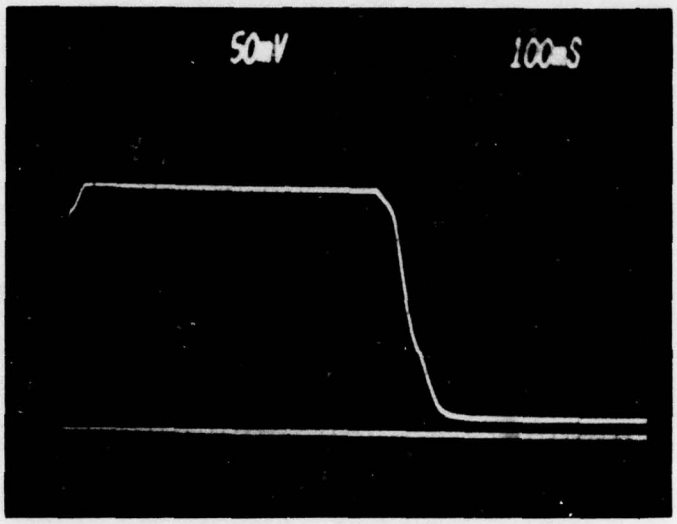

Fig. 50 (a) Contrast ratio of 5 mil, 5% cholesteryl nonanoate/BDH E-1 cell at λ = 8μm. Contrast is 14:1 for f/3 system. (Lower line = beam blocked.)

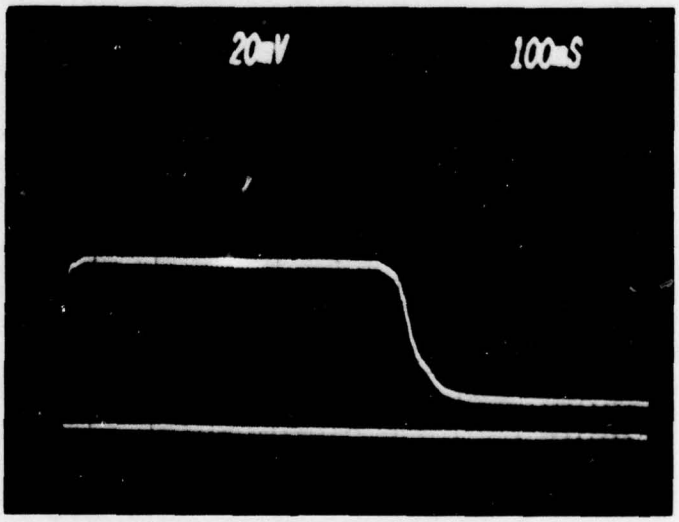

(b) Contrast ratio for above cell at λ = 10.6μm is 5.5:1.

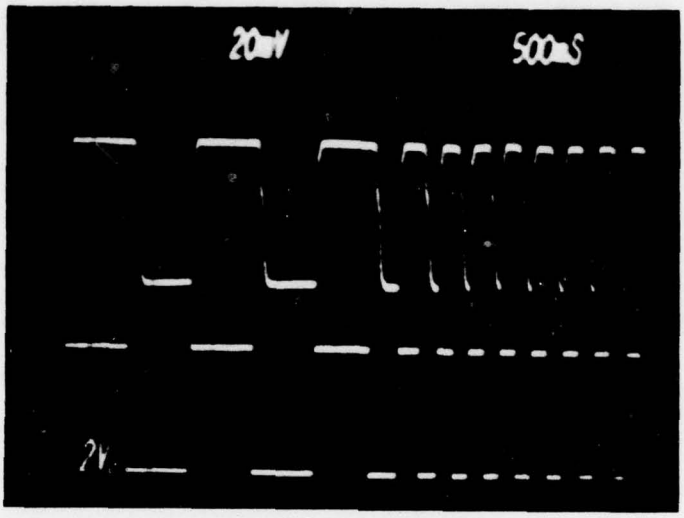

Fig. 51 5% cholesteryl nonanoate/BDH E-1 modulator response at 1 Hz (left side of photo) and 4 Hz (right side of photo). (λ = 8μm.)

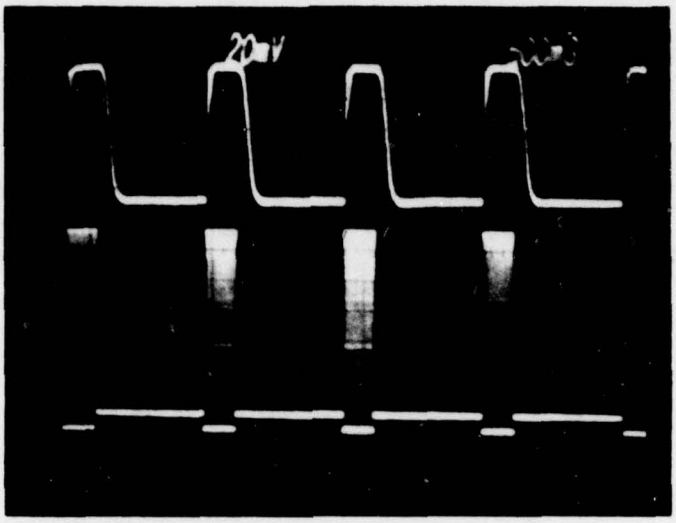

Fig. 52 (a) Response at λ = 10.6μm using AC drive technique. Cell is 5 mil 5% cholesteryl nonanoate/BDH E-1.

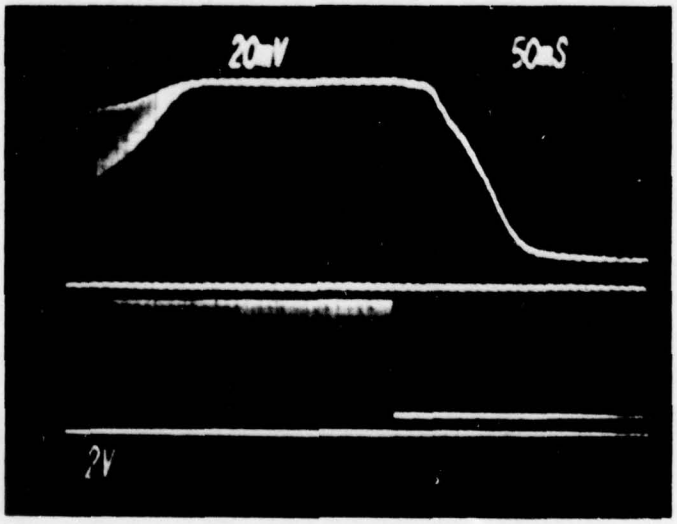

(b) Turn-on and turn-off characteristics, zero lines, and drive voltage waveforms for above cell at λ = 8μm using AC drive technique.

Varney and Davis[40] in a cell containing 10% cholesteryl nonanoate/PCB. They attribute this oscillation to the characteristic nature of the focal-conic texture in which the helix axes are aligned parallel to the cell walls. The molecules making up the helices are initially oriented at an angle to the cell walls and held in position by both wall and intermolecular forces. The ability of these molecules to align to the oscillating electric field is a function of the initial orientation angle, and at very high frequencies, the molecules can no longer follow the field and the fluctuations disappear. The fluctuations also disappear when the cell is completely turned on because the helix structure of the cholesteric liquid crystal is almost destroyed, causing the degradation of the helix elastic restoring forces. Figure 53 shows the response of a 2 mil 10% cholesteryl nonanoate/BDH E-1 cell to a low-amplitude, 30 Hz AC voltage. Notice that the modulator responds at twice the frequency of the drive voltage. This is the same behavior occurring in the turn-on portion of the above cell, but at a much lower frequency, thus making the effect more pronounced. This behavior is the basis of the partially turned-on operating mode to be discussed in Sections 5.2.5 and 5.2.6.

5.2.4 Response Time Measurements as a Function of Pitch

5.2.4.1 Introduction

In the cholesteric-nematic phase change effect, the response times and the threshold electric field are functions of the cholesteric pitch. In a nematic-cholesteric mixture, the pitch is determined by the concentration of the cholesteric component in the mixture. Pure cholesterics generally have small pitch lengths and nematics can be thought of as a cholesteric having an infinite pitch. Thus, the larger the amount of cholesteric added to the nematic, the smaller the pitch of the mixture becomes. In small-pitch materials containing large amounts of the cholesteric component, the intermolecular forces are stronger than in materials with larger pitches. Thus, in small-pitch materials, it requires a higher electric field to distort the helical structure. But once distorted by a high enough field, the strong elastic restoration forces lead to faster relaxation times than those obtained in the longer-pitch materials.

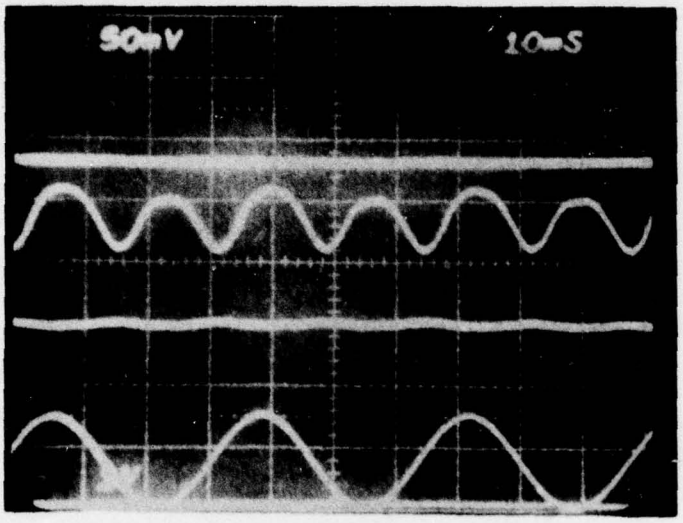

Fig. 53 Double-modulation phenomenon in a 2 mil 10% cholesteryl nonanoate/BDH E-1 cell operated with a 30 Hz AC drive voltage below the cell's threshold.

It was the purpose of these experiments to find out just what the response times actually were as a function of pitch because cholesteric materials with the longer pitch lengths had to be used for optimization of scattering, and thus, contrast in the 8-12μm region. Whatever trade-offs were required between modulator turn-off times and contrast would have to be determined. Also, the effect of cell thickness (Fig. 54 shows the difference in transmission between a 1 mil and 5 mil cell in the field induced transparent nematic state) on the response times and contrast was another parameter investigated in these experiments. An additional reason for experimenting with thicker cells was to help prevent the possible interference of cell wall surface effects on the response measurements. One unfortunate point is that surface pre-alignment experiments were not performed in these measurements. The reason for this is that only four anti-reflection coated Ge windows were available for these measurements. They had to be cleaned and re-used for each measured cell, and it was felt that additional handling with the application of surface treatments could permanently damage the coatings. As it was, the coatings began to scratch and flake off by the time the last measurements were completed. However, according to Varney,[35] there is only a minimal difference in cell response using different surface pre-alignments as long as d/P_o is large enough.

5.2.4.2 Experimental Procedure

Cells 1 mil, 2 mils and 5 mils thick containing 2%, 5%, 10%, and 14% by weight of cholesteryl nonanoate in BDH E-1 (an eutectic mixture of pentyl and heptyl cyanobiphenyl liquid crystals with a nematic temperature range of -2°C-54.3°C) were measured. Response times, contrast ratios, and scattering data were obtained. The pitch lengths for these compositions could be estimated from Fig. 55[41] which shows a plot of pitch vs concentration of cholesteryl nonanoate in PCB, which is one of the constituents of BDH E-1.

Previous response measurements were carried out using a Nernst glower and monochromotor which enabled measurements to be performed at discrete wavelengths. However, to make the measurements more appropriate for the ultimate application of the modulator, a blackbody radiation source was used with

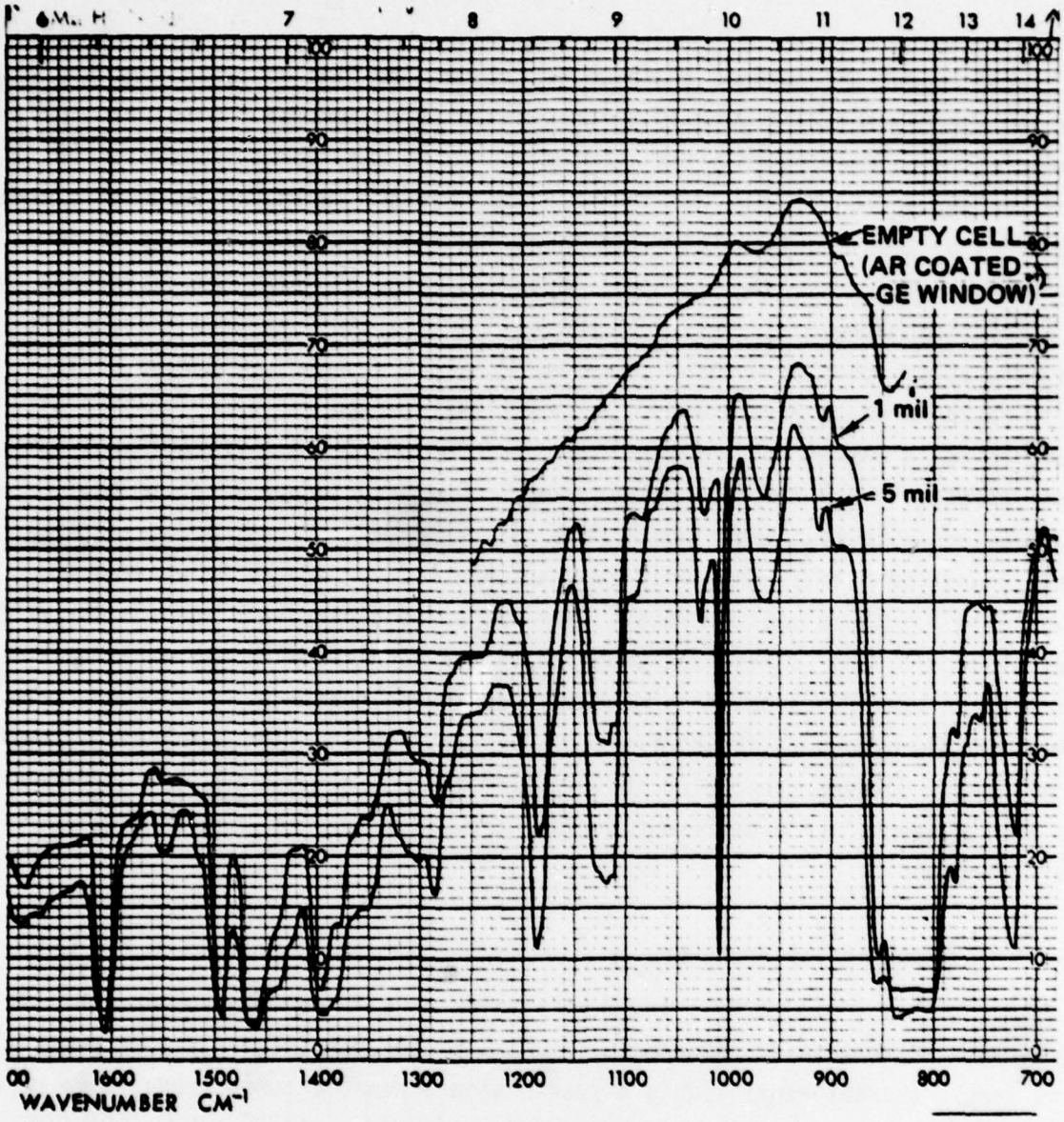

Fig. 54 Difference in transmission between 1 mil and 5 mil thick 5% cholesteryl nonanoate/BDH E-1 cells (AR coated Ge windows).

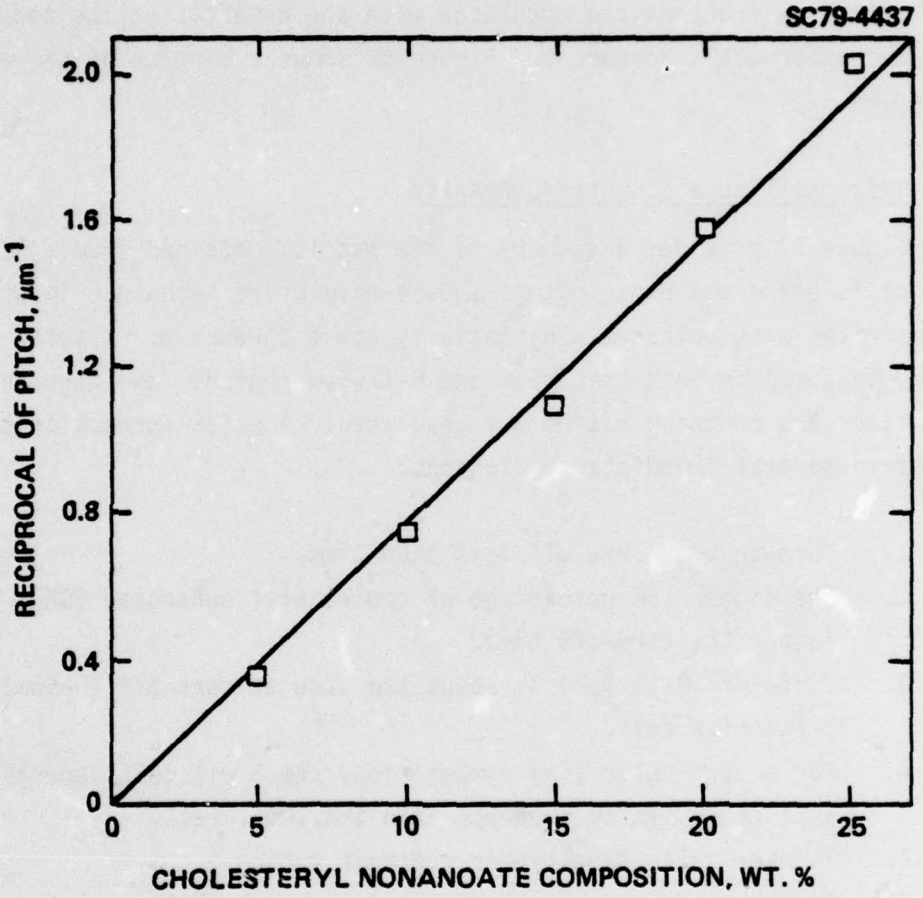

Fig. 55 Reciprocal of pitch vs cholesteric composition for cholesteryl nonanoate dissolved in 4-cyano-4'-n-pentyl biphenyl.

separate bandpass filters covering the complete 3-5μm and 8-11.5μm regions. A 25 mil PbSnTe diode sensitive from 3-11.5μm was used for the detector, the modulator was placed directly in front of the detector dewar, and an f/1.2 Ge lens was placed in front of the modulator with the detector at its focal point when the modulator was transparent. Figure 56 shows a diagram of the experimental set-up.

5.2.4.3 Response Time and Contrast Results

Figure 57 provides a summary of the results obtained from all the measured cells using the high-voltage square-wave drive technique in which the cells are driven with voltages substantially above threshold. A total of 9 cells were measured in both the 3-5μm and 8-11.5μm regions, and turn-on times, turn-off times and contrast ratios are tabulated. A quick inspection of the data leads to several immediate conclusions:

1. Turn-on times are all less than 1 ms.
2. The higher the percentage of cholesteryl nonanoate (CN), the faster the turn-off time.
3. Turn-off (8-11.5μm) is about the same as turn-off (3-5μm) for a particular cell.
4. For a particular (CN) composition, the 5 mil cell generally has a slightly faster turn-off than the 1 mil cell.
5. Thicker cells have higher contrast ratios.
6. Contrast (3-5μm) is greater than contrast (8-11.5μm) for all pitch lengths (CN compositions).

Several cells, especially pertaining to the contrast data, have values which do not fit as well into place. One possible explanation for this is that the cells seem to improve and stabilize the longer they are kept intact, although data supporting this premise are sketchy. Most of these cells were tested over a period of only a day or two, not really long enough to experience this stabilization process. Another factor is that loading the cell involves a compressive force (during which the screws are tightened) and usually a shearing force (getting holes lined up); this loading process quite

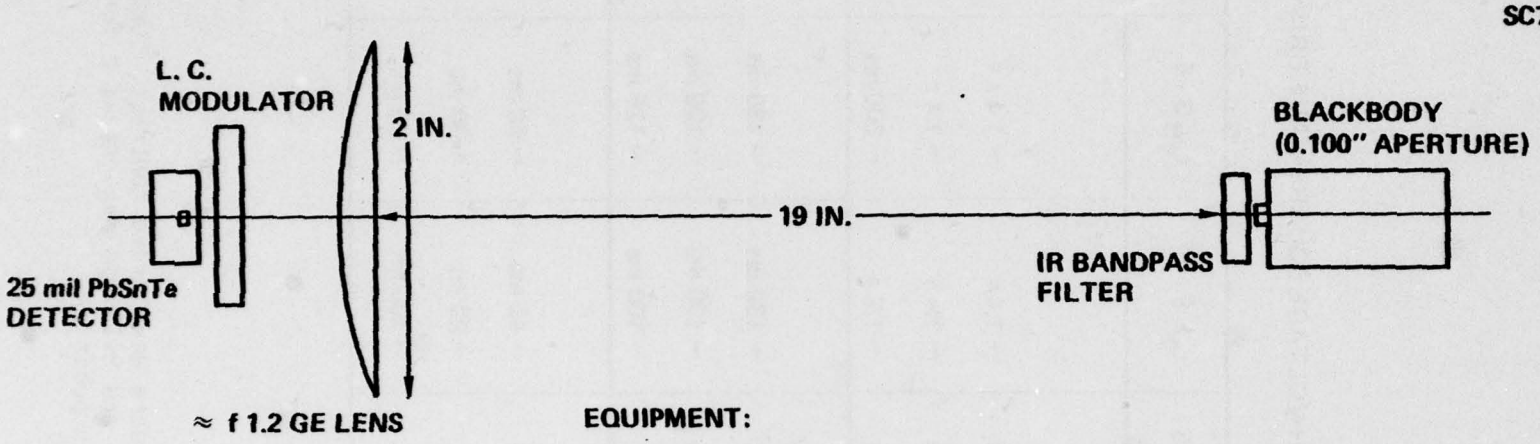

EQUIPMENT:

1) EXACT MODEL 123
   SIGNAL GENERATOR
2) BURLEIGH PZ-70 HIGH
   VOLTAGE D. C. OP-amp
3) TEKTRONIX 7834
   STORAGE OSCILLOSCOPE
4) TEKTRONIX PG-502
   PULSE GENERATOR

Fig. 56 Experimental set-up for modulator response time and contrast measurements.

HIGH-VOLTAGE SQUARE-WAVE DRIVE

	t_{on} 8 - 11	t_{on} 3 - 5	t_{off} 8 - 11	t_{off} 3 - 5	Contrast 8 - 11	Contrast 3 - 5
2% CN/E-1						
1 mil	< 1 ms	~ 500μs	~ 1.4 s	~ 1.4 s	~ 2:1	~ 4.5:1
2 mil	< 1 ms	~ 500μs	~ 1.4 s	~ 1.4 s	~ 2:1	~ 3.5:1
5 mil	~ 400μs	~ 500μs	~ 1.2 s	~ 800 ms	~ 8.5:1	~ 8:1
5% CN/E-1						
1 mil	~ 250μs	~ 500μs	~ 130 ms	~ 150 ms	~ 1.8:1	~ 6.4:1
2 mil	~ 250μs	~ 250μs	~ 100 ms	~ 125 ms	~ 1.9:1	~ 3.3:1
5 mil	< 1 ms	< 1 ms	~ 100 ms	~ 125 ms	~ 2.5:1	~ 6:1
10% CN/E-1						
1 mil	~ 250μs	~ 250μs	~ 40 ms	~ 50 ms	~ 1.9:1	~ 3.1:1
2 mil	< 1 ms	< 1 ms	~ 20 ms	~ 30 ms	~ 1.4:1	~ 3:1
5 mil	< 1 ms	< 1 ms	~ 300 ms	~ 60 ms	~ 3.5:1	~ 4.1:1

Fig. 57 High voltage Square Wave drive contrast, turn-on and turn-off values in 3-5μm and 8-11.5μm regions as a function of cell thickness and composition.

possibly imparts a pre-alignment to the cell walls which varies from cell to cell and most likely gradually disappears over a period of time. Figures 58a and 58b illustrate this process by showing the difference in contrast of a cell measured on two consecutive days. If deliberate surface pre-alignments had been used as well as sealed cells, perhaps better uniformity would have been obtained.

Figures 59a and 59b show examples of typical turn-off characteristics in the 8-11.5μm and 3-5μm regions, and Figs. 60a and 60b show examples of some of the highest measured contrast ratios for the same wavelength regions. Finally, Fig. 61 shows a plot of a 1 mil thick, 5% cholesteryl nonanoate/ BDH E-1 cell taken on the Beckman spectrophotometer in the 8-12μm regions. The upper curve is the transmission of the empty cell with two AR coated Ge windows, the lower curve is the transmission of the Grandjean semi-transparent cholesteric texture, and the middle curve is the transmission of the turned-on cell in the transparent nematic state. Because the voltage-adjusted focal-conic texture is metastable, wanting to return to the Grandjean texture, it could not be monitored in its maximum scattering state long enough to make a good plot of its transmission. However, the point designated at ≈10.8μm refers to the location of the voltage-adjusted focal-conic transmission level in this cell.

During the course of the experiments, using the high voltage square wave drive as discussed above, a partially aligned operating mode for the cholesteric-nematic phase transformation was investigated in some of the cells; a significant improvement in the cell turn-off mechanism is reported in the next section.

5.2.5 Partially Turned-On Operating Mode

After several cells had already been characterized using the high-voltage square-wave-drive technique, a remark by Fray, Hilsum and Jones[23] came to mind concerning the operation of a cell in a partially turned-on mode. With this technique, the voltage is adjusted so that the cholesteric pitch remains always finite. The axes of the liquid crystal molecules remain

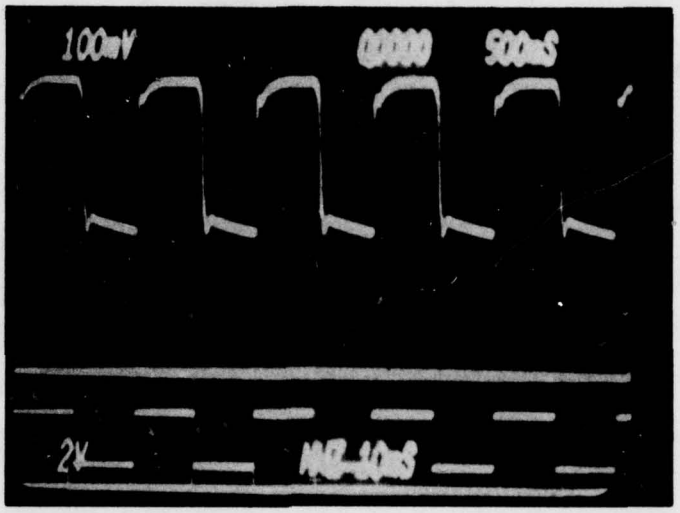

Fig. 58 (a) Contrast of 5 mil 5% cholesteryl nonanoate/BDH E-1 cell in 8-11.5μm wavelength region. (Middle line is beam blocked.) Contrast is 2.2:1.

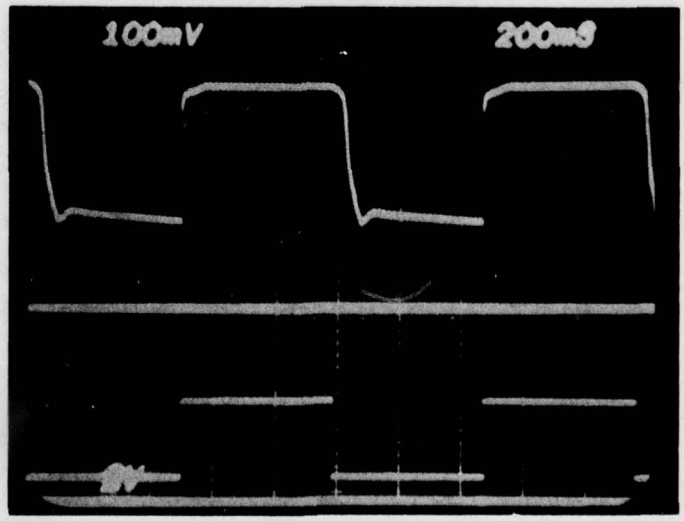

(b) Above cell one day later showing increased contrast of 2.9:1.

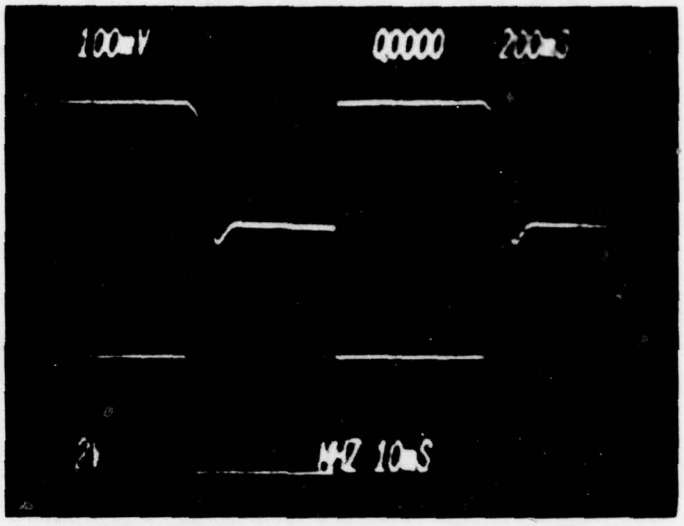

Fig. 59 (a) Turn-off of 2 mil 5% CN/E-1 cell in λ = 8-11.5μm region. Fast turn-off region is ~100 ms.

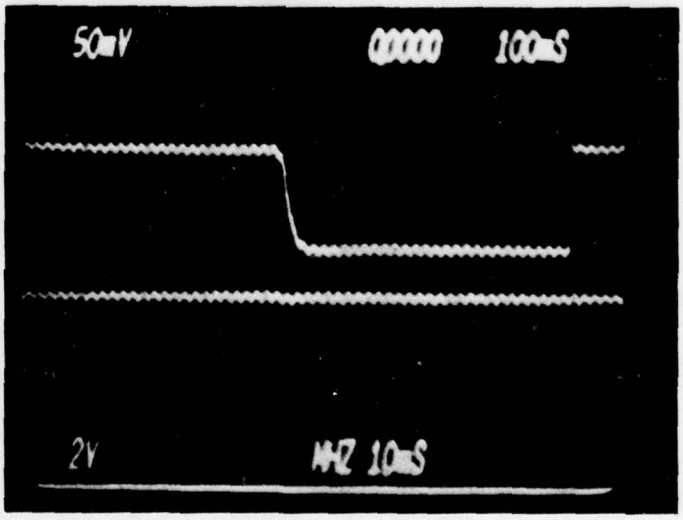

(b) Turn-off of 1 mil 10% CN/E-1 cell in λ = 3-5μm region. Turn-off is ~50 ms.

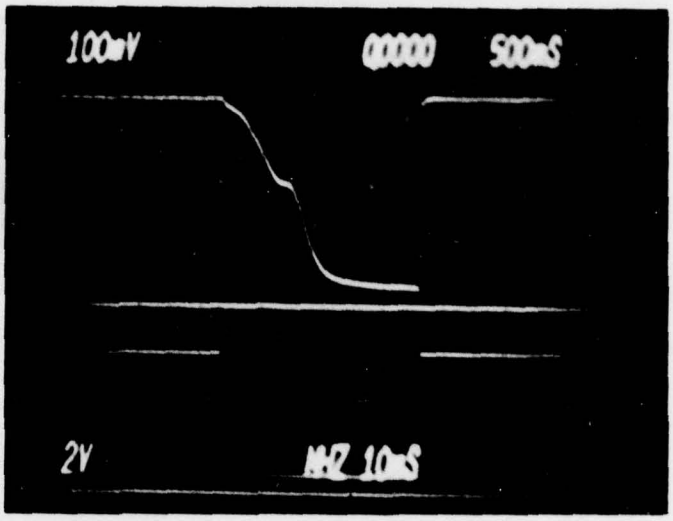

Fig. 60 (a) Contrast ratio (7:1) for 5 mil 2% CN/E-1 cell. (Center line is beam blocked.) λ = 8-11.5μm.

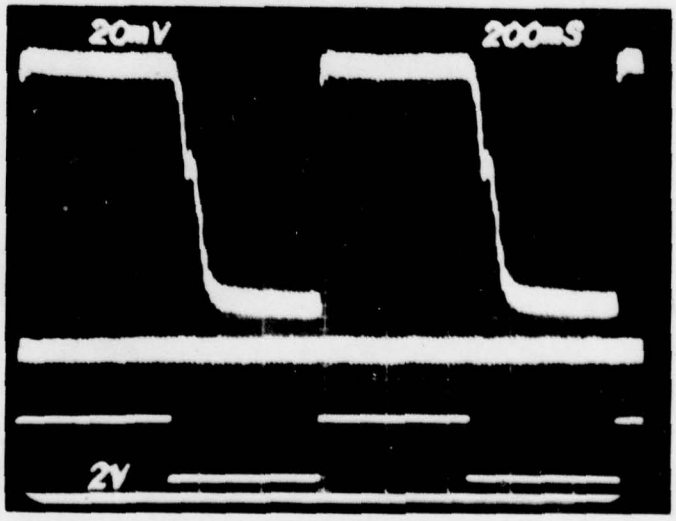

(b) Contrast ratio (6.4:1) for 1 mil 5% CN/E-1 cell. (Center line is beam blocked.) λ = 3-5μm.

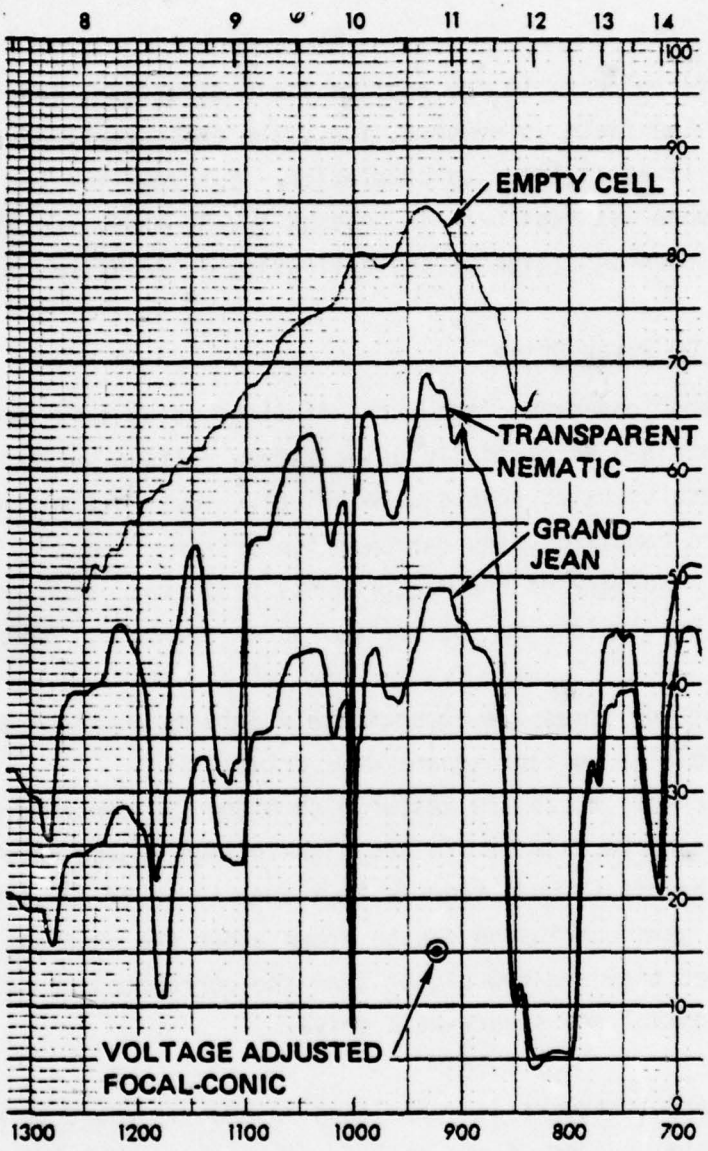

Fig. 61 Transmission of 1 mil 5% cholesteryl nonanoate/BDH E-1 cell measured on Beckman spectrophotometer. Top curve is empty cell with 2 AR-coated Ge windows, lower curve is Grandjean state transmission, middle curve is transparent nematic state, and point at ≈10.8μm is voltage-adjusted focal-conic state.

in a tilted state relative to the applied field direction, leading to a faster relaxation once the field is removed, i.e., the cholesteric-nematic phase change is not allowed to occur to completion. Evidence for the existence of this operating mode was seen back in Section 5.2.3, where oscillations were observed in the turn-on region of the cell using an AC drive technique.

5.2.5.1 Narrow DC Pulse Drive

When first observed, fast turn-off times using this operating mode could only be obtained successfully using narrow voltage pulses (Section 5.2.5.2 shows results using square-wave drive). Thus, all measurements in this section were compiled using narrow pulse drives of varying shapes. Figure 62 gives a summary of the measurements performed using this technique. Several conclusions can be arrived at by examining the available data:

1. Turn-on times are approximately 5-10 ms compared to <1 ms for the high voltage square wave drive.
2. Turn-off times are faster with higher percentages of cholesteryl nonanoate, similar to the high-voltage square-wave drive.
3. Turn-off (3-5μm) time is less than turn-off (8-11.5μm) time.
4. No hard conclusion can be drawn about the contrast ratios except that they are now higher than the corresponding cells using the high-voltage square-wave drive.

The fourth statement is surprising in that it would be expected that the contrast should be less if the cell is not turned completely on. However, as apparently shown in Figs. 63a and 63b, in the high-voltage square-wave drive mode, the cell does not return to the focal-conic scattering state after field removal, while in the partially turned-on mode it does. Thus, the contrast is actually larger in the partially turned-on cell. (In Fig. 63a, the lower line is the beam blocked, and in Fig. 63b, the upper line is the cell completely turned-on while the lower line is the beam blocked). Notice also in Fig. 63b that the turn-off time from peak transmission is about 40 ms, which is considerably faster than the turn-off shown in Fig. 63a for the same

PARTIALLY TURNED-ON OPERATING MODE

	t_{on} 8 - 11	t_{on} 3 - 5	t_{off} 8 - 11	t_{off} 3 - 5	Contrast 8 - 11	Contrast 3 - 5
2% CN/E1						
1 mil			~ 125 ms	~ 25 ms	~ 6:1	~ 2:1
2 mil			~ 100 ms	~ 40 ms	~ 4:1	~ 3:1
5 mil						
5% CN/E1						
1 mil	~ 8 ms	~ 3 ms	~ 20 ms	~ 10 ms	~ 4.6:1	~ 8.6:1
2 mil						
5 mil	~ 5 ms	~ 10 ms	~ 40 ms	~ 18 ms	~ 4.6:1	~2.6:1
10% CN/E1						
1 mil						
2 mil	~ 5 ms		~ 10 ms		~ 2.9:1	
5 mil						
14% CN/E1						
1 mil						
2 mil						
5 mil	~ 10 ms		~ 5 ms			

Fig. 62 Contrast, turn-on, and turn-off values in 3-5μm and 8-11.5μm regions as a function of cell thickness and composition for partially turned-on operating mode.

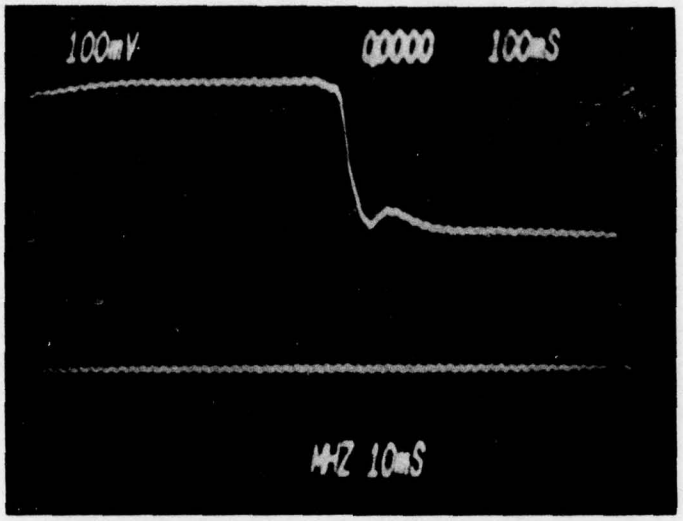

Fig. 63 (a) Turn-off and contrast of 5 mil 5% CN/E-1 cell in λ = 8-11.5μm region in high-voltage square-wave drive operating mode. (Lower line is beam blocked.)

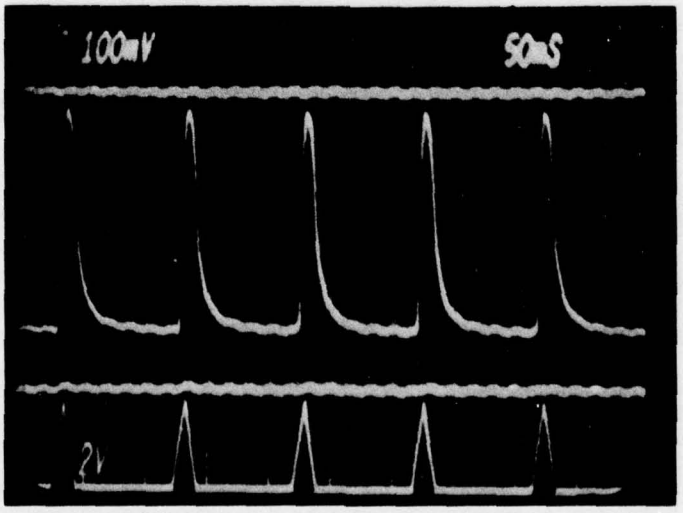

(b) Turn-off and increased contrast of above cell in partially turned-on operating mode with triangle pulse drive. (Top line is cell completely on and center line is beam blocked.)

cell using the high voltage square wave drive.

Another point to be made is that the drive in Fig. 63b is a series of triangle pulses. Besides the triangle pulses shown, haversine and rectangular pulses were also tried as driving voltages (See Figs. 64a and b). It may be that the pulse shape can be tailored to produce an optimum response characteristic. One important observation is that the partially turned-on mode works most effectively for pulses which are narrow at the peak. The reason for this can be seen from Fig. 65, which shows the response to a rectangular pulse. Notice that the cell continues to turn-on (increases transmission) during the duration of the pulse; if the pulse were wide enough, the molecules would gradually align precisely parallel to the field direction rather than remain in a slightly tilted state and thus lead to a larger turn-off time. One problem grows out of this observation: this is that a 50% duty cycle for optimum modulator performance will be more difficult to obtain using this operating mode because of the narrow pulses required for simultaneous fast response and high contrast.

Several additional experiments were performed using a 5 mil thick cell containing 5% cholesteryl nonanoate in EM Labs ZLI-1083, a mixture of phenylcyclohexane liquid crystals. This particular material was investigated because it had good 8-12μm transmission and a lower viscosity than that of the biphenyls (21 cP vs about 40 cP for the E-1 mixture). Remember that response times are optimized for low viscosity as well as short pitch lengths. The values of $\Delta\varepsilon$ are about the same for both.

Figures 66a and 66b show the cell response in the high-voltage square-wave drive mode and in the partially turned-on mode using triangle pulses. Once again, there is a faster turn-off in the partially turned-on mode. Figures 67a, b and c show the cell response as a function of rectangular pulse width with the voltage and frequency constant. As the pulse width increases causing greater molecular alignment and the resulting destruction of the cholesteric helices, the turn-off response degrades.

Figures 68a, b and c show the effect of increasing the frequency of the rectangular pulses on the cell response with voltage and pulse width kept

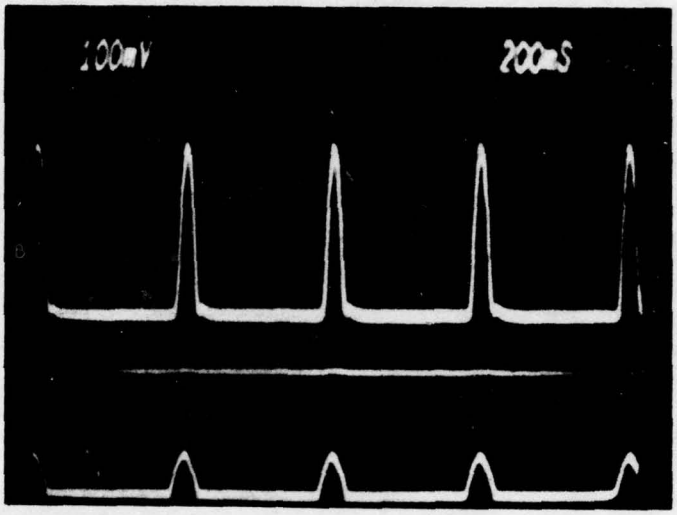

Fig. 64 (a) Response of 5 mil 5% CN/E-1 cell in 8-11.5μm region to series of Haversine pulses. (Partially turned-on operating mode.)

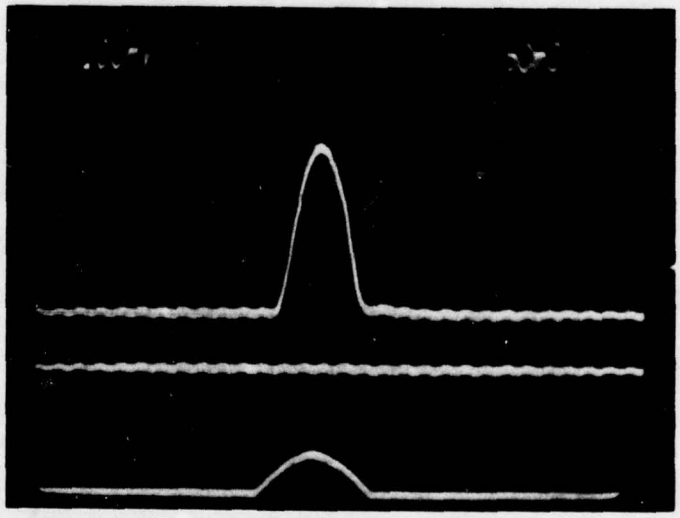

(b) Above cell response on expanded scale.

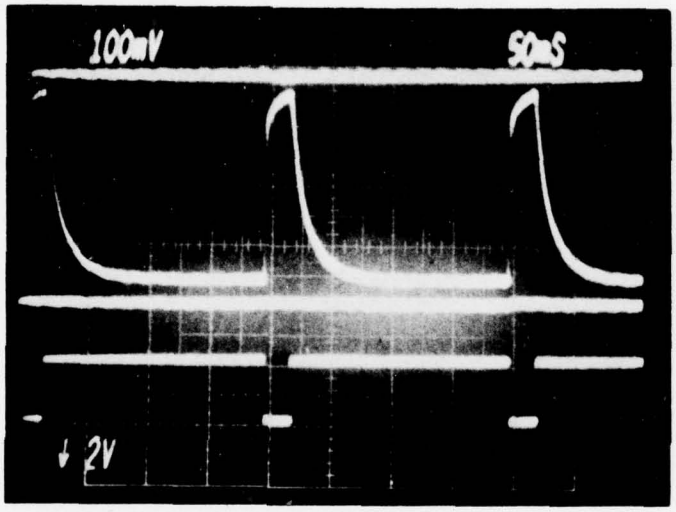

Fig. 65 Response of 5 mil 5% CN/E-1 cell to rectangular pulses in partially turned-on operating mode. Transmission begins to approach completely turned-on level (top line) during duration of pulse. (λ = 8-11.5μm.)

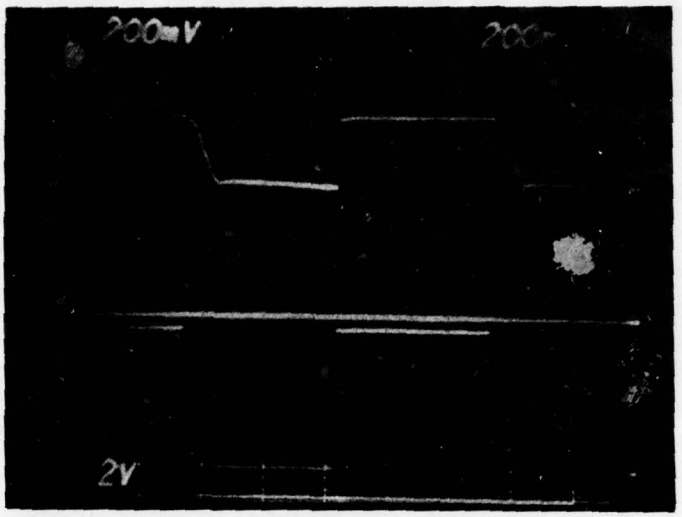

Fig. 66 (a) Turn-off of 5 mil 5% *cholesteryl nonanoate*/EM 1083 phenylcyclohexane mixture with high-voltage square-wave drive. (λ = 8-11.5μm.)

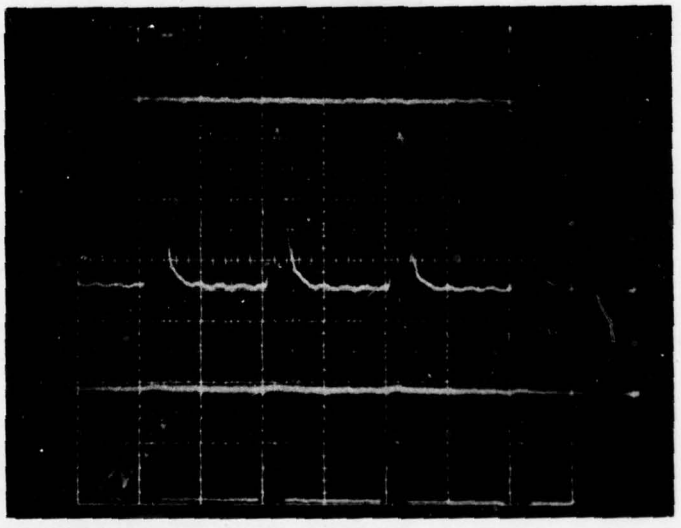

(b) Turn-off of above cell in partially turned-on operating mode using triangle drive.

(a)

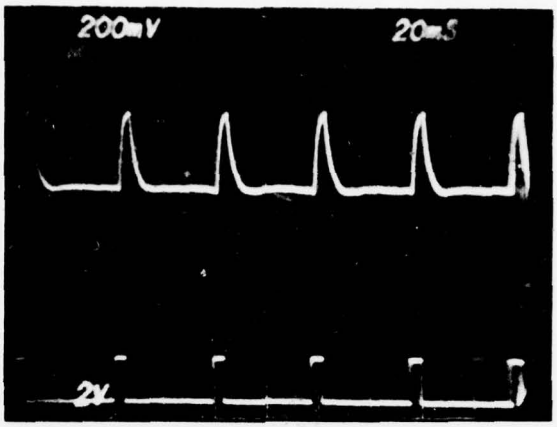

(b)

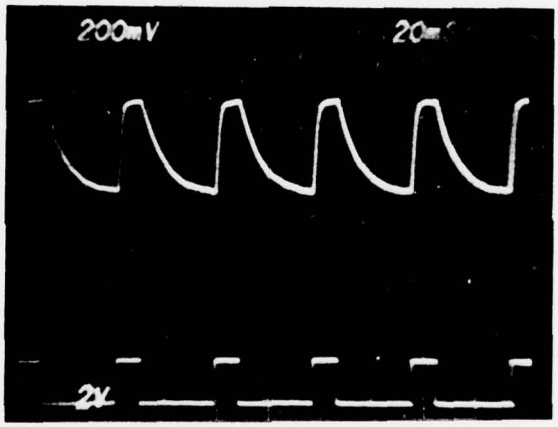

(c)

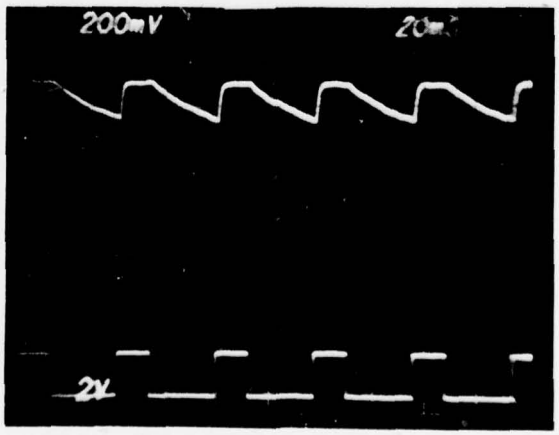

Fig. 67 Effect of rectangular pulse width (constant voltage and frequency) on turn-off and contrast of 5 mil 5% CN/EM 1083 cell in partially turned-on operating mode. (λ = 8-11.5μm.)

(a)

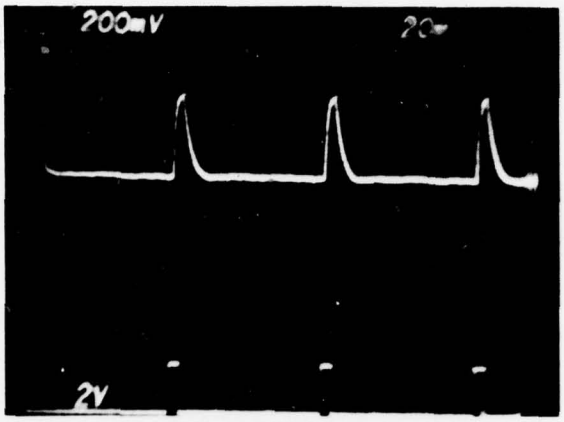

(b)

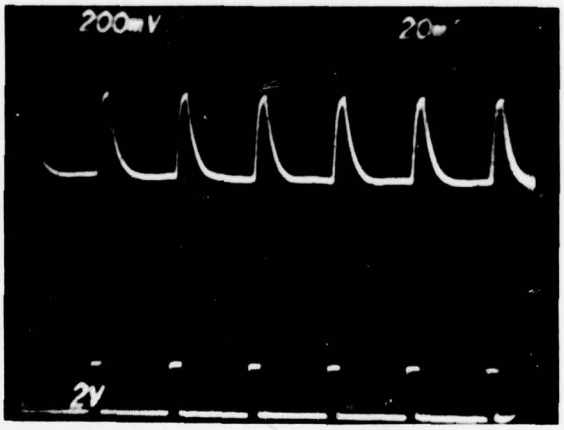

(c)

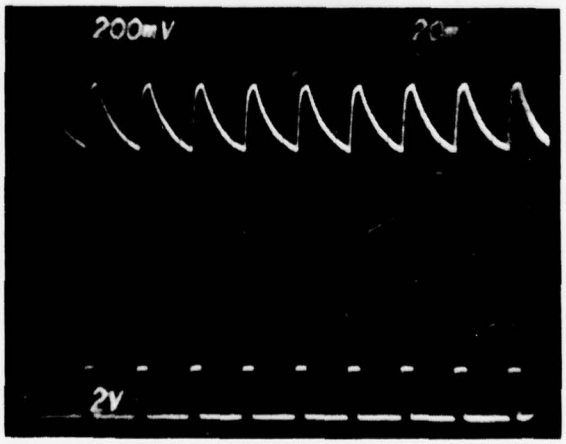

Fig. 68 Effect of rectangular pulse frequency (constant voltage and pulse width) on turn-off and contrast of 5 mil 5% CN/EM 1083 cell in partially turned-on operating mode. (λ = 8-11.5μm.)

constant. As the pulses get closer together, the turn-off also begins to degrade. Figures 69a and 69b show the effect of voltage on the cell contrast and turn-off response. When the triangular drive voltage is reduced, as in Fig. 69b, the contrast and turn-off also reduce as shown; with the reduced voltage, the liquid crystal molecules are even more tilted with respect to the field, thus maintaining the high elastic restoration force and leading to a decrease in the turn-off time. Thus, there is some trade-off between contrast and turn-off time to be considered. This was the only cell measured containing the phenylcyclohexane mixture, and no further work was performed to optimize the contrast and response.

Finally, Figs. 70a and b show the response of a 5 mil 14% cholesteryl nonanoate/BDH E-1 cell in the 8-11.5μm region using a narrow rectangular pulse drive. This material had the smallest pitch of any mixture used in the experiments. Notice, however, in Fig. 70a, that there is still a relatively large contrast even with this small-pitch cholesteric material. The obvious advantage of using this material is that the turn-off time is very fast. Figure 70b shows the cell response using two different drive voltages. The lower response curve occurs with the cholesteric material just slightly perturbed and indicates a turn-off time of about 2.5 ms. The upper response curve using a higher drive voltge clearly shows the increase in turn-off time to about 5 ms, once again reflecting the increased molecular alignment and decreased restoration forces with increasing field.

5.2.5.2 Square-Wave Drive

This section is a continuation of the previous section which discussed the partially turned-on mode using narrow pulse drive to obtain faster modulator turn-off times. Unfortunately, the use of narrow voltage pulses does not provide a square-wave output from the modulator. By additional experimentation with the drive-voltage levels, it was possible to obtain modulation with a 50% duty cycle, but, however, with a considerable decrease in contrast compared to that obtained using narrower pulses. Figure 71a shows the usual response of a 2 mil, 10% cholesteryl nonanoate/BDH E-1 cell to a series of narrow rectangular pulses. The contrast ranges from the scattering

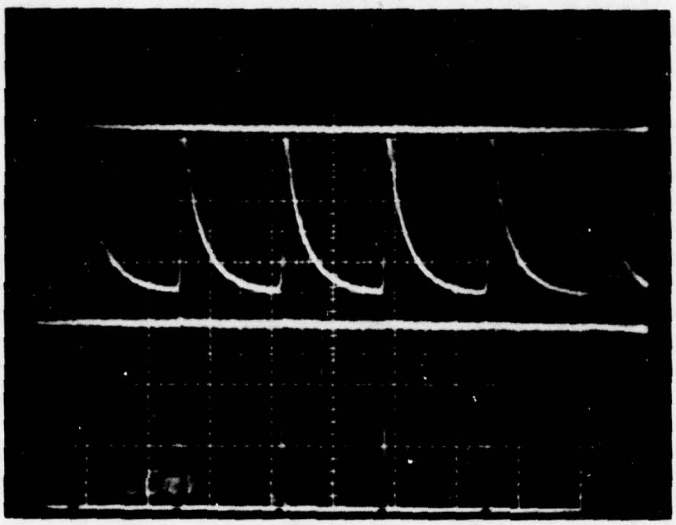

Fig. 69 (a) Response of 1 mil 2% CN/E-1 cell to series of triangular pulses in partially turned-on operating mode. (Top line is cell completely on and center line is beam blocked.) λ = 8-11.5μm.

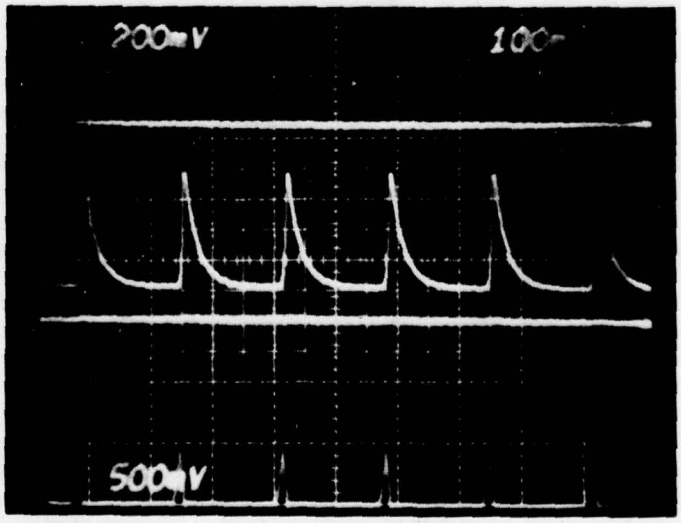

(b) Response of above cell to series of triangular pulses with reduced gain. Notice that contrast and turn-off time are reduced.

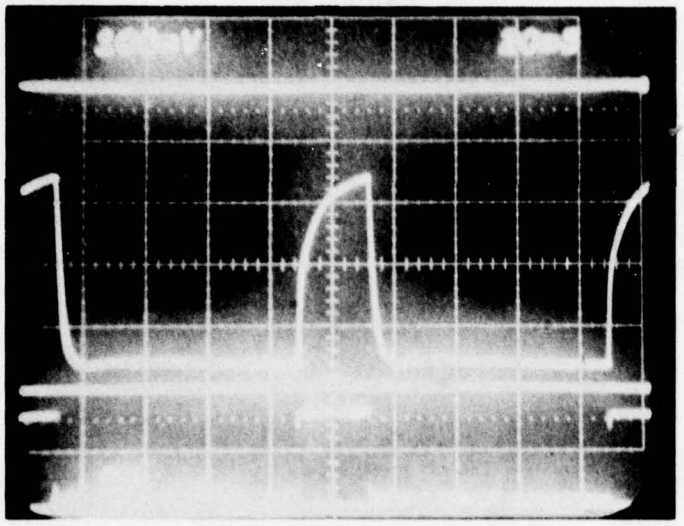

Fig. 70 (a) Partially turned-on response of 5 mil 14% cholesteryl nonanoate/BDH E-1 cell in 8-11.5μm region using narrow rectangular pulse. Turn-off is less than 10 ms.

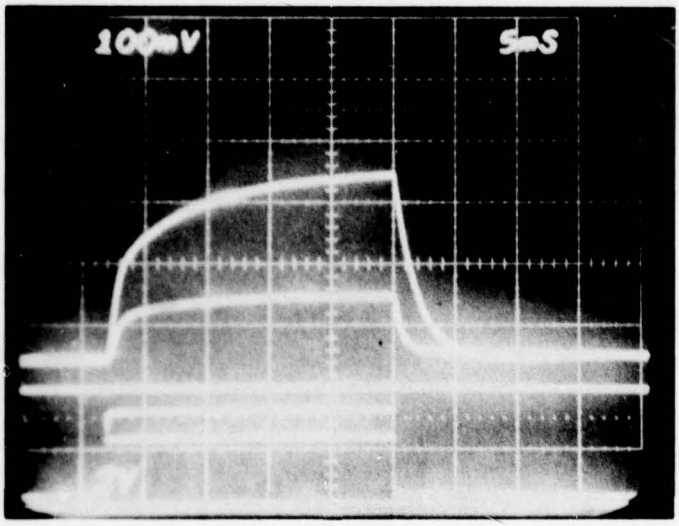

(b) Response of above cell with two different voltage pulses illustrating the effect of increasing voltage on response times. Turn-off time for lower voltage is ≈2.5 ms and for higher voltage is ≈5 ms.

(a)

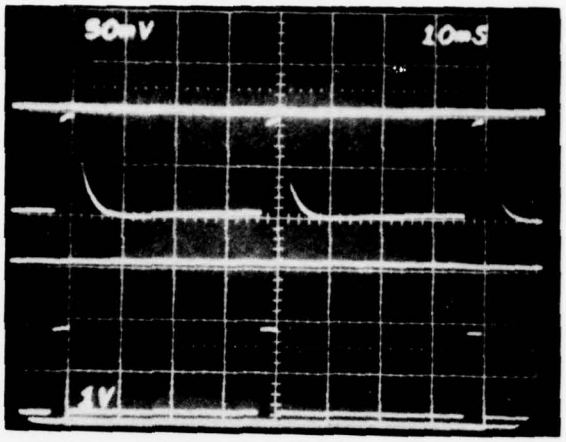

(b)

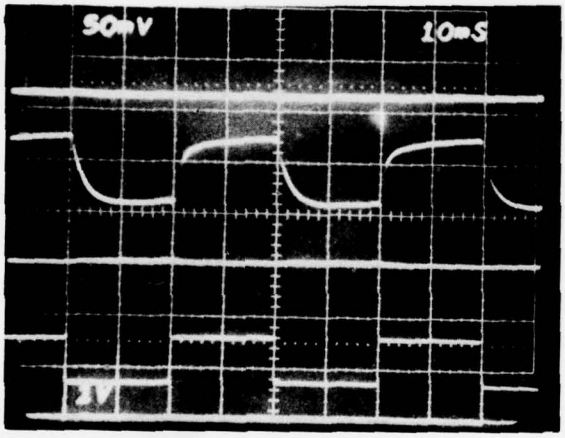

(c)

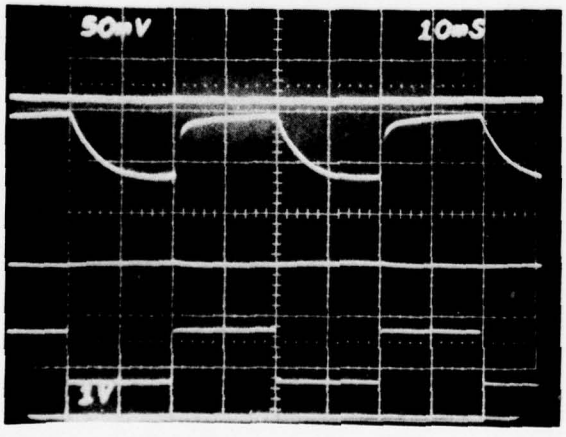

Fig. 71 (a) Response of 2 mil 10% cholesteryl nonanoate/BDH E-1 cell to narrow rectangular pulses in partially turned-on operating mode. (b) response of above cell to square-wave pulses in partially turned-on operating mode showing resulting reduction in contrast. (c) response of above cell to square-wave pulses of higher amplitude showing resulting increase in turn-off time and cell or state transmission. Effective contrast remains about the same.

focal-conic to the nearly nematic transparent states. The upper line is the cell fully transparent, while the center line is the beam blocked. Figure 71b shows the same cell using the square-wave-drive technique to achieve a nearly square wave modulator response. The maximum scattering level is still the focal-conic state, but the point of maximum transmission does not occur as close to the fully transparent line as with the case of the narrow pulse drive seen in Fig. 71a. Notice that the bias level of the square-wave drive voltage is quite different than that used for the pulse drive voltage. This was the key to obtaining square-wave modulator response in the partially turned-on operating mode. Notice also that the turn-off time is about 5-6 ms, the fastest turn-off measured up to this point of the program for a square-wave response. Figure 71c shows the same cell again, this time with the upper voltage level of the drive square-wave slightly higher than the upper voltage level used in Fig. 71b. The lower voltage levels of the drive square-waves are the same in Figs. 71b and c. In this case, the maximum scattering level is no longer the focal-conic state as in Fig. 71a and b. In addition, the transmission of the cell's on state has been increased closer to the fully transparent line with an associated degradation in the turn-off time of the cell to about 11-12 ms. However, the effective contrast (defined as transmission on minus transmission off/total transmission of cell) is about the same in both cases. The degradation in turn-off response occurs as a result of the higher drive voltage causing a greater rotation of the liquid crystal molecules toward field alignment, once again causing a reduction in the helix restoring force. Thus, there is in this case a trade-off between turn-off time and transmission of the cell in the on state, with the effective contrast being a constant.

Figures 72a, b and c show the modulator response of the 2 mil, 10% cholesteryl nonanoate/BDH E-1 cell as a function of drive frequency in the 8-11.5μm region. The bias voltage in each photo is adjusted slightly to optimize response. The drive frequencies are 30 Hz in Fig. 72a, 50 Hz in Fig. 72b, and 100 Hz in Fig. 72C. The 100 Hz modulation occurs with only a very slight decrease in the cell's effective contrast of ~45%. This measured modulation frequency is considerably improved over the 4 Hz reported initially in Section 5.2.2.

(a)

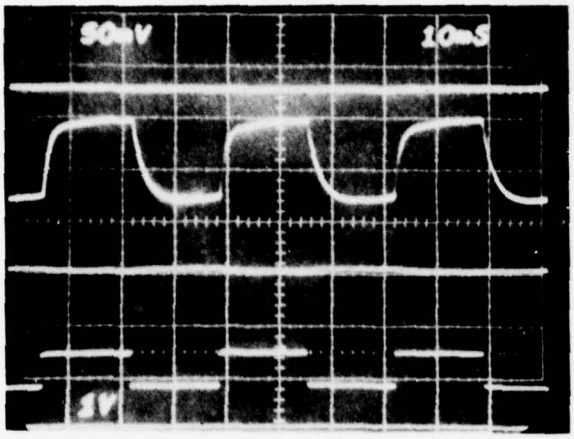

(b)

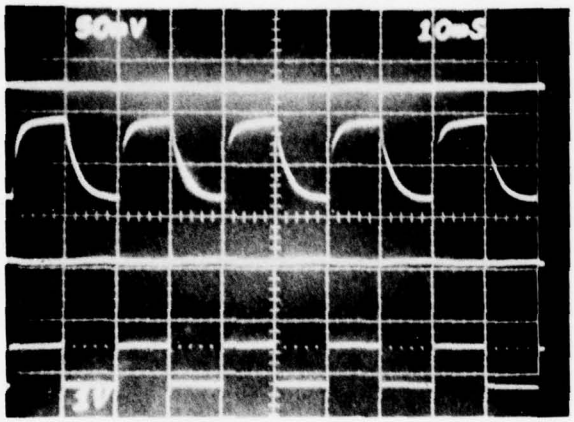

(c)

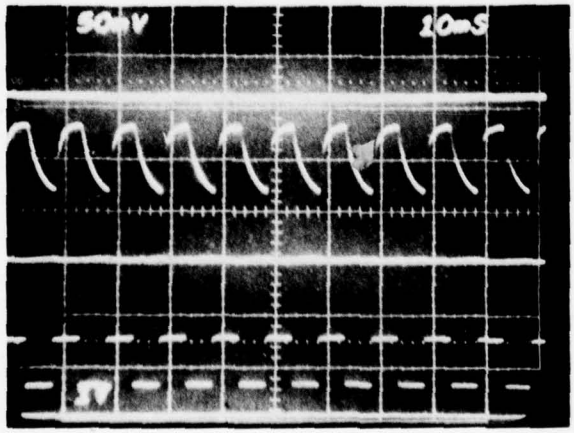

Fig. 72 (a) Response of 2 mil 10% cholesteryl nonanoate/BDH E-1 cell to 30 Hz rep rate square-wave pulses in partially turned-on operating mode. (b) Response of above cell to 50 Hz rep rate square-wave pulses. (c) Response of above cell to 100 Hz rep rate square-wave pulses showing only slight decrease in effective contrast.

Figures 73a, b, c, d and e show the sequence of cell response for a 5 mil 5% cholesteryl nonanoate/BDH E-1 cell in the 8-11.5μm region as the 10 Hz rep rate square-wave drive voltage is biased upward in each figure with the voltage difference between maximum and minimum levels kept constant. Figure 73a shows the response using a low drive voltage; the scattering level is the focal-conic state. Figures 73b show the response using a slightly higher voltage; the transmission in the on state increases and the scattering level is still the focal-conic state. Figure 73c and d shows the response as the drive voltage is increased even further. In Fig. 73c, the transmission increases, but the scattering level is no longer the focal-conic state, while in Fig. 73d, the transmission again increases slightly while the amount of scattering again decreases resulting in a decreasing effective contrast. Finally, in Fig. 73e, the cell is just about completely transparent in the on state, while the scattering, turn-off, and effective contrast have further degraded. The fastest turn-off time occurs in Fig. 73 a, where the cholesteric helix structure is least perturbed from its equilibrium state. However, the highest contrast occurs somewhere between Figs. 73 b and c, and the highest on-state transmission occurs in Fig. 73e. The trade-offs in cell turn-off, on state transmission, and contrast are thus clearly illustrated in the above figures.

Figure 74 shows the 8-11.5μm response of a 5 mil 5% cholesteryl nonanoate/BDH E-1 cell using a drive voltage having an on time slightly less than the off time. The purpose of this was to equalize the widths of the on and off times of the modulator output by taking into account the longer fall time of the modulator cell. This produced the best measured turn-off time/contrast combination of ~20 ms/55%.

Finally, Fig. 75 shows the response of a 5 mil 5% cholesteryl nononoate/EM 684 cell (EM 684 is also a biphenyl mixture). Although the contrast is now up to about 70%, the turn-off time of ~30 ms is also higher, once again illustrating the difficulty in obtaining both high contrast and fast turn-off times.

(a)

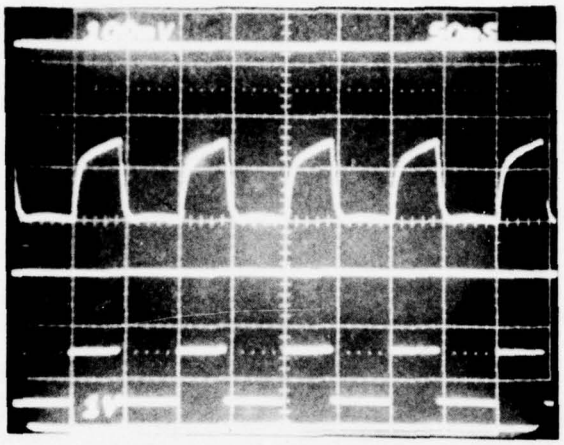

(b)

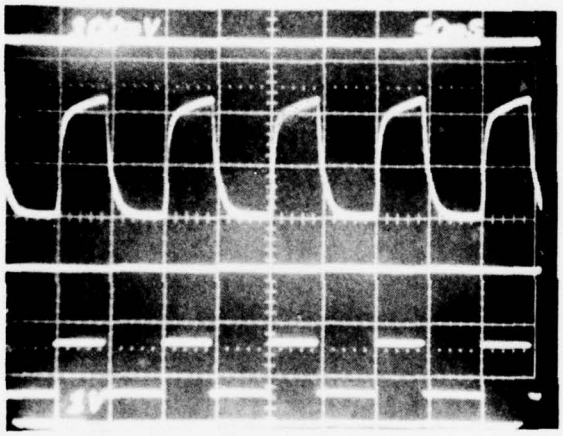

(c)

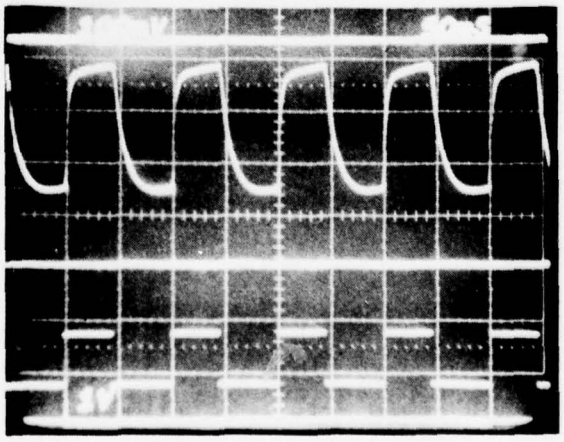

Fig. 73 Sequence of cell response of a 5 mil 5% cholesteryl nonanoate/BDH E-1 cell to a 10 Hz rep rate square wave with variable bias level. (a) shows the response using a low drive voltage, (b, c) show the highest effective contrasts, (d) shows the cell almost completely turned-on and (e) shows the response and reduced contrast of the completely turned-on cell. (λ = 8-11.5μm.)

(d)

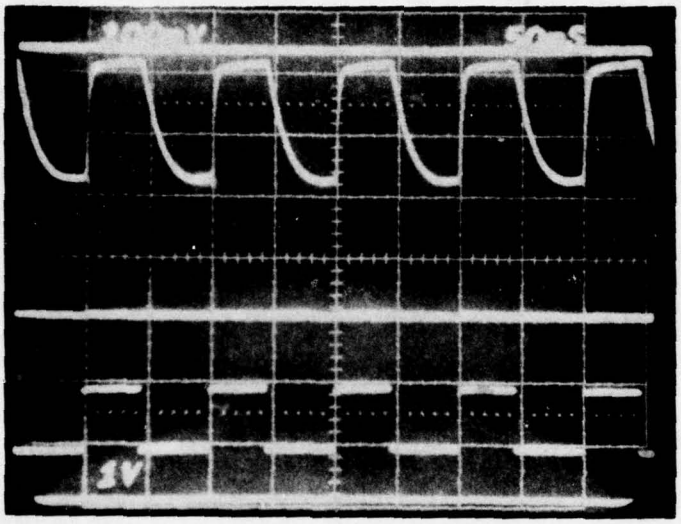

(e)

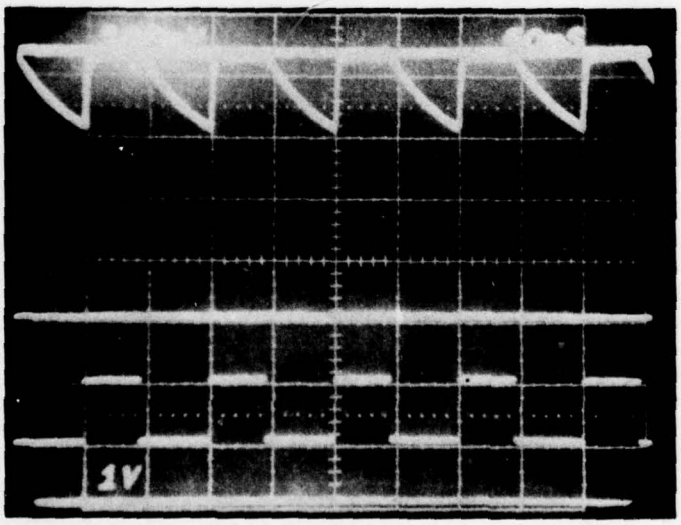

Fig. 73 (continued)

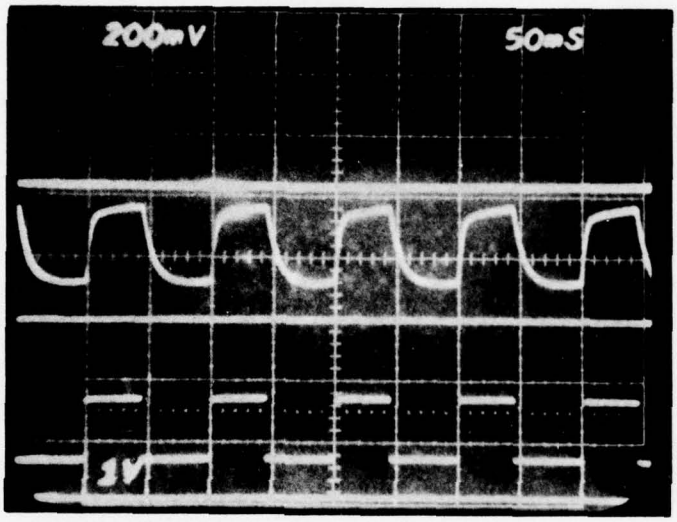

Fig. 74 Response of 5 mil 5% cholesteryl nonanoate/BDH E-1 cell to voltage pulses having an on time slightly less than the off time providing a more nearly square-wave output from the modulator. (λ = 8-11.5μm)

SC79-4491

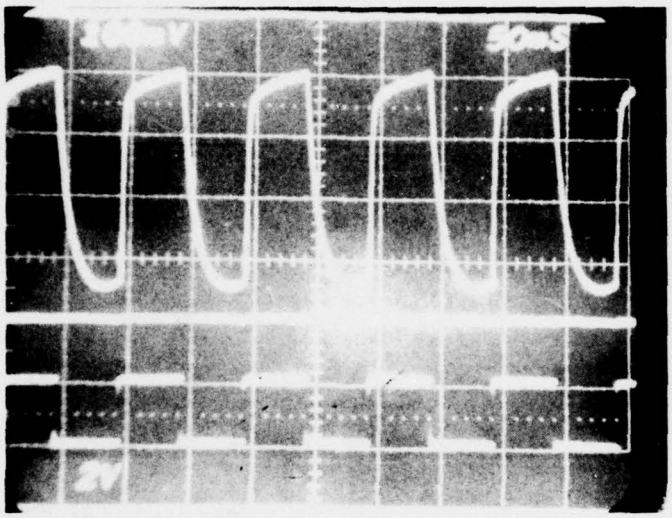

Fig. 75 Response of 5 mil, 5% cholesteryl nonanoate/EM 684 cell over λ = 8-11.5 μm band in f/1.2 system with partially turned-on operating mode. Total turn-off ≈ 30 ms and contrast modulation ≈ 70%.

Thus, the results of this section have demonstrated that fast modulator response with reasonable contrast is obtainable with the use of the partially turned-on operating mode using square wave drive.

5.3 Scattering Measurements

To obtain some idea as to the scattering mechanism involved in the cholesteric-nematic phase change effect, transmission as a function of detector position was measured for each cell; the detector was translated along a single axis and the detector output plotted on an x-y plotter with the cell first in the scattering state and then turned-on to its transparent state. Figure 76 shows a plot of typical data obtained from these measurements in the 8-11.5μm region. The upper plot is the cell turned-on, the lower plot is the cell in the voltage adjusted maximum scattering (or focal-conic) state, and the middle plot is the scattering with the cell partially turned-on (voltage less than threshold). It appears here that the scattering produces mainly a uniform decrease in the intensity of the radiation. However, Fig. 77 shows the data from the cell which had the highest measured contrast of all in the 8-11.5μm region (5 mil 2% cholesteryl nonanoate/BDH E-1); these data show almost totally diffused scattering. Also, some measurements made by hand earlier showed some smearing of the intensity of the scattered radiation as compared to the focused beam. Thus, at this point, the true nature of the scattering is not understood in great detail.

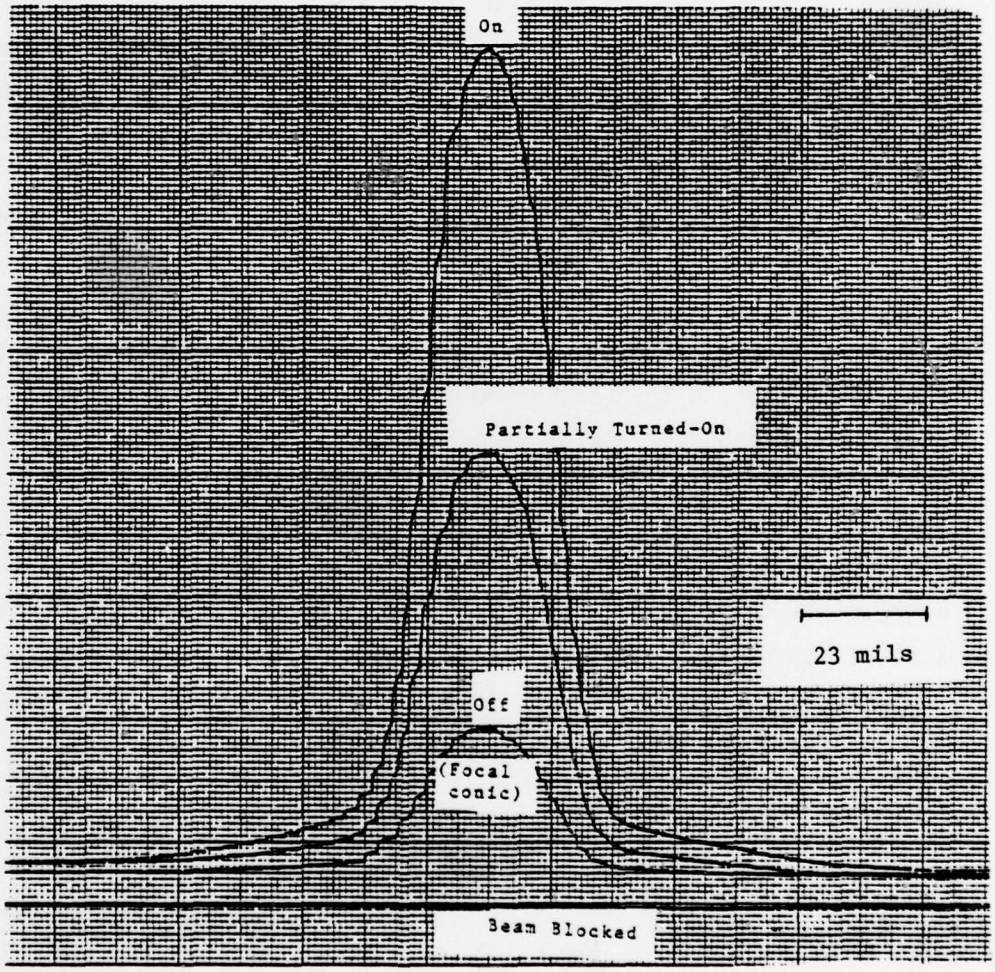

Fig. 76 Transmission vs detector position in the 8-11.5μm region for a 1 mil 5% cholesteryl nonanoate/BDH E-1 cell showing transmission in the on (transparent), off (scattering) and partially transparent states.

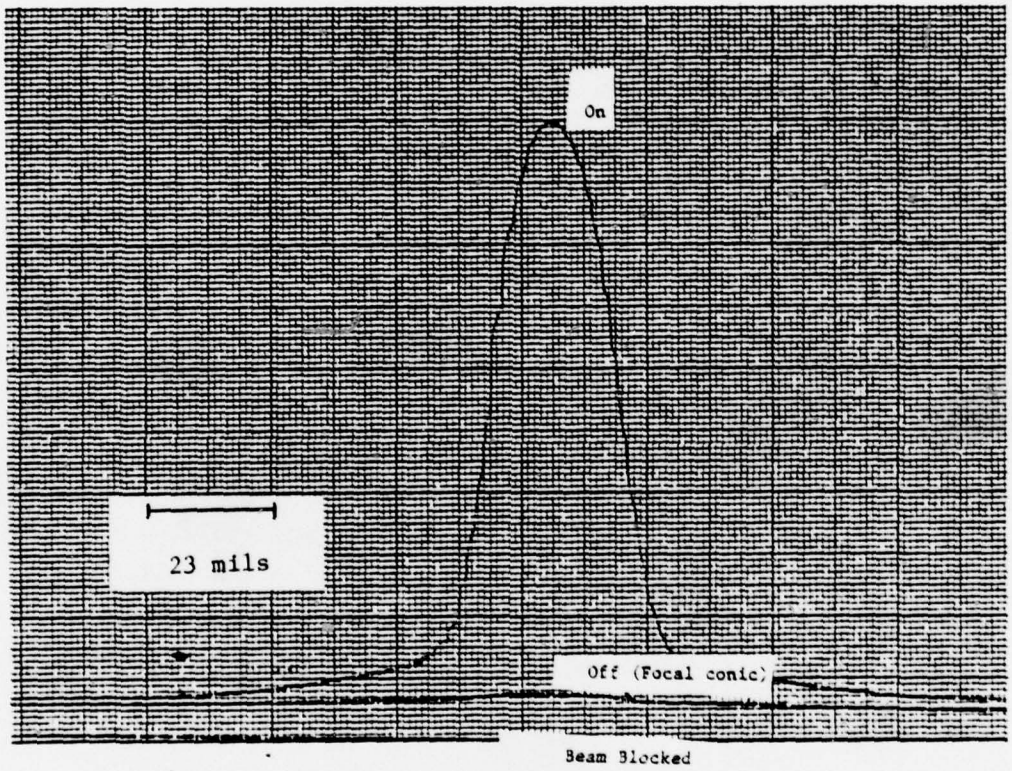

Fig. 77 Transmission vs detector position in the 8-11.5μm region for a 5 mil 2% cholesteryl nonanoate/BDH E-1 cell showing transmission in the on-state and almost totally diffuse scattering in the off-state.

6.0 SUMMARY OF PROGRAM GOALS AND ACCOMPLISHMENTS

The contract goals, as stated in the purchase description, and accomplishments for the electro-optical modulator are now summarized:

6.1 Optical:

a. Transmittance in 8-12μm regions greater than 95%:

Infrared (8-12μm) transmission of ≈87% was measured for a one mil thick sample of 4-cyano-4'-n-pentyl biphenyl liquid crystal.

b. Contrast modulation greater than 95% in 8-12μm region:

The highest measured contrast of 93%, not counting window losses and liquid crystal absorption, occurred for a 5 mil 5% cholesteryl nonanoate/BDH E-1 cell measured at λ = 8μm using ≈f/3 optics. The highest measured contrasts for λ = 8-11.5μm and λ = 3.5μm were 88% and 87%, both measured with a 5 mil 2% cholesteryl nonanoate/BDH E-1 cell using an f1.2 lens. About the best contrast/turn-off time combination to be measured for the partially turned-on operating mode using square wave drive was ≈55%/20 ms and occurred for a 5 mil 5% cholesteryl nonanoate/BDH E-1 cell in the 8-11.5μm region with an f/1.2 lens; a contrast as high as 70% was measured for a 5 mil 5% cholesteryl nonanoate/EM 684 cell, but was accompanied by an increased turn-off time of ≈30 ms.

c. Variation of transmittance, when "open", less than 5% over clear aperture:

No specific measurements were performed, but there is no reason why any variation in transmittance should occur over the clear aperture. The major contribution to non-uniformity is the dimension of the cell cavity defined by the mylar spacer. However, in a final modulator configuration, this cavity would be precisely machined into the infrared window for uniformity control.

6.2 Electrical

a. Turn-on Time (100% to 5% contrast) Less than 1 ms:

Using the high-voltage square-wave drive technique, turn-on times less than 1 ms have been achieved. However, for the preferred partially turned-on operating mode, turn-on times of several ms are obtained for the fast turn-on region, although the cell can take tens of ms for the on transmission to approach saturation.

b. Turn-off Time (0% to 90% contrast) Less than 1 ms:

The fastest measured turn-off times occur with the use of small pitch materials in the partially turned-on operating mode. Using a 5 mil 14% cholesteryl nonanoate/BDH E-1 cell, a turn-off time of ≈5 ms has been achieved in the 8-11.5μm region using a rectangular pulse drive. However, to obtain increased contrast and on state transmission as well as square wave output from the modulator, the best turn-off times are a few tens of ms.

c. Switching Power Less than 1W:

Since the cholesteric-nematic phase change effect is a field effect using a very high resistivity ($>10^{10}\Omega$-cm) liquid crystal material, current flow, and thus power dissipation should be ideally zero, although in practice, impurities can introduce negligible currents. Even with the case of dynamic scattering, in which the scattering mechanism depends on current flow, the power consumption[42] has been reported to be at most, only 500μW per cm^2, considerably less than the required 1 W limit.

6.3 Chemical

a. Material Should not have Major Absorption Bands in 8-12μm Region:

In the 8-12μm region, the biphenyl and phenylcyclohexane liquid crystal materials exhibit the highest overall transmission. Absorption bands, however, do exist in this region, although they are generally narrow and, for thin cells, still allow a very appreciable transmission even at the specific

wavelengths at which the absorption bands occur. In the 3-5μm region, every liquid crystal material measured contained a major absorption band between 3.3μm and 3.6μm due to the C-H stretching mode.

b. Operating Temperature should be Consistent with a Military Environment:

The nematic temperature range of the BDH E-1 biphenyl mixture used for the majority of the modulator measurements is -2°C to 38°C. Other biphenyl mixtures can also be used such as the E7 and E9 mixtures which have nematic temperature ranges of -10°C to 60°C and 7°C to 82.5°C. All measurements reported here were completed at room temperature. However, the viscosity of liquid crystals varies as a function of temperature, and the electro-optical response times are proportional to the viscosity. Generally, the viscosity and response times become lower for increasing temperatures. Response measurements were not made as a function of temperature, but the following data was quoted from a report by Gray[43] showing that for a twisted nematic cell, the turn-off time increases from 120 ms to 480 ms for the E7 mixture as the temperature changes from 23°C to 0°C.

c. Material should be stable against photolysis by visible and ultraviolet radiation, hydrolysis by humidity and contamination by the atmosphere:

The molecular structure of the biphenyl liquid crystals in which the linking group connecting the two benzene rings is removed makes the biphenyl liquid crystals highly chemically and photochemically stable. The weak point in the phase change application is the cholesteric material added to produce the required pitch in the biphenyl material. However, biphenyl compatible materials such as BDH C15 can be used to produce the required optically active properties of the biphenyl eutectic mixtures. Furthermore, modulator cells can be permanently sealed providing further protection against atmospheric contaminants.

Another possible degradation mechanism in the cell is electrochemical effects on the cell walls. In the dynamic scattering effect, for example, where current flow is required for cell operation, an AC voltage with

frequency greater than 50 Hz is applied in place of DC drive voltages to prevent deterioration of the electrode surfaces. Although the cholesteric-nematic phase change effect employs high-resistivity liquid crystal materials and almost all the measurements in this report were made with DC voltages, it still would be preferable to utilize a gated AC drive technique to prevent any electrochemical effects (see Section 5.2.3).

d. Material should have a vapor pressure low enough to permit vacuum operation:

Since the cells can be hermetically sealed, they should be usable in vacuum.

7.0 CONCLUSIONS AND RECOMMENDATIONS

7.1 Conclusions

The conclusions arrived at with the completion of this program are as follows:

1. The cyanobiphenyl and phenylcylohexane positive nematic liquid crystals have been identified as materials having high 8-12μm infrared transmission and are applicable as infrared electro-optical modulators utilizing the cholesteric-nematic phase change effect. A one mil thick film of 4-cyano-4'-n-pentyl biphenyl has an 8-12μm transmission of ≈87%.
2. High 8-12μm contrast is obtained with long-pitch liquid crystals, and fast turn-off times are obtained with short-pitch liquid crystals. The development of the partially turned-on operating mode has yielded modulator cells having both fast turn-off times (20-40 ms) and moderate contrast (55-70%).
3. In the partially turned-on operating mode, there are trade-offs to be made between contrast, turn-off time, and cell on state transmission, with pitch, cell thickness and drive voltage levels as parameters. It appears, with the current level of liquid crystal technology, to be not possible to simultaneously obtain the required 95% 8-12μm transmission, 95% contrast modulation, and less than 1 ms turn-on and turn-off times in a single modulator cell. These trade-offs are less severe in the 3-5μm region because of the shorter-pitch materials required for optimum scattering.

7.2 Recommendations

1. To improve liquid crystal transmission in the 3-5μm and 8-12μm regions, additional research needs to be performed on material synthesis. Fluorination or deuteration of the biphenyl materials could possibly modify infrared absorption in these regions by moving the peaks to longer wavelengths.

2. Further experiments to reduce the modulator response times need to be performed. These experiments include the investigation of different cell drive techniques and also the effect of higher temperatures on viscosity and, thus, cell response.
3. The development of a prototype line-addressable liquid crystal electro-optical modulator should be pursued.

ACKNOWLEDGMENTS

The author would like to acknowledge the useful discussions held with Drs. J. Tracy, E. Sovero, R. Chang and P. Newman of the Science Center, Dr. F. Jones of Tempor Inc., and Dr. W. Elser of the U.S. Army Night Vision and Electro-Optics Laboratory.

8.0 REFERENCES

1. T.S. Moss, "Methods of Modulating Infrared Beams," Infrared Phys. 2, 129 (1962).

2. B. Ellis and A.K. Walton, "A Bibliography on Optical Modulators," Infrared Phys. 11, 85 (1971).

3. F.K. Dolezalek and H. Jager, "Survey of Possibilities of Nonmechanical Modulation of Infrared Radiation and Consideration of Their Usefulness for Satellite Application," European Space Research Organization Report ESRP CR-26 (ESTEC Contract No. 990/70AA) (1970).

4. B. Ellis, "Solid State Modulators for Horizon Sensing Applications," Infrared Phys. 11, 147 (1971).

5. E.G. Lierke, "Infrared Modulator for Optical Sensors Based on a Vibrating Fabry-Perot Interferometer," Optical Eng. 15, 35 (1976).

6. R.H. Clarke, "A Theory for the Christiansen Filter," Appl. Optics 7, 861 (1968).

7. "Variable-Transmittance Visor for Helmet-Mounted Display," Final Technical Report for Contract F33615-71-C-1938 (Air Force Medical Research Laboratory, WPAFB).

8. C.E. Land, Sandia Laboratories Reprint SC-R-67-1219 (1967).

9. C.E. Land, P.D. Thacker and G.H. Haertling, Electro-Optic Ceramics, Academic Press.

10. D. Thacker and C.E. Land, Sandia Laboratories Reprint SC-R-69-1252 (1969).

11. R. Noel Thomas, Jens Guildberg, H.C. Nathanson and Paul R. Malmberg, "The Mirror Matrix Tube: A Novel Light Valve for Projection Displays," IEEE Trans. on Electron Devices 22, 765-775 (1975) and references contained therein.

12. L.E. Sommers, "Real Time Light Modulators for Incoherent to Coherent Image Conversion," Proc. of the Society of Photo-Optical Instrumentation Engineers 83, 31 (1976) and references contained therein.

13. Kendall Preston, Jr., "The Membrane Light Modulator and its Application in Optical Computers," Optica Acta 16, 579-585 (1969).

14. J.A. Van Raalte, "A New Schlieren Light Valve for Television Projection," Applied Optics 9, 2225-2230 (1970).

15. J.B. MacChesney and H.J. Guggenheim, "Growth and Electrical Properties of Vanadium Dioxide Single Crystals Containing Selected Impurity Ions," J. Phys. Chem. Solids 30, 225 (1969).

16. John C.C. Fan, et al., "Thin-Film VO_2 Submillimeter-Wave Modulators and Polarizers," Appl. Phys. Lett. 31, 11 (1977).

17. J. Billingsly, "Hardening Optical Systems Against Laser Countermeasures," 17th Annual IRIS Symp. on Infrared Countermeasures, Air Force Weapons Lab., Albuquerque (1979).

18. G.W. Gray, Molecular Structure and the Properties of Liquid Crystals, Academic Press, New York (1962).

19. P.G. DeGennes The Physics of Liquid Crystals, Clarendon Press, Oxford (1974).

20. L.M. Blinov, "Electro-Optical Effects in Liquid Crystals," Sov. Phys. Usp. 17, 658 (1975).

21. J.D. Margerum and L.J. Miller, "Electro-Optical Applications of Liquid Crystals," J. Colloid and Interface Sci. 58, 559 (1977).

22. T.J. Scheffer and H.C. Gruler, "Electro-Optics of Liquid Crystals," Molecular Electro-Optics, Part 2, Chester T. O'Konslsi (editor), Dekker, New York (1978).

23. A.F. Fray, C. Hilsum and D. Jones, "Some Properties of Liquid Crystals as Infrared Modulators," Infrared Phys. 18, 35 (1978).

24. M.F. Schiekel and K. Fahrenschon, "Deformation of Nematic Liquid Crystals with Vertical Orientation in Electrical Fields," Appl. Phys. Lett. 19, 391 (1972).

25. G.H. Heilmeier, L.A. Zanoni and L.A. Barton, "Dynamic Scattering: A New Electro-Optic Effect in Certain Classes of Nematic Liquid Crystals," Proc. IEEE 56, 1162 (1968).

26. G.H. Heilmeier, L.A. Zanoni and L.A. Barton, "Further Studies of the Dynamic Scattering Mode in Nematic Liquid Crystals," IEEE Trans. on Electron Dev. ED-17, 22 (1970).

27. M. Schadt and W. Helfrich, "Voltage-Dependent Optical Activity of a Twisted Nematic Liquid Crystal," Appl. Phys. Lett. 18, 127 (1971).

28. J.J. Wysocki, J. Adams and W. Haas, "Electric-Field-Induced Phase Change in Cholesteric Liquid Crystals," Phys. Rev. Lett. 20, 1024 (1968).

29. G.H. Heilmeier and J.E. Goldmacher, "Electric-Field-Induced Cholesteric-Nematic Phase Change in Liquid Crystals," J. Chem. Phys. 51, 1258 (1969).

30. J.J. Wysocki, "Continued Kinetic Study of the Cholesteric-Nematic Transition in a Liquid Crystal Film," Mol. Cryst. Liq. Cryst. 14, 71 (1971).

31. T. Ohtsuka and M. Tsukamoto, "AC Electric-Field-Induced Cholesteric-Nematic Phase Transition in Mixed Liquid Crystal Films," Jap. J. Appl. Phys. 12, 22 (1973).

32. G.H. Heilmeier, J.A. Castellano and L.A. Zanoni, "Guest-Host Interactions in Nematic Liquid Crystals," Mol. Cryst. Liq. Cryst. 8, 293 (1969).

33. H.S. Cole Jr. and S. Aftergut, "Dependence of Absorption and Optical Contrast of a Dichroic Dye Guest on the Pitch of a chiral Nematic Host," Appl. Phys. 31, 58 (1977).

34. G.H. Heilmeier and J.E. Goldmacher, "A New Electric-Field-Controlled Reflective Optical Storage Effect in Mixed-Liquid Crystal Systems," Appl. Phys. Lett. 13, 132 (1968).

35. J.C. Varney, "Liquid Crystal Display Technology," Ph.D. Thesis-Paisley College of Technology (1977).

36. E. Jakeman and E.P. Raynes, "ELectro-Optic Response Times in Liquid Crystals," Phys. Lett. 39A, 69 (1972).

37. R.A. Kashnow, J.E. Bigelow, H.S. Cole and C.R. Stein, "Comments on the Relaxation Process in the Cholesteric-Nematic Transition," Liquid Cryst. & Ordered Fluids 2, 483 (1974).

38. W. Greubel, "Bistability Behavior of Texture in Cholesteric Liquid Crystals in an Electric Field," Appl. Phys. Lett. 25, 5 (1974).

39. N. Oron and M.M. Labes," AC-DC Technique for Rapid Conical-Helical Perturbation in Cholesteric Liquid Crystals," Appl. Phys. Lett. 21, 243 (1972).

40. J.C. Varney and L.E. Davis, "Structural Oscillation in a Cholesteric-Nematic Mixture," Electron. Lett. 10, 331 (1974).

41. J. Constant and E.P. Raynes, "Cholesteric-Nematic Phase-Change Effect in Mixtures Containing the Liquid Crystal PCB," Electron. Lett. 9, 561 (1973).

42. EM Laboratories, Nematic Phases Licristal catalog, p. 9.

43. G.W. Gray, "Advances in Liquid Crystal Materials for Applications, BDH Chemicals (1978), p. 28.

9.0 APPENDIX 1. LITERATURE SURVEY SC5149.31FR

The purpose of this literature search was to locate research papers applicable to the problem of constructing a liquid crystal infrared electro-optic modulator operable in the 8-12μm wavelength region. The search was conducted back to the year 1967. Although the existence of liquid crystals has been known for many years, the first applicable published research did not appear until 1968 with the publication of the discovery of the dynamic scattering effect and the cholesteric-nematic phase change effect. This work helped launch the ever increasing volume of research and publications in the field of liquid crystals and their many applications.

With the intent of trying to make this literature search more useful, the list of articles is divided up into several sections each dealing with a separate phase of liquid crystal research. This list of papers is by no means totally inclusive. Many more could have been added, and many that are included probably could have been eliminated without adversely affecting the tone of the survey. Also, many of the papers could have been placed into categories other than the one in which they are listed. However, each paper was placed where it seemed to fit best. Any papers of importance that are published in the coming months or some from the past that may have been overlooked will be included in an addendum to be submitted at the completion of the contract.

In addition, work that relates to other types of modulators for this application will also be included. This literature survey reflects the fact that effort has concentrated on the most important goal of the program - the determination of the suitability of liquid crystals for infrared modulation.

The literature survey is divided into the following categories:

(1) Modulator and infrared material properties
(2) Books, general and review articles
(3) Liquid crystal materials
(4) Dynamic scattering effect
(5) Cholesteric-nematic phase change effect

(6) Twisted nematic, cholesteric memory, and guest host interaction effects

(7) Field effects in nematic liquid crystals

(8) Cholesteric liquid crystals, pitch and textures

(9) Alignment techniques

(10) Response time experiments

(11) Some liquid crystal applications

(12) Liquid crystal material catalogs

I. Modulator and Infrared Material Properties

This section includes papers that have a close relationship to the problem of fabricating an infrared electro-optic modulator. The most relevant paper, and probably the most relevant in the entire survey, is that by Fray, et.al., entitled "Some Properties of Liquid Crystals as Infrared Modulators " (1978). The authors discuss the dynamic scattering, cholesteric nematic phase change, and twisted nematic effects as applied to infrared modulation. The twisted nematic effect, however, requires polarizers so is not a viable contender. Included is an infrared spectrum of the positive nematic pentyl-cyano biphenyl showing an average transmittance of > 70% in the 8-14μm region. This is, as of now, the most promising material for application as an infrared modulator.

One other applicable paper, is entitled "Infrared Spectra of a Nematic Liquid Crystal in Dynamic Scattering Mode" by Y. Ohnishi (1973). The scattering of the nematic liquid crystal MBBA is studied out to 9μm with the conclusion that dynamic scattering in this material is effective only for $\lambda <$ 8μm.

Other papers study infrared absorption and vibrational modes of liquid crystals but are not complete enough to make a determination of which materials would have the highest overall 8-12μm transmission.

All the literature which follows in the remainder of this survey deals with specific aspects of liquid crystal technology. Although this technology and its applications deal primarily with modulators and displays in the visible spectral region, the physics behind this technology is directly applicable to the infrared region provided a suitable liquid crystal material can be found with the desired infrared transmission and time response characteristics. Although the dynamic scattering and cholesteric-nematic phase change effects are the two most applicable for the infrared modulator concept, papers on all of the important liquid crystal effects, including those requiring polarizers for their operation, will be included for completeness. Finally, the papers in each section will be listed chronologically to illustrate the flow of research over the last decade.

1. T. S. Moss, "Methods of Modulating Infrared Beams," Infrared Phys. 2, 129 (1962).

2. B. J. Bulkin, D. Grunbaum, and A. V. Santoro, "Vibrational Spectra of Liquid Crystals. I. Changes in the Infrared Spectrum at the Crystal-Nematic Transition," J. Chem. Phys. 51, 1602 (1969).

3. B. Ellis and A. K. Walton, "A Bibliography on Optical Modulators," Infrared Phys. 11, 85 (1971).

4. B. J. Bulkin and K. Krishnan, "Vibrational Spectra of Liquid Crystals. III. Raman Spectra of Crystal, Cholesteric, and Isotropic Cholesterol Esters, 2800-3100-cm^{-1} Region," J. Am. Chem. Soc. 93:23, 5998 (1971).

5. M. Bertolotti, S. Martellucci, F. Scudieri, and D. Sette, "Acoustic Modulation of Light by Nematic Liquid Crystals," Appl. Phys. Lett. 21, 74 (1972).

6. I. Chabay, "Absorptive and Scattering Circular Dichroism of Cholesteric Liquid Crystals in the Infrared," Chem. Phys. Lett. 17, 283 (1972).

7. B. J. Bulkin and W. B. Lok, "Vibrational Spectra of Liquid Crystals. V. Far-Infrared Study of Intermolecular Modes in 4,4'-Azoxydianisole and 4-Methoxybenzylidene-4'-n-butylaniline," J. Phys. Chem. 77, 326 (1973).

8. Y. Ohnishi, "Infrared Spectra of a Nematic Liquid Crystal in Dynamic Scattering Mode," Jap. J. Appl. Phys. 12, 1079 (1973).

9. Y. Ito, "Light Modulation with Multilayer Thin Films," Appl. Opt. 13, 2464 (1974).

10. N. Kirov and P. Simova, "Infrared Absorption Spectra of Liquid Crystals. IV. Integral Intensity Temperature Dependence of Infrared Bands in Crystal, Nematic Crystal and Isotropic Phases," Mol. Cryst. Liq. Cryst. 30, 59 (1975).

11. F. Scudieri, A. Ferrari, M. Bertolotti and D. Apostol, "Opto-Acoustic Modulator with a Nematic Liquid Crystal," Opt. Commun. 15, 57 (1975).

12. P. Simova and N. Koriv, "Infrared Spectra of Liquid Crystals. III. Rotational Diffusion in Smectic and Cholesteric Mesophase," Spectroscopy Lett. 8, 561 (1975).

13. B. J. Bulkin, "Infrared and Raman Spectroscopy of Liquid Crystals," Appl. Spectroscopy, 30, 261 (1976).

14. J. R. Fernandes and S. Venugopalan, "Infrared Spectroscopic Study of Orientational Order and Phase Transformations in Liquid Crystalline CBOOA," Mol. Cryst. Liq. Cryst. 35, 113 (1976).

15. C. Motoc, P. Sterian and E. Sofron, "Morphological Changes in Nematic Liquid Crystals and their Implications in Laser Light Modulation," Rev. Roum. Phys. 21, 638 (1976).

16. G. Vergoten, G. Fleury, R. N. Jones and A. Nadeau, "Vibrational Spectroscopy of Liquid Crystals. IV. Infrared and Far Infrared Spectra of the MBBA and EBBA Liquid Crystals," Mol. Cryst. Liq. Cryst. 36, 327 (1976).

17. G. J. Evans and M. Evans, "High and Low Frequency Torsional Absorptions in Nematic K21," J. Chem. Soc. Faraday Trans. II (GB) 73, 285 (1977).

18. A. F. Fray, C. Hilsum and D. Jones, "Some Properties of Liquid Crystals As Infrared Modulators," Infrared Phys. 18, 35 (1978).

II. Books, General and Review Articles

Many of these books and review articles provide a comprehensive introduction to liquid crystals and their applications. Among the more useful and interesting of the review articles are "Electrooptic Liquid Crystal Devices: Principles and Applications" by A. Sussman, (1972), "Electro-Optical Applications of Liquid Crystals" by T. J. Scheffer and H. C. Gruler (1978). There is also an excellent theoretical treatment entitled "The Physics of Liquid Crystals" by M. J. Stephen and J. P. Straley (1974) for those who need more than a qualitative introduction.

BOOKS

1. G. W. Gray, Molecular Structure and the Properties of Liquid Crystals, Academic Press, New York (1962).

2. J. F. Johnson and R. S. Porter, Liquid Crystals and Ordered Fluids, Vol. 1, Plenum Press, New York (1970).

3. T. Kallard (ed.), Liquid Crystals and Their Applications, Optosonic Press, New York (1970).

4. T. Kallard, Liquid Crystal Devices, Optosonic Press, New York (1973).

5. P. G. deGemes, The Physics of Liquid Crystals, Clarendon Press, Oxford (1974).

6. G. W. Gray and P. A. Winsor, Liquid Crystals and Plastic Crystals, Vol. 1 and Vol. 2, Ellis Horwood Ltd., Chichester (1974).

7. J. F. Johnson and R. S. Porter, Liquid Crystals and Ordered Fluids, Vol. 2, Plenum Press, New York (1974).

8. G. Meier, E. Sackmann, and J. G. Grabmaier, Applications of Liquid Crystals, Springer-Verlag, Berlin (1975).

9. L. Liebert (ed.), Solid State Physics, Supplement 14, ("Liquid Crystals"), Academic Press, New York (1978).

GENERAL AND REVIEW ARTICLES

1. J. L. Fergason, "Liquid Crystals," Sci. Am. p. 77, Aug.1974.

2. G. H. Brown, "Liquid Crystals and Some of their Applications in Chemistry," Analyt. Chem. 41, 26A (1969).

3. C. M. Ellis, "Liquid Crystals," School Sci. Rev. 51, 80 (1969).

4. G. H. Brown, J. W. Doane, V. D. Neff, "Structure and Physical Properties of Liquid Crystals," CRC Crit. Rev. in Sol. St. Sci. 1, 303 (1970).

5. J. A. Castellano, "Now that the Heat Is Off, Liquid Crystals Can Show their Colors Everywhere," Electronics, p. 64 (1970).

6. G. H. Heilmeier, "Liquid-Crystal Display Devices," Sci. Am. p. 100, April 1970.

7. J. A. Castellano, "Electro-Optic Properties of Liquid Crystals," Proc. 21st Electron. Compon. Conf. May 10-12, 1971.

8. L. T. Creagh, A. R. Kmetz, and R. A. Reynolds, "Performance Characteristics of Nematic Liquid Crystal Display Devices," ED-18 672 (1971).

9. B. J. Lechner, F. J. Marlowe, E. O. Nester, J. Tults, "Liquid Crystal Matrix Displays," Proc. IEEE 59, 1566 (1971).

10. J. A. Castellano, "Liquid Crystals for Electro-Optical Application," RCA Rev. 33, 296 (1972).

11. R. A. Kashnow, "Thickness Measurements of Nematic Liquid Crystal Layers," Rev. Sci. Instrum. 43, 1837 (1972).

12. G. R. Luckhurst, "Liquid Crystals," Phys. Bull. 23, (1972).

13. E. Stepke, "Liquid Crystals: Perspectives, Prospects, and Products," Electro-Opt. Syst. Design, Feb. 1972.

14. A. Sussman, "Electrooptic Liquid Crystal Devices: Principles and Applications," IEEE Trans. on Parts, Hybrids and Packaging PHP-8, 24 (1972).

15. M. Tobias, "The Fluid State of Liquid Crystals," New Scientist 14, 651 (1972).

16. G. H. Brown, "Properties and Applications of Liquid Crystals," J. Electron. Mat. 2, 403 (1973).

17. G. H. Brown, "Structure, Properties, and Some Applications of Liquid Crystals," J. Opt. Soc. of Am. 63, 1505 (1973).

18. J. A. Castellano and G. H. Brown, "Thermotropic Liquid Crystals. Part I. The Underlying Science," Chemtech, p. 47 Jan. (1973).

19. L. T. Creagh, Nematic Liquid Crystal Materials for Displays, Proc. IEEE 61, 814 (1973).

20. A. A. Groshev and V. B. Sergeev, "Liquid Crystals in Display Devices," Sov. Phys. US Pekhi 15, 515 (1973).

21. W. Helfrich, "Electric Alignment of Liquid Crystals," Mol. Cryst. & Liq. Cryst. 21, 187 (1973).

22. J. Kirton and E. P. Raynes, "Electro-Optic Effects in Liquid Crystals," Endeavour 32, 71 (1973).

23. A. R. Kmetz, "Liquid-Crystal Display Prospects in Perspective," IEEE Trans. on Electron Dev. ED-20, 954 (1973).

24. A. Saupe, "Liquid Crystals," Ann. Rev. of Phys. Chem. 24, 441 (1973).

25. R. Steinstrasser and L. Pohl, "Chemistry and Applications of Liquid Crystals," Angew. Chem. Internat. Edit. 12, 617 (1973).

26. L. M. Blinov, "Electro-Optical Effects in Liquid Crystals," Sov. Phys.-Usp. 17, 658 (1975).

27. G. H. Brown, and J. W. Doane, "Liquid Crystals and Some of their Applications," Appl. Phys. 4, 1 (1974).

28. W. H. Flygare and T. D. Gierke, "Light Scattering In Noncrystalline Solids and Liquid Crystals," Ann. Rev. of Mat. Sci. 4, 8557 (1974).

29. L. A. Goodman, "Liquid-Crystal Displays--Packaging and Surface Treatments," RCA Rev. 35, 447 (1974).

30. L. A. Goodman, "Liquid-Crystal Displays--Electro-Optic Effects and Addressing Techniques," RCA Rev. 35, 613 (1974).

31. M. J. Stephen and J. P. Straley, "Physics of Liquid Crystals," Rev. of Mod. Phys. 46, 617 (1974).

32. A. Sussman, "Liquid Crystals in Display Systems," Liq. Cryst. & Plastic Cryst. (Gray & Winsor ed.) 1, 338 (1974).

33. J. A. Castellano, "Fundamentals of Liquid Crystals and Other Liquid Display Technologies," Optics and Laser Tech. Dec. 1975.

34. I. A. Karaseva, V. I. Lebedev, T. P. Sokolova, and M. G. Tomilin, "Problems in the Fabrication and Testing of Liquid-Crystal Cells," Sov. J. Opt. Tecnnol. 42, 600 (1975).

35. S. Chandrasekhar, "Liquid Crystals" Reports on Progress in Physics 39, 613 (1976).

36. G. Durand, "Optical Properties of Liquid Crystals," Interaction of Radiation with Condensed Matter" Pt. Trieste, Italy , (Conf. Proceed.) Jan.14-Mar. 36, 1976.

37. H. Gasparoux and J. Prost, "Liquid Crystals," Ann. Rev. Phys. Chem. 27, 175 (1976).

38. G. H. Brown, "Structures and Properties of the Liquid Crystalline State of Matter," J. Coll. & Interface Sci. 58, 534 (1977).

39. G. W. Gray and A. J. Leadbetter, "Liquid Crystals, What Makes A Mesophase," Phys. Bull. p. 28, Jan. 1977.

40. J. D. Margerum and L. J. Miller, "Electro-Optical Applications of Liquid Crystals," J. Colloid and Interface Sci. 58, 559 (1977).

41. J. L. Fergason, "Liquid Crystals" A Big Case for Display," Opt. Spectra, p. 54, June 1978.

42. T. J. Scheffer and H. C. Gruler, "Electro-Optics of Liquid Crystals, Molec. Electro-Optics, Part 2, Chester T. O'Konski (Ed.), Dekker, N. Y. (1978).

III. Liquid Crystal Materials

This section lists papers which describe some of the various classes of liquid crystals and their physical and chemical properties. The most noteworthy papers are those by G. W. Gray and associates of the University of Hull, England, and researchers at the Royal Radar Establishment who synthesized and measured the properties of the now well known cyano biphenyl room temperature nematic liquid crystals. These materials have large positive dielectric anisotrooies making them useful for cholesteric-nematic phase change devices, and they also have high chemical/photochemical stability. Some of the important papers by these people include: "New Family of Nematic Liquid Crystals for Displays" (1973), "Electro-Optic Performance of a New Room-Temperature Nematic Liquid Crystal" (1973), which also describes cholesteric-nematic phase change experiments, "Synthetic Chemistry Related to Liquid Crystals" (1973), which describes the synthesis of liquid crystals to meet certain definite physical requirements, and "The Liquid Crystal Properties of Some New Mesogens" (1975). One other noteworthy paper is "Physical Properties of Nematic Phenylcyclohexanes, A New Class of Low Melting Liquid Crystals with Positive Dielectric Anisotropy" by L. Pohl, et al. We have looked at some of this material and it exhibits good transmission in the 8-12 μm region (see letter report 10).

There are many other liquid crystal material related papers especially in the various issues of the journal Molecular Crystals and Liquid Crystals, but the ones listed here have the best potential for application.

1. F. J. Kahn, "Cholesteric Liquid Crystals for Optical Applications," J. Appl. Phys., 18, 231 (1971).

2. I. Haller, "Elastic Constants of the Nematic Liquid Crystalline Phase of p-Methoxybenzylidene-p-n-Butylaniline (MBBA)," J. Chem. Phys., 57, 1400 (1972).

3. M. J. Rafuse and R. A. Soref, "Carbonate Schiff Base Nematic Liquid Crystals: Synthesis and Electro-optic Properties," Molecular Crys. & Liquid Crys., 18, 95 (1972).

4. M. Schadt, "Dielectric Properties of Some Nematic Liquid Crystals with Strong Positive Dielectric Anisotropy," J. Chem. Phys., 56, 1494 (1972).

5. C. J. Alder and E. P. Raynes, "Room-Temperature Nematic Liquid Crystal Mixtures with Positive Dielectric Anisotropy," J. Phys. D: Appl. Phys. Lett., 6, L33 (1973).

6. A. Ashford, J. Constant, J. Kirton and E. P. Raynes, "Electro-Optic Performance of a New Room-Temperature Nematic Liquid Crystal," Electronics Letters, 9, 118 (1973).

7. G. W. Gray, K. J. Harrison and J. A. Nash, "New Family of Nematic Liquid Crystals for Displays," Electronics Letters, 9, 130 (1973).

8. G. W. Gray and K. J. Harrison, "Molecular Theories and Structure. Some Effects of Molecular Structural Change on Liquid Crystalline Properties," Faraday Symposium on Liquid Crystals, London, England, 54 (1971).

9. G. W. Gray, K. J. Harrison and J. A. Nash, "New Cholesteric Liquid Crystals for Displays," Electronics Letters, 9, 616 (1973).

10. G. W. Gray, "Synthetic Chemistry Related to Liquid Crystals," Molecular Crys. & Liquid Crys., 21, 161 (1973).

11. G. W. Gray, et al. "Stable, Low Melting Nematogens of Positive Dielectric Anisotropy for Display Devices," Liquid Crys. & Ordered Fluids, 2, 617 (1974).

12. A. W. Levine, "Structure-Property Relationships in Thermotropic Organic Liquid Crystals," RCA Review, 35, 94 (1974).

13. P. G. Cummins, D. A. Dunmur and D. A. Laidler, "The Dielectric Properties of Nematic 44' n-pentylcyanobiphenyl," Molecular Crys. & Liquid Crys., 30, 109 (1975).

14. G. W. Gray and D. G. McDonnell, "New Low-Melting Cholesterogens for Electro-Optical Displays and Surface Thermography," Electronics Letters, 11, 556 (1975).

15. G. W. Gray, "The Liquid Crystal Properties of Some New Mesogens," J. de Physique (Paris) Colloque. 36, C1-337 (1975).

16. S. Ignasiak and M. J. Rafuse, "Cyano-Alkyl Diaryl Compounds: Preparation and Liquid Crystal Properties," Molecular Crys. & Liquid Crys., 30, 125 (1975).

17. J. W. Park, C. S. Bak and M. M. Labes, "Effects of Molecular Complexing on the Properties of Binary Nematic Liquid Crystal Mixtures," J. Am. Chem. Soc., 97, 4398 (1975).

18. N. V. Vijaya Raghavan and T. S. Chang, "Conjugative and Inductive Effects of Cyano Group on the Electro-Optic Properties in Substituted Cyano Phenylbenzoate Esters," J. Chem. Phys., 63, 5493 (1975).

19. D. Coates and G. W. Gray, "The Liquid Crystal Properties of Some Cyano-Substituted Aryl Esters," Molecular Crys. & Liquid Crys., 37, 249 (1976).

20. R. J. Cox and N. J. Clecak, "The Preparation of 4-Alkyl-4'-Cyanostilbenes. A New Series of Liquid Crystal Compounds," Molecular Crys. & Liquid Crys., 37, 263 (1976).

21. M. S. Davies, et al, "Dielectric and Optical Studies of a New Nematogen (4,4-n-heptyl-cyanobiphenyl)," J. Chem. Soc. Faraday Trans. II. 72, 1447 (1976).

22. G. W. Gray and D. G. McDonnell, "Synthesis and Liquid Crystal Properties of Chiral Alkyl-Cyano-Biphenyls (and -p-Terphenyls) and of Some Related Chiral Compounds Derived from Biphenyl," Molecular Crys. & Liquid Crys., 37, 189 (1976).

23. M. F. Grebenkin, V. A. Seliverstov, L. M. Blinov and V. G. Chigrinov, "Properties of Nematic Liquid Crystals with Positive Dielectric Anisotropy," Sov. Phys. Crystallogr., 20, 604 (1976).

24. J. W. Park and M. M. Labes, "Dielectric, Elastic, and Electro-optic Properties of a Liquid Crystalline Molecular Complex," J. Appl. Phys., 48, 22 (1977).

25. L. Pohl, R. Eidenschink, G. Krause and D. Erdmann, "Physical Properties of Nematic Phenylcyclohexanes, A New Class of Low Melting Liquid Crystals with Positive Dielectric Anisotropy," Phys. Lett., 60A, 421 (1977).

IV. Dynamic Scattering

Dynamic scattering is one of two effects currently being considered for use in an infrared modulator. This effect was first described by Heilmeier, et. al. in the paper "Dynamic Scattering: A New Electrooptic Effect in Certain Classes of Nematic Liquid Crystals," (1968). In dynamic scattering, with no applied field the liquid crystal is essentially transparent. With an applied field greater than a certain threshold voltage, however, a turbulent highly-scattering state is obtained. This effect occurs in nematic crystals of negative dielectric anisotropy and moderate conductivity since the scattering centers are produced by the interaction of charge carriers with the molecular dipole moments.

Current research involves studying the effects of surface alignments on dynamic scattering as well as the addition of various dopants to increase the liquid crystal conductivity and to reduce the operating voltage.

1. G. H. Heilmeier, L. A. Zanoni, and L. A. Barton, "Dynamic Scattering in Nematic Liquid Crystals, Appl. Phys. Lett. 13, 46 (1968).

2. G. H. Heilmeier, L. A. Zanoni, and L. A. Barton, "Dynamic Scattering: A New Electrooptic Effect in Certain Classes of Nematic Liquid Crystals," Proc. IEEE. 56, 1162 (1968).

3. C. Deutsch and P. N. Keating, "Scattering of Coherent Light from Nematic Liquid Crystals in the Dynamic Scattering Mode," J. Appl. Phys. 40, 4049 (1969).

4. G. H. Heilmeier, L. A. Zanoni, and L. A. Barton, "Further Studies of the Dynamic Scattering Mode in Nematic Liquid Crystals," IEEE Trans. on Electron Dev. ED-17, 22 (1970).

5. D. Jones, L. Creagh, and S. Lu, "Dynamic Scattering in a Room-Temperature Nematic Liquid Crystal," Appl. Phys. Lett. 16, 61 (1970).

6. P. A. Penz, "Voltage-Induced Vorticity and Optical Focusing in Liquid Crystals," Phys. Rev. Lett. 24, 1405 (1970).

7. G. Assouline, A. Dmitrieff, M. Hareng, and E. Leiba, "Scattering of Light by Nematic Liquid Crystals," J. Appl. Phys. 42, 2567 (1971).

8. W. W. Holloway and M. J. Rafuse, "Dynamic Scattering by a Nematic Liquid Crystal Where the Applied Electric Field Is Normal to the Incident Light," J. Appl. Phys. 42, 5395 (1971).

9. C. H. Gooch and H. A. Tarry, "Dynamic Scattering in the Homeotropic and Homogeneous Textures of a Nematic Liquid Crystal, " J. Phys. D. 5, L25 (1972).

10. A. Sussman, "Secondary Hydrodynamic Structure in Dynamic Scattering," Appl. Phys. Lett. 21, 269 (1972).

11. A. I. Baise and M. M. Labes, "Dynamic Scattering in a Liquid Crystal Having Positive Dielectric Anisotropy," J. Chem. Phys. 59, 551 (1973).

12. G. Elliott, D. Harvey, M. G. Williams, "Dielectric Anisotropy of New Liquid-Crystal Mixtures and Its Effect on Dynamic Scattering," 9, 399 (1973).

13. M. F. Grebenkin, G. S. Chilaya, V. T. Lazareva, K. V. Roitman, L. M. Blinov, and V. V. Titov,"Dynamic Scattering of Light in Liquid Crystals of the Azocompound Class," Sov. Phys. Crystallogr. 18, 274 (1973).

14. E. Jakeman and P. N. Pusey, "Light Scattering from Electrohydrodynamic Turbulence in Liquid Crystals," Phys. Lett 44A 456 (1973).

15. P. M. Alt and M. J. Freiser, "Texturing: A New Effect in the Dynamic Scattering Regime of Liquid-Crystal Cells," J. Appl. Phys. 45, 3237 (1974).

16. F. Gaspard and R. Herino, "Comments on "Effect of Charge-Transfer Acceptors on Dynamic Scattering in a Nematic Liquid Crystal," Appl. Phys. Lett. 24, 432 (1974).

17. Y. Ohnishi and M. Ozutsumi, "Properties of Nematic Liquid Crystals Doped with Hydroquinone and p-Benzoquinone: Long-Term Dynamic Scattering Under DC Excitation," Appl. Phys. Lett. 24, 213 (1974).

18. M. Zulauf, M. Bertolotti and F. Scudieri, "Photon-Correlation Measurements on Light Scattered by a Nematic Liquid Crystal Under a DC Electric Field," J. Appl. Phys. 46, 5152 (1975).

19. S. Barret, F. Gaspard, R. Herino, and F. Mondon, "Dynamic Scattering in Nematic Liquid Crystals Under DC Conditions. I. Basic Electrochemical Analysis," J. Appl. Phys. 47, 2375 (1976).

20. S. Barret, F. Gaspard, R. Herino, and F. Mondon, "Dynamic Scattering in Nematic Liquid Crystals Under DC Conditions. II. Monitoring of Electrode Processes and Lifetime Investigation," J. Appl. Phys. 47, 2378 (1976).

21. V. I. Lebedev, V. I. Mordasov, and M. G. Tomilin, "The Electro-Optic Properties of a Liquid-Crystal Cell with the Dynamic Scattering Effect," Sov. J. Opt. Technol. 43, 252 (1976).

22. V. I. Lebedev and M. G. Bomilin, "Light Scattering by Liquid-Crystal Cells," Sov. J. Opt. Technol. 43, 630 (1976).

23. H. S. Lim and J. D. Margerum, "Improved DC Dynamic Scattering with Redox Dopants in Ester Liquid Crystals," Appl. Phys. Lett. 28, 478 (1976).

24. H. S. Lim and J. D. Margerum, "Dopant Effects on D-C Dynamic Scattering in a Liquid Crystal: Microscopic Pattern Studies," J. Elec. Soc. 123, 837 (1976).

25. A. Nomura, M. Morita, and K. Yatabe, "Guest-Host Effect and Dynamic Scattering Effect in Nematic Liquid Crystals Under Flow," Jap. J. Appl. Phys. 15, 1385 (1976).

26. L. K. Vistin and S. S. Yakovenko, "Use of Infrared Spectroscopy for Determining the Orientation of the Molecules in the Strongly Light-Scattering Layers of a Liquid Crystal," Sov. Phys. Crystallogr. 21, 318 (1976.

27. T. Yamaguchi, "Statistical Properties of Scattered Field from Nematic Liquid Crystals in Dynamic Scattering Mode," J. Chem. Phys. 64, 1555 (1976).

28. Y. Hori and M. Fukai, "Liquid Crystal Mixtures for Low Voltage Dynamic-Scattering Display," J. Elec. Soc. 124, 1752 (1977).

29. H. S. Lim, J. D. Margerum, and A. Graube, "Electrochemical Properties of Dopants and the D-C Dynamic Scattering of a Nematic Liquid Crystal," J. Elec. Soc. 124, 1389 (1977).

V. Cholesteric-Nematic Phase Change Effect

This effect is the primary effect now being considered for the infrared modulator mainly because of the availability of liquid crystal materials with high average transmission in the 8-12μm region. The effect occurs in cholesteric materials with high positive dielectric anisotropy. On application of an electric field equal to a certain threshold voltage, the molecules forming the scattering cholesteric helixes align parallel to the field to form a transparent nematic phase. On removal of the field, the cholesteric phase is restored through the action of elastic forces. The discovery of this effect was reported in the paper, "Electric-Field-Induced Phase Change in Cholesteric Liquid Crystals" by J. J. Wysocki, et. al., (1968). One of the most applicable papers is that by J. Constant and E. P. Raynes entitled "Cholesteric-Nematic Phase-Change Effect in Mixtures Containing the Liquid-Crystal PCB" (1973). This paper gives plots of the critical voltage as a function of cholesteric concentration and also of cholesteric pitch as a function of cholesteric concentration for both cholesteryl chloride and cholesteryl nonanoate additives. To optimize scattering in the 8-12μm region, it is important to have the pitch length comparable to the wavelength.

1. J. J. Wysocki, J. Adams, and W. Haas, "Electric-Field-Induced Phase Change in Cholesteric Liquid Crystals," Phys. Rev. Lett. 20, 1024 (1968).

2. H. Baessler and M. M. Labes, "Relationship Between Electric Field Strength and Helix Pitch in Induced Cholesteric-Nematic Phase Transitions," Phys. Rev. Lett. 21, 1791 (1968).

3. H. Baessler and M. M. Labes, "Alternating-Current-Field Induced Cholesteric-Nematic Phase Transitions," J. Chem. Phys. 51, 5397 (1969).

4. G. Durand, L. Leger, F. Rondelez, and M. Veyssie, "Magnetically Induced Cholesteric-to-Nematic Phase Transition in Liquid Crystals," Phys. Rev. Lett. 22, 227 (1969).

5. G. H. Heilmeier and J. E. Goldmacher, "Electric-Field-Induced Cholesteric-Nematic Phase Change in Liquid Crystals," J. Chem. Phys. 51, 1258 (1969).

6. J. Wysocki, J. Adams and W. Haas, "Electric-Field Induced Phase Change in Cholesteric Liquid Crystals," Molec. Crystals & Liq. Crystals. 8, 471 (1969).

7. E. F. Carr, J. H. Parker, and D. P. McLemore, "Effects of Electric Fields on Mixtures of Nematic and Cholesteric Liquid Crystals," Liq. Cryst. & Ordered Fluids 1, 201 (1970).

8. W. Haas and J. Adams, "Electric Field Effects on the System Oleyl Cholesteryl Carbonate-Cholesteryl Chloride," J. Electrochem. Soc. 118, 1372 (1970).

9. G. H. Heilmeier, L. A. Zanoni and J. E. Goldmacher, "Some Experiments on Electric Field Induced Structural Changes in a Mixed Liquid Crystal System," Liq. Cryst. & Ordered Fluids 1, 215 (1970).

10. S. Sato and M. Wada, "Cholesteric-Nematic Phase Transitions in Compensated Liquid Crystals, Jap. J. Appl. Phys. 10, 1106 (1971).

11. J. J. Wysocki, "Continued Kinetic Study of the Cholesteric-Nematic Transition in a Liquid Crystal Film," Molec. Cryst. & Liq. Cryst. 14, 71 (1971).

12. C. J. Gerritsma and P. Van Zanten, "The Dependence of the Electric-Field-Induced Cholesteric-Nematic Transition on the Dielectric Anisotropy," Phys. Lett. 42A, 127 (1972).

13. S. Sato and M. Wada, "Cholesteric-Nematic Phase Transitions in Mixtures of Cholesteryl Chloride and Nematic Liquid Crystals," Jap. J. Appl. Phys. 11, 1752 (1972).

14. J. Constant and E. P. Raynes, "Cholesteric-Nematic Phase-Change Effect in Mixtures Containing the Liquid-Crystal PCB," Electron. Lett. 9, 561 (1973).

15. W. Greubel, "Bistability Behavior of Texture in Cholesteric Liquid Crystals in an Electric Field," Appl. Phys. Lett. 25, 5 (1974).

16. L. J. Yu and M. M. Labes, "Non-Uniform Distortions During Electric Field Induced Unwinding of a Cholesteric Liquid Crystal," Mol. Cryst. Liq. Cryst. 28, 423 (1974).

17. G. J. Sprokel, "Anisotropy Changes in the Cholesteric to Nematic Phase Transition," Mol. Cryst. Liq. Cryst. 29, 231 (1975).

18. C. Mioskowski, J. Bourguignon, S. Candau, and G. Solladie, "Photochemically Induced Cholesteric-Nematic Transition in Liquid Crystals," Chem. Phys. Lett. 38, 456 (1975).

19. J. Cuculescu and C. Motoc, "Bistability Effects in Mixtures of Cholesteric Liquid Crystals Under Electric Fields," Rev. Roum. Phys. 22, 945 (1977).

20. L. J. Yu and M. M. Labes, "Fluorescent Liquid-Crystal Display Utilizing an Electric-Field-Induced Cholesteric-Nematic Transition," Appl. Phys. Lett. 31, 719 (1977).

VI. Twisted Nematic, Cholesteric Memory, and Guest Host Interaction Effects

These effects are not applicable to the infrared modulator but are interesting nevertheless and are included for completeness. The twisted nematic effect was first described by M. Schadt and W. Helfrich in the paper "Voltage-Dependent Optical Activity of a Twisted Nematic Liquid Crystal" (1971). The twisted structure is obtained by having the nematic alignment parallel to the cell walls but with the two cell walls twisted by 90° thus enabling the variation of the rotation of linearly polarized light continuously from 0° to 90° with the application of voltage; polarizers are required for operation.

The cholesteric memory effect was first described by G. H. Heilmeier and J. E. Goldmacher in the paper "A New Electric-Field-Controlled Reflective Optical Storage Effect in Mixed-Liquid Crystal Systems" (1968). It is similar to dynamic scattering in that a turbulent scattering state occurs when a critical voltage is applied; however, the scattering state remains when the voltage is removed and very slowly relaxes to the clear state.

The guest-host interaction was first described by G. H. Heilmeier and L. A. Zanoni in "Guest-Host Interactions in Nematic Liquid Crystals: A New Electro-Optic Effect" (1968). This effect works on the principle of the inclusion of a dichroic dye (guest) in the liquid crystal material (host) whose absorption of light depends on its orientation with respect to an external electric field. Unfortunately, in a cholesteric liquid crystal the absorption of unpolarized light by the dichroic dye decreases with an increase in the pitch of the cholesteric material just opposite to the effect required for long wavelength scattering; furthermore, the dyes themselves are designed to absorb in the visible region and not the infrared region. See, for example, the paper "Dependence of Absorption and Optical Contrast of a Dichroic Dye Guest on the Pitch of a Chiral Nematic Host" by H. S. Cole and S. Aftergut (1977).

TWISTED NEMATIC EFFECT

1. M. Schadt and W. Helfrich, "Voltage-Dependent Optical Activity of a Twisted Nematic Liquid Crystal," Appl. Phys. Lett. 18, 127 (1971).

2. A. Boller, H. Scherrer, M. Schadt, P. Wild, "Low Electrooptic Threshold in New Liquid Crystals," Proc. IEEE, 1002 (1972).

3. E. P. Raynes, "Twisted Nematic Liquid-Crystal Electro-Optic Devices with Areas of Reverse Twist," Electron. Lett. 9, 101 (1973).

4. D. W. Berreman, "Dynamics of Liquid-Crystal Twist Cells," Appl. Phys. Lett. 25, 12 (1974).

5. G. D. Dixon, T. P. Brody, and W. A. Hester, "Alignment Mechanisn in Twisted Nematic Layers," Appl. Phys. Lett. 24, 47 (1974).

6. E. P. Raynes, "Improved Contrast Uniformity in Twisted Nematic Liquid-Crystal Electro-Optic Display Devices," Electron. Lett. 10, 141 (1974).

7. L. B. Stotts, A. Sussman, and M. A. Monahan, "Photoactivated Twisted Nematic Device," Appl. Opt. 13, 1752 (1974).

8. C. J. Gerritsma, J. J. M. J. de Klerk and P. van Zanten, "Changes of Twist in Twisted Nematic Liquid-Crystal Layers by Frequency Switching of Applied Electric Fields," Sol. St. Commun. 17, 1077 (1975).

9. D. Meyerhofer, "Optical Transmission of Liquid-Crystal Field-Effect Cells," J. Appl. Phys. 48, 1179 (1977).

10. F. Ogawa, C. Tani, F. Saito, "New Electro-Optical Effect: Optical Activity of Electric-Field-Induced Twisted-Nematic Liquid Crystal," Elect. Lett. 12, 70 (1976).

11. M. Schadt, "Solute-Induced Transmission Changes in Liquid Crystal Twist Cells," Phys. Lett. 57A, 442 (1976).

12. W. Haase and D. Potzsch, "Light Transmission Experiments with Nematic Liquid Crystals Showing Positive and Negative Dielectric Anisotropy," Mol. Cryst. Liq. Cryst. 38, 77 (1977).

13. D. de Rossi and J. Robert, "Electro-Optic Behavior of a Field-Induced Twisted Structure with Quasihomeotropic Boundary Conditions," J. Appl. Phys. 49, 1139 (1978).

CHOLESTERIC MEMORY EFFECT

1. G. H. Heilmeier and J. E. Goldmacher, "A New Electric-Field-Controlled Reflective Optical Storage Effect in Mixed-Liquid Crystal Systems," Appl. Phys. Lett. 13, 132 (1968).

2. G. H. Heilmeier, and J. E. Goldmacher, "A New Electric Field Controlled Reflective Optical Storage Effect in Mixed Liquid Crystal Systems," Proc. IEEE 57, 34 (1969).

3. B. Kerllenevich and A. Coche, "Erasure of Textures Stored in Nematic-Cholesteric Mixtures," Liq. Cryst. & Ordered Fluids 2, 705 (1974).

4. L. Melamed and D. Rubin, "Electric Field Hysteresis Effects in Cholesteric Liquid Crystals," Appl. Phys. Lett. 16, 149 (1970).

5. J. P. Hulin, "Parametric Study of the Optical Storage Effect in Mixed Liquid-Crystal Systems," Appl. Phys. Lett. 21, 455 (1972).

6. W. Greubel, U. Wolff and H. Kruger, "Electric Field Induced Texture Changes in Certain Nematic/Cholesteric Liquid Crystal Mixtures," Mol. Cryst. & Liq. Cryst. 24, 103 (1973).

7. D. Meyerhofer and E. F. Pasierb, "Light Scattering Characteristics in Liquid Crystal Storage Materials," Mol. Cryst. & Liq. Cryst. 20, 279 (1973).

8. W. E. L. Haas and J. E. Adams, "New Optical Storage Mode in Liquid Crystals," Appl. Phys. Lett. 25, 535 (1974).

GUEST-HOST INTERACTIONS

1. G. H. Heilmeier and L. A. Zanoni, "Guest-Host Interactions in Nematic Liquid Crystals. A New Electro-Optic Effect," Appl. Phys. Lett. 13, 91 (1968).

2. G. H. Heilmeier, J. A. Castellano and L. A. Zanoni, "Guest-Host Interactions in Nematic Liquid Crystals," Mol. Cryst. and Liq. Cryst. 8 293 (1969).

3. D. L. White and G. N. Taylor, "New Absorptive Mode Reflective Liquid-Crystal Display Device," J. Appl. Phys. 45, 4718 (1974).

4. J. Constant, J. Kirton, E. P. Raynes, I. A. Shanks, D. Coates, G. W. Gray, and D. G. McDonnell, "Pleochroic Dyes with High-Order Parameters for Liquid-Crystal Displays," Electron. Lett. 12, 514 (1976).

5. H. S. Cole and R. A. Kashnow, "A New Reflective Dichroic Liquid-Crystal Display Device," Appl. Phys. Lett. 30, 619 (19-7).

6. H. S. Cole, Jr. and S. Aftergut, "Dependence of Absorption and Optical Contrast of a Dichroic Dye Guest on the Pitch of a Chiral Nematic Host," Appl. Phhys. 31, 58 (1977).

7. Y. Nara, S. Kobayashi, and A. Miyaji, "Multiplexing for the Guest-Host Mode Using a Nematic Cholesteric Mixture with a Long Pitch," J. Appl. Phys. 49, 4277 (1978).

VII. Field Effects in Nematic Liquid Crystals

Field effects in nematic liquid crystals involve the rotation of the nematic molecules either perpendicular or parallel to the field depending on the sign of the dielectric anisotropy and the initial molecule alignment. Any devices using these field effects require polarizers for operation. The DAP effect is one such effect using nematic liquid crystals and is described by M. F. Schiekel and K. Fahrenschon in the paper "Deformation of Nematic Liquid Crystals with Vertical Orientation in Electrical Fields" (1971). In addition to field effects, several papers on acoustic excitation of liquid crystals are included in this section.

1. R. Williams, "Domains in Liquid Crystals," J. Chem. Phys. 39, 384 (1963).

2. L. K. Vistin and A. P. Kapustin, "Electrooptical Effect in Liquid Crystals," Optics and Spectroscopy 24, 348 (1969).

3. W. Haas, J. Adams, and J. B. Flannery, "New Electro-Optic Effect in a Room Temperature Nematic Liquid Crystal," Phys. Rev. Lett. 25, 1326 (1970).

4. L. W. Kessler and S. P. Sawyer, "Ultrasonic Stimulation of Optical Scattering in Nematic Liquid Crystals," Appl. Phys. Lett. 17, 440 (1970).

5. F. M. Leslie, "Distortion of Twisted Orientation Patterns in Liquid Crystals by Magnetic Fields," Molec. Cryst. and Liq. Cryst. 12, 57 (1970).

6. Orsay Liquid Crystal Group, "Theory of Light Scattering by Nematics," Liq. Cryst. & Ordered Fluids 1, 195 (1970).

7. K. Toriyama, T. Aoyagi and S. Nomura, "A Mixed Liquid Crystals with New Electrooptic Effect," Jap. J. Appl. Phys. 9, 584 (1970).

8. W. Greubel and U. Wolff, "Electrically Controllable Domains in Nematic Liquid Crystals," Appl. Phys. Lett. 19, 213 (1971).

9. S. Lu and D. Jones, "Light Diffraction Phenomena in an ac-Excited Nematic Liquid-Crystal Sample," J. Appl. Phys. 42, 2138 (1971).

10. H. Mailer, K. L. Likins, T. R. Taylor and J. L. Fergason, "Effect of Ultrasound on a Nematic Liquid Crystal," Appl. Phys. Lett. 18, 105 (1971).

11. T. Ohtsuka and M. Tsukamoto, "Electro-Optical Properties of Nematic Liquid-Crystal Films," Jap. J. of Appl. Phys. 10, 1046 (1971).

12. M. F. Schiekel and K. Fahrenschon, "Deformation of Nematic Liquid Crystals with Vertical Orientation in Electrical Fields," Appl. Phys. Lett. 19, 391 (1971).

13. W. H. DeJeu, C. J. Gerritsma, P. Van Zanten and W. J. A. Goossens, "Relaxation of the Dielectric Constant and Electrohydrodynamic Instabilities in a Liquid Crystal," Phys. Lett. 39A, 355 (1972).

14. F. J. Kahn, "Electric-Field-Induced Orientational Deformation of Nematic Liquid Crystals: Tunable Birefringence," Appl. Phys. Lett. 20, 199 (972).

15. R. A. Soref and M. J. Rafuse, "Electrically Controlled Birefringence of Thin Nematic Films," J. Appl. Phys. 43, 2029 (1972).

16. P. D. Berezin, L. M. Blinov, I. N. Kompanets, and V. V. Nikitin, "Electrooptic Switching in Oriented Liquid-Crystal Films," Sov. J. Quant. Electron. 3, 78 (1973).

17. P. D. Berezin, I. N. Kompanets, V. V. Nikitin and S. A. Pikin, "Orienting Effect of an Electric Field on Nematic Liquid Crystals," Sov. Phys. JETP. 37, 305 (1973).

18. G. Labrunie and J. Robert, "Transient Behavior of the Electrically Controlled Birefringence in a Nematic Liquid Crystal," J. Appl. Phys. 44, 4869 (1973).

19. R. A. Soref, "Transverse Field Effects in Nematic Liquid Crystals," Appl. Phys. Lett. 22, 165 (1973).

20. L. Bata, A. Buka and I. Janossy, "Reorientation of Nematic Liquid Crystal Films by Alternating and Static Fields," Sol. St. Comm. 15, 647 (1974).

21. W. Helfrich, "Polarity-Dependent Electro-Optical Effect of Nematic Liquid Crystals," Appl. Phys. Lett. 24, 451 (1974).

22. W. Jung, K. N. Kang, S. K. Min, Y. B. Chae, and Q. W. Choi, "The Electro-Optical Rotation of Vertically Aligned Nematic MBBA Layers," Proc. 5th Conf. on Sol. St. Dev., Tokyo, 43, 136 (1974).

23. R. A. Soref, "Field Effects in Nematic Liquid Crystals Obtained with Interdigital Electrodes," J. Appl. Phys. 45, 5466 (1974).

24. A. Sussman, "The Electro-Optic Transfer Function in Nematic Liquids," RCA Rev. 35, 176 (1974).

25. D. Meyerhofer, "Field Induced Distortions of a Liquid Crystal with Various Surface Alignments," Phys. Lett . 51A, 407 (1975).

26. H. J. Coles and B. R. Jennings, "Electric Birefringence of Solutions of Nematic Compounds," Molec. Phys. 31, 1225 (1976).

27. N. V. S. Rao, P. R. Kishore, T. F. S. Raj, M. N. Avadhanlu, and C. R. K. Murty, "Electric and Magnetic Field Effects in p-Methoxy Benzylidene p'-n-Butylaniline," Z. Naturforsch. 31A, 283 (1976).

28. F. Scudieri, M. Bertolotti, S. Melone and G. Albertini, "Acoustohydrodynamic Instability in Nematic Liquid Crystals," J. Appl. Phys. 47, 3781 (1976).

29. T. Shimomura, H. Mada and S. Kobayashi, "Electro-Optical Properties of Nematic Liquid Crystal Cell for Obliquely Incident Light," Jap. J. of Appl. Phys. 15, 1479 (1976).

30. V. N. Chirkov, D. F. Aliev, and A. Kh. Zeinally, "Behavior of a Nematic Liquid Crystal in Alternating Electric Fields," Sov. Phys. Crystallogr. 22, 379 (1977).

VIII. Cholesteric Liquid Crystals, Pitch and Textures

Papers in this section are important in that they provide a thorough background to the structure and behavior of cholesteric liquid crystals which are the type used in the cholesteric-nematic phase change effect. An understanding of pitch in cholesterics is crucial because it is the cholesteric pitch structure which is responsible for the scattering of light. For maximum scattering in the 8-12μm, for example, the cholesteric pitch should also be roughly 8-12μm in size. A nematic liquid crystal can be transformed to a cholesteric liquid crystal by the addition of cholesteric material, and the resultant pitch depends on the cholesteric concentration; the pitch is inversely proportional to concentration although the relationship usually isn't linear. Pitch can also be varied by the mixture of several cholesteric materials and by changes in temperature. Many of the following papers deal with the theory and measurement of pitch in cholesterics.

1. J. H. Muller, "Effects of Electric Fields on Cholesterol Nonanoate Liquid Crystals," Molec. Cryst. 2, 167 (1966).

2. E. Sackmann, S. Meiboom, and L. C. Snyder, "On the Relation of Nematic to Cholesteric Mesophases," J. Am. Chem. Soc. 89, 5981 (1967).

3. R. B. Meyer, "Effects of Electric and Magnetic Fields on the Structure of Cholesteric Liquid Crystals," Appl. Phys. Lett. 12, 281 (1968).

4. F. B. Mallory, R. L. Connner, J. R. Landrey, J. M. Zander, J. B. Greig, E. Caspi, "On the Structure of the Liquid Crystalline State of Cholesterol Derivatives," J. Am. Chem. Soc. 90, 3567 (1968).

5. H. Baessler, T. M. Laronge, and M. M. Labes, "Electric Field Effects on the Optical Rotatory Power of a Compensated Cholesteric Liquid Crystal," J. Chem. Phys. 51, 3213 (1969).

6. A. D. Buckingham, G. P. Ceasar and M. B. Dunn, "The Addition of Optically Active Compounds to Nematic Liquid Crystals," Chem. Phys. Lett. 3, 540 (1969).

7. P. Kassubek and G. Meier, "Optical Studies on Grandjean Planes in Cholesteric Liquid Crystals," Mol. Cryst. & Liq. Cryst. 8, 305 (1969).

8. P. N. Keating, "A Theory of the Cholesteric Mesophase," Mol. Cryst. & Liq. Cryst. 8, 315 (1969).

9. R. B. Meyer, "Distortion of a Cholesteric Structure by a Magnetic Field," Appl. Phys. Lett. 14, 208 (1969).

10. H. Baessler and M. M. Labes, "Determination of the Pitch of a Cholesteric Liquid Crystal by Infrared Transmission Measurements," Molec. Cryst. & Liq. Cryst. 6, 419 (1970).

11. W. J. A. Goossens, "A Molecular Theory of the Cholesteric Phase," Phys. Lett. 31A, 413 (1970).

12. W. Haas, J. Adams, and J. B. Flannery, "ac-Field Induced Grandjean Plane Texture in Mixtures of Room-Temperature Nematics and Cholesterics," Phys. Rev. Lett. 24, 577 (1970).

13. W. Helfrich, "Deformation of Cholesteric Liquid Crystals with Low Threshold Voltage," Appl. Phys. Lett. 17, 531 (1970).

14. F. J. Kahn, "Electric-Field-Induced Color Changes and Pitch Dilation in Cholesteric Liquid Crystals," Phys. Rev. Lett. 24, 209 (1970).

15. H. Stegemeyer and K.-J. Mainusch, "Optical Rotatory Power of Liquid Crystal Mixtures," Chem. Phys. Lett. 6, 5 (1970).

16. C. J. Gerritsma and P. van Zanten, "Periodic Perturbations in the Cholesteric Plane Texture," Phys. Lett. 37A, 47 (1971).

17. W. Helfrich, "Electrohydrodynamic and Dielectric Instabilities of Cholesteric Liquid Crystals," J. Chem. Phys. 55, 839 (1971).

18. B. Kerllenevich and A. Coche, "Effects of the Addition of Cholesterics on Nematic Liquid Crystal Properties," J. Appl. Phys. 42, 5313 (1971).

19. T. Nakagiri, "Helical Twisting Power In Mixtures of Nematic and Cholesteric Liquid Crystals," Phys. Lett. 36A, 427 (1971).

20. S. C. Chou, L. Cheung and R. B. Meyer, "Effects of a Magnetic Field on the Optical Transmission in Cholesteric Liquid Crystals," Sol. St. Commun. 11, 977 (1972).

21. F. Rondelez and H. Arnould, "Electrohydrodynamic Effects in Cholesteric Liquid Crystals under ac Electric Fields," Phys. Rev. Lett. 28, 735 (1972).

22. T. Wako and K. Nakamura, "Voltage Effect on Cholesteric Liquid Crystals," Molec. Cryst. and Liq. Cryst. 19, 141 (1972).

23. T. J. Scheffer, "Electric and Magnetic Field Investigations of the Periodic Gridlike Deformation of a Cholesteric Liquid Crystal," Phys. Rev. Lett. 28, 593 (1972).

24. N. A. Clark and P. S. Pershan, "Light Scattering by Deformation of the Plane Texture of Smectic and Cholesteric Liquid Crystals," Phys. Rev. Lett. 30, 3 (1973).

25. P. Dreher and G. Meier, "Light Propagation in Helicoidal Structures," Sol. St. Commun. 13, 607 (1973).

26. N. Oron, J. L. Yu, and M. M. Labes, "Angular Dependence of Optical Scattering in Mixed Nematic-Cholesteric Liquid Crystals," Appl. Phys. Lett. 23, 217 (1973).

27. J. Voss and E. Sackmann, "Solute and Temperature Induced Pitch Changes and Pretransitional Effects in Cholesteric Liquid Crystals," Z. Naturforsch. 28a, 1496 (1973).

28. G. A. Dir, J. Adams and W. Haas, "Dynamics of Texture Transitions in Cholesteric-Nematic Mixtures," Mol. Cryst. Liq. Cryst. 25, 19 (1974).

29. G. Dir, J. Adams and W. Haas, "Conductivity Differences in the Cholesteric Textures," Liq. Cryst. & Ordered Fluids 2, 429 (1974).

30. C. J. Gerritsma and G. van Zanten, "Electro-Optical Properties of Imperfectly Ordered Planar Cholesteric Layers," Liq. Cryst. & Ordered Fluids 2, 437 (1974).

31. H. W. Gibson, J. M. Pochan, and D. Hinman, "Effect of Cholesteryl Alkanoate Structure on the Pitch of the Cholesteric Mesophase," Liq. Cryst. & Ordered Fluids 2, 593 (1974).

32. F. Nakano, K. Toriyama, M. Sato, T. Muroi, "Light Scattering in Nematic-Cholesteric Mixtures at a Low Electric Field," Suppl. to J. Jap. Soc. of Appl. Phys. 43, 141 (1974).

33. A. Wulf, "Helical Pitch in Mixtures of Cholesteric Liquid Crystals," J. Chem. Phys. 60, 3994 (1974.

34. C. S. Bak and M. M. Labes, "Pitch-Concentration Relationships in Multicomponent Liquid Crystal Mixtures," J. Chem. Phys. 62, 3066 (1975).

35. C. S. Bak and M. M. Labes, "Analysis of Pitch-Concentration Dependences in Some Binary and Ternary Liquid Crystal Mixtures," J. Chem. Phys. 63, 805 (1975).

36. M. DeZwart and Th.W. Lathouwers, "Electric Field-Induced Pitch Contraction in the Planar Cholesteric Texture of a Liquid Crystal with a Large Negative Dielectric Anisotropy," Phys. Lett 55A, 41 (1975).

37. F. Gharadjedaghi and J. Robert, "Optical and Electro-Optical Behaviour of a Liquid Crystal Helicoidal Structure," Revue de Phys. Appl. 10, (1975).

38. H. Hanson, A. J. Dekker, and F. van der Woude, "Analysis of the Pitch in Binary Cholesteric Liquid Crystal Mixtures," J. Chem. Phys. 62, 1941 (1975).

39. H. Kozawaguchi, and M. Wada, "Helical Twisting Power in Cholesteric Liquid Crystal Mixtures. I. Experimental Results," Jap. J. of Appl. Phys. 14, 651 (1975).

40. M. Tsukamoto, T. Ohtsuka, K. Morimoto, and Y. Murakami, "Pitch and Sense of Helix in Mixtures of Optically Active Azo or Azoxy Compounds and Nematic Liquid Crystal," Jap. J. of Appl. Phys. 14, 1307 (1975).

41. F. Fischer, "Critical Pitch in Thin Cholesteric Films with Homeotropic Boundaries," Z. Naturforsch 31a, 41 (1976).

42. E. K. Galanov, "Theory of Some Optical Properties of Liquid Cholesteric Crystals," Opt. Spectrosc. 41, 253 (1977).

43. G. Gottarelli, B. Samori and C. Stremmenos, "A Model for the Induction of a Cholesteric Mesophase in Nematic MBBA By the Addition of Optically Active 1-Phenylethanol," Chem. Phys. lett. 40, 308 (1976).

44. N. L. Kramarenko, I. V. Kurnosov, and Yu. V. Naboikin, "Light Scattering by Liquid Crystals in an Electric Field," Phys. Stat. Sol. (a) 33, 773 (1976).

45. E. H. Korte, "Infrared Rotatory Dispersion of Binary Cholesteric Mixtures," J. Chem. Phys. 66, 99 (1977).

46. H. Kozawaguchi and M. Wada, "Dependence of Helical Pitch on Composition in Mixtures of Nematic and Cholesteric Liquid Crystals," Mol. Cryst. Liq. Cryst. 44, 97 (1978).

IX. Alignment Techniques

Another important aspect of liquid crystal technology is the uniform alignment of liquid crystal molecules. Two basic alignments or textures of nematic liquid crystals are commonly used, the homogeneous alignment in which the long molecules are aligned parallel to the cell walls and the homeotropic alignment in which the long molecules are aligned perpendicular to the cell walls. The following papers describe techniques by which these alignments can be reproducibly obtained in liquid crystal cells. Some of the techniques used for homogeneous alignment include rubbing the cell walls with a cloth or paper, oblique evaporation of a thin film material on the cell walls, and the use of various surfactants. Homeotropic alignment is generally obtained by placing surfactants in the liquid crystal material.

The alignment of cholesteric liquid crystals is a little more complicated. In this case, it is the helix axis that is aligned in a certain orientation. In the planar or Grandjean texture, the axes are perpendicular to the cell walls, and in the focal conic texture the axes are parallel to the cell walls. Similar techniques are used to align cholesterics as are used for nematics.

1. D. W. Berreman, "Solid Surface Shape and the Alignment of an Adjacent Nematic Liquid Crystal," Phys. Rev. Lett., 26, 1683 (1972).

2. J. L. Janning, "Thin Film Surface Orientation for Liquid Crystals," Appl. Phys. Lett., 21, 173 (1972).

3. J. E. Proust, L. T.-Saraga and E. Guyon, "Orientation of a Nematic Liquid Crystal by Suitable Boundary Surfaces," Solid State Communications, 11, 1227 (1972).

4. L. T. Creagh and A. R. Kmetz, "Mechanism of Surface Alignment in Nematic Liquid Crystals," Molecular Crys. & Liquid Crys., 24, 59 (1973).

5. F. J. Kahn, "Orientation of Liquid Crystals by Surface Coupling Agents," Appl. Phys. Lett., 22, 386 (1973).

6. F. J. Kahn, G. N. Taylor and H. Schonhorn, "Surface-Produced Alignment of Liquid Crystals," Proc. IEEE, 61, 823 (1973).

7. I. Haller, "Alignment and Wetting Properties of Nematic Liquids," Appl. Phys. Lett., 24, 349 (1974).

8. U. Wolff, W. Greubel and H. Kruger, "The Homogeneous Alignment of Liquid Crystal Layers," Molecular Crys. & Liquid Crys., 23, 187 (1973).

9. W. Urbach, M. Boix and E. Guyon, "Alignment of Nematics and Smectics on Evaporated Films," Appl. Phys. Lett., 25, 479 (1974).

10. W. A. Crossland, J. H. Morrissy and B. Needham, "Tilt Angle Measurements of Nematic Phases of Cyano-Biphenyls Aligned by Obliquely Evaporated Films," J. Phys. D: Appl. Phys., 9, 2001 (1976).

11. J. C. Dubois, M. Gazard and A. Zann, "Liquid-Crystal Orientation Induced by Polymeric Surfaces," J. Appl. Phys., 47, 1270 (1976).

12. S. Matsumoto, D. Nakagawa, N. Kaneko and K. Mizunoya, "Surface-Produced Parallel Alignment of Nematic Liquid Crystals by Polynuclear Dicarboxylatochromium Complexes," Appl. Phys. Lett., 29, 67 (1976).

13. F. Nakano and M. Sato, "Alignmental Deterioration of Homeotropically Aligned Liquid Crystal Cells under D. C. Electric Field. I. Effect of Liquid Crystal Composition and Surface Treatment," Japanese J. Appl. Phys., 15, 1937 (1976).

14. K. Fahrenschon and M. F. Schiekel, "Properties of Pretilted Liquid Crystal Structures," J. Electrochem. Soc., 124, 953 (1977).

15. G. J. Sprokel and R. M. Gibson, "Liquid Crystal Alignment Produced by RF Plasma Deposited Films," J. Electrochem. Soc., 124, 557 (1977).

X. Response Time Experiments

The one really major problem area in the realization of a liquid crystal infrared modulator is the time response behavior of the cell. Liquid crystals are inherently slow in response, and many experiments have been performed to understand this behavior and to attempt to optimize their performance. Several techniques have been investigated to try to reduce liquid crystal relaxation times. For instance, in the paper, "AC-DC Technique for Rapid Conical-Helical Perturbation in Cholesteric Liquid Crystals," by N. Oron and M. M. Labes (1972), the simultaneous application of an AC and DC field in a four-electrode cell leads to a fast turn-on and relaxation in a cholesteric-nematic phase change cell. E. Jakeman and E. P. Raynes in "Electro-Optic Response Times in Liquid Crystals," (1972) discuss some of the parameters affecting response times in the cholesteric-nematic phase change effect. They find that the response times are minimized in liquid crystals having a low viscosity, small pitch and large dielectric anisotropy. Decay times of 60 μs are reported, but this occurs in their cells containing short pitch material.

Relaxation time reductions are also produced in the dynamic scattering mode by application of simultaneous AC and DC fields as reported in "A Method for Reducing the Decay Time of a Liquid Crystal" by A. Alimonda and V. Meyer (1973), so it appears that the application of AC fields is a viable technique in reducing relaxation times. Used in conjunction with optimizing material properties, short response times in infrared modulator cells may be possible.

1. G. H. Heilmeier and W. Helfrich, "Orientation Oscillation in Nematic Liquid Crystals," Appl. Phys. Lett., 16, 155 (1970).

2. C. R. Stein and R. A. Kashnow, "A Two-Frequency Coincidence Addressing Scheme for Nematic-Liquid-Crystal Displays," Appl. Phys. Lett., 19, 343 (1971).

3. P. J. Wild and J. Nehring, "Turn-On Time Reduction and Contrast Enhancement in Matrix-Addressed Liquid-Crystal Light Valves," Appl. Phys. Lett., 19, 335 (1971).

4. E. Jakeman and E. P. Raynes, "Electro-Optic Response Times in Liquid Crystals," Phys. Lett., 39A, 69 (1972).

5. N. Oron and M. M. Labes, "AC-DC Technique for Rapid Conical-Helical Perturbation in Cholesteric Liquid Crystals," Appl. Phys. Lett., 21, 243 (1972).

6. A. A. Vasil'ev, I. N. Kompanets and V. V. Nikitin, "Reduction of the Switching Time of a Liquid-Crystal Optical Transparency," Sov. J. Quant. Electron., 2, 263 (1972).

7. A. Alimonda and V. Meyer, "A Method for Reducing the Decay Time of a Liquid Crystal," IEEE Trans. Elec. Devices, p. 332 (March, 1973).

8. R. A. Kashnow, J. E. Bigelow, H. S. Cole and C. R. Stein, "Transient Observations of Field-Induced Nematic-Cholesteric Relaxation," Appl. Phys. Lett., 23, 290 (1973).

9. B. Kerllenevich and A. Coche, "Relaxation of Light Scattering in Nematic Crystals and in Nematic-Cholesteric Mixtures," Molecular Crys. & Liquid Crys., 24, 113 (1973).

10. T. Ohtsuka and M. Tsukamoto, "AC Electric-Field-Induced Cholesteric-Nematic Phase Transition in Mixed Liquid Crystal Films," Japanese J. Appl. Phys., 12, 22 (1973).

11. T. S. Chang, P. E. Greene and E. E. Loebner, "Kinetics of Field Alignment and Elastic Relaxation in Twisted Nematic Liquid Crystals," Liquid Crys. & Ordered Fluids, 2, 115 (1974).

12. T. S. Chang and E. E. Loebner, "Crossover Frequencies and Turn-Off Time Reduction Scheme for Twisted Nematic Liquid Crystal Displays," Appl. Phys. Lett., 25, 1 (1974).

13. C. J. Gerritsma, C. Z. Van Doorn and P. Van Zanten, "Transient Effects in the Electrically Controlled Light Transmission of a Twisted Nematic Layer," Phys. Lett., 48A, 263 (1974).

14. R. A. Kashnow, J. E. Bigelow, H. S. Cole, and C. R. Stein, "Comments on the Relaxation Process in the Cholesteric-Nematic Transition," Liquid Crys. & Ordered Fluids, 2, 483 (1974).

15. J. P. Sumner, "Fast-Switching Twisted Nematic Electro-Optical Shutter and Colour Filter," Electronics Letters, 10, 114 (1974).

16. C. S. Bak, K. Ko and M. M. Labes, "Fast Decay in a Twisted Nematic Induced by Frequency Switching," J. Appl. Phys., 46, 1 (1975).

17. M. Kawachi, O. Kogure, S. Yoshii and Y. Kato, "Field-Induced Nematic-Cholesteric Relaxation in a Small Angle Wedge," Japanese J. Appl. Phys., 14, 1063 (1975).

18. S. Aftergut and H. S. Cole, Jr., "Decay Time of Twist Cells with Liquid Crystals of Shortened Pitch," Appl. Phys. Lett., 30, 363 (1977).

19. M. Kawachi and O. Kogure, "Hysteresis Behavior of Texture in the Field-Induced Nematic-Cholesteric Relaxation," Japanese J. Appl. Phys., 16, 1673 (1977).

20. S. K. Kwok and Y. Liao, "Transient Phenomena of Relaxation from Electric-Field-Induced Nematic Phase to Cholesteric Phase," J. Appl. Phys., 49, 3970 (1978).

XI. Some Liquid Crystal Applications

This section lists several applications utilizing liquid crystals that demonstrates the versatility of these interesting materials.

1. J. D. Margerum, J. Nimoy and S.-Y. Wong, "Reversible Ultraviolet Imaging with Liquid Crystals," Appl. Phys. Lett., 17, 51 (1970).

2. D. L. White and M. Feldman, "Liquid-Crystal Light Valves," Electronics Letters, 6, 837 (1970).

3. J. Adams, W. Haas and J. Dailey, "Cholesteric Films as Optical Filters," J. Appl. Phys., 42, 4096 (1971).

4. J. D. Margerum, T. D. Beard, W. P. Bleha, Jr. and S.-Y. Wong, "Transparent Phase Images in Photoactivated Liquid Crystals," Appl. Phys. Lett., 19, 216 (1971).

5. N. G. Basov, et al, "Phase Modulation of Coherent Light with the Aid of Liquid Crystals," JETP Lett., 15, 138 (1972).

6. T. O. Carroll, "Liquid-Crystal Diffraction Grating," J. Appl. Phys., 43, 767 (1972).

7. T. D. Beard, W. P. Bleha and S.-Y. Wong, "AC Liquid-Crystal Light Valve," Appl. Phys. Lett., 22, 90 (1973).

8. D. J. Channin, "Optical Waveguide Modulation Using Nematic Liquid Crystal," Appl. Phys. Lett., 22. 365 (1973).

9. J. P. Sheridan, J. M. Schnur and T. G. Giallorenzi, "Electro-optic Switching in Low-Loss Liquid-Crystal Waveguides," Appl. Phys. Lett., 22, 560 (1973).

10. P. D. Berezin, I. N. Kompanets and V. V. Nikitin, "Liquid-Crystal Deflector," Sov. J. Quant. Electron, 4, 693 (1974).

11. G. Labrunie and S. Valette, "Nematic Liquid Crystal Digital Light Deflector," Appl. Optics, 13, 1802 (1974).

12. F. Scudieri, M. Bertolotti and R. Bartolino, "Light Scattered by a Liquid Crystal: A New Quasi-Thermal Source," Appl. Optics, 13, 181 (1974).

13. J. P. Sheridan and T. G. Giallorenzi, "Electro-optically Induced Deflection in Liquid-Crystal Waveguides," J. Appl. Phys., 45, 5160 (1974).

14. J. C. Filippini and Y. Poggi, "Nematic Liquids: A New Class of Materials for Kerr Cells," J. Phys. D: Appl. Phys. Lett., 8, L152 (1975).

15. A. F. Fray and D. Jones, "Large-Angle Beam Deflector Using Liquid Crystals," Electronics Letters, 11, 358 (1975).

16. J. Grinberg, "A New Real-Time Non-Coherent to Coherent Light Image Converter. The Hybrid Field Effect Liquid Crystal Light Valve," Optical Engineering, 14, 217 (1975).

17. L. M. Klyukin, I. D. Samodurova and A. S. Sonin, "Use of Nematic Liquid Crystals in Recording Long-Wavelength Radiation," Sov. J. Quant. Electron., 5, 249 (1975).

18. Y. A. Bykovskii, A. V. Makovkin, V. L. Smirnov and V. N. Sorokovikov, "Modulation of Laser Radiation in Liquid Thin-Film Waveguides," Sov. J. Quant. Electron., 5, 1361 (1976).

19. V. L. Kalinovskii, I. D. Samodurova and A. S. Sonin, "Reduction of Optical Radiation by Means of Nematic Liquid Crystals," Instum. & Exp. Tech., 19, 214 (1976).

20. A. S. Sonin, I. N. Shibaev and M. I. Epshtein, "Visualizer with a Wide Dynamic Range," Sov. J. Quant. Electron., 7, 295 (1977).

21. W. P. Bleha, et al, "Application of the Liquid Crystal Light Valve to Real-Time Optical Data Processing," Optical Engineering, 17, 371 (1978).

22. R. Denis, "Characterization of Ultrasonic Transducers Using Cholesteric Liquid Crystals," Ultrasonics, p. 37 (Jan., 1978).

23. S. R. Jost, "A New Light-Modulated Liquid-Crystal Light Valve," J. Appl. Phys., 49, 5332 (1978).

XII. Liquid Crystal Material Catalogs

1. BDH Liquid Crystals
2. Eastman Liquid Crystal Products
3. EM Nematic Phases Licristal
4. EM Nematic Phases Licristal (Phenylcyclohexanes)
5. Atomergic Liquid Crystals

10.0 APPENDIX 2 - PATENT SURVEY

I. Optical and Electro-Optical Devices

U.S. Patent No.	Title	Date
1,906,803	Means for Controlling Radiations	May 2, 1933
2,029,401	Method of and Apparatus for Obtaining Optical Effects by Electrical Means	Feb. 4, 1936
2,062,468	Optical Device	Dec. 1, 1936
2,387,587	Light Modulating Apparatus	June 23, 1942
2,335,659	Light Controlling Device	Nov. 30, 1943
2,692,950	Valve for Infrared Energy	Oct. 26, 1954
2,692,952	Semiconductive Light Valve	Oct. 26, 1954
3,158,678	Optical Device	Nov. 24, 1964
3,158,746	Light Modulation in a Semiconductor Body	Nov. 24, 1964
3,164,665	Electro-Optical Light Shutter	Jan. 5, 1965
3,169,163	Electro-Optical Light Valve Utilizing Charged Particle Migration	Feb. 9, 1965
3,183,359	Optical Modulator Employing Reflection From Piezoelectric-Semiconductive Material	May 11, 1965
3,190,177	Electrochemical Shutters	June 22, 1965
3,196,743	Light Modulation Device Employing a Scotophoric Light Valve	July 27, 1965
3,213,752	Optical Valve Responsive to Intense Light Flash	Oct. 26, 1965
3,238,843	Electro-Optical Devices Utilizing the Stark Shift Phenomenon	March 8, 1966
3,242,805	Semiconductor Light Modulator or Detector	March 29, 1966

3,245,313	Light Modulating Means Employing a Self-Erasing Plating Solution	April 12, 1966
3,247,765	Light Switching Means	April 26, 1966
3,259,014	Light Modulator using a Variable Spacing Diffraction Grating	July 5, 1966
3,259,016	Tunable Semiconductor Optical Modulator	July 5, 1966
3,278,749	Optical Wave Modulator	Oct. 11, 1966
3,280,701	Optically Variable One-Way Mirror	Oct. 25, 1966
3,294,469	Optical Shutters	Dec. 27, 1966
3,307,897	Light Modulator	March 7, 1967
3,367,733	Apparatus for Modulating Laser Radiation	Feb. 6, 1968
3,376,089	High Speed Optical Shutter	April 2, 1968
3,386,789	Reflective Element	June 4, 1968
3,393,033	Radiation Modulation Cell Utilizing a Magnetic Polymer	July 16, 1968
3,415,591	High Speed Optical Shutter	Dec. 10, 1968
3,429,636	Electro-Optical Light Modulation Means using Birefringent Crystals	Feb. 25, 1968
3,433,554	Electro-Optical Modulation of Radiation Pattern using Curved Electrodes	March 18, 1969
3,443,859	Variable Light Filtering Device	May 13, 1969
3,454,325	Optical Wave Modulator with Suppressed Piezoelectric Resonances	July 8, 1969
3,460,884	Electro-Optical Devices Utilizing the Stark Shift Phenomenon	Aug. 12, 1969
3,463,572	Optical Phase Modulation Apparatus	Aug. 26, 1969
3,473,863	Variable Transmission Windows	Oct. 21, 1969

AD-A072 095 ROCKWELL INTERNATIONAL THOUSAND OAKS CA SCIENCE CENTER F/G 20/6
FIR OPTICAL MODULATION PHENOMENA.(U)
MAY 79 J G PASKO DAAK70-78-C-0003
UNCLASSIFIED SC5149.31FR NL

3 OF 3
AD A072095

END
DATE FILMED
9-79
DDC

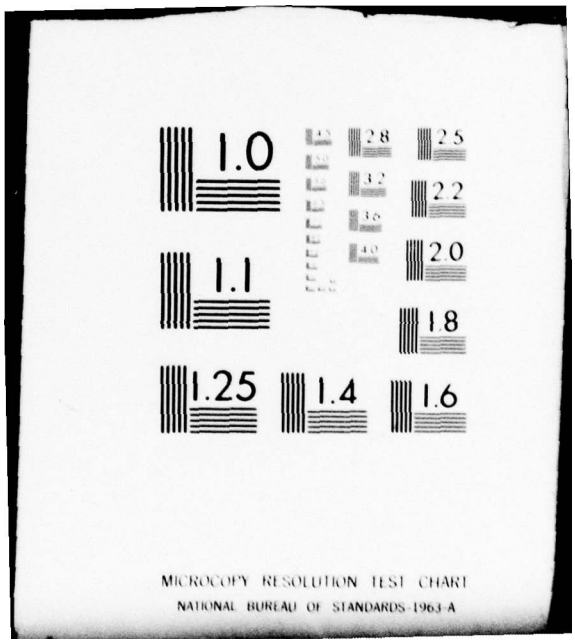
1.0
1.1
1.25
1.4
1.6
2.8
2.5
2.2
2.0
1.8
MICROCOPY RESOLUTION TEST CHART
NATIONAL BUREAU OF STANDARDS-1963-A

3,476,460	Electrochemically Controlled Light Reflection	Nov. 4, 1969
3,479,109	Optical Phase Modulator	Nov. 18, 1969
3,480,348	Apparatus for use in Phase Modulating a Beam of Light	Nov. 25, 2969
3,495,893	Optical Limiter Utilizing Multiphoton Absorbing Material	Feb. 17, 1970
3,499,112	Electro-Optical Device	March 3, 1970
3,499,704	Ferroelectric Ceramic Electro-Optical Device	March 10, 1970
3,516,727	Multipass Interferometric Optical Modulator	June 23, 1970
3,516,728	Infrared Intensity Modulator Wherein the Optical Absorption Spectrum of Cadmium Telluride Doped with Iron Ions is Varied	June 23, 1970
3,517,982	Coherent Light Modulating System	June 30, 1970
3,535,022	Electrostatic Variable Light Reflecting Arrangement	Oct. 20, 1970
3,551,028	Electro-Optical Light Modulator Low Voltage	Dec. 19, 1970
3,561,842	Light Disrupter	Feb. 9, 1971
3,572,896	Switchable Light Modulating Device	Mar. 30, 1971
3,572,897	Optical Modulator having Dissipative Matching Boundaries	Mar. 30, 1971
3,575,489	Liquid Cell Shutter	April 20, 1971
3,584,934	Non-Mechanical Shutter	June 15, 1971
3,586,416	Light Modulator by Gated Interferometry	June 22, 1971
3,614,201	Acoustically Absorbent Mounting Method & Apparatus for Optical Modulator	Oct. 19, 1971
3,614,203	High Speed Optical Shutter	Oct. 19, 1971

3,652,149	Variable Light-Filtering Device with a Redox Compound which Functions as its own Electrolyte	Mar. 28, 1972
3,653,744	Optical Modulator Utilizing a Slow Wave Circuit	April 4, 1972
3,656,835	Modulation by a Magnetic Field of Electromagnetic Radiation Produced by the Decay of Triplet States	April 18, 1972
3,656,836	Light Modulator	April 18, 1972
3,664,726	Optical Shutter for Laser or Maser Modulation	May 23, 1972
3,667,829	Electro-Optical Phase Modulator	June 6, 1972
3,671,105	Light Regulator	June 26, 1972
3,702,724	Ferroelectric Ceramic Plate Electro-Optical Light Scattering Device and Method	Nov. 14, 1972
3,703,332	Light Modulator and Display Device	Nov. 21, 1972
3,704,058	Light Modulating Device Controlled by a Divertable Fluid Stream	Nov. 28, 1972
3,712,709	Variable Light Transmission Device	Jan 23, 1973.
3,726,585	Electrically Modulated Radiation Filters	April 10, 1973
3,730,608	Electrolytic Light Modulation Systems	May 1, 1973
3,736,045	Fast Optical Guided Wave Modulator and Digital Deflector	May 29, 1973
3,790,250	Thermally-Activated Optical Absorber	Feb. 5, 1974
3,791,718	Wideband Traveling Wave Microstrip Meander-Line Light Modulator	Feb. 12, 1974
3,794,413	Strontium Formate Nonlinear Device	Feb. 26, 1974
3,804,489	Electro-Optic Thin-Film Diffraction Loss Modulator	April 16, 1974
3,833,286	Nonlinear Optical Component	Sept. 3, 1974

3,848,964	Forced Closure Dipolar Electro-Optic Shutter and Method	Nov. 19, 1974
3,850,506	Modulation by a Magnetic Field of Electromagnetic Radiation Produced by the Decay of Triplet States	Nov. 26, 1974
3,854,795	Light Modulation Device	Dec. 17, 1974
3,873,187	Light Modulator Array and Method of Making It	Mar. 25, 1975
3,912,367	Optical Multipactor	Oct. 14, 1975
3,923,380	Electro-Optic Modulator Utilizing Multiple Interference	Dec. 2, 1975
3,930,717	Variable Light Transmission Device Containing Ferrous Ammonium Sulfate as an Auxialiary Redox System	Jan 6, 1976
3,951,521	Reversible Radiant Energy Filter and Process of using Same	April 20, 1976
3,955,880	Infrared Radiation Modulator	May 11, 1976
3,958,862	Electro-Optical Modulator	May 25, 1976
3,970,364	Depletion Layer Laser Beam Modulator and Deflector	July 20, 1976
3,994,566	Synchronous Traveling Wave Electro-Optic Light Pipe Modulator	Nov. 30, 1976
4,003,631	Device for Blocking a Laser Beam	Jan. 18, 1977
4,030,813	Control Element having Liquid Layer Attainable to Geometrically Uneven State in Response to Electrical Signal	June 21, 977
4,036,554	Laser Modulator for Producing Dark Pulses	July 19, 1977
4,066,338	Electro-Optic Light Modulator	Jan. 3, 1978
4,068,923	Electro-Optical Cell	Jan 17, 1978
RE.28,199	Electro-Optical Device having Variable Optical Density	Oct. 15, 1974

II. DEFORMABLE MEMBRANE DEVICES

3,619,032	Temporal Light Modulator using Deflectable Membrane	Nov. 9, 1971
3,796,480	Membrane Light Modulator	Mar. 12, 1974
3,877,791	Deformable Mirror Light Valve and Method of Making the Same	April 15, 1975
3,897,997	Electrostatic Display Device with Variable Reflectivity	Aug. 5, 1975
3,905,683	Deformable Mirror Light Valve for Real Time Operation	Sept. 16, 1975
3,912,370	AC Deformable Mirror Light Valve	Oct. 14, 1975
3,990,783	Light Modulating Device	Nov. 9, 1976
4,013,345	Deformable Mirror Light Valve and Method of Operating the Same	Mar. 22, 1976

III. SUSPENDED PARTICLE DEVICES

3,329,110	Electromagnetic Radiation Valve	June 27, 1967
3,341,274	Electrically Responsive Light Controlling Device Employing Suspended Dipole Particles in a Plastic Film	Sept. 12, 1967
3,451,742	Multiple Iris Raster	June 24, 1969
3,512,876	Dipolar Electro-Optic Structures	May 19, 1970
3,594,065	Multiple Iris Raster	July 20, 1971
3,788,729	Thermal Convection Flow Light Valve	Jan. 29, 1974
3,841,732	Dipolar Electro-Optic Structures and Method	Oct. 15, 1974
3,876,288	Light Controlling Device	April 8, 1975
4,025,163	Light Valve, Light Valve Suspension Materials and Suspension Therefor	May 24, 1977

4,046,456	Electro-Optic Cell with Transverse Electric Field	Sept. 6, 1977

IV. ACOUSTO-OPTICAL DEVICES

3,730,609	Thermally Compensated Ultrasonic Light Modulator	May 1, 1973
3,746,427	Acousto-Optical System with Simplified Optics	July 17, 1973
3,759,603	Acousto-Optical Light Deflector having Increased Bandwidth and Short Excess Time	Sept. 18, 1973
3,764,196	Reentrant Acousto-Optic Light Modulators and Deflections	Oct. 9, 1973
3,765,750	Acousto-Optic Device	Oct. 16, 1973
3,771,856	Acousto-Optical Light Diffraction Device	Nov. 13, 1973
3,822,929	Electronically Tunable Optical Filter using Acoustic Waves	July 9, 1974
3,843,234	Acoustic-Optical Element utilizing Univalent Mercury Halogenide Crystals	Oct. 22, 1974
3,851,951	High Resolution Laser Beam Recorder with Self-Focusing Acousto-Optic Scanner	Dec. 3, 1974
3,891,308	Acousto-Optic Modulator	June 24, 1975
3,938,881	Acousto-Optic Modulation Device	Feb. 17, 1976
3,944,334	Acousto-Optic Filter	March 16, 1976
3,944,335	Acousto-Optic Filter	March 16, 1976
3,958,863	Tl_3TaS_4 and TL_3TaSe_4 Crystals and Acousto-Optical Devices	May 25, 1976
3,977,770	$Tl_3VS_4Tl_3NbS_4$ Crystals and Acousto-Optical Devices	Aug. 31, 1976
3,994,569	$TlPSe_4$ Compound, Single Crystals, and Acousto-Optical Devices	Nov. 30, 1976

4,025,166	Acousto-Optic Light Beam Scanner	May 24, 1977
4,032,221	Mounting Arrangements for Acousto-Optic Modulators	June 28, 1977
4,037,933	Light Deflector of Acousto-Optic Interaction Type	July 26, 1977
4,040,722	Light Beam Controller	Aug. 9, 1977

V. OPTICAL SCANNING AND DEFLECTOR DEVICES

2,836,652	Deviation of Light by Utilizing Electrical Field	May 27, 1958
2,915,943	Method and Apparatus for Displacing a Light Beam	Dec. 8, 1959
3,357,771	Light Beam Deflector Employing Electro-Optic Crystal	Dec. 12, 1967
3,360,324	Light Displacement Control System	Dec. 26, 1967
3,395,961	Light Deflector	Aug. 6, 1968
3,400,992	Coplanar Light Beam Deflection and Selection Apparatus	Sept. 10, 1968
3,434,778	Radiation Beam Deflection System	March 25, 1969
3,442,570	Piezoelectric Laser Beam Deflector	May 6, 1969
3,485,552	Phased Array-Type Beam Scanner with Dispersion Compensation	Dec. 23, 1969
3,485,553	Electro-Optic Light Beam Deflector	Dec. 23, 1969
3,492,061	Light Beam Deflector in Which the Light is Diffracted by Magnetic Waves	Jan. 17, 1970
3,492,063	Multiple Passage Light Beam Deflection System	Jan. 27, 1970
3,495,894	Optical Beam Deflection Utilizing $LiNbO_3$ or $LiTbO_3$	Feb. 17, 1970
3,497,285	Resolvable Element Enhancement for Optical Scanning	Feb. 24, 1970

3,498,693	Radiation Translating Devices	March 3, 1970
3,503,671	Multiple Pass Light Deflection Modulator	March 31, 1970
3,512,870	Optical Scanning Apparatus	May 19, 1970
3,515,458	Radiation Scanning System	June 2, 1970
3,531,183	Light Beam Deflector	Sept. 29, 1970
3,539,244	Electromagnetic Radiation Deflection Apparatus Employing Electro-Optic or Electro-Acoustical Devices	Nov. 10, 1970
3,612,653	Digital Light Deflector Having Liquid and Vapor States	Oct. 12, 1971
3,625,594	Electric Field Gradient Beam Deflector	Dec. 7,1971
3,627,404	Electrical Focusing Devices	Dec. 14, 1971
3,650,602	Parallel Array Light Beam Deflector with Variable Phase Plate	Mar. 21, 1972
3,736,044	Dispersive Acoustical Deflector for Electromagnetic Waves	May 29, 1973
3,753,151	Mode Selector for Scan Laser	Aug. 14, 1973
3,787,111	Electro-Optic Grating for Scanning a Beam of Light	Jan. 22, 1974
3,799,652	Optical Deflection System with Acousto-Optical Cell and Associated Prisms	March 26, 174
3,801,184	Closed Vessel Comprising a Digital Light Deflection System	April 2, 1974
3,804,490	Pulse Modulation and Cavity Dumping Lasers	April 16, 1974
3,869,197	Light Deflecting System for Effecting Bragg Diffraction of a Wide Bandwidth	Mar. 4, 1975
3,874,785	Optical Deflector Arrangement for use in Holographic Data Storage Devices	April 1, 1975

3,894,792	Method and Device for Deflecting Light Beam	July 15, 1975
4,006,967	Directing Optical Beam	Feb. 8, 1977

VI. ELECTROCHROMIC DEVICES AND DISPLAYS

3,451,741	Electrochromic Devices	June 24, 1969
3,453,038	Compartmented Electrochromic Device	July 1, 1969
3,560,078	Color Reversible Light Filter Utilizing Solid State Electrochromic Substances	Feb. 2, 1971
3,704,057	Electrochromic Device having Identical Display and Counter Electrode Materials	Nov. 28, 1972
3,712,710	Solid State Electrochromic Mirror	Jan. 23, 1973
3,819,252	Additives that Increase the Stability of Electrochromic Films in Electrochromic Devices	June 25, 1974
3,827,784	Simple, Bonded Graphite Counter Electrode for Electrochromic Devices	Aug. 6, 1974
3,840,286	Electrochromic Device	Oct. 8, 1974
3,840,287	Symmetrical Electrochromic Cell	Oct. 8, 1974
3,840,288	Electrochromic Display having Electro Catalyst	Oct. 8, 1974
3,847,468	Ammonia-Treated Electrochromic (EC) Electrodes	Nov. 12, 1974
3,854,794	Image Display Cell	Dec. 17, 1974
3,879,108	Electrochromic Devices	April 22, 1975
3,892,472	Self-Supporting Pigment Layers for Electrochromic Display	July 1, 1975
3,940,205	Electrochromic Device having an Indium Electrode	Feb. 24, 1976
3,944,333	Electrochromic Display with Porous Separator	March 16, 1976

3,950,077	Lead Reference and Counter Electrode for an Electrochromic Display	April 13, 1976
3,961,842	Regenerating Electrode for Electrochromic Display Cell	June 8, 1976
3,970,365	Additives that Increase the Stability of Electrochromic Films in Electrochromic Devices	July 20, 1976
3,971,624	Controllable Electrochromic Indicator Device with Ionic Conducting Intermediate Layer and Non-Polarizable Electrodes	July 27, 1976
3,973,829	Electrochromic Devices with Partially Pre-Charged Counterelectrodes	Aug. 10, 1976
3,981,560	Electrochromic Display Device	Sept. 21, 1976
3,995,943	All Solid Electrochromic Display	Dec. 7, 1976
3,998,525	Edge Lighted Electrochromic Displays	Dec. 21, 1976
4,006,966	Process for Preparation of an Electrode Structure Containing WO_3 use of the Structure in an Electrochromic Cell	Feb. 8, 1977
4,009,935	Electrochromic Device having a Dopant Therein to Improve its Color Center Absorption Characteristics	March 1, 1977
4,019,809	Electrochromic Display Device	April 26, 1977
4,021,100	Electrochromic Device having an Electrolyte Contained in a Solid Porous Insulating Layer	May 3, 1977
4,036,551	Display Apparatus	July 19, 1977
4,053,209	Electrochromic Device	Oct. 11, 1977
4,060,311	Electrochromic Device	Nov. 29, 1977
4,066,336	Electrode for a Controllable Electrochromic Indicator Device and Method of Manufacture	Jan. 3,1 978

4,068,928	Process for Preparation of an Electrode Structure containing WO_3 use of the Structure in an Electrochromic Cell	Jan. 17, 1978
4,073,570	Electrochromic Display Device	Feb. 14, 1978
4,076,386	Segmented Electrochromic Display General	Feb. 28, 1978

VII. OTHER DISPLAYS AND OPTICAL SYSTEMS

2,896,507	Arrangement for Amplifying the Light Intensity of an Optically Projected Image	July 28, 1959
2,929,922	Masers and Maser Communications Systems	March 22, 1960
3,044,358	Color Projection System	July 17, 1962
3,063,331	Projection System	Nov. 13, 1962
3,084,590	Optical System	April 9, 1963
3,100,817	Image Converter and Amplifier	Aug. 13, 1963
3,137,162	Arrangement for Amplifying the Brightness of an Optically Formed Image	June 16, 1964
3,450,461	Color Picture Projecting System	June 17, 1969
3,450,462	Color Projection System	June 17, 1969
3,459,466	Optical Beam Peak Power Amplifier and Buncher	Aug. 5, 1969
3,485,550	Arrangement for Reinforcement of the Intensity of Optically Produced Images	Dec. 28,1969
3,497,286	Variable Reflectance Display Device	Feb. 24, 1970
3,527,522	Image Intensifier for Optically Produced Images	Sept. 8, 1970
3,544,964	Apparatus for Reproducing Television Pictures	Dec. 1, 1970
3,583,788	Display Device with Uniformly Decreasing Electric Field	June 8, 1971

3,656,837	Solid State Scanning by Detecting the Relief Profile of a Semiconductor Body	April 18, 1972
3,601,470	Light Valve Projection System Employing Coaxial Beams of Colored Light	Aug. 24, 1971
3,667,830	Display System Utilizing a Selectively Deformable Light Reflecting Element	June 6, 1972
3,698,793	Solid State Display	Oct. 17, 1972
3,698,794	Sonic Page Composer for Holographic Memory	Oct. 17, 1972
3,704,936	Achromatic Depth-of-Field Correction for Off-Axis Optical System	Dec. 5, 1972
3,765,749	Optical Memory Storage and Retrieval System	Oct. 16, 1973
3,806,229	Image Display Apparatus	April 23, 1974
3,834,793	Dichromic Mirror having Multilayer Thin Films Including Vanadium Dioxide	Sept. 10, 1974
3,864,024	Optical Display Device	Feb. 4, 1975
3,844,552	Invisible to Visible Light Image Converter	May 20, 1975
2,892,380	Arrangement for Amplifying the Light Intensity of an Optically Projected Image	June 30, 1959
3,941,456	Device for Reducing the Granulation in the Transmission of Optical Information by Means of a Highly Coherent Beam of Radiation	March 2, 1976
3,957,350	Device for Displaying a Laser Beam	May 18, 1976
3,960,440	Light Optic Data Handling System	June 1, 1976
3,963,314	Color Display Device	June 15, 1976
3,985,428	Light Optic Data Handling System	Oct. 12, 1976
3,988,055	Light Optic Data Handling System	Oct. 26, 1976
3,995,940	Luminous Display Device	Dec. 7, 1976

4,000,939	Light Optic Data Handling Systems	Jan. 4, 1977
4,004,847	Light Optic Data Handling Systems	Jan. 25, 1977
4,013,343	Electro-Optical Display Arrangement with Storage Effect using a Solid Electrolyte	March 22, 1977
4,025,165	Electro-Optical Imaging Device	May 24, 1977
4,032,220	Light Optic Data Handling System	June 28, 1977
4,035,061	Honeycomb Display Devices	July 12, 1977
4,037,928	Visual Image Display Device	July 26, 1977
4,039,255	Color Display Device with Dye and Synthetic Oil Solution	Aug. 2, 1977
4,050,787	Electro-Optic Display Device	Sept. 27, 1977
4,068,927	Electrophoresis Display with Buried Lead Lines	Jan. 17, 1978
4,076,387	Magnetic Display	Feb. 28, 1978
4,078,855	Electro-Optical Display Device	March 14, 1978

11.0 APPENDIX 3

LITERATURE SURVEY ADDENDUM

I.P. Kaminow and E.H. Turner, "Electro-Optic Light Modulators", Appl. Optics, Vol. 5, No. 10, Oct. 1966.

R.H. Clarke, "A Theory for the Christiansen Filter", Appl. Optics, Vol. 7, No. 5, May 1978.

H. Baessler and M.M. Labes, "Helical Twisting Power of Steroidal Solutes in Cholesteric Mesophases", J. of Chem. Physics, Vol. 52, No. 2, Jan. 15, 1970.

F.K. Dolezalek and H. Jager, "Survey of Possibilities of Nonmechanical Modulation of Infrared Radiation and Consideration of their Usefulness for Satellite Application", ESTEC Contract No. 990/70, Oct. 1970.

J.A. Castellano, "Mesomorphic Materials for Electro-Optical Application", Ferroelectrics, 3, 29-38 (1971).

L.S. Cosentino, "Transient Scattering of Light by Pulsed Liquid Crystal Cells", SID (1971).

B. Ellis, "Solid State Modulators for Horizon Sensing Applications", Infrared Physics 11, 147-193 (1971).

R.A. Kashnow, "Nematic Liquid Crystals - Cinemicrograhy of Electrohydrodynamic Instabilities", SID (1971).

R.A. Soref, "The Physics and Chemistry of Liquid Crystals", SID Digest of Tech. Papers, Philadelphia, PA 1971.

L. Goodman, "Light Scattering in Electric Field Driven Nematic Liquid Crystals", SID Digest of Tech. Papers, Philadelphia, PA 1971.

W.H. DeJeau, C.J. Gerritsma and A.M. Van Boxtel, "Electrohydrodynamic Instabilities in Nematic Liquid Crystals", Physics Lett., Vol. 34A, No. 4, Mar. 8, 1971.

G.A. Dir, J.H. Becker, J.J. Wysocki, W.E. Haas, J.E. Adams, L.B. Leder, B. Mechiowitz, J.L. Daily and F.D. Saeva, "Cholesteric Liquid Crystal Texture Change Displays", SID Digest of Tech. Papers, Philadelphia, PA 1971.

J.J. Wysocki, J.H. Becker, G.A. Dir, R. Madrid, J.E. Adams, W.E. Haas, L.B. Leder, B. Mechlowitz and F.D. Saeva, "Cholesteric-Nematic Phase Transition Displays", SID Digest of Tech. Papers, Philadelphia, PA 1971.

B.J. Lechner, F.J. Marlowe, E.O. Nester and J. Tults, "Liquid Crystal Matrix Displays", Proc. of the IEEE, Vol. 59, No. 11, November 1971

J. Borel and J. Robert, "An MOS-Driven Liquid Crystal Display", SID Digest of Tech. Papers, Philadelphia, PA 1971.

L.S. Cosentino, "On the Transient Scattering of Light by Pulsed Liquid Crystal Cells", IEEE Trans. on Electron Devices, Dec. 1971.

S. Aftergut and H.S. Cole, "Effect of Boundary Conditions on the Performance of Nematic Liquid Crystal Displays", SID Symp. Digest of Tech. Papers, Philadelphia, PA 1972.

G. Barzilai, P. Maltese, C.M. Ottavi and P. Reali, "Fast Liquid Crystal Cells Suitable for Television Displays", IEEE Conf. on Display Devices, New York, 1972.

W.H. De Jeu and C.J. Gerritsma, "Electrohydrodynamic Instabilities in Some Nematic Azoxy Compounds with Dielectric Anisotropies of Different Sign", J. of Chem. Phys, Vol. 56, No. 10, May 15, 1972.

W.J. De Jeu, C.J. Gerritsma and Th.W. Lathouwers, "Instabilities in Electric Fields of Nematic Liquid Crystals with Positive Dielectric Anisotropy: Domains, Loop Domains and Reorientation", Chem. Physics Lett., Vol. 14, No. 4, June 15, 1972.

G.A. Dir, J.J. Wysocki, J.H. Becker, J.E. Adams, W.E. Haas, L.B. Leader, B. Mechlowitz and E.D. Saeva, "Cholesteric Liquid Crystal Texture Change Displays", Proc. of SID, Vol. 13/2, 1972.

B. Ellis, "Fabry-Perot Modulator for Space Use", Infrared Physics 12, 197-217, 1972.

C.J. Gerritsma and P. Van Zanten, "The Dependence of the Electric Field Induced Cholesteric-Nematic Transition on the Dielectric Anisotropy", Physics Lett., Vol. 42A, No. 2, Nov. 20, 1972.

L. Goodman, "Angular Distribution of Light Scattering from Electric-Field Driven Nematic Liquid Crystals", Proc. of SID, Vol. 13/2, 1972.

F. Rondelez and J.P. Hulin, "Distorsions of a Planar Cholesteric Structure Induced by a Magnetic Field", Solid Stte Commun. 10, 1012 (1972).

J.J. Wysocki, et al., "Cholesteric-Nematic Phase Transition Displays", Proc. SID, Vol. 13/2, 1972.

G.W. Gray, K.J. Harrison and J.A. Nash, "New Cholesteric Liquid Crystals for Displays", Elec. Lett., Vol. 9, No. 26, Dec. 27, 1973.

R.A. Soref, "Liquid Crystals", SPIE Electro-Optical Principles and Applications, 1973.

A.I. Baise and M.M. Labes, "Effect of Dielectric Anisotropy on Twisted Nematics", Appl. Phys. Lett., Vol. 24, No. 7, April 1 1974.

G.W. Gray, K.J. Harrison and J.A. Nash, "Wide Range Nematic Mixtures Incorporating 4'-n-Alykl-4-Cyano-p-Terphenyls", J. Chem. Soc. Chem. Comm., 1974.

D.S. Hulme and E.P. Raynes, "Eutectic Mixtures of Nematic 4'-Substituted 4-Cyanobiphenyls", J. Chem. Soc. Chem. Comm., 1974.

V.I. Lebedev, V.I. Mordasov and M.G. Tomilin, "Liquid Crystals in Optics", Sov. J. Opt. Technol., Vol. 41, No. 7, July 1974.

E.P. Raynes, "Improved Contrast Uniformity in Twisted Nematic Liquid Crystal Electro-Optic Display Devices", Elect. Lett., Vol. 10, No. 8, May 2, 1974.

I.A. Shanks, "Liquid Crystal Materials and Device Developments", Electronic Engineering, August 1974.

J.C. Varney and L.E. Davis, "Structural Oscillation in a Cholesteric-Nematic Mixture", Elec. Lett., Vol. 10, No. 16, Aug. 8, 1974.

J.E. Bigelow, R.A. Kashnow and C.R. Stein, "Contrast Optimization in Matrix-Addressed Liquid Crystal Displays", IEEE Trans. on Electron Devices, January 1975.

J.A. Castellano, "Fundamentals of Liquid Crystals and Other Liquid Display Technologies", SID Digest, 1975.

G. Elliott, "Electro-Optical Displays using Liquid Crystals", GEC J. of Sci. & Tech., Vol. 42, No. 2, 1975.

L. Goodmand and D. Meyerhofer, "Liquid Crystal Field Effect Devices Operating in the Multiplexed Mode", SID Digest, 1975.

F.J. Kahn and R.A. Burmeister, Jr., "Multiplexed Twisted Nematic Liquid Crystal Display", SID Digest, 1975.

L.T. Lipton, M.A. Meyer and D.O. Massetti, "A Liquid Crystal Television Display using a Silicon-on-Sapphire Switching Array", SID Digest, 1975.

K.Uehara, H. Mada and S. Kobayashi, "A Realtime Matrix Liquid Crystal Display", SID Digest, 1975.

J.E. Adams, G.A. Dir, I.P. Gates, W.E. Haas, K.F. Nelson, J.F. Stepany and S. Tutihasi, "Improved Liquid Crystal Image Storage Device", SID Digest, 1975.

W.L. Carl and C.R. Stein, "A Non-Scanning Matrix Addressing Scheme for Certain Liquid Crystal Displays", SID Digest, 1975.

D.J. Channin, "Triode Optical Gate Liquid Crystal Devices for Dynamic Image Display", SID Digest, 1976.

D. Coates and G.W. Gray, "Properties of the Liquid Crystals formed by Some 4'-Substituted 4-(β-p-Substituted Arylethyl)biphenyls", J. Chem. Soc. Perkin II, 1976.

G. Elliott, "Recent Developments in Liquid Crystals and other New Display Techniques", Radio and Elec. Engineer, Vol. 46, No. 6, June 1976.

G.W. Gray and A. Mosley, "Trends in the Nematic-Isotropic Liquid Transition Temperatures for the Homologous Series of 4-n-Alkoxy- and 4-n-Alykl-4'-Cyanobiphenyls", J. Chem. Soc. Perkin II, 1976.

A.R. Kmetz, "Twisted Nematic Displays for Multiplexing", SID Digest, 1976.

V.I. Lebedev, V.I. Mordasov and M.G. Tomilin, "The Electro-Optic Properties of a Liquid-Crystal Cell with the dynamic Scattering Effect", Sov. J. Opt. Technol., Vol. 43, No. 4, April 1976.

E.G. Lierke, "Infrared Modulator for Optical Sensors Based on a Vibrating Fabry-Perot Interferometer", Opt. Engineering, Vol. 15, No. 1, Jan. 1976.

W.L. Martin, "Human Factors Design Criteria for Liquid Crystal Displays", SID Digest, 1976.

K. Ono, E. Matani, E. Kaneko and M. Sato, "Large-Scale Liquid Crystal Matrix Display", SID Digest, 1976.

S. Sherr, "A Liquid Crystal Bar Graph Meter", SID Digest, 1976.

C.P. Stephens and L.T. Lipton, "A Multichip MOS Video Rate Liquid Crystal Display", SID Digest 1976.

M. Yamashita and Y. Amemiya, "Effect of Substrate Surface on Alignment of Liquid Crystal Molecules", Jap. J. of Appl. Phys., Vol. 15, No. 11, Nov. 1976

S. Aftergut and H.S. Cole, Jr., "Technique for Reducing Decay Time in Twisted Nematic Cells", SID Digest, 1977.

G. Bauer and W. Greubel, "Fluorescence Activated Liquid Crystal Display", SID Digest, 1977.

J.E. Bigelow, D.E. Castleberry and C.R. Stein, "A Multiplexed 64 Character Liquid Crystal Display with Improved Optics", SID Digest, 1977.

W.P. Bleha, J. Grinberg, A.D. Jacobson and G.D. Myer, "The Use of the Hybrid Field Effect Mode Liquid Crystal Light Valve with Visible Spectrum Projection Light", SID Digest, 1977.

H.S. Cole, Jr. and R.A. Kashnow, "A New Display Configuration for Dichroic Liquid Crystals", SID Digest, 1977.

B. Dargent and J. Robert, "Twisted Nematic Flat-Panel Display", SID Digest, 1977.

W.H. De Jeu and J. Van der Veen, "Liquid Crystals for Numerical Displays", Philip Tech. Rev. 37, 131-150 (1977).

A.G. Dewey, J.T. Jacobs, B.G. Huth, G.T. Sincerbox, G.J. Sprokel, A. Juliana and R.W. Koepcke, "A 2000-Character Thermally-Addressed Liquid Crystal Projection Display", SID Digest, 1977.

R. Eidenschink, D. Erdmann, J. Krause and L. Pohl, "Substituted Phenycyclohexanes - A New Class of Liquid Crystalline Compounds", Angew. Chem. Int. Ed. Engl. 16 (1977).

R. Eidenschink, L.M. Pohl, J. Krause and D. Erdmann, "A New Class of Low Melting Nematic Compounds", SID Digest, 1977.

J.C. Fan, H.R. Fetterman, F.J. Bachner, P.M. Zavracky and C.D. Parker, "Thin-Film VO_2 Submillimeter-Wave Modulators and Polarizers", Appl. Phys. Lett., Vol. 31, No. 1, July 1977.

M. Kawachi, K. Kato and O. Kogure, "Light Scattering Properties of a Nematic-Cholesteric Mixture with Positive Dielectric Anisotropy", Japan. J. Appl. Phys. 16, 7 (1977).

M. Kawachi, O. Kogure and K. Kato, "Nucleation of Focal-Conic Domains in the Field-Induced Nematic Texture of a Cholesteric Liquid Crystal", Japan. J. of Appl. Phys. 17, 2 (1977).

L.T. Lipton, C.P. Stephens and R.B. Lloyd, "A Fully Integrated MOS Liquid Crystal Video-Rate Matrix Display", SID Digest, 1977.

K.F. Nelsen, J.M. Pollack, J.F. Stephany, G.A. Dir, I.P. Gates, J.E. Adams and W.E. Haas, "A Ten-Thousand Element Liquid Crystal Matrix Display", SID Digest, 1977.

J.C. Varney, "Liquid Crystal Display Technology", Ph.D. Thesis, Paisley College of Technology, May 1977.

R.K. Waring, Jr., "Christiansen Effect Display Element", Proc. of IEEE, July 1977.

H.S. Cole, Jr. and S. Aftergut, "Absorption and Pitch Relationships in Dichroic Guest-Host Liquid Crystal Systems", J. Chem. Phys. 68(3), Feb. 1978.

G.A. Dir, I.P. Gates and K.F. Nelson, "A Vacuum Deposition Alignment Technique for Tilt Control in Liquid Crystals", SID Digest, 1978.

R. Eidenschink, L. Pohl, J. Krause, D. Erdman and R. Macklin, "Low-Melting Nematic Compounds/CCH", SID Digest, 1978.

J.L. Fergason, "Liquid Crystals: A Big Case for Display", Optical Spectra, June 1978.

N.P. Gracheva and S.I. Zhdanov, "Liquid Crystal Electrochemistry. Oxidation of p,p'-Phenyl Benzoates at the Rotating Platinum Electrode", Sov. Electrochem. 14(5), 590 (1978).

G.W. Gray, "Advances in Liquid Crystal Materials for Applications",

C. Hilsum, R.J Holden and E.P. Raynes, "A Novel Method of Temperature Compensation for Multiplexed Liquid Crystal Displays", Elect. Lett. 14, 14 (1978).

S.R. Jost, A New Light-Modulated Liquid-Crystal Light Valve", J. Appl. Phys. 49, 10 (1978).

F.J. Kahn, "Reflective Mode, 40-Character, Alphanumeric Twisted-Nematic Liquid Crystal Displays", SID Digest, 1978.

E. Kaneko, H. Kawakami and H. Hanmuar, "Liquid Crystal Television Display", SID Digest, 1978.

A.R. Kmetz, "Characterization and Optimization of Twisted Nematic Displays for Multiplexing", SID Digest, 1978.

G.M. Kurdyumov, V.A. Molochko and O.P. Chernova, "Selection of Low Melting Liquid Crystal Compositions having High Mesophase Stability", J. App. Chem. of U.S.S.R. 51, 167 (1978).

L.T. Lipton, C.P. Stephens, R.B. Lloyd, S.E. Shields, A.G. Toth and R.C. Tsai, "A 2.5" Diagonal, High Contrast, Dynamic Scattering Liquid Crystal Matrix Display wiht Video Drivers", SID Digest, 1978.

G.R. Luckhurst, "Liquid Crystals: The Fourth State of Matter", Proc. Royal Inst. (GB) 49, 159 (1978).

F.C. Lueo, W.A. Hester and T.P. Brody, "Alphanumeric and Video Performance of a 6"x6" 30 Lines-Per-Inch Thin-Film Transistor-Liquid Crystal Display Panel", SID Digest, 1978.

K. Odawara, T. Ishibashi, K. Toriyama, M. Kohyama and H. Sakurada, "Alphanumeric Liquid-Crystal Display System for Portable Computer Terminals", SID Digest, 1978.

P.A. Penz, "A Figure of Merit Characterizing the Anisotropic Viewing Properties of the Twisted Nematic LCD", SID Digest, 1978.

L. Pohl, R. Eidenschink, J. Krause and G. Weber, "Nematic Liquid Crystals with Positive Dielectric and Negative Diamagnetic Anisotropy", Phys. Lett. 65A, 2 (1978).

E.P. Raynes, "Recent Advances in Liquid Crystal Materials and Display Devices", (1978).

S. Saito and H. Yamamoto, "Transient Behaviors of Field-Induced Reorientation in Variously Oriented Nematic Liquid Crystals", Japan. J. of Appl. Physics 17, 2 (1978).

I.A. Shanks, P.A. Holland and A.J. Hughes, "Liquid Crystal Oscilloscope Displays", SID Digest, 1978.

C.Z. Van Doorn and J.J.M. De Klerk, "Two-Frequency, 100-Line Addressing of a Reflective Twisted Nematic Liquid Crystal Matrix Display", SID Digest, 1978.

J.C. Varney and L.E. Davis, "The Effect of Surface Preparation on Voltage Threshold in Liquid Crystal Phase-Change Cells", Elect. Lett. 14, 25 (1978).

H. Wedel and W. Haase, "Substituted Phenylcyclohexanes and Cyclohexylcyclohexanes. Two New Classes of Liquid Crystals as Anisotropic Solvents in Optical Absorption Spectroscopy", Chem. Phys. Lett. 55, 1 (1978).

M. Bertolotti, G. Sansoni and F. Scudieri, "Dye Laser Emission in Liquid Crystal Hosts", Appl. Optics 18, 4 (1979).